THE UNIVERSITY
of ADELAIDE

Faculty of Sciences

Department of Physics

Generalised Parton Distributions from Lattice Feynman-Hellmann Techniques

Alec Hannaford Gunn

Supervisors:
A. Prof. Ross Young
A. Prof. James Zanotti

February 2020

Contents

Abstract

Generalised parton distributions (GPDs) are observables that contain an abundance of previously inaccessible information about hadron structure. However, GPDs have proven difficult to measure from experiment, and first principles calculations in lattice Quantum Chromodynamics (QCD) have largely been limited to their lowest Mellin moments.

In this thesis, we outline a completely novel approach to determine GPD-related information using Feynman-Hellmann techniques in lattice QCD. We present both the formalisms that make this numerical computation possible, and an exploratory calculation using this method. The results appear very promising.

First, we show how lattice Feynman-Hellmann techniques can be applied to calculate the off-forward Compton tensor (OFCT). The result is a relation between the OFCT and the energy shifts of a two-point function for a carefully chosen perturbed Lagrangian. Moreover, since the OFCT is both off-forward and second order, the Lagrangian mixes momentum eigenstates in a non-trivial way. Therefore, we also show how to control this mixing by a careful choice of the parameters in our perturbed Lagrangian.

Second, we need a form of the OFCT with kinematics that are suitable for the Euclidean lattice. We use an operator product expansion to derive an expression for the leading order (twist-two) contribution to the OFCT in terms of the Mellin moments of GPDs. This result can be compared to a lattice calculation of the OFCT for large momentum transfer, and hence allows us to extract the moments of GPDs.

Finally, we present our calculation of the Euclidean OFCT using lattice Feynman-Hellmann techniques. Our results exhibit behaviour that is consistent with the theoretical expressions derived in the previous chapters. We find that the magnitude of our results is significantly larger than what is expected from a simple phenomenological model, but that the t dependence of our results is consistent with this model.

As such, this study paves the way for a first principles calculation of higher GPD moments. Moreover, it allows us to investigate the behaviour of the OFCT in the Euclidean region as it pertains to scaling, factorisation, and other properties of interest.

Declaration

I certify that this work contains no material which has been accepted for the award of any other degree or diploma in my name in any university or other tertiary institution and, to the best of my knowledge and belief, contains no material previously published or written by another person, except where due reference has been made in the text. In addition, I certify that no part of this work will, in the future, be used in a submission in my name for any other degree or diploma in any university or other tertiary institution without the prior approval of the University of Adelaide and where applicable, any partner institution responsible for the joint award of this degree. I give permission for the digital version of my thesis to be made available on the web, via the University's digital research repository, the Library Search and also through web search engines, unless permission has been granted by the University to restrict access for a period of time.

I acknowledge the support I have received for my research through the provision of an Australian Government Research Training Program Scholarship.

Acknowledgements

Over the past two years, I have had the immense good fortune of being surrounded and supported by some really wonderful people, both in my academic and personal life.

First and foremost, I want to thank my supervisors, Ross Young and James Zanotti, who have been consistently encouraging and generous with their time and knowledge. I have greatly appreciated the openness of their teaching styles and the guidance and support they have given me in my research.

I have also had the privilege of being surrounded by a fantastic cohort of fellow students, during my undergraduate and Master's. In particular, I would like to thank the students I graduated with and the students of room 123. Our constant conversations about physics have sharpened my understanding significantly, and been a great source of pleasure.

I would also like to express my gratitude for my family and friends. Mum and Dad, Hannah and Ian, thank you for the constant love and support. And to my friends, thank you for keeping me sane, with quizzes, D&D, our extremely successful and highly athletic social soccer team, and other distractions.

And, best for last, thank you Georg, for making the past two years a wonderful time.

Chapter 1

Introduction

> What is a hadron?
>
> In practice, the answer to this question depends upon the energy scale of interest.
>
> *S. J. Brodsky, G. P. Lepage* [1].

Hadrons, the bound states of Quantum Chromodynamics (QCD), account for almost all observable matter: every ion, atom and molecule in the universe is composed of them. Despite their ubiquity, the phenomena of hadronic matter are some of the least understood in all particle physics.

It has been a long and winding road that led to QCD, our best theory of hadronic matter. We can begin our story in 1909, with Geiger and Marsden's famous experiment involving the scattering of alpha particles off gold foil [2]. In 1911, Rutherford was the first to propose that the anomalous 'back-scattering' observed in these experiments could be explained if atoms were made of a positively charged and tightly bound nucleus, orbited by electrons [3]. The discovery of protons and neutrons followed. However, if the nucleus is composed of multiple positively charged particles, surely some even stronger force would be responsible for overcoming their electromagnetic repulsion and holding them together? An early and successful theory of this strong nuclear force was proposed in 1934 by Yukawa [4]. His model had protons and neutrons as fundamental particles, bound together by the exchange of massive particles dubbed 'mesons'.

In the 1950s, our understanding of the strong interaction changed significantly, as a new generation of high-energy experiments began to discover a 'zoo' of strongly interacting particles. With the proliferation of new types of particles came a proliferation of new theoretical frameworks: S-matrix methods, current algebra and its sum rules, and the various iterations of the quark model all sought to circumvent the need for quantum field theory (QFT) of the strong force altogether.

The quark model of Gell-Mann and Zweig [5], developed in the early '60s, appeared to clear up the mess of new particles significantly. According to this model, the newly discovered particles were not fundamental, but were instead composites (collectively called hadrons), made up of the truly fundamental particles, quarks. The elegance of the quark model seemed to speak for its truthfulness. However, it offered little to explain how quarks were held together. In fact, the force binding quarks would have to be immensely powerful to keep them forever bound within the hadron, never seen in experiment.

Then, in 1969, the first deep inelastic scattering experiments took place at the Stanford Linear Accelerator (SLAC), scattering electrons off of protons with unprecedentedly high

energies [6]. These experiments revealed the extraordinary property of 'Bjorken scaling', which suggested that the proton could be described as a collection of *weakly* interacting particles. Although at first this seemed entirely at odds with the idea that quarks in hadrons were strongly bound together, it was in fact the final piece of the puzzle for QCD. In the few years after the SLAC experiment, this property of being strongly bound at low energies and weakly bound at high energies (asymptotic freedom) led finally to QCD as the QFT of the strong force.

Quantum chromodynamics describes how quarks interact strongly via the exchange of gluons. The strong *nuclear* force, which binds protons and neutrons in the nucleus, then emerges as a residual force, much like molecular forces between atoms. As with any quantum field theory, QCD is summarised by its Lagrangian; in principle, all predictions of the theory are contained in this equation. But QCD is not so simple: since the strong force between quarks is so strong, the coupling is too large to apply perturbation theory. Therefore, quantitative predictions require computational simulations. The first formulation of numerical solutions to the QCD equations of motion (lattice QCD) was provided in 1974 by Wilson [7]. However, it wasn't until the late 1980s that lattice QCD became computationally feasible.

So, with one of the greatest achievements of modern particle physics — a QFT of the strong force — how much more do we know about what's really going on inside hadrons? For a long time, two observables encompassed almost all there was to know about hadron structure: (1) parton distribution functions (PDFs), which describe the probability density of quarks and gluons in a hadron as one dimensional functions of the 'longitudinal momentum fraction'; and (2) electromagnetic form factors, from which one can obtain the charge and magnetisation densities of the hadron. Hence for a more complete description of hadron structure, new observables would need to be constructed.

Generalised parton distributions (GPDs) were first considered as an extension of the standard PDFs [8]. Ji then showed in 1996 that GPDs could give insights into the spin structure of the proton [9], thereby offering to solve the decades-old 'proton spin crisis'. Since then, it has also been shown that GPDs are the Fourier transform of the spatial distribution of quarks and gluons in a plane transverse to the motion of a high-energy hadron [10]. Moreover, recent work has uncovered the connection between GPDs and a hadron's 'mechanical' properties [11]. Therefore, the measurement of generalised parton distributions would offer an unprecedented window into hadron structure.

However, as we have already established, nothing in QCD is ever easy. As such, GPDs are very difficult to measure experimentally. This is partly a result of the experiments that measure them: hard, exclusive scattering processes, which are more difficult to get a clean measurement of than inclusive deep inelastic scattering. Moreover, even once the necessary cross section has been extracted, phenomenological determination of GPDs from this data requires even more work. Global fits of GPDs, which are most desired, lean heavily on our theoretical understanding, which is lacking. Nonetheless, there have been multiple experiments aiming to measure GPDs (HERA, COMPASS and JLab). The proposed electron-ion collider (EIC) is a major experimental undertaking, specifically to probe hadronic structure by measuring hadronic observables such as GPDs.

In terms of lattice calculations, the progress has been mostly limited to the lowest few Mellin moments of GPDs. More recently, there has been one study of pion quasi-GPDs. The lack of lattice calculations of GPDs reflects a more general difficulty in reconciling the

light-cone physics that is so useful in describing high-energy scattering and the Euclidean spacetime of lattice calculations, our only first principles way to calculate parton distributions. The present thesis offers a novel way to determine GPD-related quantities from lattice QCD, by first calculating the off-forward Compton tensor (OFCT) in the Euclidean region and relating this to GPD moments.

To begin this thesis, in chapter 2 we give a brief outline of QCD and lattice QCD. In chapter 3, we give a detailed account of deep inelastic scattering (DIS). In particular, we show how the non-perturbative structure of the amplitude for this process can be parameterised by a basis of local operators from the operator product expansion (OPE), or by non-local light-cone operators. In chapter 4, we outline all things GPD: their basic properties and relation to other variables, their physical content, and the ways in which they can be measured experimentally or calculated on the lattice.

Then we begin our results in chapter 5. The Feynman-Hellmann method, as applied to lattice QCD, involves adding perturbing terms to the lattice Lagrangian that depend on arbitrary parameters. As in the perturbation theory of regular quantum mechanical systems, the shift in the energy can be shown to be proportional to the matrix elements of operators. Hence we show how the energy shifts calculated from lattice two-point functions can be related to the OFCT.

In chapter 6, we investigate the theoretical behaviour of the OFCT, the quantity in our Feynman-Hellmann relation. Even though the OFCT is very well-studied, much of these studies only consider light-cone kinematics (in the infinite momentum frame), and hence aren't suitable for comparison to the Euclidean lattice. Therefore, by performing an OPE on the OFCT, we show how the Compton tensor can be parameterised in terms of the Mellin moments of GPDs.

Finally, in chapter 7, we present the results of a proof-of-principle lattice calculation. Remarkably, given the subtleties involved in both our Feynman-Hellman relation and the OPE, the lattice results appear in good agreement with what we expect from previous chapters. Therefore, the exploratory results presented in this chapter open up a multitude of possibilities for future studies: the calculation of many higher GPD moments, exploring the factorisation and scaling behaviour of the OFCT, and ultimately the reconstruction of full GPDs may all be possible.

Now, more than one hundred years after Rutherford first proposed the existence of atomic nuclei, we may be afforded a new window into the internal structure of nucleons through the determination of GPDs. According to our best theory of matter, all the information about such structure is contained in the Lagrangian of QCD. Therefore, in this thesis we present a new method to numerically calculate these observables from lattice QCD.

Chapter 2

Quantum Chromodynamics

The Standard Model (SM) of particle physics is one of the most successful theories in the history of science. It predicted the existence of the W and Z bosons, top and charm quarks, and the Higgs boson, as well as many of the properties of these particles. To give an example of the SM's predictive power, precision tests of QED agree with one another to more than ten significant figures*, making them the most accurate predictions in all science.

Roughly speaking, the SM applies to the universe on the small scale, where gravity is negligible. As such, the SM describes three of the four fundamental forces in nature (electromagnetism, the weak force and the strong force) in terms of gauge field theories (GFTs); that is, a field theory in which the Lagrangian is invariant under a group of continuous, local transformations.

Quantum Chromodynamics (QCD) is the GFT that describes the strong force: the force responsible for binding quarks together to form hadrons. The strong force also gives rise to the strong nuclear force that binds protons and neutrons together to form atomic nuclei. It is therefore QCD that describes the interactions that make almost all observable matter possible.

However, QCD is the outlier of the three GFTs of the SM: due to the size of the strong coupling ($\alpha_S \approx 1$ at standard energy scales), we cannot apply perturbation theory to QCD. Even though the QCD Lagrangian in principle contains all possible strong interactions, there are few analytic methods for making quantitative predictions apart from perturbation theory. Therefore, the only first principles method to calculate non-perturbative quantities in QCD is computational: lattice QCD, a technique that only became feasible in the late 1980s.

The structure of this chapter follows: first, we introduce quarks and gluons, the basic constituents of QCD, and then introduce some of the formal properties of the theory, such as local gauge invariance and the Lagrangian. Next, we give a brief account of asymptotic freedom, and how it gives rise to perturbative and non-perturbative regimes. Finally, we introduce some of the formalism and techniques of lattice QCD. We omit a detailed discussion of the quantisation of the Lagrangian and the construction of Feynman rules, as these topics are not essential to the present thesis.

*QED makes predictions about observables (e.g. the anomalous magnetic moment of the electron and muon, the Lamb shift etc.) in terms of the fine structure constant α_{QED} (equivalently the QED coupling). These observables can then be measured, and hence the value of α_{QED} determined from different processes. These measurements of α_{QED} agree with one another to an extremely high degree of accuracy [12].

2.1 Elements of QCD

In this section we start with a qualitative description of the quark model, and then give a more formal treatment of the theory of QCD.

2.1.1 Quarks and Hadrons

The basic elements of QCD are quarks (the fermions) and gluons (the gauge bosons). Quarks and gluons both carry 'colour' charge. The different types of quarks are known as different 'flavours' of quark, given in the table below. The flavour of a quark determines its electric charge, spin and mass. Note that each flavour of quark listed below has its own anti-particle (e.g. the anti-up quark).

Strong interactions only occur between colour charged particles. In strong interactions, there are three types of charge: red, green and blue (with corresponding anti-red, -green and -blue for the anti-particles). In contrast with electromagnetism, the gauge bosons of QCD (gluons) are themselves carriers of colour charge. Apart from the fact that the anti-quarks carry anti-charge, the flavour of a quark and its colour charge are independent.

Particle	electric charge	spin	mass (MeV/c^2)
Up quark	+2/3	1/2	2.2
Down quark	-1/3	1/2	4.7
Charm quark	+2/3	1/2	1.28×10^3
Strange quark	-1/3	1/2	96
Top quark	+2/3	1/2	173×10^3
Bottom quark	-1/3	1/2	4.18×10^3
Gluons	0	1	massless

Note the difference in masses of the different types of quarks: the up, down and strange are all comparatively light, while the others (especially the top!) are significantly heavier.

Bound States

Individual quarks and gluons are never observed. Instead, we always measure colour neutral bound states, collectively called hadrons. There are two main types of hadron: mesons and baryons, defined by their *valence quarks*. A meson has two valence quarks (a quark and an anti-quark), whereas baryons have three valence quarks. These valence quarks determine the quantum numbers that define a particular hadron. Examples of some hadrons are given in the table below.

In addition to the valence quarks, hadrons also contain *sea quarks* and gluons. The sea quarks always occur in quark anti-quark pairs, and hence do not alter the quantum numbers of the hadron. As our knowledge of QCD has developed further, we have come to understand that the sea quarks and gluons determine more of a hadron's properties than was first thought (see for instance the 'proton spin crisis' [13]). The existence of this 'sea' of quarks and gluons within hadrons is a large part of the reason their internal structure is so complicated.

Hadron	electric charge	valence quarks	spin	mass (MeV/c^2)
Proton	+1	uud	1/2	938.27
Neutron	-1	udd	1/2	939.56
Pion +	+1	$u\bar{d}$	0	139.57
Pion 0	0	$\frac{1}{\sqrt{2}}(u\bar{u}+d\bar{d})$	0	134.98
Pion -	-1	$d\bar{u}$	0	139.57

2.1.2 Formal Properties of QCD

We now move from a qualitative account of the quark model to describing some of the formal properties of QCD. Quantum chromodynamics is defined by its local gauge invariance: the QCD Lagrangian (and all QCD observables) must be invariant under the SU(3) group of transformations. Moreover, these quantities must be *locally* invariant, meaning that different spacetime points have independent gauge spaces, and hence transform differently under SU(3) transformations.

An element of SU(3) can be expressed as

$$V(x) = \exp\left[i\alpha^a(x)t^a\right], \tag{2.1}$$

where $\alpha^a(x)$ are parameters that depend on some spacetime point x (that is, they are local), and t^a are the generators of the group[†]. In the language of Lie groups, t^a are elements of the Lie algebra and the $V(x)$ are elements of the Lie group. In particular, the elements of SU(3) don't commute, which has important physical implications we will discuss later.

The fermion (quark) fields transform like

$$\psi_i(x) \to \psi_i'(x) = [V(x)]_{ij}\psi_j(x), \tag{2.2}$$

where i, j are colour indices[‡].

Now we need to construct a gauge invariant Lagrangian. To start, note that the derivative is not well-defined, since we can't meaningfully subtract two quark fields with different gauge spaces and different transformations:

$$n^\mu\partial_\mu\psi(x) = \lim_{\varepsilon\to 0}\frac{\psi(x^\mu+\varepsilon n^\mu)-\psi(x^\mu)}{\varepsilon}. \tag{2.3}$$

Therefore we need a way to 'compare' different gauge spaces.

As such, we define the Wilson line $U(x_1, x_2)$ that transforms like

$$U(x_1, x_2) \to V(x_1)U(x_1, x_2)V(x_2)^{-1}, \tag{2.4}$$

and constructed to ensure that $U(x+\varepsilon n, x)\psi(x)$ transforms like $\psi(x+\varepsilon n)$.

[†]In the fundamental representation of SU(3), we can write $t^a = \frac{\lambda^a}{2}$, where λ^a are known as the Gell-Mann matrices.

[‡]There are two types of colour indices we make explicit: first, indices of the 3×3 SU(3) matrices in the fundamental representation: i, j. Second, the indices that label the individual generators t^a fo SU(3): a, b, c.

Explicitly, the Wilson line is

$$U(x_1, x_2) \equiv \mathcal{P} \exp\Big\{ig \int_{x_2}^{x_1} dx^\mu t^a A_\mu^a(x)\Big\}, \tag{2.5}$$

where $\mathcal{P}$ denotes path-ordering. The Wilson line is a way to parallel transport in gauge space: it gives a way of 'comparing' local gauge geometries at different spacetime points.

Therefore, for an infinitesimal path,

$$U(x + \varepsilon n, x) = \mathbb{I} + i\varepsilon n^\mu g A_\mu^a(x) t^a, \tag{2.6}$$

and hence, by comparison with Eq. 2.3, we get the *covariant derivative*:

$$D^\mu = \partial^\mu - igA_a^\mu t^a, \tag{2.7}$$

where A_μ^a are the gluon fields. Since there are eight SU(3) generators, there are eight types of gluon.

Then the derivative of quark fields has the transformation law

$$D_{ij}^\mu \psi_j(x) \to [V(x)]_{ij} D_{jk}^\mu \psi_k(x), \tag{2.8}$$

and hence kinetic terms such as $\bar{\psi} D_\mu \psi$ are gauge invariant.

The field strength tensor $F_{\mu\nu}^a$ is defined by

$$[D_\mu, D_\nu] = -igF_{\mu\nu}^a t^a. \tag{2.9}$$

The Classical Lagrangian

The two main properties the classical QCD Lagrangian density must satisfy are: (1) local gauge invariance, and (2) renormalisability (that is, it must have mass dimension four: $[\mathcal{L}] = 4$). It is then a straightforward exercise to enumerate all possible terms made up of quark and gluon fields and eliminate those that don't satisfy these constraints [14]. The resultant Lagrangian density is,

$$\mathcal{L} = \sum_f \bar{\psi}_f^i \big(\not{D}^{ij} - \delta^{ij} m_f\big) \psi_f^j - \frac{1}{4} F^{a\mu\nu} F_{\mu\nu}^a. \tag{2.10}$$

Here, f is the flavour index that runs over $u, d, s....$

Note that, since the elements of SU(3) don't commute, there will be interaction terms in the Lagrangian that are cubic and quartic in the A_μ^a fields. Physically, these interaction terms mean that the vector bosons of QCD (gluons) interact with one another, an extremely important property.

For the quantised QCD Lagrangian density, we must include ghost terms that arise from the gauge-fixing condition, and counter-terms from renormalization. For the purposes of our simple description of QCD, we omit such terms.

2.1.3 Asymptotic Freedom

One of the most important emergent properties of QCD is asymptotic freedom: at short distances (or equivalently high energies), the effective strength of strong interactions *de-*

Figure 2.1: Left: the one-loop vacuum polarisation term for quarks. Right: the one-loop vacuum bubble for gluons.

creases. Therefore, it becomes possible at short distances to apply perturbative techniques to QCD.

Asymptotic freedom is the result of gluon self-interaction. To demonstrate this qualitatively, consider the case of screening in quantum electrodynamics (QED): a lone electron will emit an electric field, which will in turn create virtual electron-positron pairs in the vacuum. The positrons will be pulled towards the inital electron, resulting in a *screening* of the charge: the further away the observer from the charge, the more vacuum is in the way, and hence more screening. Therefore, at long distances the charge will be weaker.

For a lone quark with some colour charge, the same process as above will occur (see figure 2.1 left), resulting in a screening of the colour charge. However, unlike QED, gluon self-interaction implies that gluons may also be created from the vacuum (see figure 2.1 right). Since gluons are spin 1 bosons rather than spin 1/2 fermions, they are affected differently by the presence of the strong charge: they act as colour-anti-colour dipoles, oriented to align with the direction of the inital charge [15, 16]. As a result, they *anti-screen* the colour charge, increasing its strength at long distances. The anti-screening of the gluons dominates the screening of the quarks, resulting in the extraordinary property of asymptotic freedom.

Quantitatively, we must use renormalisation group methods. The one-loop result for the strong coupling is

$$\alpha_S(\mu) \propto \frac{1}{\log(\mu/\Lambda_{\mathrm{QCD}})}. \tag{2.11}$$

Here μ is the energy scale and $\Lambda_{\mathrm{QCD}} \approx 0.2$ GeV is the natural scale of QCD, which is on the order of low-lying hadronic masses (pions, nucleons etc.). Therefore, for large energy scales $\mu \gg \Lambda_{\mathrm{QCD}}$, the coupling is small. This dependence on the energy scale μ is known as the 'running' of the coupling.

2.1.4 Confinement

The fundamental constituents of QCD so far introduced (quarks and gluons) all carry colour charge, but observed states in QCD are colour neutral (colourless). Therefore, we say that colour charged states are always confined within the colourless bound state. However, confinement is an emergent property of QCD: it is not fundamental to the QCD Lagrangian (Eq. 2.10), in which all the fields have colour charge, but instead emerges from the interactions of those fields.

Intuitively, confinement can be thought of as a result of asymptotic freedom: since the strength of the strong coupling grows with the separation of colour charges, colourless

bound states are always 'energetically favourable'. Despite this, so far no first principles proof exists of the property of confinement, and as such, it is part of one of the Millennium Prize Problems (the 'Yang-Mills mass gap' problem) [17].

2.1.5 Perturbative and Non-Perturbative QCD

Apropos our discussion of asymptotic freedom, the running of the strong coupling divides QCD into two regimes: the high-energy/short distance regime, where perturbative techniques are applicable, and the low-energy/long distance regime, where only non-perturbative techniques can be used.

However, even at high energies, there is still some non-perturbative contribution to the amplitude. This is manifest in a property called factorisation: a high-energy amplitude factorises into its short distance (perturbative) and long distance (non-perturbative) parts. This is demonstrated below:

$$\sigma = \big(\text{long distance effects}\big) \otimes \big(\text{short distance effects}\big), \tag{2.12}$$

where $\otimes$ represents some convolution integral. While we can calculate the short distance component using perturbation theory, the long-distance effects can only be calculated with non-perturbative methods (e.g. lattice QCD) or measured from experiment. This is a highly desirable property, since it means we can extract the interesting non-perturbative part of the process, which gives us information about internal hadronic structure.

Factorisation is particularly important to the present thesis, since we will show how the quantity we calculate on the lattice factorises (chapter 6), and as a result we can extract the non-perturbative part of this amplitude (see chapter 7).

2.2 Lattice QCD

Lattice QCD, first proposed by Wilson [7], is the only first principles, systematically improvable way to calculate non-perturbative quantities in QCD. Simply put, it is a method to calculate Euclidean path integrals on a finite volume lattice of points. The finite distance between adjacent points (the lattice spacing) serves as a natural ultraviolet regularisation, while the finite volume provides an infrared regularisation. Lattice simulations have been applied very successfully to the hadronic spectrum, the structure of the QCD vacuum and the structure of hadrons, among other properties of QCD.

2.2.1 Euclidean Path Integrals

In the path integral formulation of QCD, the expectation value of some operator $\mathcal{O}$ is given by

$$\langle\Omega|\mathcal{O}|\Omega\rangle = \frac{\int \mathcal{D}A_\mu \mathcal{D}\bar{\psi}\mathcal{D}\psi \mathcal{O} e^{iS_{\text{QCD}}}}{\int \mathcal{D}A_\mu \mathcal{D}\bar{\psi}\mathcal{D}\psi e^{iS_{\text{QCD}}}}, \tag{2.13}$$

where $|\Omega\rangle$ is the vacuum state and $\mathcal{D}\phi$ gives the functional volume element for some field ϕ. Hence the path integral is an integration over all possible configurations of *classical* fields.

Here,

$$S_{\text{QCD}} = \int d^4x \mathcal{L}_{\text{QCD}}(x), \tag{2.14}$$

where the Lagrangian density is given in Eq. 2.10.

Note that, even with discretisation, the expression in Eq. 2.13 is near-impossible to evaluate, due to the highly oscillatory factor $e^{iS_{\text{QCD}}}$. To deal with this problem, we use a fundamental property of any QFT, analytic continuity, to 'Wick rotate' to Euclidean spacetime: $t \to -i\tau$. Under this transformation, the action goes to $S_{\text{QCD}} \to iS^{\text{Euc}}_{\text{QCD}}$, and hence

$$\langle\Omega|\mathcal{O}|\Omega\rangle = \frac{\int \mathcal{D}A_\mu \mathcal{D}\bar{\psi}\mathcal{D}\psi\mathcal{O}e^{-S^{\text{Euc}}_{\text{QCD}}}}{\int \mathcal{D}A_\mu \mathcal{D}\bar{\psi}\mathcal{D}\psi e^{-S^{\text{Euc}}_{\text{QCD}}}}. \tag{2.15}$$

Since each configuration of fields is now weighted by a decaying exponential, providing that the field configurations are generated to conform to this probability distribution, we have that

$$\langle\Omega|\mathcal{O}|\Omega\rangle \approx \frac{1}{N_{\text{conf}}}\sum_{i=0}^{N_{\text{conf}}}\mathcal{O}[\phi_i], \tag{2.16}$$

where ϕ_i represents the i^{th} configuration of the relevant particle fields.

Despite making lattice calculations computationally feasible, the Wick rotation doesn't come without consequences. For instance, after the Wick rotation the invariant length of a four-vector is

$$x^2 = -\tau^2 - |\mathbf{x}|^2 < 0.$$

Hence the lattice is Euclidean: there is no sign difference between the spatial and temporal components. Therefore, lattice calculations can only involve spacelike vectors (for spatial separations, momenta etc.). This makes it difficult to extract information related to parton distributions, as we will discuss in future chapters.

2.2.2 Discretisation

For lattice QCD, discretisation is quite an involved exercise; as with most discretisation procedures, the choice of discretisation is not unique. Moreover, the choice of procedure is further complicated by the desire to preserve the physics.

Discretisation begins with introducing the lattice spacing a, which is related to a spacetime point by

$$x^\mu = an^\mu,$$

where $n^\mu \in \mathbb{Z}$. Note that the choice of n^μ is restricted since the lattice has finite volume.

Now we would like to construct a gauge invariant lattice action. We can separate out the gauge and fermion parts of the action: $S_{\text{latt}} = S^G_{\text{latt}} + S^F_{\text{latt}}$. To construct gauge invariant quantities, we again need to use the Wilson line from Eq. 2.5. In particular, we will use the Wilson line (Eq. 2.4) to define the *link variable*:

$$U_\mu(x) \equiv U(x, x + a\hat{\mu}) = \exp\left\{2iagt^a A^a_\mu(x + a\hat{\mu}/2)\right\}, \tag{2.17}$$

where $\hat{\mu}$ is the unit vector point along the axis x_μ. Note that the link variable pointing in the $-\hat{\mu}$ direction is $U_{-\mu}(x) = U^\dagger_\mu(x - a\hat{\mu})$.

Then, the discretised covariant derivative is

$$D_\mu\psi(x) = \frac{U_\mu(x)\psi(x + a\hat{\mu}) - U^\dagger_\mu(x - a\hat{\mu})\psi(x - a\hat{\mu})}{2a}. \tag{2.18}$$

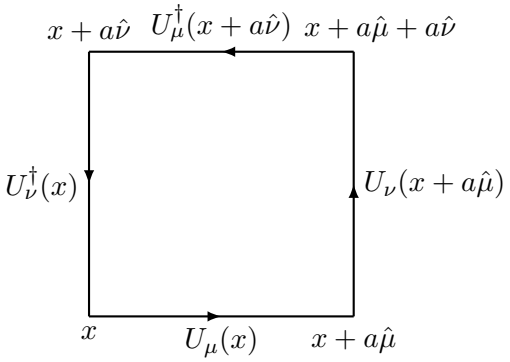

Figure 2.2: Visual representation of the gauge invariant plaquette.

Unlike in the continuum case (Eq. 2.7), we can't take a to be infinitesimal, and therefore we don't have the straightforward relationship between the covariant derivative and the gauge boson fields A_μ as in Eq. 2.7. Hence all gauge invariant quantities on the lattice must be constructed from the link variables in Eq. 2.17.

Gauge Component

To construct the gauge term, we introduce the plaquette (see figure 2.2):

$$\mathcal{P}^{\mu\nu}(x) \equiv U_\nu^\dagger(x) U_\mu^\dagger(x + a\hat{\nu}) U_\nu(x + a\hat{\mu}) U_\mu(x). \tag{2.19}$$

It is trivial to show that this is gauge invariant, using the transformation law of the Wilson line Eq. 2.4.

Then, using the identity $e^{a+b} = \exp\left\{a + b + \frac{1}{2}[a, b] + ...\right\}$, and Taylor expanding the vector fields,

$$A_\nu(x + \hat{\mu}) = A_\nu(x) + a\partial_\mu A_\nu(x) + \mathcal{O}(a^2),$$

one can derive the following

$$\mathcal{P}^{\mu\nu}(x) = \exp\left\{ia^2 F^{\mu\nu}(x) + \mathcal{O}(a^2)\right\}, \tag{2.20}$$

where $F^{\mu\nu}$ is the QCD field strength tensor from Eq. 2.9. Hence the standard discretisation of the gauge term is

$$S^G_{\text{latt}} = \frac{2}{g^2} \sum_{\text{sites}} \sum_{\mu<\nu} \text{Re trace}\big[\mathbb{I} - \mathcal{P}^{\mu\nu}(x)\big]. \tag{2.21}$$

Fermion Component

Building a gauge invariant fermion component of the lattice action at first glance seems simpler than the gauge component. We use the discretised form of the covariant derivative from Eq. 2.18,

$$S^F_{\text{naive}} = \sum_{\text{sites}} \left[\bar{\psi}(x)\gamma_\mu \frac{U_\mu(x)\psi(x + a\hat{\mu}) - U_\mu^\dagger(x - a\hat{\mu})\psi(x - a\hat{\mu})}{2a} + m\bar{\psi}(x)\psi(x)\right], \tag{2.22}$$

which has $\mathcal{O}(a^2)$ errors. However, this naive fermion action suffers from a difficulty known as 'fermion doubling'. To remove the doubling, the 'Wilson term' is added to the naive action. However, this term introduces $\mathcal{O}(a)$ errors, which can be removed by the inclusion of the Sheikholeslami-Wolhert (or 'clover') term [18]. Therefore, the final clover action is $\mathcal{O}(a)$ improved, and doesn't suffer from fermion doubling. See Refs. [19, 20] for a much more complete treatment of this problem and its solution.

2.2.3 Hadron Spectroscopy

One of the most common applications of lattice QCD is the calculation of energies of hadronic states. For the present thesis, this is particularly important, since such methods are the foundation of Feynman-Hellmann lattice techniques.

First, we define the nucleon two-point correlation function[§]:

$$c_{\chi\chi}(z', z) \equiv \langle\Omega|\chi(z')\chi^\dagger(z)|\Omega\rangle, \tag{2.23}$$

where χ is the nucleon interpolating operator that couples to states with the same quantum numbers as the nucleon:

$$\begin{aligned}\chi_\alpha(x) &= \epsilon^{ijk}[\psi_u]^i_\alpha(x)\Big([\psi_u]^j_\beta(x)[C\gamma_5]_{\beta\gamma}[\psi_d]^k_\gamma(x)\Big),\\ \chi^\dagger_\alpha(x) &= \epsilon^{ijk}\Big([\bar{\psi}_{\bar{u}}]^i_\beta(x)[C\gamma_5]_{\beta\gamma}[\bar{\psi}_{\bar{d}}]^j_\gamma(x)\Big)[\bar{\psi}_{\bar{u}}]^k_\alpha(x).\end{aligned} \tag{2.24}$$

Here, i, j, k are fermion colour indices and α, β, γ are Dirac indices.

Then, we define the set of momentum eigenstates $\{|X(\mathbf{k})\rangle\}$, where X is the hadronic state and $\mathbf{k}$ is the momentum, whose components are quantised to integer values of $2\pi/L$ for L the spatial extent of the lattice. These states are eigenstates of the Hamiltonian and satisfy the normalisation condition

$$H_{\text{QCD}}|X(\mathbf{k})\rangle = E_X(\mathbf{k})|X(\mathbf{k})\rangle, \quad \langle Y(\mathbf{p})|X(\mathbf{k})\rangle = 2E_X(\mathbf{k})L^3\delta_{X,Y}\delta_{\mathbf{p},\mathbf{k}}. \tag{2.25}$$

We then define $C(\tau, \mathbf{k})$ the Fourier-projected two-point function[**]:

$$C(\tau, \mathbf{k}) \equiv \sum_{\mathbf{z}} e^{-i\mathbf{k}\cdot\mathbf{z}}\langle\Omega|\chi(\tau, \mathbf{z})\chi^\dagger(0)|\Omega\rangle. \tag{2.26}$$

Then inserting a complete set of states

$$\begin{aligned}C(\tau, \mathbf{k}) =& \sum_{\mathbf{z}} e^{-i\mathbf{k}\cdot\mathbf{z}}\langle\Omega|\chi(\tau, \mathbf{z})\chi^\dagger(0)|\Omega\rangle\\ =& \mathcal{N}\sum_{X,\mathbf{k}'}\sum_{\mathbf{z}} e^{-i\mathbf{k}\cdot\mathbf{z}}\langle\Omega|\chi(\tau, \mathbf{z})|X(\mathbf{k}')\rangle\langle X(\mathbf{k}')|\chi^\dagger(0)|\Omega\rangle,\end{aligned} \tag{2.27}$$

[§]We often refer to lattice correlation functions by the number of spacetime points their operators have. So some matrix element $\langle\Omega|\phi_1(x_1)...\phi_n(x_n)|\Omega\rangle$ is an n-point function.

[**]For the rest of this thesis, we simply refer to the Fourier-projected quantity as the 'two-point function' or 'correlator'.

where $\mathcal{N}$ is some appropriate normalisation of the complete set of states. Using the translational invariance of the interpolating operators in Euclidean space, we get

$$\begin{aligned} C(\tau, \mathbf{k}) =& \mathcal{N} \sum_{X, \mathbf{k}'} \sum_{\mathbf{z}} e^{-i\mathbf{k}\cdot\mathbf{z}} \langle \Omega | e^{H\tau - i\hat{\mathbf{p}}\cdot\mathbf{z}} \chi(0) e^{-H\tau + i\hat{\mathbf{p}}\cdot\mathbf{z}} | X(\mathbf{k}') \rangle \langle X(\mathbf{k}') | \chi^\dagger(0) | \Omega \rangle \\ =& \mathcal{N} \sum_{X, \mathbf{k}'} e^{-E_X(\mathbf{k}')\tau} \sum_{\mathbf{z}} e^{-i(\mathbf{k}-\mathbf{k}')\cdot\mathbf{z}} \langle \Omega | \chi(0) | X(\mathbf{k}') \rangle \langle X(\mathbf{k}') | \chi^\dagger(0) | \Omega \rangle \\ =& \sum_{X} e^{-E_X(\mathbf{k}')\tau} |\langle \Omega | \chi(0) | X(\mathbf{k}) \rangle|^2, \end{aligned} \tag{2.28}$$

which we simply write as

$$C(\tau, \mathbf{k}) = \sum_X A_X(\mathbf{k}) e^{-E_X(\mathbf{k})\tau}. \tag{2.29}$$

Therefore, for large τ, the term in the sum of X with the lowest energy will dominate: the nucleon. Hence

$$C(\tau, \mathbf{k}) \approx A_N(\mathbf{k}) e^{-E_N(\mathbf{k}')\tau}, \quad \tau \gg a. \tag{2.30}$$

This allows us to extract the ground state nucleon. In particular, we define the *effective mass*:

$$\Delta E_{\text{eff}}(\tau) \equiv \frac{1}{\delta\tau} \log \left(\frac{C(\tau, \mathbf{k})}{C(\tau + \delta\tau, \mathbf{k})} \right). \tag{2.31}$$

When the effective mass is approximately constant, the ground state is dominant. Therefore, we can calculate the nucleon mass from first principles. Moreover, by varying the interpolating operators or with more advanced techniques, we can also calculate the masses of different hadrons and excited states.

Although thoroughly compactified, this section presents all the basic ideas of QCD that will be necessary in subsequent chapters. In the next chapter, we narrow our focus considerably to a single QCD process.

Chapter 3

Forward Scattering

In this chapter, we discuss deep inelastic scattering (DIS). This scattering process is extremely important for a few reasons: first, from a historical perspective, DIS was instrumental in guiding theorists towards QCD at a time when there was great confusion about how the strong force should be described. Second, the parton distribution functions (PDFs) that are measured from DIS are some of the most important observables for describing hadron structure. Finally, for the purposes of the present thesis, we are concerned with calculating generalised parton distributions (GPDs). Since GPDs are generalisations of PDFs and the processes one uses to access them are generalisations of DIS, an analysis of DIS serves as a natural gateway to discussions of GPDs and their measurement and calculation.

In the early 1960s Gell-Mann's eight-fold way and the quark model [5] provided an elegant description of the observed hadronic spectrum without introducing a quantum field theory (QFT). Moreover, methods such as current algebra [21] seemed to supplant the need for a QFT of the strong force altogether. By 1969, however, results from the Stanford linear accelerator (SLAC) would lead to breakthroughs in the understanding of hadron structure, and eventually a field theory of the strong force: QCD. The electron-proton scattering (DIS) experiments at SLAC were performed at unprecedented high-energies. In particular, they showed that the DIS cross section exhibited behaviour known as 'Bjorken scaling' [6], which suggested that hadronic structure was best described at high-energies as a collection of weakly interacting particles. The first iteration of a model of weakly interacting hadron constituent was the naive parton model [22, 23].

Later, it was proven that the only QFT that could have this behaviour would have to have to be asymptotically free [24]. Furthermore it was shown that only non-Abelian gauge theories could exhibit this asymptotic freedom [25, 26], which, combined with the symmetries described by the quark model and eight-fold way, confirmed that QCD was a good description of the strong force.

Deep inelastic scattering is more than just historically interesting, though. Parton distribution functions, which are extracted from DIS, have enormous significance to almost any physics that involves high-energy scattering with hadrons [27]. Not only are PDFs one of the most important observables for describing hadron structure, they are also used to parameterise non-perturbative behaviour in scattering events, allowing for phenomenological tests of standard model and beyond standard model physics.

For our purposes, DIS has a special importance. The tools and methods introduced in this chapter will be used over and over in later chapters to extract GPD-related quantities from a lattice calculation (see chapters 5, 6 and 7). Moreover, an introduction to the

simpler case of DIS and PDFs may help to clarify many of the properties of GPDs that can seem arbitrary or confusing when they are introduced in chapter 4.

The structure of this chapter is as follows: first in section 3.1, we will discuss the basic kinematics and cross section of DIS, and its behaviour in the high-energy limit. Furthermore, we will briefly discuss the parton model, indicating the properties that make it a good description of experiment.

Then, in section 3.2, we will discuss the application of the operator product expansion (OPE) to DIS. This section is especially significant, since it forms the basis of our OPE analysis in chapter 6. In addition to a more or less standard presentation of the OPE, we will emphasise properties of the OPE that make it good for comparing to lattice calculations.

Finally, in section 3.3, we will introduce the light-cone operators, which are essential tools for understanding the definition and properties of parton distributions.

Therefore, the outline of this chapter is to present a general description of DIS in section 3.1, and then show how DIS can be parameterised in the high-energy limit in terms of two types of operators: first, the local operators introduced by way of the OPE, and then non-local light-cone operators. The similarities and contrasts between these two types of operators is especially important for how we connect lattice quantities to physical Minkowski quantities, as will be discussed in depth in later chapters.

3.1 Deep Inelastic Scattering

Deep inelastic scattering is a hard inclusive* process, given by $e^-(k)+N(P) \to e^-(k')+X$, where X is some unspecified final hadronic state. See figure 3.1 for a Feynman diagram. In our discussion, we always take the target to be a nucleon, but in principle it could be another hadron. Moreover, we will limited ourselves to discussing only spin averaged scattering; that is, where a particular spin polarisation is not enforced, and hence there is an average over the spins in experiment.

Qualitatively, our understanding of DIS is that the very high-energy electron transmits enough momentum to eject one of the nucleon's constituent quarks. As the quark is pulled out of its nucleon, the strong force between it and the colour-charged remnants of the nucleon increases with the distance between them, until this force is strong enough to create particles from the QCD vacuum. The products of DIS are then a collection of colour neutral hadrons. This violent process of 'smashing open' a nucleon gives us insight into its internal structure. In the rest of this chapter, we will furnish the technical details to this qualitative account of DIS†.

3.1.1 Kinematics

The kinematics of DIS are:

- the incoming nucleon has momentum P;
- the incoming/outgoing electrons have momentum k/k', respectively;

*In a particle physics context, 'hard' means that the momentum transferred between the particles is much greater than the relevant particle masses, and 'inclusive' means that the outgoing hadronic states are not specified.

†Where no citation is given, the material of this chapter is drawn from Refs. [14, 28–32].

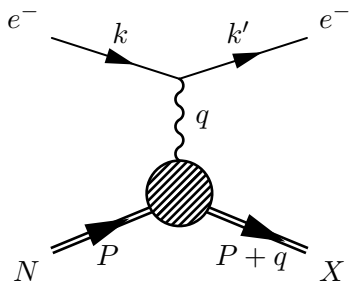

Figure 3.1: The Feynman diagram for deep inelastic scattering. As with all Feynman diagrams in this thesis, time increases left to right.

- the virtual photon exchanged by the electron and nucleon has momentum $q = k - k'$.

Given these variables, it is useful to define some Lorentz scalars.

- $\nu = \frac{P \cdot q}{M}$, which is the energy transferred to the nucleon in the nucleon's rest frame: $\nu = k^0 - k'^0$.
- $Q = \sqrt{-q^2}$, which is always real, since q^μ is spacelike. This is the momentum transferred to the nucleon.
- $x = \frac{Q^2}{2P \cdot q}$, the 'Bjorken scaling variable'. In the nucleon's rest frame, this is proportional to the ratio of momentum transfer to energy transfer.
- $\omega = x^{-1}$, the inverse Bjorken variable. This variable is particularly useful for the OPE.
- M, the nucleon mass.
- m_f the mass of a quark of flavour f.
- $M_X^2 = (P+q)^2$, the invariant mass of the outgoing state X.

Physical Region of Scalars

Now we will determine what the physically allowed region is for each Lorentz scalar defined above.

First, note that in the nucleon's rest frame the electron transfers energy to the proton and hence $\nu \geq 0$, and since this is a Lorentz scalar it is non-negative in all frames.

Then, since $q = k - k'$ and k and k' are future-pointing timelike vectors, we can use the inverse Minkowski triangle inequality to get $q^2 = (k-k')^2 \leq |k^2 - k'^2| = m_{e^-}^2 - m_{e^-}^2 = 0$ (see appendix A). Therefore, q is a spacelike vector, and hence $-q^2 = Q^2 \geq 0$. The region for inelastic scattering starts at $Q^2 \gtrsim 2\text{GeV}^2$.

In inelastic scattering, the momentum transfer to the nucleon is very large, and hence $M_X^2 = (P+q)^2 \gtrsim M^2$. Therefore,

$$P^2 + 2P \cdot q - Q^2 \gtrsim P^2 \quad \Rightarrow \quad 2P \cdot q \gtrsim Q^2 \quad \Rightarrow \quad \omega = \frac{2P \cdot q}{Q^2} \gtrsim 1. \tag{3.1}$$

Hence the physical region of x is $[0, 1]$, and for ω it is $[1, \infty)$.

3.1.2 Cross Section

The scattering amplitude for spin averaged DIS is

$$i\mathcal{M} = (-ie)^2\Big(\frac{-ig_{\mu\nu}}{q^2}\Big)\langle k'|j^{\mu}_{\mathrm{e}^-}(0)|k\rangle\langle X|j^{\nu}_{h}(0)|P\rangle, \tag{3.2}$$

where we leave out spin variables in the state vectors, since we only consider the spin averaged case. Note that $j^{\mu}_{\mathrm{e}^-}$ and j^{μ}_{h} are the electromagnetic Noether currents for electrons and hadrons, respectively:

$$j^{\mu}_{\mathrm{e}^-}(z) = -\bar{\psi}_{\mathrm{e}^-}(z)\gamma^{\mu}\psi_{\mathrm{e}^-}(z), \quad j^{\mu}_{h}(z) = \sum_f e_f\bar{\psi}_f(z)\gamma^{\mu}\psi_f(z), \tag{3.3}$$

where f denotes the flavour of the quark, e_f is the charge for quark of flavour f in units of the magnitude of the electron charge e (e.g. for the down quark $e_f = -1/3$), and ψ_f is the quark field for quark of flavour f.

Therefore, the scattering cross section for spin averaged DIS is

$$\begin{aligned} d\sigma &= \frac{1}{2}\sum_{X,\text{spins}}\int\frac{d^3P_X}{(2\pi)^3}\frac{1}{2E_X}\int\frac{d^3k'}{(2\pi)^3 2k'^0}\frac{(2\pi)^4\delta^{(4)}(k+P-k'-P_X)}{2k^0 2M}|\mathcal{M}|^2 \\ &= \frac{e^4}{Q^4}\frac{1}{2}\sum_{X,\text{spins}}\int\frac{d^3P_X}{(2\pi)^3}\frac{1}{2E_X}\int\frac{d^3k'}{(2\pi)^3 2k'^0}\frac{(2\pi)^4\delta^{(4)}(k+P-k'-P_X)}{2k^0 2M} \\ &\times\langle P|j^{\mu}_{h}(0)|X\rangle\langle X|j^{\nu}_{h}(0)|P\rangle L_{\mu\nu}, \end{aligned} \tag{3.4}$$

where we have introduced P_X the momentum of the outgoing state X. Also note that we used the hermiticity of the currents to get $\langle\alpha|j|\beta\rangle = (\langle\beta|j|\alpha\rangle)^{\dagger}$. And moreover, we introduced $L_{\mu\nu}$ the *leptonic tensor*, defined as

$$L_{\mu\nu} \equiv \frac{1}{2}\sum_{\text{spins}}\langle k'|j^{\mu}_{\mathrm{e}^-}(0)|k\rangle\langle k|j^{\nu}_{\mathrm{e}^-}(0)|k'\rangle.$$

Now we would like a similar tensor for the hadronic contributions to this scattering process. Hence we define the *hadronic tensor*:

$$W^{\mu\nu} \equiv \frac{1}{2}\sum_{X,\text{spins}}\int\frac{d^3P_X}{(2\pi)^3}\frac{1}{2E_X}(2\pi)^4\delta^{(4)}(k+P-k'-P_X)\langle P|j^{\mu}_{h}(0)|X\rangle\langle X|j^{\nu}_{h}(0)|P\rangle. \tag{3.5}$$

We can simplify expression 3.5 significantly. First, using the integral representation of the Dirac delta and the fact that $q = k - k'$, we can re-write

$$W^{\mu\nu} = \frac{1}{2}\sum_{X,\text{spins}}\int\frac{d^3P_X}{(2\pi)^3}\frac{1}{2E_X}\int d^4z e^{i(q+P-P_X)\cdot z}\langle P|j^{\mu}_{h}(0)|X\rangle\langle X|j^{\nu}_{h}(0)|P\rangle. \tag{3.6}$$

By the transational invariance of the current operator

$$j^{\mu}(z) = e^{i\hat{P}\cdot z}j^{\mu}(0)e^{-i\hat{P}\cdot z}.$$

Therefore,

$$W^{\mu\nu} = \frac{1}{2}\sum_{X,\text{spins}} \int \frac{d^3P_X}{(2\pi)^3}\frac{1}{2E_X}\int d^4z e^{iq\cdot z}\langle P|j_h^\mu(z)|X\rangle\langle X|j_h^\nu(0)|P\rangle. \tag{3.7}$$

Finally, since $\{|X\rangle\}$, the set of all hadronic states, is a complete set, the identity in this space is

$$\mathbb{I} = \sum_X \int \frac{d^3P_X}{(2\pi)^3}\frac{1}{2E_X}|X\rangle\langle X|. \tag{3.8}$$

Therefore,

$$W^{\mu\nu} = \frac{1}{2}\sum_{\text{spin}} \int d^4z e^{iq\cdot z}\langle P|j^\mu(z)j^\nu(0)|P\rangle, \tag{3.9}$$

where we have dropped the h subscripts on the currents, since from now on we will only consider the hadronic current. Therefore, the cross section in Eq. 3.4 can be written as,

$$d\sigma = \frac{e^4}{Q^4}\int \frac{d^3k'}{(2\pi)^3 2k'^0}\frac{1}{4k^0 M}W^{\mu\nu}L_{\mu\nu}. \tag{3.10}$$

The purpose of isolating the leptonic (electron) and hadronic (nucleon) contributions to the scattering process is so that we can independently examine the hadronic part of the process. Leptons have trivial structure, and their contribution can be calculated perturbatively. By contrast, due to the complicated nature of the strong force, the hadronic tensor is highly non-trivial.

We can constrain the form of the hadronic tensor by noting that it must satisfy its Ward identity $q_\mu W^{\mu\nu} = 0 = q_\nu W^{\mu\nu}$. Further, the spin averaged hadronic tensor can only depend on the Lorentz tensors, P^μ, q^μ and the Minkowski metric $g^{\mu\nu}$. Therefore, after writing out the most general ansatz and applying the Ward identity, we arrive at the tensor decomposition for the spin averaged hadronic tensor:

$$W^{\mu\nu} = F_1(x,Q^2)\left(-g^{\mu\nu} + \frac{q^\mu q^\nu}{q^2}\right) + \frac{F_2(x,Q^2)}{P\cdot q}\left(P^\mu - \frac{P\cdot q}{q^2}q^\mu\right)\left(P^\nu - \frac{P\cdot q}{q^2}q^\nu\right), \tag{3.11}$$

where $F_{1,2}$ are called the *structure functions*, whose variables are the only Lorentz scalar variables we can form: q^2 and $P\cdot q$, or equivalently Q^2 and x.

3.1.3 The Bjorken Limit

In 1967, Bjorken predicted that the DIS cross section should exhibit a behaviour now known as 'Bjorken scaling' [33]. That is, as $Q^2 \to \infty$ with x fixed, the DIS cross section asymptotically approaches a finite non-zero value:

$$\lim_{Q^2\to\infty} F_{1,2}(x,Q^2) = F_{1,2}(x). \tag{3.12}$$

This behaviour was later confirmed by experiment, leading to the discovery of QCD as the QFT of the strong force, as discussed in the introduction. Note that there are large

logarithmic deviations from Bjorken scaling behaviour, as predicted by perturbative QCD; however, we will not discuss these in the present thesis.

Therefore, it is useful to introduce the *Bjorken limit*:

$$Q^2 \to \infty,\ P \cdot q \to \infty,\ \ x, \omega \text{ fixed to finite values.} \tag{3.13}$$

Coordinate Space Behaviour

Recall the hadronic tensor from Eq. 3.9:

$$W^{\mu\nu} = \frac{1}{2} \sum_{\text{spin}} \int d^4 z e^{iq\cdot z} \langle P | j^\mu(z) j^\nu(0) | P \rangle.$$

It is instructive to ask how this object behaves in the Bjorken limit.

To begin, consider the Riemann-Lebesgue lemma:

$$\lim_{p\to\infty} \int_{-\infty}^{\infty} dx e^{ipx} f(x) = 0, \tag{3.14}$$

where $f(x)$ is an integrable function of one variable. Compare this to the hadronic tensor in the Bjorken limit

$$\lim_{Q^2, P\cdot q \to \infty} \frac{1}{2} \sum_{\text{spin}} \int d^4 z e^{iq\cdot z} \langle P | j^\mu(z) j^\nu(0) | P \rangle. \tag{3.15}$$

Clearly, from the Riemann-Lebesgue lemma, some regions of the hadronic tensor will vanish. However, since we are in Minkwoski space, where $q \cdot z = 0$ does not imply $|q||z| = 0$, we may have regions where the argument of the exponential vanishes, and hence these regions will have non-vanishing contributions. In particular, in the nucleon's rest frame [34],

$$q \cdot z \approx \frac{\omega Q^2}{2M}(z^0 - r) - \frac{M}{\omega} r, \tag{3.16}$$

for $r = \mathbf{q} \cdot \mathbf{z}/|\mathbf{q}|$. Therefore, it is not too difficult to show that this implies

$$|z^2| \lesssim \frac{c_1}{Q^2}, \quad |z^\mu| \lesssim c_2 \omega, \tag{3.17}$$

where $|z^\mu|$ indicates the magnitude of the μ^{th} component of the separation between currents z, and $c_{1,2}$ are finite non-zero scalars. Hence in the Bjorken limit the contributions that dominate are those for which the current separation is lightlike (see figure 3.2). Intuitively, we can think of this as, at infinite momentum, a massive particle's trajectory asymptotically approaches a lightlike trajectory[‡].

3.1.4 The Parton Model

In response to the SLAC experiments, Feynman [22] and Bjorken and Paschos [23] recognised that Bjorken scaling behaviour could be recovered if one assumed that the nucleon was composed of non-interacting fundamental particles, which they called partons.

[‡]For a full discussion of light-cone dominance, we need to consider the singularities of the current product [35–38]. However, in the interest of brevity, this heuristic explanation must suffice.

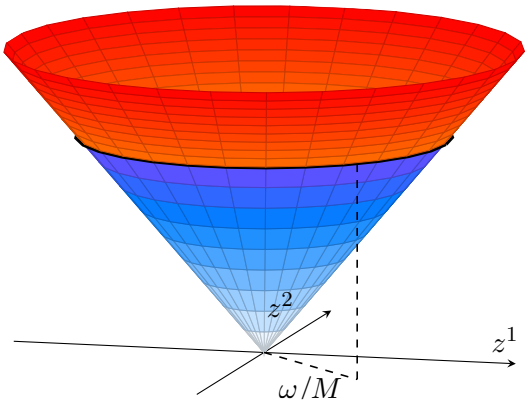

Figure 3.2: Light-cone in (2+1) dimensions. In the Bjorken limit, the blue region is dominant, while the red region and everything outside the light-cone is suppressed.

Today, the theory of parton-like calculations is very advanced [27]; however, for the naive parton model, the assumptions are simple:

- hadrons are constituted point-like particles called partons;
- these partons don't interact with one another, but can interact electromagnetically with the incoming electron;
- with P the nucleon momentum, a given parton has momentum $p = yP$, where y is the fraction of the nucleon's momentum carried by the parton (so we ignore any components of the parton's momentum transverse to the nucleon's);
- parton model calculations always use the infinite momentum frame, where the nucleon and parton momenta are lightlike. In the Bjorken limit, this is simply the centre of mass frame.

Parton Model Hadronic Tensor

In particular, the fact that the partons don't interact with one another means that we can simply split up the hadronic tensor into its contributions from each species of parton:

$$W^{\mu\nu} = \sum_f \int_0^1 dy q_f(y) W_f^{\mu\nu}, \tag{3.18}$$

where $q_f(y)$ is the probability density to find a parton of species f and momentum fraction y in the nucleon and $W_f^{\mu\nu}$ is the hadronic tensor of a given parton species. These probability densities are known as parton distribution functions (PDFs). For the moment, they are *ad hoc* inclusions necessary to conserve probability. However, the future sections of this chapter will be devoted to parameterising them in terms of QCD operators. Furthermore, Eq. 3.18 is an example of the factorisation of short- and long-distance contributions to a cross section. In perturbative QCD these relations, known as 'factorisation theorems', are extremely important.

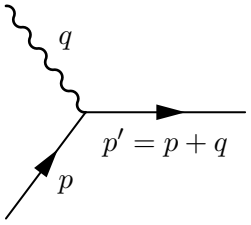

Figure 3.3: The Feynman diagram for γ^* parton $\rightarrow$ parton$'$ scattering.

Therefore, in the parton model the contribution to the hadronic tensor (Eq. 3.5) given by the struck parton can be calculate independently:

$$W_f^{\mu\nu} = \frac{1}{2}\sum_{\text{spins}}\int \frac{d^3p'}{(2\pi)^3 2p'^0}\frac{1}{y}(2\pi)^4\delta^{(4)}(q+p-p')\langle p|j_f^\mu(0)|p'\rangle\langle p'|j_f^\nu(0)|p\rangle, \tag{3.19}$$

where $j_f^\mu(z) = e_f\bar{\psi}_f(z)\gamma^\mu\psi_f(z)$, for parton field ψ_f. We include the factor of $1/y$ since the hadronic tensor is normalised for $1/2P^0$.

Note that, since the partons are structureless particles (see figure 3.3), we can calculate this amplitude using the standard trace techniques:

$$\begin{aligned}\frac{1}{2}\sum_{\text{spins}}\langle p|j_f^\mu(0)|p'\rangle\langle p'|j_f^\nu(0)|p\rangle &= \frac{1}{2}e_f^2\text{tr}\left[(\not{p}' - m_f)\gamma^\mu(\not{p} - m_f)\gamma^\nu\right] \\ &\approx 2e_f^2\left(p'^\mu p^\nu + p^\mu p'^\nu - g^{\mu\nu}p\cdot p'\right) = 2e_f^2\left(2y^2P^\mu P^\nu + y(P^\mu q^\nu + P^\mu q^\nu) - g^{\mu\nu}yP\cdot q\right),\end{aligned} \tag{3.20}$$

where we have used the fact that m_f and M, the parton and nucleon mass, may be neglected. Now we can use the identity

$$\int \frac{d^3p'}{(2\pi)^3 2p'^0} = \int \frac{d^4p'}{(2\pi)^4}(2\pi)\delta\Big((p+q-p')^2\Big) = \int \frac{d^4p'}{(2\pi)^4}\frac{\pi}{P\cdot q}\delta(x-y), \tag{3.21}$$

and hence we can make the equivalence of the Bjorken variable and the momentum fraction $x = y$ in the parton model. So in the parton model $p = xP$.

Putting Eqs. 3.20 and 3.21 into Eq. 3.19:

$$W_f^{\mu\nu} = \frac{2\pi}{P\cdot q}\delta(x-y)e_f^2\Big(2yP^\mu P^\nu + (P^\mu q^\nu + P^\mu q^\nu) - g^{\mu\nu}P\cdot q\Big). \tag{3.22}$$

Therefore, the full hadronic tensor for the parton model is

$$\begin{aligned}W^{\mu\nu} &= 2\pi\sum_f\int_0^1 dy e_f^2 q_f(y)\frac{\delta(x-y)}{P\cdot q}\Big(2yP^\mu P^\nu + (P^\mu q^\nu + P^\mu q^\nu) - g^{\mu\nu}P\cdot q\Big) \\ &= 2\pi\sum_f e_f^2 q_f(x)\left[\Big(-g^{\mu\nu} + \frac{q^\mu q^\nu}{q^2}\Big) + \frac{2x}{P\cdot q}\Big(P^\mu - \frac{P\cdot q}{q^2}q^\mu\Big)\Big(P^\nu - \frac{P\cdot q}{q^2}q^\nu\Big)\right].\end{aligned} \tag{3.23}$$

By comparison with Eq. 3.11, the parton model structure functions are:

$$F_1(x) = 2\pi \sum_f e_f^2(q_f(x) + \bar{q}_f(x)), \quad F_2(x) = 2\pi 2x \sum_f e_f^2(q_f(x) + \bar{q}_f(x)). \tag{3.24}$$

Note that we have pre-empted the identification of partons with quarks by introducing the anti-parton distribution $\bar{q}_f(x)$.

From Eq. 3.24, we recover Bjorken scaling: the structure functions of the parton model are independent of Q^2. Note that F_1 and F_2 are linearly dependent:

$$F_2(x) = 2xF_1(x), \tag{3.25}$$

which is known as the Callan-Gross relation.

3.2 Operator Product Expansion

The parton model reproduces the observed property of Bjorken scaling and imbues the structure functions of Eq. 3.11 with a simple physical interpretation of probability densities. So far, however, we have made little reference to the properties of QCD outlined in chapter 2. Therefore, in this section we will show that the partonic results can be recovered from QCD via a theoretical tool known as the operator product expansion (OPE).

Recall from chapter 2 that we discussed a property of QCD called asymptotic freedom. Due to this property, the strong coupling as a function of energy scale μ behaves like

$$\alpha_S(\mu) \propto \frac{1}{\log(\mu/\Lambda_{\text{QCD}})}.$$

In DIS, our energy scale is $\mu = Q$, and hence in the region where Q is large, the coupling is small and we can use perturbation theory. Of course, in the Bjorken limit the coupling vanishes altogether, and hence QCD becomes very similar to the parton model.

However, it is not immediately clear how to apply perturbative techniques to the DIS cross section. For instance, even if one of the nucleon's quarks is struck by the high-energy electron and made asymptotically free, the rest of the nucleon — a mass of gluons and quarks — will still be dominated by low-energy degrees of freedom. Therefore, we can't simply apply the Feynman rules of QCD to this problem, since the amplitude still contains non-perturbative components.

Ideally, we would like to show that at large momentum scales the scattering amplitude can factorise; that is, to show that it can break up into its high-energy/short-distance component and low-energy/long-distance component:

$$\mathcal{M}_{\text{DIS}} = \mathcal{M}_{\text{short distance}} \times \mathcal{M}_{\text{long distance}}. \tag{3.26}$$

Then for an asymptotically free theory, the short distance component can be calculated in perturbation theory, allowing for the purely non-perturbative (i.e. interesting) part of the amplitude to be extracted. This is exactly what the OPE allows us to do.

3.2.1 The Compton Tensor

Before we apply the OPE to DIS and perform a perturbative calculation, we first need to recall that for perturbation theory to work, we need time-ordered operators. By contrast the hadronic tensor,

$$W^{\mu\nu} = \frac{1}{2}\sum_{\text{spin}} \int d^4z e^{iq\cdot z}\langle P|j^\mu(z)j^\nu(0)|P\rangle,$$

is not time-ordered. However, we can relate the hadronic tensor to a time-ordered operator through the optical theorem[§]:

$$2\text{Im}\mathcal{M}(A\to A) = \sum_X \int \frac{d^2p_X}{(2\pi)^3}\frac{1}{2P_X^0}(2\pi)^4\delta^{(4)}(p_A - p_X)|\mathcal{M}(A\to X)|^2. \tag{3.27}$$

Note that this only works for inclusive processes, where there is a sum over the final states.

Therefore, if we define the forward Compton tensor as

$$T^{\mu\nu} \equiv i\int d^4z e^{iq\cdot z}\langle P|T[j^\mu(z)j^\nu(0)]|P\rangle, \tag{3.28}$$

the optical theorem implies

$$2\text{Im}T^{\mu\nu} = W^{\mu\nu}. \tag{3.29}$$

It is then convenient to use the translational invariance of the current operators to re-express Eq. 3.28 as

$$T^{\mu\nu} = i\int d^4z e^{iq\cdot z}\langle P|T[j^\mu(z/2)j^\nu(-z/2)]|P\rangle. \tag{3.30}$$

Note that from now on, we will suppress the spin averaging; nonetheless we are only interested in the spin averaged Compton tensor. The Feynman diagram for the Compton tensor is given in figure 3.4.

Unlike the hadronic tensor, the Compton tensor satisfies the crossing symmetry:

$$T^{\mu\nu}(P,q) = T^{\nu\mu}(P,-q), \tag{3.31}$$

and therefore the physical range of its ω variable is $|\omega| \geq 1$ and for x, $|x| \leq 1$. Since the hadronic tensor has the decomposition given in Eq. 3.11, the Compton tensor similarly has the decomposition:

$$T^{\mu\nu} = T_1(x,Q^2)\left(-g^{\mu\nu} + \frac{q^\mu q^\nu}{q^2}\right) + \frac{T_2(x,Q^2)}{P\cdot q}\left(P^\mu - \frac{P\cdot q}{q^2}q^\mu\right)\left(P^\nu - \frac{P\cdot q}{q^2}q^\nu\right), \tag{3.32}$$

where $T_{1,2}$ are the Compton form factors. From the optical theorem (Eq. 3.29), these can be related to the hadronic structure functions by

$$2\text{Im}\big\{T_i(x,Q^2)\big\} = F_i(x,Q^2), \quad \text{for } i = 1,2. \tag{3.33}$$

[§]The field theory optical theorem, just as in the quantum mechanical case, follows from the unitarity of the S-matrix; derivations can be found in most QFT textbooks [29, 30].

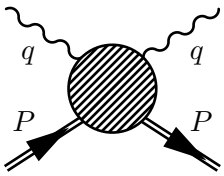

Figure 3.4: The Feynman diagram for forward $N\gamma \to N\gamma$ scattering.

Now we are ready to perform the OPE on the Compton tensor.

3.2.2 Wilson's Operator Product Expansion

For two operators, A and B, Wilson [39] conjectured the following relationship:

$$A(z)B(0) \xrightarrow{z\to 0} \sum_i c_i(z)\mathcal{O}_i(0). \tag{3.34}$$

The c_i are complex-valued functions called 'Wilson coefficients'; at least some of these will be singular as $z^\mu \to 0$, and moreover they are arranged by the strength of their singularity, with c_0 having the greatest divergence. The operators $\mathcal{O}_i(0)$ are local and regular (not divergent). Or, equivalently in momentum space:

$$\int d^4z e^{iq\cdot z} A(z)B(0) \xrightarrow{q\to 0} \sum_i \tilde{c}_i(q)\tilde{\mathcal{O}}_i(0). \tag{3.35}$$

Note that the momentum space coefficients $\tilde{c}_i(q)$ may not be singular. Equations 3.34 and 3.35 are operator product expansions.

Immediately, we can see that if an OPE could be performed on the Compton tensor, factorisation would follow. For instance, in the matrix element of the OPE,

$$\int d^4z e^{iq\cdot z} \langle \text{out}|A(z)B(0)|\text{in}\rangle \xrightarrow{q\to 0} \sum_i \tilde{c}_i(q)\langle \text{out}|\tilde{\mathcal{O}}_i(0)|\text{in}\rangle, \tag{3.36}$$

the local operators are not sensitive to the large momentum transfer q and hence their matrix elements contain low-energy (long-distance) information, which relates to the non-perturbative strucutre of the hadron. On the other hand, the Wilson coefficients are entirely dependent on the large momentum transfer, and therefore parameterise the high-energy (short-distance) part of the matrix element. Therefore, in an asymptotically free theory, the Wilson coefficients can be calculated perturbatively, while the local operators can not. This is the desired property of factorisation we mentioned previously.

Validity of the OPE

The OPE statement (Eq. 3.34) was first proven by Zimmermann [40]. This and all subsequent proofs are in renormalised perturbation theory; that is, where the entire matrix element can be calculated perturbatively. By contrast, many applications of the OPE, including its application to DIS, are for matrix elements that contain non-perturbative components. The main difficulty in a non-perturbative proof of the OPE is that one cannot preclude infinite oscillations in the matrix element of the operator product as $z \to 0$.

However, once these oscillations are assumed to vanish, a non-perturbative proof is possible [41, 42].

In the case of DIS, the OPE has been very successful at providing a theoretical framework for describing experiment, and it is this property, not a rigorous mathematical proof, that speaks for its validity. More advanced justifications of the OPE and its application to different non-perturbative processes can be found in, for instance, Ref. [43].

Moreover, the OPE as it is proven in perturbation theory is best understood as a Euclidean relation [28]: it is true in the short-distance limit, taking all the components of $z^\mu \to 0$, rather than the Minkowski product $z^2 \to 0$. Similarly, it is in the limit of 'large Euclidean momentum' (see the next paragraph) that relations like Eq. 3.35 hold in perturbation theory. Even for non-perturbative physics, the OPE is still thought of as a Euclidean relation [43–45]. Therefore, it has a natural correspondence with lattice calculations, as we will see.

Large Euclidean Momentum

In momentum space, the OPE applies for large Euclidean momentum. In general, this means that momentum scalars have values that are accessible in Euclidean space, but does not necessarily mean we need to perform our calculations in Euclidean space [14, 28, 31]. For the case of DIS, we have in Euclidean kinematics

$$\omega = \frac{2P \cdot q}{Q^2} \sim \frac{|P|}{|q|}. \tag{3.37}$$

Therefore, we can't access the Bjorken limit $Q^2 \to \infty$ and ω fixed without making target mass corrections $|P|/|q|$ blow up. If we allow our target mass corrections to blow up, we would spoil any possibility of relating our results back to the physical light-cone limit.

Instead, we take the large Euclidean momentum limit:

$$Q^2 \to \infty, \quad \omega \sim 0. \tag{3.38}$$

This is also evident from our discussion of light-cone dominance (recall figure 3.2), where we saw that the individual components of the current separation go like $|z^\mu| \lesssim \frac{\omega}{M}$, and hence as we take $\omega \to 0$, we get the short-distance limit $|z^\mu| \to 0$. Therefore, the limit of large Euclidean momentum, whether in Euclidean or Minkowski space, picks out the short distance limit.

However, because we ultimately wish to analytically continue this expression back to the Minkowski region where $|\omega| \geq 1$, we keep terms of all powers of ω but throw away target mass corrections such as P^2/Q^2, even though in Euclidean kinematics these are of approximately the same order.

Finally, for the purposes of this thesis, the fact that the OPE uses Euclidean kinematics makes it very useful to compare to the lattice calculation, which also uses the Euclidean signature.

3.2.3 Operator Product Expansion for DIS

The method for doing a more rigorous and complete OPE is outlined in appendix B. However, in this section we will simply expand the Compton tensor in the Bjorken limit: at

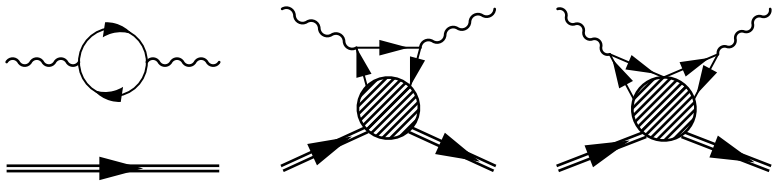

Figure 3.5: Feynman diagrams corresponding to terms in Eq. 3.40: the trace term (left), the two terms with a single contraction (center), the term with no contraction (right).

$\alpha_S = 0$, the free field approximation. Our results are equivalent to the OPE from appendix B for the leading-order basis of operators with their corresponding Wilson coefficients taken to leading-order, too.

Free Field Approximation

To begin, note that the current product is

$$T[j^\mu(z)j^\nu(y)] = \sum_f e_f^2 T[\bar\psi_f(z)\gamma^\mu\psi_f(z)\bar\psi_f(y)\gamma^\nu\psi_f(y)]. \tag{3.39}$$

Since we take $\alpha_S = 0$ and hence the fields in Eq. 3.39 as free, we can apply Wick's theorem:

$$\begin{aligned} T\big[\bar\psi_f(z)\gamma^\mu\psi_f(z)\bar\psi_f(y)\gamma^\nu\psi_f(y)\big] &= -\,\mathrm{trace}[\gamma^\mu\overbrace{\psi_f(z)\bar\psi_f}(y)\gamma^\nu\overbrace{\psi(y)_f\bar\psi_f}(z)] \\ &+ :\bar\psi_f(z)\gamma^\mu\overbrace{\psi_f(z)\bar\psi_f}(y)\gamma^\nu\psi_f(y): + :\overbrace{\bar\psi_f(z)\gamma^\mu\psi_f(z)\bar\psi_f(y)\gamma^\nu\psi_f}(y): \\ &+ :\bar\psi_f(z)\gamma^\mu\psi_f(z)\bar\psi_f(y)\gamma^\nu\psi_f(y):, \end{aligned} \tag{3.40}$$

where the contractions yield free quark propagators, $S_F(z-y)$, which are singular both in the limit that $z \to y$ and $(z-y)^2 \to 0$ [14].

Therefore, in the short-distance limit $z \to y$, the trace term will be the most singular of Eq. 3.40, the second two terms less singular. The last term corresponds to a power-suppressed cat's ears diagram (See Figure 3.5). We are only interested in the most singular terms. Therefore, we can ignore the cat's ears term. Further, the trace term (vacuum polarisation) doesn't contribute to the scattering process, so we ignore this term too. This leaves us with the two terms that have only one propagator each: the 'handbag' terms.

Coordinate Space OPE

So the relevant part of the free current product are the handbag terms from Eq. 3.40:

$$\begin{aligned} T[j^\mu(z/2)j^\nu(-z/2)] = \sum_f e_f^2\big(&:\bar\psi_f(z/2)\gamma^\mu\overbrace{\psi_f(z/2)\bar\psi_f}(-z/2)\gamma^\nu\psi_f(-z/2): \\ &+ :\overbrace{\bar\psi_f(z/2)\gamma^\mu\psi_f(z/2)\bar\psi_f(-z/2)\gamma^\nu\psi_f}(-z/2):\big). \end{aligned} \tag{3.41}$$

With some manipulation this becomes

$$\begin{aligned} &T[j^\mu(z/2)j^\nu(-z/2)] = \\ &\quad\sum_f e_f^2\big(:\bar\psi_f(z/2)\gamma^\mu S_F(z)\gamma^\nu\psi_f(-z/2): + :\bar\psi_f(-z/2)\gamma^\nu S_F(-z)\gamma^\mu\psi_f(z/2):\big). \end{aligned} \tag{3.42}$$

The free fermion propagator in coordinate space is

$$S_F(z-y) = \frac{i}{2\pi^2}\frac{(z-y)^\alpha \gamma_\alpha}{((z-y)^2 - i\epsilon)^2} + \text{less singular terms}, \tag{3.43}$$

where we will ignore the less singular terms. Therefore, for our present purposes, it is useful to define the reduced propagator:

$$S^\mu(z) \equiv \frac{i}{2\pi^2}\frac{(z-y)^\mu}{((z-y)^2 - i\epsilon)^2} \quad \Rightarrow \quad \gamma_\mu S^\mu(z) = S_F(z). \tag{3.44}$$

Therefore,

$$\begin{aligned} &T[j_\mu(z/2)j_\nu(-z/2)] = \\ &\quad \sum_f e_f^2 S^\rho(z)\big(: \bar\psi_f(z/2)\gamma_\mu\gamma_\rho\gamma_\nu\psi_f(-z/2) - \bar\psi_f(-z/2)\gamma_\nu\gamma_\rho\gamma_\mu\psi_f(z/2) : \big). \end{aligned} \tag{3.45}$$

From Dirac algebra $\gamma_\mu\gamma_\rho\gamma_\nu = g_{\mu\rho}\gamma_\nu + g_{\rho\nu}\gamma_\mu - g_{\mu\nu}\gamma_\rho + i\epsilon_{\mu\rho\nu\kappa}\gamma^\kappa\gamma^5 = (\mathcal{S}_{\mu\rho\nu\kappa} + i\epsilon_{\mu\rho\nu\kappa}\gamma^5)\gamma^\kappa$, where we denote $\mathcal{S}_{\mu\rho\nu\kappa} = g_{\mu\rho}g_{\nu\kappa} + g_{\mu\kappa}g_{\nu\rho} - g_{\mu\nu}g_{\rho\kappa}$. Substituting this into Eq. 3.45, we get

$$\begin{aligned} T[j_\mu(z/2)j_\nu(-z/2)] &= \sum_f e_f^2 S^\rho(z)\big(: \bar\psi_f(z/2)(\mathcal{S}_{\mu\rho\nu\kappa} + i\epsilon_{\mu\rho\nu\kappa}\gamma^5)\gamma^\kappa\psi_f(-z/2) \\ &\quad - \bar\psi_f(-z/2)(\sigma_{\nu\rho\mu\kappa} + i\epsilon_{\nu\rho\mu\kappa}\gamma^5)\gamma^\kappa\psi_f(z/2) : \big) \\ &= \sum_f e_f^2 S^\rho(z)\big(\mathcal{S}_{\mu\rho\nu\kappa} : \bar\psi_f(z/2)\gamma^\kappa\psi_f(-z/2) - \bar\psi_f(-z/2)\gamma^\kappa\psi_f(z/2) : \\ &\quad - i\epsilon_{\mu\rho\nu\kappa} : \bar\psi_f(z/2)\gamma^\kappa\gamma^5\psi_f(-z/2) + \bar\psi_f(-z/2)\gamma^\kappa\gamma^5\psi_f(z/2) : \big), \end{aligned} \tag{3.46}$$

by symmetry properties of $\mathcal{S}_{\mu\rho\nu\kappa}$ and $\epsilon_{\mu\rho\nu\kappa}$, and the anti-commutation of γ^5 and γ^μ.

We can now Taylor expand the Dirac bilinears $\bar\psi_f(z/2)\gamma^\mu\psi_f(-z/2)$ and $\bar\psi_f(z/2)\gamma^\mu\psi_f(-z/2)$, since the singular part of the operator has been factored out. Doing so, we get

$$\bar\psi_f(-z/2)\gamma^\mu\psi_f(z/2) = \sum_{n=0}^{\infty}\frac{1}{n!}z_{\mu_1}...z_{\mu_n}\Big(\bar\psi_f(X)\gamma^\mu \overset{\leftrightarrow}{D}{}^{\mu_1}...\overset{\leftrightarrow}{D}{}^{\mu_n}\psi(X)\Big)\big|_{X=0}, \tag{3.47}$$

where $\overset{\leftrightarrow}{D} = (\vec{D} - \overleftarrow{D})/2$, for D the covariant derivative. The appearance of the covariant derivatives instead of the regular partial derivatives is due to the Wilson line, which we chose to suppress earlier.

Now notice that any terms in the operator in Eq. 3.47 that are proportional to $g^{\mu_i\mu_j}$ (traces) will contract with the z vectors to give z^2, thereby reducing the power of the singularity. Hence, to get the leading (in terms of the strength of the singularity) term of Eq. 3.47, we must subtract the traces.

Moreover, each of the derivative terms in Eq. 3.47 is contracted with $z_{\mu_1}...z_{\mu_n}$, a totally symmetric tensor. Therefore, the indices of the covariant derivatives are totally symmetrised. Moreover, it can be shown, by considering the further contractions of Lorentz indices in Eq. 3.46, and the restriction of current conservation, that all the Lorentz indices of the operator in Eq. 3.47 must be symmetrised.

Therefore, the component of Eq. 3.47 that is leading-order is

$$\bar{\psi}_f(-z/2)\gamma^\mu\psi_f(z/2) = \sum_{n=0}^{\infty}\frac{1}{n!}z_{\mu_1}...z_{\mu_n}\Big(\bar{\psi}_f(X)\gamma^{\{\mu}\overset{\leftrightarrow}{D}^{\mu_1}...\overset{\leftrightarrow}{D}^{\mu_n\}}\psi(X) - \text{traces}\Big)\big|_{X=0}. \quad (3.48)$$

See appendix A for our symmetrisation convention. Following the above Taylor expansion it is easy to see that

$$\bar{\psi}_f(z/2)\gamma^\mu\psi_f(-z/2) = \sum_{n=0}^{\infty}\frac{(-1)^n}{n!}z_{\mu_1}...z_{\mu_n}\Big(\bar{\psi}_f(X)\gamma^{\{\mu}\overset{\leftrightarrow}{D}^{\mu_1}...\overset{\leftrightarrow}{D}^{\mu_n\}}\psi(X) - \text{traces}\Big)\big|_{X=0}. \quad (3.49)$$

The expansion of the polarised terms is identical except for the inclusion of a γ^5 matrix.

We have, therefore, arrived at the basis of leading-order local quark operators (vector and axial vector, respectively):

$$\mathcal{O}_f^{(n)\mu_1...\mu_n}(X) = \bar{\psi}_f(X)\gamma^{\{\mu_1}i\overset{\leftrightarrow}{D}^{\mu_2}...i\overset{\leftrightarrow}{D}^{\mu_n\}}\psi_f(X) - \text{traces}, \quad (3.50)$$

$$\tilde{\mathcal{O}}_f^{(n)\mu_1...\mu_n}(X) = \bar{\psi}_f(X)\gamma^{\{\mu_1}\gamma^5 i\overset{\leftrightarrow}{D}^{\mu_2}...i\overset{\leftrightarrow}{D}^{\mu_n\}}\psi_f(X) - \text{traces}. \quad (3.51)$$

Note that in the standard jargon of the OPE these operators are referred to as *twist-two* operators. For more explanation of this terminology see appendix B, but for our purposes all we need note is that 'twist-two', 'leading-order' and 'leading-twist' may be used interchangeably to refer to the term that is leading-order as $|z^\mu| \to 0$ or as $Q^2 \to \infty$. Moreover, we will suppress the dependence on X of the above operators.

Then the bilinears become

$$:\bar{\psi}_f(z/2)\gamma^\mu\psi_f(-z/2) - \bar{\psi}_f(-z/2)\gamma^\mu\psi_f(z/2): \\ = -2\sum_{n=1,3,5}^{\infty}\frac{(-i)^n}{n!}z_{\mu_1}...z_{\mu_n}\mathcal{O}_f^{(n+1)\mu\mu_1...\mu_n}(0), \quad (3.52)$$

$$:\bar{\psi}_f(z/2)\gamma^\mu\gamma^5\psi_f(-z/2) + \bar{\psi}_f(-z/2)\gamma^\mu\gamma^5\psi_f(z/2): \\ = -2\sum_{n=0,2,4}^{\infty}\frac{(-i)^n}{n!}z_{\mu_1}...z_{\mu_n}\tilde{\mathcal{O}}_f^{(n+1)\mu\mu_1...\mu_n}(0). \quad (3.53)$$

Therefore, the current product is

$$T[j_\mu(z/2)j_\nu(-z/2)] = -2\sum_f e_f^2 S^\rho(z)\Big\{\mathcal{S}_{\mu\rho\nu\kappa}\sum_{n=1,3,5}^{\infty}\frac{(-i)^n}{n!}z_{\mu_1}...z_{\mu_n}\mathcal{O}_f^{(n+1)\kappa\mu_1...\mu_n} \\ - i\epsilon_{\mu\rho\nu\kappa}\sum_{n=0,2,4}^{\infty}\frac{(-i)^n}{n!}z_{\mu_1}...z_{\mu_n}\tilde{\mathcal{O}}_f^{(n+1)\kappa\mu_1...\mu_n}\Big\}. \quad (3.54)$$

For the rest of this thesis, we will focus on the symmetric part of Eq. 3.54 and the unpolarised operators:

$$\begin{aligned} T[j_\mu(z/2)j_\nu(-z/2)]_{\text{symm}} = &-2\sum_f e_f^2 S^\rho(z) \\ &\times \Big\{\mathcal{S}_{\mu\rho\nu\kappa}\sum_{n=1,3,5}^{\infty}\frac{(-i)^n}{n!}z_{\mu_1}...z_{\mu_n}\mathcal{O}_f^{(n+1)\kappa\mu_1...\mu_n}\Big\}. \end{aligned} \tag{3.55}$$

The forward matrix element of Eq. 3.55 is therefore

$$\begin{aligned} \langle P|T[j_\mu(z/2)j_\nu(-z/2)]_{\text{symm}}|P\rangle = &-2\sum_f e_f^2 S^\rho(z) \\ &\times \Big\{\mathcal{S}_{\mu\rho\nu\kappa}\sum_{n=1,3,5}^{\infty}\frac{(-i)^n}{n!}z_{\mu_1}...z_{\mu_n}\langle P|\mathcal{O}_f^{(n+1)\kappa\mu_1...\mu_n}|P\rangle\Big\}. \end{aligned} \tag{3.56}$$

Then, from Lorentz symmetry, we have that

$$\langle P|\mathcal{O}_f^{(n)\mu_1...\mu_n}|P\rangle = a_n^f P^{\mu_1}...P^{\mu_n}, \tag{3.57}$$

where a_n^f is a Lorentz scalar. Therefore, Eq. 3.56 becomes

$$\langle P|T[j_\mu(z/2)j_\nu(-z/2)]_{\text{symm}}|P\rangle = -2\sum_f e_f^2 S^\rho(z)\Big\{\mathcal{S}_{\mu\rho\nu\kappa}\sum_{n=1,3,5}^{\infty}\frac{(-i)^n}{n!}(P\cdot z)^n a_n^f\Big\}. \tag{3.58}$$

Fourier Transform

Inserting Eq. 3.54 into the expression for the Compton tensor (Eq. 3.30), we get that the leading-order Compton tensor is

$$T_{\mu\nu} = -2i\sum_f e_f^2\int d^4z e^{iq\cdot z}S^\rho(z)\mathcal{S}_{\mu\rho\nu\kappa}P^\kappa\sum_{n=1,3,5}^{\infty}\frac{(-i)^n}{n!}(P\cdot z)^n a_{n+1}^f. \tag{3.59}$$

A useful identity from distribution theory [46] is

$$\int_a^b dx\mathcal{F}(x)\frac{\partial^n}{\partial x^n}\delta(x-y) = (-1)^n\frac{\partial^n}{\partial x^n}\mathcal{F}(x)\Big|_{x=y} \quad y\in(a,b). \tag{3.60}$$

Hence we have that

$$(P\cdot z)^n = i^n\int d\chi e^{i\chi P\cdot z}\frac{\partial^n}{\partial\chi^n}\delta(\chi). \tag{3.61}$$

So, inserting Eq. 3.61 into the Compton tensor we get

$$T_{\mu\nu} = -2i\sum_f e_f^2\mathcal{S}_{\mu\rho\nu\kappa}P^\kappa\sum_{n=1,3,5}^{\infty}\frac{1}{n!}a_{n+1}^f\int d\chi\frac{\partial^n}{\partial\chi^n}\delta(\chi)\int d^4z e^{i(q+\chi P)\cdot z}S^\rho(z). \tag{3.62}$$

Now, Fourier expanding the reduced propagator, we get

$$\begin{aligned}\int d^4z e^{i(q+\chi P)\cdot z} S^\mu(z) &= \frac{i(q^\mu+\chi P^\mu)}{(q+\chi P)^2} = \frac{i(q^\mu+\chi P^\mu)}{\chi^2 P^2 + 2\chi P\cdot q - Q^2} \\ &= \frac{i(q^\mu+\chi P^\mu)}{\chi^2 P^2 + 2\chi P\cdot q - Q^2} = -\frac{1}{Q^2}\frac{i(q^\mu+\chi P^\mu)}{1-2\chi P\cdot q/Q^2}.\end{aligned} \tag{3.63}$$

Note that, by Eq. 3.60, we have

$$\begin{aligned}&\int d\chi \frac{\partial^n}{\partial\chi^n}\delta(\chi)\int d^4z e^{i(q+\chi P)\cdot z} S^\rho(z) \\ &\qquad = -\int d\chi \frac{\partial^n}{\partial\chi^n}\delta(\chi)\frac{1}{Q^2}\frac{i(q^\mu+\chi P^\mu)}{1-2\chi P\cdot q/Q^2} \\ &\qquad = (-1)^{n+1}\frac{i}{Q^2}\frac{\partial^n}{\partial\chi^n}(q^\rho+\chi P^\rho)\sum_{k=0}^{\infty}\chi^k\Big(\frac{2P\cdot q}{Q^2}\Big)^k\Big|_{\chi=0} \\ &\qquad = (-1)^{n+1}\frac{i}{Q^2}\sum_{k=0}^{\infty}(\delta_{k,n}k!q^\rho + \delta_{k+1,n}(k+1)!P^\rho)\omega^k,\end{aligned} \tag{3.64}$$

where we can Taylor expanded around $\chi = 0$, since this is where the derivative is evaluated. Inserting Eq. 3.64 back into Eq. 3.62, we get

$$\begin{aligned}T_{\mu\nu} &= -\frac{2}{Q^2}\sum_f e_f^2 \mathcal{S}_{\mu\rho\nu\kappa}P^\kappa \sum_{n=1,3,5}^{\infty} a_{n+1}^f \frac{(-1)^n}{n!}\sum_{k=0}^{\infty}(\delta_{k,n}k!q^\rho + \delta_{k+1,n}(k+1)!P^\rho)\omega^k \\ &= \frac{2}{Q^2}\sum_f e_f^2 \mathcal{S}_{\mu\rho\nu\kappa}P^\kappa \sum_{n=1,3,5}^{\infty} a_{n+1}^f \omega^{n-1}(\omega q^\rho + P^\rho).\end{aligned} \tag{3.65}$$

Then, recalling that $\mathcal{S}_{\mu\rho\nu\kappa} = g_{\mu\rho}g_{\nu\kappa} + g_{\mu\kappa}g_{\nu\rho} - g_{\mu\nu}g_{\rho\kappa}$, we get

$$\begin{aligned}T^{\mu\nu} &= \frac{2}{Q^2}\sum_f e_f^2 \sum_{n=1,3,5}^{\infty} a_{n+1}^f \omega^{n-1}\Big(\omega(P_\mu q_\nu + P_\nu q_\mu) + 2P_\mu P_\nu - \omega P\cdot q g_{\mu\nu}\Big) \\ &= \sum_f e_f^2 \sum_{n=2,4,6}^{\infty} a_n^f \omega^n\left(\frac{P_\mu q_\nu + P_\nu q_\mu}{P\cdot q} + \frac{Q^2}{(P\cdot q)^2}P_\mu P_\nu - g_{\mu\nu}\right).\end{aligned} \tag{3.66}$$

So, as in the parton model, we recover the Bjorken scaling prediction and the Callan-Gross relation.

If all we wanted to do was compare to a lattice simulation, Eq. 3.66 would be sufficient, since it matches on to the Euclidean kinematics of the lattice, where $\omega \sim 0$. However, to relate this to the physical Minkowski region, we need a way to connect Eq. 3.66 to the Compton tensor for the physical region $|\omega| \geq 1$.

3.2.4 Dispersion Relation

First, recall the definition of $T_1(x, Q^2)$ and $T_2(x, Q^2)$ in Eq. 3.32. So, from Eq. 3.66, we have that

$$T_1(x, Q^2) = \sum_f e_f^2 \sum_{n=2,4,6}^{\infty} a_n^f \omega^n, \quad T_2(x, Q^2) = 2x \sum_f e_f^2 \sum_{n=2,4,6}^{\infty} a_n^f \omega^n, \tag{3.67}$$

for $Q^2 \to \infty$ and $\omega \sim 0$. Then, recall that the hadronic tensor structure functions F_i are related to T_i by $2\text{Im}\{T_i(x, Q^2)\} = F_i(x, Q^2)$. Comparing the OPE and parton model (Eq. 3.24) structure functions have that

$$\frac{1}{\pi}\text{Im}\left\{ \sum_{n=2,4,6}^{\infty} a_n^f \omega^n \right\} = q_f(x) + \bar{q}_f(x), \tag{3.68}$$

which is our first connection between fundamental QCD and partonic physics. However, Eq. 3.68 is not exactly what we want: it is in the region of $\omega \to 0$ and hence $x \to \infty$. Instead, we would like to find a way to relate this to our physical region.

Leading Order Dispersion Relation

To start, we use the property of analytic continuity, which is a fundamental assumption of QFT: we extend the variable ω to the complex plane. For convenience, define $T_1^f(\omega)$ as the contribution to the Compton form factor for one flavour of quark. Then, if we take a contour $\mathcal{C}_1$, that is a small closed loop around the origin, by Cauchy's theorem

$$\frac{1}{2\pi i} \oint_{\mathcal{C}_1} d\omega \frac{T_1^f(\omega)}{\omega^{N+1}} = \frac{1}{2\pi i} \sum_{n=2,4,6}^{\infty} \oint_{\mathcal{C}_1} d\omega \frac{a_n^f \omega^n}{\omega^{N+1}} = a_N^f, \tag{3.69}$$

where N is some even integer ≥ 2. Equation 3.69 follows from the fact that the integral of a complex contour enclosing the Laurent series $\sum_n z^{-n}$ only picks out the z^{-1} term.

The Compton tensor has discontinuities along the real axis for $|\omega| \geq 1$ (see figure 3.6). We show how to determine the cuts in the complex plane for the Compton tensor in appendix C. More details can be found in section 6.3.

We can deform $\mathcal{C}_1$ to $\mathcal{C}_2$, the contour given in Figure 3.6. We assume that the parts of the contour near the real axis are an infinitesimal distance ϵ away from it. Hence

$$\frac{1}{2\pi i} \oint_{\mathcal{C}_1} d\omega \frac{T_1^f(\omega)}{\omega^{N+1}} = \frac{1}{2\pi i} \left[\int_1^{\infty} d\omega + \int_{-\infty}^{-1} d\omega \right] \frac{T_1^f(\omega + i\epsilon) - T_1^f(\omega - i\epsilon)}{\omega^{N+1}} + \text{arc contributions}. \tag{3.70}$$

Here, we will assume that the contributions from the arcs vanish. Note that by the Schwarz reflection principle [47], we have that $T_1^f(\omega) = [T_1^f(\omega^*)]^*$, and hence

$$T_1^f(\omega + i\epsilon) - T_1^f(\omega - i\epsilon) = 2i\text{Im}[T^f(\omega + i\epsilon)] = iF_1^f(\omega + i\epsilon).$$

From now on, we will suppress the infinitesimal ϵ.

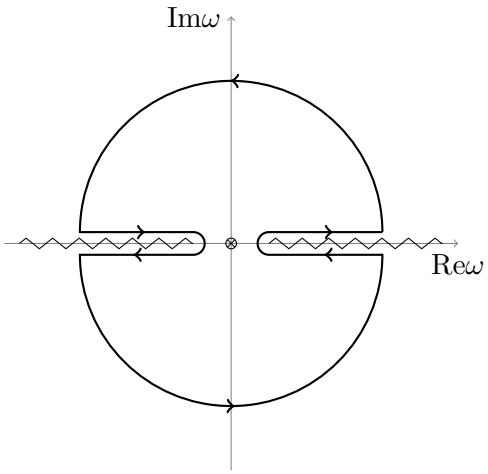

Figure 3.6: Contour $\mathcal{C}_2$ and the discontinuities of the Compton tensor.

Therefore, Eq. 3.70 becomes

$$\begin{aligned}\frac{1}{2\pi i}\oint_{\mathcal{C}_1} d\omega \frac{T_1^f(\omega)}{\omega^{N+1}} &= \frac{1}{2\pi}\left[\int_1^\infty d\omega + \int_{-\infty}^{-1} d\omega\right]\frac{F_1^f(\omega)}{\omega^{N+1}}. \\ &= \frac{1}{2\pi}\int_{-1}^{1} dx x^{N-1} F_1^f(x) = \int_{-1}^{1} dx x^{N-1}(q_f(x)+\bar{q}_f(x)).\end{aligned} \tag{3.71}$$

Comparing Eqs. 3.69 and 3.71, we have

$$\int_{-1}^{1} dx x^{n-1}(q_f(x)+\bar{q}_f(x)) = a_n^f. \tag{3.72}$$

Using symmetry properties of PDFs, we note that $q_f(x) = -\bar{q}_f(-x)$. Therefore, it is simple to show that Eq. 3.72 implies

$$2\int_{-1}^{1} dx x^{n-1} q_f(x) = a_n^f, \tag{3.73}$$

and

$$2\int_{0}^{1} dx x^{n-1}(q_f(x)+\bar{q}_f(x)) = a_n^f. \tag{3.74}$$

Therefore, for instance, $\frac{1}{2}a_2^f$ gives the fraction of the nucleon's total momentum contributed quarks of flavour f and their anti-quarks**.

In general we define the n^{th} *Mellin moment* M_n of a function $f(x)$ as

$$M_n \equiv \int_{-1}^{1} dx x^{n-1} f(x) \tag{3.75}$$

Equation 3.73 completes our connection between local parton distribution functions and a basis of *local* operators (Eq. 3.50). In the next section, we will show the connection

**Note that it is more common [29,30] to see the notation $\langle P|\mathcal{O}_f^{(n)\mu_1\cdots\mu_n}|P\rangle = 2a_n^f P^{\mu_1}...P^{\mu_n}$, which differs from our definition (Eq. 3.57) by a factor of 1/2.

between PDFs and *non-local* light-cone operators. This is desired, since it short-cuts the complicated relationship between local operators and PDFs.

3.3 Light-Cone Operators

Parton distribution functions $q_f(x)$ were introduced as the probability density of finding a proton constituent with flavour f and momentum xP. Probability densities in quantum mechanics are always interpreted as the mod squared of some state function. Therefore, we should be able to write

$$q_f(x) = \int \frac{d^4p_X}{(2\pi)^4} \sum_X |\langle X|\psi_f|P\rangle|^2 \delta(xP - p) = \langle P|\psi_f^\dagger \psi_f|P\rangle \delta(xP - p), \tag{3.76}$$

where p is the parton momentum.

However, as we saw in the parton model section, it's not that $p^\mu = xP^\mu$, but rather that the components of p^μ transverse to the nucleon's momentum were taken to be very small compared to the components parallel to the nucleon's momentum. Obviously, this is not true in all frames — in the nucleon's rest frame, for instance.

Therefore, we start by choosing to work in the *centre of mass frame*, where $q^\mu = (0, 0, 0, Q)$. In this frame, the nucleon momentum must be $P^\mu = (E, P^1, P^2, -\frac{P\cdot q}{Q})$. Since $P \cdot q \sim Q^2$ in the Bjorken limit, $P \cdot q/Q \sim Q$, which goes to infinity. Then, noting that $E = \sqrt{\mathbf{P}^2 + M^2} \simeq \sqrt{Q^2 + M^2} \approx Q$, we have that $P^\mu \simeq (E, 0, 0, -E)$, a lightlike vector in this frame.

Since our nucleon momentum is lightlike, it is convenient to project all the vector quantities into light-cone coordinates with two light-cone vectors: $a^\mu = \Lambda(1, 0, 0, 1)$ and $\bar{a}^\mu = (1, 0, 0, -1)/(2\Lambda)$, for Λ a parameter set so that $a \cdot P = 1$. Hence $P^\mu = \bar{a}^\mu + (M^2/2)a^\mu$ (see appendix D).

Therefore, the relationship between the parton and nucleon momentum becomes $p \cdot a = xP \cdot a$. So, we can make Eq. 3.76 a precise relation:

$$q_f(x) = \int \frac{d^4p_X}{(2\pi)^4} \sum_X |\langle X|\psi_f|P\rangle|^2 \delta(p \cdot a - xP \cdot a), \tag{3.77}$$

where the above equation describes a nucleon splitting into one constituent parton of momentum p, and the left-over parts of the nucleon X with momentum p_X. So we have the momentum conservation $P = p + p_X$, which we can insert as a momentum conserving delta function into Eq. 3.77:

$$\begin{aligned} q_f(x) &= \int \frac{d^4p}{(2\pi)^4} \int \frac{d^4p_X}{(2\pi)^4} \sum_X (2\pi)^4 \delta^{(4)}(p + p_X - P) |\langle X|\psi_f|P\rangle|^2 \delta(p \cdot a - xP \cdot a) \\ &= \int \frac{d^4p_X}{(2\pi)^4} \sum_X |\langle X|\psi_f|P\rangle|^2 \delta((P - p_X) \cdot a - xP \cdot a) \\ &= \int \frac{d^4p_X}{(2\pi)^4} \int \frac{d\lambda}{2\pi} \sum_X \langle P|\psi_f^\dagger(0)|X\rangle\langle X|\psi_f(0)|P\rangle e^{-i\lambda a\cdot(P - xP - p_X)}, \end{aligned} \tag{3.78}$$

where we have introduced some parameter λ, the Fourier conjugate of $a \cdot (P - xP - p_X)$. Then, using translational invariance, Eq. 3.78 becomes

$$\begin{aligned} q_f(x) &= \int \frac{d^4p_X}{(2\pi)^4} \int \frac{d\lambda}{2\pi} \sum_X \langle P|\psi_f^\dagger(-\lambda a/2)|X\rangle\langle X|\psi_f(\lambda a/2)|P\rangle e^{i\lambda x P\cdot a} \\ &= \int \frac{d\lambda}{2\pi} e^{i\lambda x}\langle P|\bar{\psi_f}(-\lambda a/2)\gamma^0\psi_f(\lambda a/2)|P\rangle, \end{aligned} \tag{3.79}$$

removing the complete set of states, and using the relations $(\gamma^0)^2 = \mathbb{I}$ and $P \cdot a = 1$. From the Dirac equation, we have that $0 = (\not{p} - m_f)\psi_f \approx \not{p}\psi_f \approx p \cdot \bar{a}\not{a}\psi_f$, using the fact that we neglect quark masses, and that most of the quark's momentum is in the $\bar{a}^\mu$ direction (i.e. in the same direction as the proton's momentum). So $\not{a}\psi_f \approx 0$, and therefore $\gamma^0\psi = -\mathbf{a}\cdot\gamma\psi$, implying that $2\gamma^0\psi = \not{a}\psi$[††]. Therefore, we have the final expression of a PDF in light-cone coordinates.

$$q_f(x) = \int \frac{d\lambda}{2\pi} e^{i\lambda x}\langle P|\bar{\psi_f}(-\lambda a/2)\frac{\not{a}}{2}\psi_f(\lambda a/2)|P\rangle. \tag{3.80}$$

More generally, we can introduce the non-local light-cone operator

$$\mathcal{O}^f_{\mathrm{LC}}(x) = \int \frac{d\lambda}{2\pi} e^{i\lambda x}\bar{\psi_f}(-\lambda a/2)\not{a}\psi_f(\lambda a/2). \tag{3.81}$$

So that we can simply write $q_f(x) = \frac{1}{2}\langle P|\mathcal{O}^f_{\mathrm{LC}}(x)|P\rangle$.

3.3.1 Correspondence Between Light-Cone and Local Operators

So far, we have managed to connect parton distributions to fundamental QCD through two very different formalisms: the local operators of section 3.2 and the light-cone operators of section 3.3. However, we should be able to connect these, since we stated in 3.2 that the matrix elements of the local operators were the Mellin moments of PDFs.

Therefore, from Eqs. 3.73 and 3.80, we have

$$a_{\mu_1}...a_{\mu_m}\langle P|\mathcal{O}_f^{(m)\mu_1...\mu_m}|P\rangle = \int_{-1}^{1} dx x^{m-1}\langle P|\mathcal{O}^f_{\mathrm{LC}}(x)|P\rangle. \tag{3.82}$$

In fact, we can show something more general. First, we Taylor expand along the light-cone to get

$$a_{\mu_1}\bar{\psi_f}(-\lambda a/2)\gamma^{\mu_1}\psi_f(\lambda a/2) = \sum_{k=0}^{\infty}\frac{\lambda^k}{k!}a_{\mu_1}...a_{\mu_{k+1}}\Big(\bar{\psi_f}(y)\gamma^{\mu_1}\overleftrightarrow{D}^{\mu_2}...\overleftrightarrow{D}^{\mu_{k+1}}\psi(y)\Big)\Big|_{y=0}. \tag{3.83}$$

Notice that any term in the operator on the LHS of Eq. 3.83 that are proportional to $g^{\mu_i\mu_j}$ (traces) will result in an $a^2 = 0$. Therefore, we can subtract off the traces without changing the overall expression. Moreover, the operator on the LHS of Eq. 3.83 is contracted with $a_{\mu_1}...a_{\mu_{k+1}}$, a totally symmetric tensor, which will kill off any anti-symmetric components

[††]To make the expression gauge invariant it is necessary to insert a Wilson line; however, as is commonly done, we will neglect this term by choosing light-cone gauge, $A \cdot a = 0$.

of this operator. Hence Eq. 3.83 becomes

$$\begin{aligned} a_{\mu_1}\bar{\psi}_f(-\lambda a/2)\gamma^{\mu_1}\psi_f(\lambda a/2) & \\ &= \sum_{k=0}^{\infty}\frac{\lambda^k}{k!}a_{\mu_1}...a_{\mu_{k+1}}\Big(\bar{\psi}_f(y)\gamma^{\{\mu_1}\overset{\leftrightarrow\mu_2}{D}...\overset{\leftrightarrow\mu_{k+1}\}}{D}\psi(y) - \text{traces}\Big)\Big|_{y=0} \\ &= \sum_{k=0}^{\infty}\frac{\lambda^k}{k!}(-i)^k a_{\mu_1}...a_{\mu_{k+1}}\mathcal{O}_f^{(k+1)\mu_1...\mu_{k+1}}, \end{aligned} \tag{3.84}$$

where we have used the definition of the local twist-two operators Eq. 3.50. Inserting this into the definition of the light-cone operators, Eq. 3.81, we get

$$\mathcal{O}^f_{\text{LC}}(x) = \int\frac{d\lambda}{2\pi}e^{i\lambda x}\sum_{k=0}^{\infty}\frac{\lambda^k}{k!}(-i)^k a_{\mu_1}...a_{\mu_{k+1}}\mathcal{O}_f^{(k+1)\mu_1...\mu_{k+1}}. \tag{3.85}$$

Then, the m^{th} moment is

$$\begin{aligned} &\int_{-1}^{1}dx x^{m-1}\int_{-\infty}^{\infty}\frac{d\lambda}{2\pi}e^{i\lambda x}\sum_{k=0}^{\infty}\frac{\lambda^k}{k!}(-i)^k a_{\mu_1}...a_{\mu_{k+1}}\mathcal{O}_f^{\mu_1...\mu_{k+1}} \\ &= \sum_{k=0}^{\infty}\frac{1}{k!}(-i)^k a_{\mu_1}...a_{\mu_{k+1}}\mathcal{O}_f^{\mu_1...\mu_{k+1}}\int_{-1}^{1}dx x^{m-1}\int_{-\infty}^{\infty}\frac{d\lambda}{2\pi}e^{i\lambda x}\lambda^k \\ &= \sum_{k=0}^{\infty}\frac{1}{k!}(-i)^k a_{\mu_1}...a_{\mu_{k+1}}\mathcal{O}_f^{\mu_1...\mu_{k+1}}\int_{-1}^{1}dx x^{m-1}(-i)^k\frac{\partial^k}{\partial x^k}\int_{-\infty}^{\infty}\frac{d\lambda}{2\pi}e^{i\lambda x} \\ &= \sum_{k=0}^{\infty}\frac{1}{k!}(-i)^k a_{\mu_1}...a_{\mu_{k+1}}\mathcal{O}_f^{\mu_1...\mu_{k+1}}\int_{-1}^{1}dx x^{m-1}(-i)^k\frac{\partial^k}{\partial x^k}\delta(x). \end{aligned} \tag{3.86}$$

Finally, using the identity in Eq. 3.60, we have

$$\int_{-1}^{1}dx x^{m-1}\frac{\partial^k}{\partial x^k}\delta(x) = (-1)^k\frac{\partial^k}{\partial x^k}x^{m-1}\Big|_{x=0} = \delta_{k,m-1}(-1)^k k! \tag{3.87}$$

So putting this back into Eq. 3.86, we get

$$\sum_{k=0}^{\infty}\frac{1}{k!}(-i)^k a_{\mu_1}...a_{\mu_{k+1}}\mathcal{O}_f^{\mu_1...\mu_{k+1}}(-i)^k(-1)^k k!\delta_{k,m-1} = a_{\mu_1}...a_{\mu_m}\mathcal{O}_f^{\mu_1...\mu_m}. \tag{3.88}$$

Therefore, we get the very nice result that

$$a_{\mu_1}...a_{\mu_m}\mathcal{O}_f^{\mu_1...\mu_m} = \int_{-1}^{1}dx x^{m-1}\mathcal{O}^f_{\text{LC}}(x). \tag{3.89}$$

This final result is a very neat way to short-cut the connection between non-local light-cone operators, which inherently are Minkowski space objects, and the local twist-two operators, which are related to the Euclidean Compton tensor. Therefore, as we will discuss in future chapters, this provides a way to calculate parton distribution related quantities in lattice QCD.

Chapter 4

Generalised Parton Distributions

For a long time, parton distribution functions (PDFs) and electromagnetic (EM) form factors (see appendix E) encompassed almost all there was to know about hadron structure. However, more recent research has uncovered the potential of a new class of hadronic observable, generalised parton distribtuions (GPDs)*, which contain an abundance of hitherto inaccessible physical information. As their name suggests, GPDs are generalisations of PDFs to kinematics where the outgoing parton (quark or gluon) has a different momentum to the incoming parton. Therefore, they do not have the standard probability interpretation that PDFs do. Moreover, GPDs can only be extracted from a class of hard, exlcusive†, off-forward scattering experiments, which are in some ways generalisations of deep inelastic scattering (DIS). The unifying feature of off-forward scattering processes is that they all involve a non-zero momentum transfer to the scattered hadron. And hence just like GPDs the incoming and outgoing hadronic states have different momenta.

While there were some early studies of off-forward processes, widespread interest in off-forward scattering began in the mid 1990s with a string of papers on GPDs [8,9,48,49]. Importantly, Ji [9] showed that the GPDs contained valuable information about the proton's spin structure, offering to resolve the decades-old 'proton spin crisis'. Moreover, it was proven [50] that the scattering amplitude of some off-forward processes do indeed factorise into a hard perturbative part and a non-perturbative component containing GPDs, making GPDs experimentally accessible.

Since then, it has been shown that GPDs and off-forward scattering contain more information about hadron structure. In particular, from the work of Burkardt [10], GPDs give access to the spatial distribution of partons in a hadron, in the plane transverse to the hadron's motion. More recent work [11, 51–53] has explored the relation of GPDs to 'mechanical' properties of hadrons: forces, distribution of pressure, and radius of hadrons. Hence GPDs offer the possibility of unprecedented access to information about hadron structure.

Despite the intense theoretical interest in GPDs, they have proven extremely difficult to measure from experiment. Even once an experimental cross section has been measured — itself a task beset with difficulties — determining GPDs from the cross section is extremely difficult. The main way to extract GPDs is to assume a functional form of the GPD, leaving some parameters adjustable, and fit this to experimental data [54, 55]. Such a method

*Older literature may refer to them as 'off-forward', 'off-diagonal', 'non-forward' or 'skewed' parton distributions; these terms all refer to the same observable.

†In contrast to inclusive processes like DIS, exclusive processes have all of their final state particles specified.

clearly leans heavily on the theoretical understanding of GPD-behaviour. Therefore, GPD phenomenology can be greatly aided by improvements in theoretical constraints.

Since the experimental determination of GPDs is so difficult, first principles lattice calculations of GPD-related quantities are highly valuable. So far, lattice results have been limited to the lowest few Mellin moments of GPDs [56–64], and one quasi-GPD calculation [65].

In this chapter, we start in section 4.1 by introducing off-forward processes that can probe GPDs. Then, we will show how GPDs are defined and explore some of their basic properties. In section 4.2, we will outline the physical information that GPDs give access to. In section 4.3 we will review the current status of off-forward scattering experiments, and the phenomenological methods of extracting GPDs from these experiments. Finally, in section 4.4, we will look at the various methods of calculating parton distributions and related quantities using lattice QCD. In particular, we will mention which of these methods has been applied to GPDs.

4.1 Definition and Properties

In this section, we define what GPDs are and how they relate to off-forward scattering processes. Moreover, we derive some of their basic features, such as polynomiality and their relation to PDFs and EM form factors.

4.1.1 Off-Forward Scattering Processes

The off-forward scattering processes we focus on are those that contain the sub-process $\gamma^{(*)}(q) + N(P) \to \gamma^{(*)}(q') + N(P')$[‡]. Note that the incoming/outgoing photons need not be virtual; however, in any process that probes inelastic hadron structure, at least one of them must be deeply virtual (q^2 and/or q'^2 much greater than the nucleon mass). This sub-process is illustrated in figure 4.1.

General Off-Forward Kinematics

The kinematics of this off-forward sub-process are:

- The incoming/outgoing photon has momentum q/q'.
- The incoming/outgoing nucleon has momentum P/P'.
- We use the standard basis

$$\bar{P} = \frac{1}{2}(P + P'), \quad \bar{q} = \frac{1}{2}(q + q'), \quad \Delta = P' - P = q - q'. \tag{4.1}$$

- Hence we can form at most four possible linearly independent momentum scalar variables

$$\bar{P} \cdot \bar{q}, \quad \bar{q}^2, \quad \bar{q} \cdot \Delta, \quad \Delta^2. \tag{4.2}$$

[‡]In general, the target hadron need not be a nucleon, but that is the focus of this thesis.

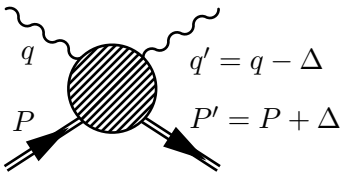

Figure 4.1: The Feynman diagram for off-forward $N\gamma \to N\gamma$ scattering.

- We will use an equivalent basis of scalars:

$$\bar{Q}^2 = -\bar{q}^2, \quad \bar{\omega} = \frac{2\bar{P}\cdot\bar{q}}{\bar{Q}^2}, \quad t = \Delta^2, \quad \xi = -\frac{\bar{q}\cdot\Delta}{2\bar{P}\cdot\bar{q}}. \tag{4.3}$$

- Note that $\bar{P}\cdot\Delta = 0$ and $\bar{P}^2 = M^2 - t/4$, and hence these are not linearly independent Lorentz scalars.

The amplitude of this sub-process is

$$i\mathcal{M}(\gamma N \to \gamma N) = \epsilon^*_\mu \epsilon_\nu T^{\mu\nu}(P, q; P', q'), \tag{4.4}$$

where we have introduced the off-forward Compton tensor (OFCT):

$$T^{\mu\nu}(P, q; P', q') \equiv i \int d^4z e^{i\bar{q}\cdot z} \langle P'|T\big[j^\mu(z/2)j^\nu(-z/2)\big]|P\rangle, \tag{4.5}$$

which is clearly just a generalisation of the forward Compton tensor introduced in the previous chapter (Eq. 3.30).

Physical Processes

While this sub-process of off-forward Compton scattering and the OFCT is the main focus of this thesis, it is worth outlining the physical processes that can measure the OFCT.

Of all the physical processes that can probe the OFCT and GPDs, *deeply virtual Compton scattering* DVCS is the most thoroughly studied, theoretically and experimentally. It is given by $e^-(k) + N(P) \to e^-(k') + \gamma^*(q') + N(P')$ (see figure 4.2 left). The scattering amplitude for DVCS is

$$i\mathcal{M}(e^- N \to e^- N\gamma) = e^3 \bar{u}(k')\gamma_\mu u(k)\varepsilon^*_\nu T^{\mu\nu}(P, q; P', q'), \tag{4.6}$$

where $T^{\mu\nu}$ is the OFCT.

Similarly, we can measure the OFCT from doubly deeply virtual Compton scattering (DDVCS) $e^-(k) + N(P) \to e^-(k') + \ell^+ + \ell^- + N(P')$, where ℓ is some lepton (see figure 4.2 right).

Each of these physical processes define a limit on the allowed values of the off-forward Lorentz scalars in Eq. 4.3:

$$\text{DIS:} \quad \Delta = 0, \quad \xi = t = 0, \tag{4.7}$$

$$\text{DVCS:} \quad \xi \simeq \bar{\omega}^{-1}, \quad q'^2 = 0, \quad \bar{Q}^2 \simeq \frac{-q^2}{2}, \tag{4.8}$$

$$\text{DDVCS:} \quad \bar{\omega}^{-1} < \xi, \quad q^2 < 0, \qquad q'^2 > 0. \tag{4.9}$$

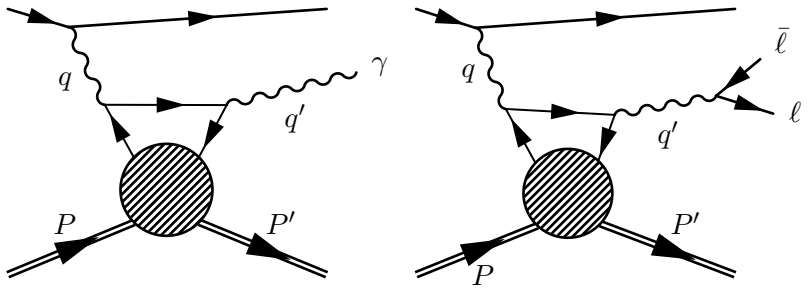

Figure 4.2: Left: the Feynman diagram for deeply virtual Compton scattering. Right: the Feynman diagram for doubly deeply virtual Compton scattering. Note that both diagrams are expanded to leading-order in the strong coupling.

Note that $\simeq$ means 'equal up to $t/\bar{Q}^2$ and $M^2/\bar{Q}^2$ terms', which are suppressed in the scaling limit of each process. In all off-forward processes, we can use the Minkowski triangle inequality to show that $t \leq (P')^2 - P^2$, and hence t is always spacelike.

Finally, note that all these processes are exclusive: their outgoing states are specified. Contrast this to DIS where we had a sum over all possible outgoing states. This makes them harder to measure experimentally, since it means lower luminosity of the cross section and interference with other processes (e.g. Bethe-Heitler scattering). Furthermore, exclusivity means scattering amplitudes of these processes can't be related to the imaginary part of a cross section through the optical theorem, unlike in DIS. Therefore, there is no analogous 'off-forward hadronic tensor' that is the imaginary part of the OFCT.

4.1.2 Generalised Parton Distributions: Definition

To define GPDs, we work in the centre of mass frame as in section 3.3. In this frame, the averaged momentum of the incoming/outgoing nucleons is dominated by lightlike contributions. Therefore, we introduce two lightlike vectors similar to those in section 3.3: $a^\mu = \Lambda(1,0,0,1)$ and $\bar{a}^\mu = (1,0,0,-1)/(2\Lambda)$, where the normalising factor is chosen such that $a \cdot \bar{P} = 1$. With these lightlike vectors in hand, one can show (see appendix D) that $\xi = -a \cdot \Delta/2$, which is the more common expression for ξ [66], the 'skewness' variable. It should be noted that in some of Ji's earlier work [9,49] a variable that is equivalent to our 2ξ is labelled ξ.

Like PDFs, GPDs are defined as the matrix element of the non-local light-cone operators (Eq. 3.81). The difference being that PDFs are the 'forward' matrix element (between two nucleon states of the same momenta), whereas GPDs are 'off-forward' matrix elements (between two nucleon states with different momenta):

$$\begin{aligned}\langle P'|\mathcal{O}^f_{\mathrm{LC}}(x)|P\rangle &= \int \frac{d\lambda}{2\pi} e^{i\lambda x}\langle P'|\bar{\psi}_f(-\lambda a/2)\not{a}\psi_f(\lambda a/2)|P\rangle \\ &= H^f(x,\xi,t)\bar{u}(P')\gamma^\mu a_\mu u(P) + E^f(x,\xi,t)\bar{u}(P')\frac{i\sigma^{\mu\nu}a_\mu\Delta_\nu}{2M}u(P),\end{aligned} \tag{4.10}$$

where $H^f(x,\xi,t)$ and $E^f(x,\xi,t)$ are the nucleon GPDs. Here, x is the momentum fraction in the $\bar{P}$ direction. That is, the incoming nucleon momentum is $P = \bar{P} - \Delta/2$, and hence the incoming parton momentum p has longitudinal component $a \cdot p = x + \xi$, and the outgoing parton has momentum $x - \xi$. As in section 3.3, we are working in light-cone

gauge, where the gauge fields are such that $A \cdot a$, and hence we need not write out the Wilson line for gauge invariance.

Note that unlike regular parton distributions functions (Eq. 3.80), the off-forward matrix element of the light-cone operator needs two Dirac bilinears to span it, similar to EM form factors. This is why there are two unpolarised twist-two GPDs, but only one such PDF. The GPD E^f is sometimes referred to as the 'helicity-flip' GPD, since it vanishes if the incoming/outgoing states have the same helicity. Correspondingly, the H^f GPD vanishes if the incoming/outgoing states don't have the same helicity.

Note that, since GPDs are off-forward matrix elements, they can not be immediately interpreted as a probability density in the same way as PDFs. Instead, as in good old fashioned quantum mechanics, we can interpret them as an interference or transition amplitude between two different proton states: the mod square of a GPD is the probability for a high-energy quark to be ejected from its hadron and re-enter with momentum transfer Δ.

Moreover, as we will discuss in section 4.2, GPDs can in some sense be interpreted as the Fourier transform of the spatial distribution of quarks.

4.1.3 Relation to DVCS

So far, we have discussed GPDs and off-forward scattering processes independently. In this subsection, we will show how generalised parton distributions can be extracted from the OFCT. In particular, the twist-two component of the OFCT for DVCS kinematics is

$$\begin{aligned} T^{\mu\nu}(P,q;P',q') = &-\frac{1}{2}(a^\mu \bar{a}^\nu + a^\nu \bar{a}^\mu - g^{\mu\nu}) \int_{-1}^{1} dx \left(\frac{1}{x-\xi+i\epsilon} + \frac{1}{x+\xi+i\epsilon} \right) \\ &\times \left[H(x,\xi,t)\bar{u}(P')\not{\bar{a}}u(P) + E(x,\xi,t)\bar{u}(P')\frac{i\sigma^{\alpha\beta}\bar{a}_\alpha \Delta_\beta}{2M}u(P) \right] \\ &- \frac{i}{2}\epsilon^{\mu\nu\alpha\beta} a_\alpha \bar{a}_\beta \int_{-1}^{1} dx \left(\frac{1}{x-\xi+i\epsilon} + \frac{1}{x+\xi+i\epsilon} \right) \\ &\times \left[\tilde{H}(x,\xi,t)\bar{u}(P')\not{\bar{a}}\gamma_5 u(P) + \tilde{E}(x,\xi,t)\frac{\Delta\cdot\bar{a}}{2M}\bar{u}(P')\gamma_5 u(P) \right], \end{aligned} \tag{4.11}$$

where a^μ and $\bar{a}^\mu$ are the collinear lightlike vectors we defined in the previous section. Note that $\tilde{H}$ and $\tilde{E}$ are the polarised GPDs, which will not be the focus of the calculation in this thesis, and therefore we will neglect them. The method of perturbative expansion used to derive Eq. 4.11 is known as 'collinear factorisation'[§]; details of this method can be found in Ref. [67,68]. Furthermore, the calculation leading to Eq. 4.11 can be found in Ref. [9,49].

From Eq. 4.11 it is clear that GPDs can be extracted from DVCS, and their relation to the OFCT is analogous to the relation of PDFs to the forward Compton tensor. Similar expressions hold for non-DVCS kinematics.

[§]In chapter 6, we will derive an expression equivalent to Eq. 4.11 but more suited to comparison with lattice calculations.

4.1.4 GPD Moments

Given the relation Eq. 3.89, we would like to find a relationship between the GPDs defined in Eq. 4.10 and the local twist-two operators defined in Eq. 3.50:

$$\mathcal{O}_f^{(n)\mu_1\ldots\mu_n} = \bar{\psi}_f \gamma^{\{\mu_1} i\overset{\leftrightarrow}{D}^{\mu_2} \ldots i\overset{\leftrightarrow}{D}^{\mu_n\}} \psi_f - \text{traces},$$

suppressing the coordinate argument.

To start, we write out all possible Lorentz and Dirac structures for the off-forward matrix elements:

$$\begin{aligned}\langle P'|\mathcal{O}_f^{(n+1)\kappa\mu_1\ldots\mu_n}|P\rangle &= \bar{u}(P')\gamma^{\{\kappa}u(P)\sum_{i=0}^{n} X^f_{n+1,i}(t)\Delta^{\mu_1}\ldots\Delta^{\mu_i}\bar{P}^{\mu_{i+1}}\ldots\bar{P}^{\mu_n\}} \\ &+ \bar{u}(P')u(P)\bar{P}^{\{\kappa}\sum_{i=0}^{n} Y^f_{n+1,i}(t)\Delta^{\mu_1}\ldots\Delta^{\mu_i}\bar{P}^{\mu_{i+1}}\ldots\bar{P}^{\mu_n\}} \\ &+ \bar{u}(P')u(P)\Delta^{\{\kappa}\sum_{i=0}^{n} Z^f_{n+1,i}(t)\Delta^{\mu_1}\ldots\Delta^{\mu_i}\bar{P}^{\mu_{i+1}}\ldots\bar{P}^{\mu_n\}}.\end{aligned} \tag{4.12}$$

Then, using the Gordon identity

$$\bar{u}(P')\gamma^{\mu}u(P) = \bar{u}(P')\left(\frac{\bar{P}^{\mu}}{M} + \frac{i\sigma^{\mu\nu}\Delta_{\nu}}{2M}\right)u(P), \tag{4.13}$$

we can reorganise Eq. 4.12 into

$$\begin{aligned}\langle P'|\mathcal{O}_f^{(n+1)\kappa\mu_1\ldots\mu_n}|P\rangle &= \bar{u}(P')\gamma^{\{\kappa}u(P)\sum_{i=0}^{n} A^f_{n+1,i}(t)\Delta^{\mu_1}\ldots\Delta^{\mu_i}\bar{P}^{\mu_{i+1}}\ldots\bar{P}^{\mu_n\}} \\ &+ \bar{u}(P')\frac{\sigma^{\{\kappa\alpha}i\Delta_{\alpha}}{2M}u(P)\sum_{i=0}^{n} B^f_{n+1,i}(t)\Delta^{\mu_1}\ldots\Delta^{\mu_i}\bar{P}^{\mu_{i+1}}\ldots\bar{P}^{\mu_n\}} \\ &+ C^f_{n+1}(t)\frac{1}{M}\bar{u}(P')u(P)\Delta^{\{\kappa}\Delta^{\mu_1}\ldots\Delta^{\mu_n\}},\end{aligned} \tag{4.14}$$

where we can not use the Gordon identity to reorganise those terms with the C_n^f structure function, since these contain no $\bar{P}^{\mu_i}$ term.

Finally, using time-reversal symmetry, one can show that Eq. 4.14 must be invariant under the transformation $\Delta \to -\Delta$ [69]. Hence all terms containing an odd number of uncontracted Δ^{μ_i} vanish ($\sigma^{\kappa\alpha}i\Delta_{\alpha}$ doesn't change sign under time-reversal, though). Then, we arrive at the standard decomposition given by Ji [66]:

$$\begin{aligned}\langle P'|\mathcal{O}_f^{(n+1)\kappa\mu_1\ldots\mu_n}|P\rangle &= \bar{u}(P')\gamma^{\{\kappa}u(P)\sum_{i=0,2,4}^{n} A^f_{n+1,i}(t)\Delta^{\mu_1}\ldots\Delta^{\mu_i}\bar{P}^{\mu_{i+1}}\ldots\bar{P}^{\mu_n\}} \\ &+ \bar{u}(P')\frac{\sigma^{\{\kappa\alpha}i\Delta_{\alpha}}{2M}u(P)\sum_{i=0,2,4}^{n} B^f_{n+1,i}(t)\Delta^{\mu_1}\ldots\Delta^{\mu_i}\bar{P}^{\mu_{i+1}}\ldots\bar{P}^{\mu_n\}} \\ &+ C^f_{n+1}(t)\text{mod}(n,2)\frac{1}{M}\bar{u}(P')u(P)\Delta^{\{\kappa}\Delta^{\mu_1}\ldots\Delta^{\mu_n\}}.\end{aligned} \tag{4.15}$$

The form factors ($A^f_{n,i}$, $B^f_{n,i}$, C^f_n) are known as *generalised form factors* (GFFs)**.

Now from Eq. 3.89 we know that

$$a_{\mu_1}...a_{\mu_n}\langle P'|\mathcal{O}_f^{\mu_1\cdots\mu_n}|P\rangle = \int dx x^{n-1}\langle P'|\mathcal{O}^f_{\rm LC}(x)|P\rangle. \tag{4.16}$$

Therefore, inserting Eq. 4.15 into Eq. 4.16, we get

$$\begin{aligned}
&\bar{u}(P')\not{a}u(P)\sum_{i=0,2,4}^{n} A^f_{n+1,i}(t)(-2\xi)^i + \bar{u}(P')\frac{\sigma^{\kappa\alpha}i\Delta_\alpha a_\kappa}{2M}u(P)\sum_{i=0,2,4}^{n} B^f_{n+1,i}(t)(-2\xi)^i \\
&+ C^f_{n+1}(t)\mathrm{Mod}(n,2)\frac{1}{M}(-2\xi)^{n+1}\left(\bar{u}(P')\not{a}u(P) - \bar{u}(P')\frac{\sigma^{\kappa\alpha}\Delta_\kappa a_\alpha}{2M}u(P)\right) \\
&= \int dx x^{n-1}\left[H^f(x,\xi,t)\bar{u}(P')\not{a}u(P) + E^f(x,\xi,t)\bar{u}(P')\frac{i\sigma^{\kappa\alpha}\Delta_\kappa a_\alpha}{2M}u(P)\right],
\end{aligned} \tag{4.17}$$

where we have used the facts that $a\cdot\bar{P} = 1$ and $a\cdot\Delta = -2\xi$. Furthermore, we used the Gordon identity to re-express

$$\frac{1}{M}\bar{u}(P')u(P) = \bar{u}(P')\not{a}u(P) - \bar{u}(P')\frac{\sigma^{\alpha\beta}i\Delta_\alpha a_\beta}{2M}u(P). \tag{4.18}$$

Matching the Dirac structures in Eq. 4.17, we have the following relations

$$\int_{-1}^{1} dx x^n H^f(x,\xi,t) = \sum_{i=0,2,4}^{n}(-2\xi)^i A^f_{n+1,i}(t) + \mathrm{mod}(n,2)(-2\xi)^{n+1}C^f_{n+1}(t), \tag{4.19a}$$

$$\int_{-1}^{1} dx x^n E^f(x,\xi,t) = \sum_{i=0,2,4}^{n}(-2\xi)^i B^f_{n+1,i}(t) - \mathrm{mod}(n,2)(-2\xi)^{n+1}C^f_{n+1}(t). \tag{4.19b}$$

Therefore, the Mellin moments of GPDs can be related expressed in terms of GFFs. This relation is known as the 'polynomiality' property of GPDs, since the moments of GPDs are polynomials in ξ.

4.1.5 Relation to Other Observables

We can see from Eq. 4.10 that in the limit that $P' = P$, we have $\langle P'|\mathcal{O}^f_{\rm LC}(x)|P\rangle = 2q_f(x)$, the familiar parton distribution function. Noting that

$$\begin{aligned}
\bar{u}(P')\gamma^\mu a_\mu u(P)\Big|_{P=P'} &= 2P\cdot a = 2 \\
\bar{u}(P')\frac{i\sigma^{\mu\nu}a_\mu\Delta_\nu}{2M}u(P)\Big|_{P=P'} &= 0,
\end{aligned} \tag{4.20}$$

we see that

$$H^f(x,0,0) = q_f(x), \quad x>0, \quad \text{and} \quad H^f(x,0,0) = -\bar{q}_f(-x), \quad x<0, \tag{4.21}$$

where $\bar{q}_f(x)$ is the PDF for the anti-quark of flavour f.

**Sometimes the $n=2$, $i=0$ GFFs are referred to as 'gravitational form factors'.

Moreover, using Eq. 4.16 for $n = 1$, we have

$$a_\mu \langle P'|\bar{\psi}\gamma^\mu\psi|P\rangle = \int_{-1}^{1} dx\Big(H^f(x,\xi,t)\bar{u}(P')\gamma^\mu a_\mu u(P) + E^f(x,\xi,t)\bar{u}(P')\frac{i\sigma^{\mu\nu}a_\mu\Delta_\nu}{2M}u(P)\Big). \tag{4.22}$$

Noting that the LHS of Eq. 4.22 can be parameterised by the EM form factors (see appendix E for a review), we get

$$\begin{aligned} a_\mu \langle P'|\bar{\psi}\gamma^\mu\psi|P\rangle &= F_1^f(t)\bar{u}(P')\gamma^\mu a_\mu u(P) + F_2^f(t)\bar{u}(P')\frac{i\sigma^{\mu\nu}a_\mu\Delta_\nu}{2M}u(P) \\ &= \int_{-1}^{1} dx\Big(H^f(x,\xi,t)\bar{u}(P')\gamma^\mu a_\mu u(P) + E^f(x,\xi,t)\bar{u}(P')\frac{i\sigma^{\mu\nu}a_\mu\Delta_\nu}{2M}u(P)\Big), \end{aligned} \tag{4.23}$$

where $F_1^f(t)$ and $F_2^f(t)$ are the EM form factors. Hence, matching Dirac structures, we get

$$\int_{-1}^{1} dx H^f(x,\xi,t) = F_1^f(t), \quad \int_{-1}^{1} dx E^f(x,\xi,t) = F_2^f(t). \tag{4.24}$$

The relationship between GPDs and PDFs and EM form factors is important for two reasons: firstly, PDFs and EM form factors are two of the most important and most studied hadronic observables; the fact that the information contained in both is entirely contained in GPDs is therefore significant. Secondly, as we discussed earlier, the main way to extract GPDs from experiment is to fit experimental data to a functional form. By relating GPDs to better understood observables, therefore, the functional form of GPDs can be better constrained.

4.2 Physical Content of GPDs

Despite the fact that GPDs by themselves have many interesting properties, the main reason we're interested in them is that they contain a great deal of otherwise inaccessible physical information. As we mentioned in the introduction, the three main pieces of physical information that are unique to GPDs are:

1. Access to the orbital angular momentum of quarks and gluons within a hadron.
2. The distribution of quarks in 'impact parameter space', interpreted as their distribution in a plane transverse to the hadron's motion.
3. Mechanical properties of hadrons; in particular the distribution of forces and pressure within a hadron, and its mechanical radius.

In this section, we will outline how this information is related to GPDs.

4.2.1 GPDs and Nucleon Spin Structure

GPDs first emerged as an attempt to solve the 'proton spin crisis': the proton is a spin 1/2 particle, as are its constituent quarks. Therefore, it was believed that the valence

quarks would carry all or almost all the proton's spin (two with aligned spin polarisation, one with opposite) [70].

However, experiments at the European Muon collaboration showed that the proton's valence quarks carry far less of the total spin than expected [71]. In fact, about 85% of the proton's spin is due to orbtial and gluonic contributions! As a result, there have been many theoretical and experimental efforts to find the source of the proton's missing spin, expected to be in the spins and orbital angular momentum of the remaining gluons and sea quarks. In the first paper on GPDs, Ji [9] showed that the individual components of quark and gluons spin and orbtial angular momentum could be measured through DVCS.

The general argument starts with the Belifanté energy-momentum tensor (EMT) for QCD[††]:

$$\mathcal{T}^{\mu\nu} = \mathcal{T}_q^{\mu\nu} + \mathcal{T}_g^{\mu\nu}, \tag{4.25}$$

an operator that is symmetric in its Lorentz indices.

Here, the quark component for a given quark of flavour f is

$$\mathcal{T}_q^{\mu\nu} = \bar{\psi}_f \gamma^{\{\mu} \overleftrightarrow{D}^{\nu\}} \psi_f. \tag{4.26}$$

And the gluon component is

$$\mathcal{T}_g^{\mu\nu} = \frac{1}{4} g^{\mu\nu} F^{\alpha\beta} F_{\alpha\beta} + F^{\mu\alpha} F_\alpha{}^\nu, \tag{4.27}$$

where $F^{\mu\nu}$ is the usual QCD field strength tensor. If we write out the tensor decomposition of a generic matrix element of the QCD EMT using Lorentz covariance, we get

$$\begin{aligned} \langle P'|\mathcal{T}_{q,g}^{\mu\nu}|P\rangle =& \bar{u}(P')\Big[A_{q,g}(t)\gamma^{\{\mu}\bar{P}^{\nu\}} + B_{q,g}(t)\frac{i\sigma^{\{\mu\alpha}\Delta_\alpha}{2M}\bar{P}^{\nu\}} \\ &+ D_{q,g}(t)\frac{\Delta^\mu\Delta^\nu - g^{\mu\nu}\Delta^2}{M} - g^{\mu\nu}\bar{c}_{q,g}(t)M\Big]u(P). \end{aligned} \tag{4.28}$$

Note that the quark EMT Eq. 4.26 is the $n = 2$ operator defined in Eq. 3.50: $\mathcal{O}_f^{(n)\mu\nu}$ without its traces subtracted. Hence the scalar EMT form factors in Eq. 4.28 are

$$A_q^f(t) = A_{2,0}^f(t), \quad B_q^f(t) = B_{2,0}^f(t), \quad C_q^f(t) = C_2^f(t). \tag{4.29}$$

Hence the quark EMT can be calculated from GPDs. Recall the orbital angular momentum operator from non-relativistic quantum mechanics: $L^i = \epsilon^{ijk}x^j p^k$. And the density of momentum in the i direction is $\mathcal{T}^{i0} = \mathcal{T}^{0i}$. Hence the angular momentum density operator in QCD is

$$M^{\alpha\mu\nu}(x) = \mathcal{T}_f^{\alpha\mu}x^\nu - \mathcal{T}_f^{\alpha\nu}x^\mu, \tag{4.30}$$

[††]The EMT is defined through Noether's theorem: $\Theta^{\mu\nu} = \sum_i \frac{\partial\mathcal{L}}{\partial(\partial_\nu\phi_i)}\partial^\mu\phi_i - g^{\mu\nu}\mathcal{L}$. In QCD the Noether EMT is not symmetric in its Lorentz indices. Therefore, to construct an EMT that is symmetric (so as to agree with the EMT from torsionless General Relativity), one can use the procedure attributed to Belifanté [72]. The resulting operator $\mathcal{T}^{\mu\nu}$ is known as the 'Belifanté EMT'.

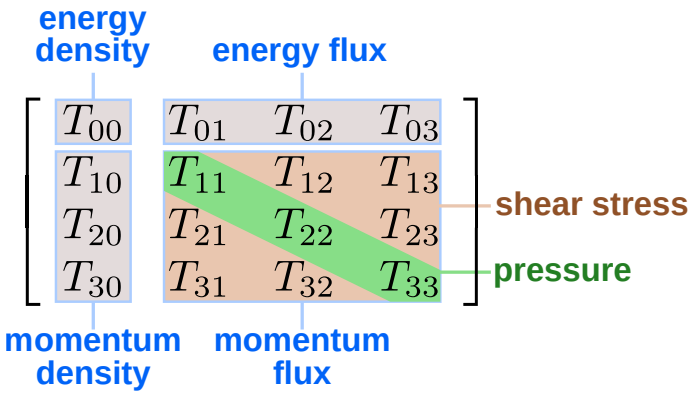

Figure 4.3: The energy-momentum tensors components in matrix form [73].

where x is the position at which the angular momentum density is measured, and $\mathcal{T}_f^{\mu\nu}$ is the Belifanté EMT for a single flavour of quarks. The angular momentum operator is then

$$J_f^i = \frac{1}{2}\epsilon^{ijk}\int d^3x\Big(\mathcal{T}_f^{0k}x^j - \mathcal{T}_f^{0j}x^k\Big). \tag{4.31}$$

Substituting Eq. 4.28 into Eq. 4.31 and taking the matrix element in the forward limit, we get the Ji sum rule:

$$\begin{aligned}\langle J_f^3\rangle &= \lim_{P'\to P}\langle P'|J_f^3|P\rangle \\ &= \frac{1}{2}[A_{2,0}^f(0) + B_{2,0}^f(0)] = \frac{1}{2}\int_{-1}^{1} dx x\Big[H^f(x,\xi,t) + E^f(x,\xi,t)\Big]\Big|_{t=0}.\end{aligned} \tag{4.32}$$

An analogous relation holds for gluons and their GPDs. Combining this with results from polarised DIS, one could determine the contributions to the proton's spin from the orbital angular momentum of its constituents.

However, as we have already discussed, GPDs are difficult to extract from experiment. Not only would evaluating the explicit value of Eq. 4.32 require a very precise determination of GPDs, it would also require a determination of both H and E GPDs over a wide range of x, ξ and t values.

4.2.2 Nucleon Tomography

Shortly after the connection between GPDs and nucleon spin structure was shown by Ji, Burkardt [10,74] showed that GPDs also contain information about the spatial distribution of quarks in a nucleon. This led not only to further interest in GPDs, but also a new physical interpretation of them.

To motivate this argument, we start with a very nice analogy between EM form factors and GPDs [10]: an EM form factor is an off-forward matrix element of the current operator $\bar{\psi}_f\gamma^\mu\psi_f$. The forward matrix element of this operator is just the charge $\mathcal{Q}$ of the hadron. And the Fourier transform of an EM form factor is the charge density $\rho(\mathbf{r})$ (strictly speaking, this interpretation is only valid in the infinite momentum frame — see appendix E). So *the Fourier transform of the off-forward matrix element is the density of the forward matrix element in position space.*

If we could extend this analogy to GPDs, we would have that the Fourier transform of a GPD $H^f(x,\xi,t)$ is the density of its forward matrix element, the PDF $q_f(x)$, in position space.

Operator	Off-foward Matrix Element	Forward Matrix Element	Position space
$\bar{\psi}_f\gamma^\mu\psi_f$	$F_{1,2}(t)$	$\mathcal{Q}$	$\rho(\mathbf{r})$
$\mathcal{O}_{\mathrm{LC}}(x)$	$H^f(x,\xi,t)$	$q_f(x)$	$q_f(x,\mathbf{r})$ (??)

The idea, then, is that the Fourier transform of the H^f GPD gives the probability density of finding a parton of flavour f with longitudinal momentum fraction x and position from the centre of the nucleon $\mathbf{r}$ in certain frames.

Impact Parameter Dependent PDFs

First, to meaningfully define the spatial distribution of partons in a given nucleon, the nucleon needs to be localised by working in the centre of mass (COM) frame (equivalently the infinite momentum frame, as discussed in section 3.3). In this frame, the nucleon is infinitely Lorentz contracted along the direction of its motion into a 'pancake' with no longitudinal extent. Therefore, its partons will all be in a two-dimensional plane transverse to the nucleon's motion.

Then, we introduce an operator that is identical to the light-cone operator from Eq. 3.81, except the position of the quark operators is shifted by $\mathbf{b}_\perp$, a vector in this transverse plane ($\mathbf{b}_\perp \cdot a = 0 = \mathbf{b}_\perp \cdot \bar{a}$):

$$\tilde{\mathcal{O}}^f_{\mathrm{LC}}(x,\mathbf{b}_\perp) \equiv \int \frac{d\lambda}{2\pi} e^{i\lambda x} \bar{\psi}_f\big(-\lambda a/2 + \mathbf{b}_\perp\big) \not{a} \psi_f\big(\lambda a/2 + \mathbf{b}_\perp\big). \tag{4.33}$$

We refer to $\mathbf{b}_\perp$ as the *impact parameter*. At $\mathbf{b}_\perp = 0$ this new operator coincides with the regular light-cone operator: $\tilde{\mathcal{O}}^f_{\mathrm{LC}}(x,\mathbf{b}_\perp = 0) = \mathcal{O}^f_{\mathrm{LC}}(x)$.

Now we define the nucleon centre of momentum in the transverse plane: $\mathbf{R}_\perp$. In intuitive partonic terms, this is $\mathbf{R}_\perp = \sum_i x_i \mathbf{r}_{i,\perp}$, were x_i is the longitudinal momentum fraction of a parton and $\mathbf{r}_{i,\perp}$ is its position, and the sum is over all the nucleon's partons. To localise the nucleon wave-packet we choose a nucleon state with $\mathbf{R}_\perp = 0$ [74], and with light-cone momentum P^+ and some spin value λ: $|P^+, \mathbf{R}_\perp = 0, \lambda\rangle$. In particular, these states have the property

$$|P^+, \mathbf{R}_\perp = 0, \lambda\rangle = \mathcal{N} \int \frac{d^2\mathbf{p}_\perp}{(2\pi)^2} |P^+, \mathbf{p}_\perp, \lambda\rangle. \tag{4.34}$$

This is a property of light-cone helicity eigenstates which we will not justify; the properties of such states are given in e.g. Refs. [10, 75].

Then we define the *impact parameter dependent PDFs*:

$$q_f(x,\mathbf{b}_\perp) \equiv \langle P^+, \mathbf{R}_\perp = 0, \lambda | \tilde{\mathcal{O}}^f_{\mathrm{LC}}(x,\mathbf{b}_\perp) | P^+, \mathbf{R}_\perp = 0, \lambda\rangle. \tag{4.35}$$

Note that it isn't by definition true that this quantity is a probability density; this interpretation requires further justification.

Fourier transformed GPD

Consider the GPD definition in terms of light-cone operators from Eq. 4.10. If we fix the helicity of the incoming and outgoing particles to be the same, then the helicity-flip GPD $E^f(x,\xi,t)$ vanishes. Moreover, if we let $\xi = 0$[‡‡], so that $a \cdot \Delta = 0$, then we have $a \cdot P = a \cdot P'$, and therefore $\bar{u}(P')\not{a}u(P) = 2a \cdot P = 2a \cdot \bar{P} = 2$. So the off-forward matrix element of the light-cone operator is

$$\langle P', \lambda | \mathcal{O}^f_{\mathrm{LC}}(x) | P, \lambda \rangle = 2H^f(x, \xi = 0, t), \tag{4.36}$$

where from now on we will adopt the notation $H^f(x, \xi = 0, t) = H^f(x, t)$.

It is now a straight-forward calculation to show that the impact parameter dependent PDF is the Fourier transform of a GPD for $\xi = 0$:

$$\begin{aligned} q_f(x, \mathbf{b}_\perp) =& \langle P^+, \mathbf{R}_\perp = 0, \lambda | \tilde{\mathcal{O}}^f_{\mathrm{LC}}(x, \mathbf{b}_\perp) | P^+, \mathbf{R}_\perp = 0, \lambda \rangle \\ =& |\mathcal{N}|^2 \int \frac{d^2\mathbf{p}'_\perp}{(2\pi)^2} \int \frac{d^2\mathbf{p}_\perp}{(2\pi)^2} \langle P^+, \mathbf{p}'_\perp, \lambda | \tilde{\mathcal{O}}^f_{\mathrm{LC}}(x, \mathbf{b}_\perp) | P^+, \mathbf{p}_\perp, \lambda \rangle \\ =& |\mathcal{N}|^2 \int \frac{d^2\mathbf{p}'_\perp}{(2\pi)^2} \int \frac{d^2\mathbf{p}_\perp}{(2\pi)^2} e^{-i\mathbf{b}_\perp \cdot (\mathbf{p}'_\perp - \mathbf{p}_\perp)} \langle P^+, \mathbf{p}'_\perp, \lambda | \tilde{\mathcal{O}}^f_{\mathrm{LC}}(x, 0) | P^+, \mathbf{p}_\perp, \lambda \rangle \\ =& |\mathcal{N}|^2 \int \frac{d^2\boldsymbol{\Delta}_\perp}{(2\pi)^2} \int \frac{d^2\bar{\mathbf{p}}_\perp}{(2\pi)^2} e^{-i\mathbf{b}_\perp \cdot (\mathbf{p}'_\perp - \mathbf{p}_\perp)} \langle P^+, \mathbf{p}'_\perp, \lambda | \tilde{\mathcal{O}}^f_{\mathrm{LC}}(x, 0) | P^+, \mathbf{p}_\perp, \lambda \rangle, \end{aligned} \tag{4.37}$$

where we have introduced the variables $\boldsymbol{\Delta}_\perp = \mathbf{p}'_\perp - \mathbf{p}_\perp$ and $\bar{\mathbf{p}}_\perp = \frac{1}{2}(\mathbf{p}'_\perp + \mathbf{p}_\perp)$. Then, using Eqs. 4.36 and 4.37, and the fact that the integrand doesn't depend on $\bar{\mathbf{p}}_\perp$, we have that

$$q_f(x, \mathbf{b}_\perp) = \int \frac{d^2\boldsymbol{\Delta}_\perp}{(2\pi)^2} H^f(x, -\boldsymbol{\Delta}^2_\perp) e^{-i\mathbf{b}_\perp \cdot \boldsymbol{\Delta}_\perp}. \tag{4.38}$$

Probability Density Interpretation

Finally, as we mentioned previously, it is not *ipso facto* true that Eq. 4.35 defines the desired probability density. It can be shown [74] that $q_f(x, \mathbf{b}_\perp)$ is non-negative for $x > 0$ for all $\mathbf{b}_\perp$, and non-positive for $x < 0$ for all $\mathbf{b}_\perp$. These constraints strongly suggest the probability interpretation of $q_f(x, \mathbf{b}_\perp)$. Therefore, the most common interpretation is that $q_f(x, \mathbf{b}_\perp)$ is the probability density to find a parton with momentum fraction x and $\mathbf{b}_\perp$ distance from the centre of mass of the nucleon in the infinite momentum frame. Hence GPDs may be interpreted as Fourier transforms of the spatial distribution of quarks in the transverse plane.

As a result, it is possible to extract profiles of the distribution of partons in the transverse plane from hard exclusive scattering experiments [77, 78]. This technique is known as 'nucleon tomography' by analogy with a process of x-ray cross section.

4.2.3 Mechanical Properties

The spin structure and transverse position distribution are certainly the best known and most studied physical aspects of GPDs. However, due to their relation to the QCD energy-

[‡‡] These ideas have been extended to $\xi \neq 0$ [76].

momentum tensor, GPDs contain an abundance of other information about the properties of hadrons. In particular, in a series of papers [11, 51, 52] Polyakov and collaborators have shown, from the so-called 'D-term'[§§] of the EMT (Eq. 4.29), one can calculate the distribution of shear forces and pressure in a hadron, as well as its mechanical radius. Moreover, from analyses of the OFCT using dispersion relations, multiple studies [82–85] have shown that this D-term is experimentally accessible. Recently, the D-term was measured experimentally via DVCS [86] — a very exciting development.

Recall that the EMT form factors A, B and D are equivalent to the GFFs $A_{2,0}$, $B_{2,0}$ and C_2, respectively. The EMT $\mathcal{T}_f^{\mu\nu}$, in the Breit frame where $\Delta^\mu = (0, \boldsymbol{\Delta})$, can be related to the *static EMT* $\hat{T}_f^{\mu\nu}$:

$$\hat{T}_f^{\mu\nu}(\boldsymbol{r}, \boldsymbol{s}) = \int \frac{d^3\boldsymbol{\Delta}}{(2\pi)^3 2E} e^{-i\boldsymbol{r}\Delta} \langle p'|\mathcal{T}_f^{\mu\nu}|p\rangle. \tag{4.39}$$

From this tensor, we can get many physical properties of hadronic systems (see Ref. [11] for a review):

- $\hat{T}^{00}$ gives the energy density in terms of A, B and D EMT form factors. Moreover, the energy density at the centre of the hadron can be calculated entirely in terms of A and D form factors.
- $\hat{T}^{ij}$ is the stress tensor [51]. Since the stress tensor is related to the pressure and shear force distributions,

  $$\hat{T}^{ij}(\boldsymbol{r}) = \left(\frac{r^i r^j}{r^2} - \frac{1}{3}\delta^{ij}\right) s(r) + \delta^{ij} p(r), \tag{4.40}$$

  these may be calculated from EMT form factors, and hence GPDs. These pressure and shear force distributions can be calculated entirely from the D-term.
- Moreover, the mechanical radius and surface tension of a hadron may be calculated from its D-term.
- Finally, it has been suggested [53] that the EMT may shed light on the equation of state of quark matter in compact stars.

A full measurement of GPDs would, therefore, provide an unprecedented level of description of hadron structure: information about spin composition, spatial distribution of partons, and mechanical properties in far greater detail than what is currently available. As we mentioned previously, however, the determination of GPDs from experiment, while in principle possible, is highly non-trivial.

[§§] The etymology of the 'D-term' is particularly confusing. In older papers, 'the D-term' also refers to a scalar function in the double distribution representation of GPDs [79–81], which also relates to the C GFFs! We will use the convention of more recent literature, and exclusively use the 'D-term' to refer to the EMT form factor.

4.3 Experiment and Phenomenology

In this section, we will outline the experimental progress in measuring GPDs, and give some idea of the phenomenological methods to attempt to extract them from hard exclusive processes.

4.3.1 Experiment

Generalised parton distributions can only be calculated from hard exclusive processes: scattering events in which the momentum transfer of a virtual photon is very large, and in which the final products of the experiment are specified. The main processes so far measured in experiment are deeply virtual Compton scattering (DVCS) and deeply virtual meson production (DVMP), with experiments carried out at HERA [87–91], COMPASS [92], and JLab [93–96]. Moreover, the proposed election-ion collider (EIC) [97] is a major experimental undertaking designed specifically to investigate hadron structure, including through DVCS, DVMP, and doubly deeply virtual Compton scattering (DDVCS) (recall figure 4.2).

4.3.2 Phenomenology

There are a number of fitting methods used to extract GPDs, including local fitting algorithms [98] and machine learning methods [99]. However, we are most interested in global fitting procedures, which would give access to GPDs over the full range of their kinematic variables [100–105]. Global fits use a functional form with free parameters to fit to experiment; the parameterisation is determined by both model dependent and independent constraints (see Refs. [54, 55] for a review). While global fitting has had great success with PDFs and EM form factors, for GPDs the situation is more difficult because they are functions of three variables, not one. Moreover, there can be significant discrepancies between fits that use different constraints (see for instance Ref. [100]).

Given the difficulty of fitting GPDs from experiment, and the reliance of these fits on theoretical priors, lattice calculations of GPDs are therefore especially valuable, both to guide and compare to phenomenological extractions.

4.4 Lattice Calculations

The present thesis is primarily concerned with determining GPD-related quantities (specifically GFFs) from a calculation using lattice QCD. Here, we will outline other lattice methods that could in principle calculate GPD-related quantities — a few of these have been put into practice. However, a theme that runs through all of these methods is the incompatibility of the lightlike description of parton distributions (Eq. 4.10), which is a good approximation for high-energy experiments, and the Euclidean spacetime of lattice QCD. In all the methods given in this section, a different trick (or set of) must be employed to get information about the light-cone parton distributions from the lattice.

4.4.1 Euclidean vs. Minkwoski Space

Recall from section 2.2 that currently the only computationally feasible method to calculate the expectation values of QCD operators is to use Euclidean spacetime. This reduces

the light-cone from a hypercone to a single point, and only admits the possibility of spacelike vectors.

First, note that the matrix element of a local operator has the same value in Minkowski as in Euclidean space. Hence it is not really proper to refer to local matrix elements as belonging to Minkowski or Euclidean space — they are 'spacetime agnostic' to use the phrase from Ref. [106].

Now consider the product of two local operators, $\mathcal{A}$ and $\mathcal{B}$, which are respectively at two spacetime points, $x_1 = (0, \mathbf{x}_1)$ and $x_2 = (0, \mathbf{x}_2)$. Then the value of their product doesn't depend on whether it is calculated using a Euclidean or Minkowski signature [106]:

$$\langle k_1 | \mathcal{A}_{\text{Euc}}(\mathbf{x}_1) \mathcal{B}_{\text{Euc}}(\mathbf{x}_2) | k_2 \rangle = \langle k_1 | \mathcal{A}_{\text{Mink}}(\mathbf{x}_1) \mathcal{B}_{\text{Mink}}(\mathbf{x}_2) | k_2 \rangle. \tag{4.41}$$

We can see this by simply applying translational invariance and inserting a complete set of states to the above equation. This reduces the above equation to the product of the matrix elements of two local operators, with no dependence on the Wick-rotated temporal coordinate.

Since any spacelike separation can be Lorentz transformed to one for which there is no temporal separation, the above argument also applies to the matrix element of any two spacelike separated operators. Therefore, two spacelike separated operators (or local operators) have the same matrix element in Euclidean and Minkowski space — they, too, are signature agnostic.

However, light-cone operators (Eq. 3.81) are lightlike separate, not spacelike separated. Therefore, they can not be directly calculated using lattice QCD. The trick, therefore, is to *relate light-cone operators to spacelike separated or local operators that can be calculated in lattice QCD.*

4.4.2 GPD Moments

We have already spent some time discussing the relation between local operators from Eq. 3.50 and light-cone operators from Eq. 3.81. We found that the Mellin moments of GPDs could be expressed as the off-forward matrix elements of the *local* operators (Eq. 4.19), and hence these moments can be calculated on the lattice. Naively, we should be able to calculate these matrix elements from the vacuum expectation value of the operator

$$\chi(x_3) \mathcal{O}_f^{(n)\mu_1 \cdots \mu_n}(x_2) \chi^\dagger(x_1),$$

with the correct choice of momentum transfer. There have been quite a few such calculations of off-forward matrix elements of local operators [56–64].

However, this method suffers a difficulty called operator mixing. The twist-two local operators defined in Eq. 3.50 belong to an irreducible representation of the Lorentz group (some further discussion is given in appendix B). Since lattice QCD is formulated on a hypercubic grid of points, it breaks Lorentz symmetry. Instead of the usual continuum orthogonal group $O(4)$ of transformations, only a finite subgroup of $O(4)$, the hypercubic subgroup, survives on the lattice. As a result, the usual leading-twist operators mix under renormalisation with other operators on the lattice.

For the lowest $n = 2$ operator, this mixing can be controlled systematically [107], but as n gets larger the mixing becomes harder to control [108]. Therefore, few studies go beyond the $n = 3$ moment. In particular, for GPDs the highest GFFs calculated so far are

$A_{3,0}$, $B_{3,0}$ [61]. Most studies, however, calculate only the lowest moments, $A_{2,0}$, $B_{2,0}$ and C_2. From our discussion in section 4.2, this is a sensible choice, since these GFFs contain lots of the information that is physically interesting. On the other hand, for comparison to experiment and nucleon tomography, the full GPD is required. Hence calculation of higher GFFs or the full GPD itself is desirable.

4.4.3 Quasi-GPDs

Quasi-distributions are another method to calculate parton distribution-related quantities, first proposed by Ji [109]. Quasi distributions are defined by the operator

$$\mathcal{O}^f_{\text{quasi}}(x) = \int \frac{d\lambda}{2\pi} e^{iP\cdot zx} \bar{\psi}_f(-z/2)\gamma^3 \text{exp}\bigg(- ig \int_0^z dz' A(z')\cdot z \bigg) \psi_f(z/2), \tag{4.42}$$

where $z^\mu = (0,0,0,k\lambda)$. Clearly, this operator is similar to the light-cone operator define in Eq. 3.81 but for spacelike separations. Since z is spacelike, the operator in Eq. 4.42 is signature agnostic, and hence the matrix element of it is the same in Euclidean and Minkowski space. The forward matrix element of the operator in Eq. 4.42 is a quasi-PDF, while the off-forward a quasi-GPD. In principle, any distribution that is defined by a light-cone operator can be related to a similar quasi-distribution defined by an operator like Eq. 4.42.

The main difficulty, therefore, is in comparing the quasi-distributions to light-cone distributions. In theory this is possible through large momentum effective field theory (LaMET) [109,110]. Through this matching procedure, quasi-distributions are equivalent to light-cone distributions up to terms of order Λ_{QCD}/P_z (higher twist effects), where P_z is the z-component of the spacelike nucleon momenta. Intuitively, the idea is that, by taking $P_z \to \infty$, the current separation approaches the light-cone asymptotically, and hence the matrix element of Eq. 4.42 approaches the corresponding parton distribution.

The possibility presented by quasi-distributions to finally calculate parton distributions from first principles has generated a great deal of interest in them, and no doubt will generate more in the future. So far, calculations involving quasi-distributions have largely been limited to quasi-PDFs (see Ref. [111] for a review). More recently pion quasi-GPDs were calculated [65]. However, like the local operators, the matching procedure and the renormalisation involved are non-trivial (see Ref. [111] for a review). Moreover, it has been argued that the limit $P_z \to \infty$ doesn't recover the light-cone operator as it would in the continuum due to lattice operator mixing [112,113].

4.4.4 Current Product Methods

Finally, there are lattice calculations that attempt to calculate the matrix element of the product of currents, such as the Compton tensor (time-ordered currents) or the hadronic tensor (unordered). Of course, apropos the previous discussion on the Euclidean signature, for the product of currents $j_\mu(z)j_\nu(0)$ the separation z must be spacelike in a lattice calculation.

In this class of calculations are four-point function extractions of the hadronic tensor [114–118], fictitious heavy quark insertion [119,120], a proposed method of calculating a 'lattice cross section' [121], and the Feynman-Hellmann method [122,123]. In all these calculations, however, the matrix elements are forward. Therefore, the present thesis is

the first attempt to calculate the current product on the lattice for off-forward kinematics (the OFCT).

A major advantage of this method is that vector currents have a simple multiplicative renormalisation procedure on the lattice, in contrast to quasi-distributions and local twist-two operators. On the other hand, one of the main difficulties of this method is relating the matrix element of the spacelike current product to a physical quantity in Minkowski space. The OPE discussed in chapter 3 is therefore very useful for this purpose since it expands a non-local operator in terms of local (that is, signature agnostic) operators. We will extend this discussion in chapter 6. The application of Feynman-Hellmann techniques to off-forward second order scattering is given in the next chapter.

Chapter 5

Feynman-Hellmann Techniques

The Feynman-Hellmann (FH) theorem is a result from non-relativistic quantum mechanics (QM) that relates energy shifts to matrix elements of operators [124–126]. Suppose we have a Hamiltonian $H(\lambda)$ with eigen-energies that are differentiable functions of a parameter λ. Then, for a normalised eigenstate of the Hamiltonian $|n\rangle$, one can show that

$$\frac{\partial E_n}{\partial \lambda}\bigg|_{\lambda=0} = \langle n|\frac{\partial H}{\partial \lambda}|n\rangle\bigg|_{\lambda=0}. \tag{5.1}$$

This statement was originally used as a tool to calculate forces within molecules. However, the Feynman-Hellmann theorem is also a generalisation of perturbation theory: in the special case that $H(\lambda) = H_0 + \lambda V$, where H_0 is a Hamiltonian with analytically solvable eigenstates, Eq. 5.1 reduces to the usual first order energy shift in QM perturbation theory, $\Delta E_n = \lambda\langle n|V|n\rangle$.

Therefore, we generally don't think of Feynman-Hellmann methods in terms of Eq. 5.1 or forces in molecules, but simply as a generalisation of perturbation theory, where the unperturbed Hamiltonian is not necessarily completely solvable and where the λ-dependence is not necessarily a one-dimensional linear relationship.

Lattice Feynman-Hellmann Techniques

The form of Eq. 5.1 presents applications to lattice QCD, where calculating energies is simple but calculating matrix elements of operators may be more difficult.

The FH theorem was first applied to lattice QCD in the calculation of sigma terms [127–130]. In these calculations the mass of a given hadron is varied with respect to the quark mass. From a Feynman-Hellmann relation, we then have that

$$m_f \frac{\partial M_X}{\partial m_f} = m_f \langle X|\bar{\psi}_f \psi_f|X\rangle = \sigma_f, \tag{5.2}$$

for some hadron $|X\rangle$.

In the calculation of sigma terms, an input of the QCD Lagrangian (the quark mass) is varied. However, in more recent applications of the FH theorem, extra terms are added to the QCD Lagrangian that depend on arbitrary parameters. Using this method and related methods, lattice studies have calculated the axial coupling [131–133] and the Gamow-Teller matrix element [134]. Moreover, the CSSM and QCDSF/UKQCD collaborations have used lattice FH techniques to calculate multiple matrix elements of physical interest [135–139]. In particular, this collaboration has used second order FH techniques to calculate the

forward Compton tensor [122, 123, 140]. The present thesis is an extension of these works to the off-forward Compton tensor (OFCT).

In this chapter, we will show that the OFCT as defined in Eq. 4.5 can be calculated from the energy shifts of two-point functions, when the lattice action has been altered by additional terms. The OFCT must be treated with extra care in our FH proof for two reasons: first, it is *second order*, which essentially means that it is the matrix element of an operator that depends on two spacetime points. Second, it is off-forward, meaning that the initial and final states have different momenta. The combination of these properties requires us to take extra care in our derivation of the suitable FH relation.

We will start in section 5.1 by considering a simple example from degenerate QM perturbation theory that captures many of the properties of the actual FH proof. However, it needs to be stressed that the results of this section are not substitutes for a comprehensive proof of a FH relation using Euclidean path integrals. In section 5.2, we will prove the necessary FH relation, allowing us to calculate the OFCT. Finally, in section 5.3 we will look in more depth at the properties of the perturbed correlator, and in doing so justify some of the assumptions we make in the FH proof and further show how to calculate the energy shifts.

5.1 Toy-Model Example

For the FH derivation in the next section, a great deal of effort will go into performing long and quite tedious calculations, and hence the basic physics can easily be obscured. To avoid losing the forest in the trees, in this section we give an outline of the arguments that lead us to the FH relation. In particular, we consider a much simpler quantum system that nonetheless preserves many of the properties of the lattice calculation.

We consider a system with the following properties:

- The Hamiltonian is $H_{\boldsymbol{\lambda}} = H_0 + V_{\boldsymbol{\lambda}}$, where H_0 is the unperturbed Hamiltonian and $V_{\boldsymbol{\lambda}}$ is the perturbing potential. Note that $\boldsymbol{\lambda} = (\lambda_1, \lambda_2)$, and hence our perturbation depends on two perturbing parameters.
- $H_{\boldsymbol{\lambda}} \to H_0$, as $\boldsymbol{\lambda} \to 0$.
- We consider a set of eight states: $\{|p_i\rangle | i \in [1, 8]\}$.
- These states are eigenstates of the unperturbed Hamiltonian H_0 and the unperturbed momentum operator; we assume all states have the same mass, so that if $|p_i| = |p_j|$, then the energies of these two states are the same.
- In particular, we let $|p_1\rangle$ and $|p_2\rangle$ be *degenerate low-energy states*, whose energy, E_0, is the lowest energy of all the states.
- For every state in our system, $|p_i\rangle$, we can always find another state in our system $|p_j\rangle$ that has momentum satisfying $p_j = p_i \pm q$ or $p_j = p_i \pm q'$, where q and q' are momentum vectors (see figure 5.1).

In particular, the perturbing potential mixes states of different momentum:

$$V_{\boldsymbol{\lambda}}|p_i\rangle = J\Big[\lambda_1(|p_i + q\rangle + |p_i - q\rangle) + \lambda_2(|p_i + q'\rangle + |p_i - q'\rangle)\Big], \tag{5.3}$$

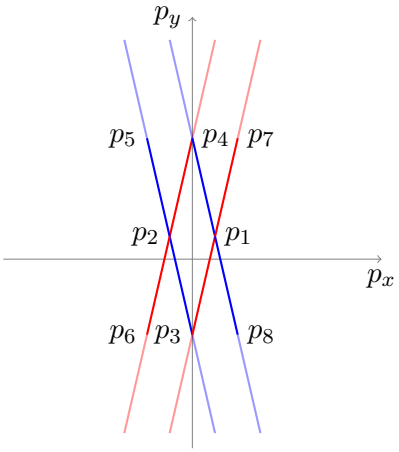

Figure 5.1: Diagram in momentum space showing how each state is mixed by the perturbing potential. The red lines are q vectors, and the blue lines are q' vectors. The semi-transparent lines are even higher energy terms that we do not consider.

for some Hermitian operator J; it is convenient to assume that the matrix elements of J are all real. So the λ_1 perturbation is associated with the transfer of momentum q, and likewise for λ_2 and momentum q'.

Therefore, in matrix form the Hamiltonian operator is

$$H = \begin{pmatrix} E_0 & 0 & \lambda_1 J & \lambda_2 J & 0 & 0 & \lambda_1 J & \lambda_2 J \\ 0 & E_0 & \lambda_2 J & \lambda_1 J & \lambda_2 J & \lambda_1 J & 0 & 0 \\ \lambda_1 J & \lambda_2 J & E_1 & 0 & 0 & 0 & 0 & 0 \\ \lambda_2 J & \lambda_1 J & 0 & E_2 & 0 & 0 & 0 & 0 \\ 0 & \lambda_2 J & 0 & 0 & E_3 & 0 & 0 & 0 \\ 0 & \lambda_1 J & 0 & 0 & 0 & E_4 & 0 & 0 \\ \lambda_1 J & 0 & 0 & 0 & 0 & 0 & E_3 & 0 \\ \lambda_2 J & 0 & 0 & 0 & 0 & 0 & 0 & E_4 \end{pmatrix}, \tag{5.4}$$

where we let $E_i \gg E_0$ for $i \in [1, 4]$.

Since $V_{\boldsymbol{\lambda}}$ doesn't commute with the momentum operator, the momentum eigenstates $\{|p_i\rangle\}$ *aren't eigenstates of the perturbed Hamiltonian.* Instead, the low-energy eigenstates of $H_{\boldsymbol{\lambda}}$ are (up to λ^2 at least) linear combinations of the eight states in $\{|p_i\rangle\}$. Let the perturbed spectrum of states be $\{|k_i\rangle_{\boldsymbol{\lambda}}\}$, which are eigenstates of the perturbed Hamiltonian with energies $E_i^{\boldsymbol{\lambda}}$. And let $|k_1\rangle_{\boldsymbol{\lambda}}$ and $|k_2\rangle_{\boldsymbol{\lambda}}$ be states such that

$$H_0|k_1\rangle_{\boldsymbol{\lambda}=0} = E_0|k_1\rangle_{\boldsymbol{\lambda}=0}, \quad H_0|k_2\rangle_{\boldsymbol{\lambda}=0} = E_0|k_2\rangle_{\boldsymbol{\lambda}=0}. \tag{5.5}$$

That is, these perturbed states reduce to linear combinations of $|p_1\rangle$ and $|p_2\rangle$ as the perturbation couplings go to zero. Then, we can write these two terms as

$$|k_{(1,2)}\rangle_{\boldsymbol{\lambda}} = \sum_{i=1}^{8} c_i^{(1,2)}|p_i\rangle + \mathcal{O}(\lambda^2), \tag{5.6}$$

where c_1 and c_2 are $\mathcal{O}(1)$, and c_i are $\mathcal{O}(\lambda)$ for $i = 3, 4, ..., 8$.

We will approximate the energy eigenstates and eigenvalues of the Hamiltonian, Eq. 5.4, by constructing an effective Hamiltonian, as in Ref. [141]. The effective Hamiltonian is an operator whose eigen-energies approximate the eigen-energies of the actual Hamiltonian to up to order $\mathcal{O}(\lambda^2)$, and its eigenstates approximate the eigenstates of the actual Hamiltonian up to order $\mathcal{O}(1)$. In other words, the eigenstates of the effective Hamiltonian are linear combinations of $|p_1\rangle$ and $|p_2\rangle$.

Using the result from Gottfried [141], the effective Hamiltonian is

$$\langle p_i|H_{\text{eff}}|p_j\rangle = E_0\delta_{i,j} + \langle p_i|V_{\boldsymbol{\lambda}}|p_j\rangle + \sum_{k=3}^{8}\frac{\langle p_i|V_{\boldsymbol{\lambda}}|p_k\rangle\langle p_k|V_{\boldsymbol{\lambda}}|p_j\rangle}{E_0 - E_{p_k}}, \tag{5.7}$$

where $i, j \in \{1, 2\}$. Therefore, each component of the effective Hamiltonian is

$$\begin{aligned}
\langle p_1|H_{\text{eff}}|p_1\rangle - E_0 &= \lambda_1^2\left(\frac{(J_{13})^2}{E_0 - E_1} + \frac{(J_{17})^2}{E_0 - E_3}\right) + \lambda_2^2\left(\frac{(J_{14})^2}{E_0 - E_2} + \frac{(J_{18})^2}{E_0 - E_4}\right),\\
\langle p_1|H_{\text{eff}}|p_2\rangle = \langle p_2|H_{\text{eff}}|p_1\rangle &= \lambda_1\lambda_2\left(\frac{J_{13}J_{23}}{E_0 - E_1} + \frac{J_{14}J_{24}}{E_0 - E_2}\right),\\
\langle p_2|H_{\text{eff}}|p_2\rangle - E_0 &= \lambda_2^2\left(\frac{(J_{23})^2}{E_0 - E_1} + \frac{(J_{25})^2}{E_0 - E_3}\right) + \lambda_1^2\left(\frac{(J_{24})^2}{E_0 - E_2} + \frac{(J_{26})^2}{E_0 - E_4}\right),
\end{aligned}$$

where we use the notation $J_{ij} = \langle p_i|J|p_j\rangle$, which we assume are real. Note that there are no terms linear in the λ variables in the above equations.

Compare the expressions in the equations above with the form of the Compton tensor where the position space integral has been performed (see appendix C for a derivation):

$$\begin{aligned}
T^{\mu\nu}_{\text{fwd}} &= \sum_X\left[\frac{\langle P|j^\mu(0)|X\rangle\langle X|j^\nu(0)|P\rangle}{E_X - (E_N + q^0)} + \frac{\langle P|j^\mu(0)|X\rangle\langle X|j^\nu(0)|P\rangle}{E_X - (E_N - q^0)}\right],\\
T^{\mu\nu}_{\text{off-fwd}} &= \sum_X\left[\frac{\langle P'|j^\mu(0)|X\rangle\langle X|j^\nu(0)|P\rangle}{E_X - (E_N + q^0)} + \frac{\langle P'|j^\mu(0)|X\rangle\langle X|j^\nu(0)|P\rangle}{E_X - (E_N - q'^0)}\right],
\end{aligned} \tag{5.8}$$

where $E_N = P^0$. Therefore, if we think of J as a current, and $|p_1\rangle$ as $|P\rangle$ and $|p_2\rangle$ as $|P'\rangle$, we can re-write the effective Hamiltonian as

$$H_{\text{eff}} - E_0 = \begin{pmatrix} \lambda_1^2 T(\omega_1) + \lambda_2^2 T(\omega_2) & \lambda_1\lambda_2\tilde{T}(\bar{\omega}) \\ \lambda_1\lambda_2\tilde{T}(\bar{\omega}) & \lambda_2^2 T(\omega_1) + \lambda_1^2 T(\omega_2) \end{pmatrix}, \tag{5.9}$$

where T is the simplified forward Compton tensor, and $\tilde{T}$ is the simplified off-forward Compton tensor. We have further assumed that, by some symmetries of our system, $J_{13} = J_{24}$, $J_{17} = J_{26}$, $J_{14} = J_{23}$, and $J_{18} = J_{25}$.

The eigenvalues of the effective Hamiltonian are

$$E^{\pm}_{\boldsymbol{\lambda}} = E_0 + \frac{A + B}{2} \pm \frac{1}{2}\sqrt{4C^2 + (A - B)^2} + \mathcal{O}(\lambda^3), \tag{5.10}$$

where

$$\begin{gathered}
A + B = (\lambda_1^2 + \lambda_2^2)\big(T(\omega_1) + T(\omega_2)\big), \quad A - B = (\lambda_1^2 - \lambda_2^2)\big(T(\omega_1) - T(\omega_2)\big),\\
C = \lambda_1\lambda_2\tilde{T}(\bar{\omega}).
\end{gathered} \tag{5.11}$$

If we let $\lambda_1 = \pm\lambda_2 = \lambda$, the eigenvalues become

$$E_\lambda^\pm = E_0 + \lambda^2\big(T(\omega_1) + T(\omega_2)\big) \pm \lambda^2|\tilde{T}(\bar{\omega})| + \mathcal{O}(\lambda^3). \tag{5.12}$$

And the eigenvectors are $v_\pm = \frac{1}{\sqrt{2}}(1, \pm 1)$. Therefore, the simplifed off-forward Compton tensor is

$$|\tilde{T}(\bar{\omega})| = \frac{E_\lambda^+ - E_\lambda^-}{2\lambda^2} + \mathcal{O}(\lambda).$$

This toy-model example captures the basic idea of the Feynman-Hellmann proof in the next section. We introduce a shift to our Lagrangian/Hamiltonian that mixes states of different momentum at *second order* through a current. Then, we show that the second order energy shift contains matrix elements with two insertions of the current. And since two different momenta are transferred through the currents, part of the shift is the off-forward Compton tensor.

5.2 Second-Order Off-Forward Feynman-Hellmann

In this section, we show the necessary FH relation of the form

$$\left.\frac{\partial^2 E}{\partial\lambda_1\partial\lambda_2}\right|_{\lambda_1\lambda_2=0} \simeq T^{33}(P, q; P', q'), \tag{5.13}$$

where T^{33} is the $\mu = \nu = 3$ component of the OFCT, as defined in Eq. 4.5. Here, the λ variables are couplings of the FH perturbation, and E is the energy extracted from a two-point function. The proof will use Euclidean path integrals that *have not been discretised in space and time.* A discretised derivation would be equivalent, except with Dirac delta functions replaced by Kronecker deltas and integrals replaced by sums.

The plan of the following section is:

1. Choose an appropriate perturbation to the QCD Lagrangian, and show the effect of this perturbation on the nucleon correlator (two-point correlation function).

2. Take the derivatives of the perturbed correlator with respect to λ in two ways: (1) the 'direct' derivative (we will define this later), and (2) path integral derivative.

3. Compare the Euclidean time dependence of terms from the direct and path integral derivatives, and equate terms either side of the equation with the same time-dependence. The energy shift (LHS of Eq. 5.13) comes from the direct derivative, while the matrix element (RHS) comes from the path integral derivative.

4. A relation of the form Eq. 5.13 follows.

5.2.1 Modified Action

The key element of a FH calculation is a perturbation to the action that depends on arbitrary parameters. The Lagrangian density is,

$$\mathcal{L} = \mathcal{L}_{\text{QCD}} + \mathcal{L}_{\text{FH}}, \tag{5.14}$$

where $\mathcal{L}_{\text{FH}}$ is the FH shift, which depends on the parameters $\boldsymbol{\lambda} = (\lambda_1, \lambda_2)$; we take these parameters to be small. Specifically, we choose $\mathcal{L}_{\text{FH}}$ to be

$$\mathcal{L}_{\text{FH}} = \Big[\lambda_1\big(e^{i\mathbf{q}\cdot\mathbf{z}} + e^{-i\mathbf{q}\cdot\mathbf{z}}\big) + \lambda_2\big(e^{i\mathbf{q}'\cdot\mathbf{z}} + e^{-i\mathbf{q}'\cdot\mathbf{z}}\big)\Big]J(\mathbf{z},\tau), \tag{5.15}$$

where $J(z) = \bar{\psi}_f(z)\gamma^3\psi_f(z)$ is the EM quark current (unit charge), with the choice of flavour f corresponding to the flavour of generalised form factor we wish to extract. Note that the combination of exponentials of the form $e^{ia} + e^{-ia}$ is used to keep the Lagrangian Hermitian, and therefore ensure its eigenvalues are real.

This perturbation to the Lagrangian density induces a perturbation to the Hamiltonian density $\mathcal{H} = \mathcal{H}_{\text{QCD}} + \mathcal{H}_{\text{FH}}$. We can find $\mathcal{H}_{\text{FH}}$ explicitly by using the relation between Lagrangian and Hamiltonian densities:

$$\mathcal{H} = \sum_f \frac{\partial\mathcal{L}}{\partial(\dot{\psi}_f)}\dot{\psi}_f + \sum_a \frac{\partial\mathcal{L}}{\partial(\dot{A}^a_\mu)}\dot{A}^a_\mu - \mathcal{L}. \tag{5.16}$$

Since

$$\frac{\partial\mathcal{L}_{\text{FH}}}{\partial(\dot{\psi}_f)} = 0 = \frac{\partial\mathcal{L}_{\text{FH}}}{\partial(\dot{A}^a_\mu)}, \tag{5.17}$$

we have that

$$\mathcal{H} = \mathcal{H}_{\text{QCD}} + \mathcal{H}_{\text{FH}} = \sum_f \frac{\partial\mathcal{L}_{\text{QCD}}}{\partial(\dot{\psi}_f)}\dot{\psi}_f + \sum_a \frac{\partial\mathcal{L}_{\text{QCD}}}{\partial(\dot{A}^a_\mu)}\dot{A}^a_\mu - \mathcal{L}_{\text{QCD}} - \mathcal{L}_{\text{FH}}. \tag{5.18}$$

Therefore, comparing $\boldsymbol{\lambda}$-dependence on each side, we have $\mathcal{H}_{\text{FH}} = -\mathcal{L}_{\text{FH}}$.

Since $\mathcal{L}_{\text{FH}}$ doesn't commute with the momentum operator (it mixes states of different momentum), neither does the perturbation to the Hamiltonian $\mathcal{H}_{\text{FH}}$. Of course, $\mathcal{H}_{\text{QCD}}$ commutes with the momentum operator. Therefore, the whole Hamiltonian density $\mathcal{H}$ doesn't commute with the momentum operator, $\hat{\mathbf{P}}$, and hence *our momentum eigenstates are not eigenstates of the perturbed Hamiltonian.* The translation operator is $\exp\{i\hat{\mathbf{P}}\cdot\mathbf{x}\}$, and therefore the Hamiltonian also doesn't commute with this operator.

Consider the nucleon correlator (two-point function) with a FH perturbation*:

$$\begin{aligned} C_{\boldsymbol{\lambda}}(\tau,\mathbf{p}') &= \int d^3z e^{-i\mathbf{p}'\cdot\mathbf{z}}\langle\Omega|\chi(\mathbf{z},\tau)\chi^\dagger(0)|\Omega\rangle \\ &= \sum_Y \int \frac{d^3k}{(2\pi)^3}\frac{1}{2E_Y(\mathbf{k})}\int d^3z e^{-i\mathbf{p}'\cdot\mathbf{z}}\langle\Omega|\chi(\mathbf{z},\tau)|Y(\mathbf{k})\rangle\langle Y(\mathbf{k})|\chi^\dagger(0)|\Omega\rangle \\ &= \sum_Y \int \frac{d^3k}{(2\pi)^3}\frac{1}{2E_Y(\mathbf{k})}\int d^3z e^{-i\mathbf{p}'\cdot\mathbf{z}}\langle\Omega|\chi(\mathbf{z},0)e^{-H(\boldsymbol{\lambda})\tau}|Y(\mathbf{k})\rangle\langle Y(\mathbf{k})|\chi^\dagger(0)|\Omega\rangle, \end{aligned} \tag{5.19}$$

where $|\Omega\rangle$ is the *perturbed* vacuum state, and hence it is an eigenstate of the perturbed Hamiltonian with eigenvalue zero. Here, χ is the nucleon interpolating operator from Eq. 2.24.

Now, we introduce another basis of eigenstates, $\{|X(a)\rangle\}$, that are eigenstates of the perturbed Hamiltonian and span the same space as the basis of momentum eigenstates,

*The standard notation in this chapter and chapter 7 is to always use $\mathbf{p}'$ to denote the sink momentum.

$\{|Y(\mathbf{k})\rangle\}$. These states are labelled by a new quantum number a with corresponding operator $\mathcal{A}$. We will hold off on discussing explicitly what this operator is until section 5.3.

For finite volume, the relation between these two bases is

$$|Y(\mathbf{k}_i)\rangle = \sum_{X,a} c_{X,a}(\mathbf{k}_i, Y)|X(a)\rangle, \quad |X(a)\rangle = \sum_{Y,i} (c_{X,a}(\mathbf{k}_i, Y))^* |Y(\mathbf{k}_i)\rangle. \tag{5.20}$$

Since we have relativistic normalisation $\langle X(\mathbf{p})|Y(\mathbf{k})\rangle = 2E_X(\mathbf{p})\delta_{X,Y}(2\pi)^2\delta^{(3)}(\mathbf{p}-\mathbf{k})$, the coefficients $c_{X,a}(\mathbf{k})$ are not simply the overlap $\langle X(a)|Y(\mathbf{k})\rangle$. However, by unitarity, we must still have $\sum_{X,a}|c_{X,a}(\mathbf{k}_i)|^2$. We use X to label the new states $|X(a)\rangle$, even though strictly speaking these states can be the superposition of multiple different hadronic states. It is simplest to think of X as the hadronic state of $|X(a)\rangle$ in the limit that $\boldsymbol{\lambda} \to 0$.

Using Eq. 5.20, we have

$$e^{-H(\boldsymbol{\lambda})\tau}|Y(\mathbf{k})\rangle = e^{-H(\boldsymbol{\lambda})\tau}\sum_{X,a} c_{a,X}(\mathbf{k}, Y)|X(a)\rangle = \sum_{X,a} c_{a,X}(\mathbf{k}, Y)e^{-E_{X,a}\tau}|X(a)\rangle. \tag{5.21}$$

Inserting Eq. 5.21 into Eq. 5.19, we get

$$\begin{aligned} C_{\boldsymbol{\lambda}}(\tau, \mathbf{p}') = \sum_{X,a} e^{-E_{X,a}\tau} \sum_{Y} \int \frac{d^3k}{(2\pi)^3}\frac{1}{2E_Y(\mathbf{k})} \\ \times \int d^3z e^{-i\mathbf{p}'\cdot\mathbf{z}} c_{a,X}(\mathbf{k}, Y)\langle\Omega|\chi(\mathbf{z}, 0)|X(a)\rangle\langle Y(\mathbf{k})|\chi^\dagger(0)|\Omega\rangle. \end{aligned} \tag{5.22}$$

We can re-express this as

$$C_{\boldsymbol{\lambda}}(\tau, \mathbf{p}') = \sum_{X,a} A_{X,a} e^{-E_{X,a}\tau}, \tag{5.23}$$

where the coefficient $A_{X,a}$ is just the appropriate terms taken from Eq. 5.22. We will further discuss what $\mathcal{A}$ can be and find a more explicit form of the perturbed correlator in section 5.3.

5.2.2 Derivatives of the Correlator

The rest of the Feynman-Hellmann proof will then be to compare the 'direct' derivative of Eq. 5.23 to the same derivative expressed as the derivative of a path integral. The former will give us an energy derivative, while the latter will give us a matrix element, and hence from both we will get a FH relation of the form Eq. 5.13.

Direct Derivative

We will assume that $C_{\boldsymbol{\lambda}}$ is at least twice-differentiable in its λ variables, if not analytic in them. Therefore, from Eq. 5.23,

$$\left.\frac{\partial C_{\boldsymbol{\lambda}}}{\partial \lambda_i}\right|_{\lambda_i=0} = \sum_{X,a}\left(\frac{\partial A_{X,a}}{\partial \lambda_i} - \tau\frac{\partial E_{X,a}}{\partial \lambda_i}\right)e^{-E_{X,a}\tau}\Bigg|_{\lambda_i=0}. \tag{5.24}$$

Hence the mixed second derivative is

$$\begin{aligned}\left.\frac{\partial^2 C_{\boldsymbol{\lambda}}}{\partial\lambda_1\partial\lambda_2}\right|_{\lambda_1=\lambda_2=0} = \sum_{X,a}\Bigg[&\frac{\partial^2 A_{X,a}}{\partial\lambda_1\partial\lambda_2} - \tau\frac{\partial E_{X,a}}{\partial\lambda_1}\frac{\partial A_{X,a}}{\partial\lambda_2} - \tau\frac{\partial E_{X,a}}{\partial\lambda_2}\frac{\partial A_{X,a}}{\partial\lambda_1} \\ &+ \tau^2\frac{\partial E_{X,a}}{\partial\lambda_2}\frac{\partial E_{X,a}}{\partial\lambda_1}A_{X,a} - \tau\frac{\partial^2 E_{X,a}}{\partial\lambda_1\partial\lambda_2}A_{X,a}\Bigg]e^{-E_{X,a}\tau}\Bigg|_{\lambda_1=\lambda_2=0}.\end{aligned} \tag{5.25}$$

Note that the terms in Eqs. 5.24 and 5.25 have different τ-dependencies. In particular, the terms that will give us the FH relation are those that have τ-dependence like $\tau e^{-E\tau}$; we call these terms τ-*enhanced*.

Path Integral Derivative

Now we compare these direct derivatives (Eqs. 5.24 and 5.25) to a derivative of the path integral expression.

As we discussed in section 2.2, the vacuum matrix element[†] of an operator in the Euclidean path integral formalism is

$$\langle\mathcal{O}\rangle = \frac{\int\mathcal{D}\phi\mathcal{O}e^{-S}}{\int\mathcal{D}\phi e^{-S}}, \tag{5.26}$$

where $\mathcal{D}\phi$ indicates a functional integral over all fermion and gauge fields. Then one can show, using Eq. 5.26, that

$$\frac{\partial\langle\mathcal{O}\rangle}{\partial\lambda_i} = \langle\mathcal{O}\rangle\left\langle\frac{\partial S}{\partial\lambda_i}\right\rangle - \left\langle T\left\{\mathcal{O}\frac{\partial S}{\partial\lambda_i}\right\}\right\rangle, \quad i=1,2. \tag{5.27}$$

Then taking the derivative of Eq. 5.27 with respect to the opposite λ,

$$\frac{\partial^2\langle\mathcal{O}\rangle}{\partial\lambda_2\partial\lambda_1} = \frac{\partial\langle\mathcal{O}\rangle}{\partial\lambda_2}\left\langle\frac{\partial S}{\partial\lambda_1}\right\rangle + \langle\mathcal{O}\rangle\frac{\partial}{\partial\lambda_2}\left\langle\frac{\partial S}{\partial\lambda_1}\right\rangle - \frac{\partial}{\partial\lambda_2}\left\langle T\left\{\mathcal{O}\frac{\partial S}{\partial\lambda_1}\right\}\right\rangle. \tag{5.28}$$

The derivatives of the action are

$$\frac{\partial S}{\partial\lambda_1} = \int_{-\infty}^{\infty}d\tau\int d^3y\big(e^{i\mathbf{q}\cdot\mathbf{y}} + e^{-i\mathbf{q}\cdot\mathbf{y}}\big)J(\mathbf{y},\tau), \tag{5.29}$$

$$\frac{\partial S}{\partial\lambda_2} = \int_{-\infty}^{\infty}d\tau\int d^3y\big(e^{i\mathbf{q}'\cdot\mathbf{y}} + e^{-i\mathbf{q}'\cdot\mathbf{y}}\big)J(\mathbf{y},\tau). \tag{5.30}$$

From Eqs. 5.29 and 5.30, the action itself has no cross terms in λ_1 and λ_2, and hence the second term on the RHS of Eq. 5.28 vanishes. Moreover, we can use Eq. 5.27 to

[†]We use the notation $\langle\mathcal{O}\rangle$ and $\langle\Omega|\mathcal{O}|\Omega\rangle$ interchangeably; they are equivalent.

evaluate the first and third terms on the RHS of Eq. 5.28:

$$\begin{aligned}\frac{\partial^2\langle\mathcal{O}\rangle}{\partial\lambda_2\partial\lambda_1} =& \Big(\langle\mathcal{O}\rangle\Big\langle\frac{\partial S}{\partial\lambda_2}\Big\rangle - \Big\langle T\Big\{\mathcal{O}\frac{\partial S}{\partial\lambda_2}\Big\}\Big\rangle\Big)\Big\langle\frac{\partial S}{\partial\lambda_1}\Big\rangle \\ &- \Big\langle T\Big\{\mathcal{O}\frac{\partial S}{\partial\lambda_1}\Big\}\Big\rangle\Big\langle\frac{\partial S}{\partial\lambda_2}\Big\rangle + \Big\langle T\Big\{\mathcal{O}\frac{\partial S}{\partial\lambda_1}\frac{\partial S}{\partial\lambda_2}\Big\}\Big\rangle \\ =&\langle\mathcal{O}\rangle\Big\langle\frac{\partial S}{\partial\lambda_2}\Big\rangle\Big\langle\frac{\partial S}{\partial\lambda_1}\Big\rangle - \Big\langle T\Big\{\mathcal{O}\frac{\partial S}{\partial\lambda_2}\Big\}\Big\rangle\Big\langle\frac{\partial S}{\partial\lambda_1}\Big\rangle \\ &- \Big\langle T\Big\{\mathcal{O}\frac{\partial S}{\partial\lambda_1}\Big\}\Big\rangle\Big\langle\frac{\partial S}{\partial\lambda_2}\Big\rangle + \Big\langle T\Big\{\mathcal{O}\frac{\partial S}{\partial\lambda_1}\frac{\partial S}{\partial\lambda_2}\Big\}\Big\rangle.\end{aligned} \tag{5.31}$$

For the operator $\mathcal{O}$ we use

$$\int d^3z e^{-i\mathbf{p}'\cdot\mathbf{z}}\Gamma_{\beta\alpha}\chi_\alpha(\mathbf{z},\tau)\chi^\dagger_\beta(0), \tag{5.32}$$

where we assume $\tau > 0$, and Γ is some projection matrix in Dirac space. Here, χ is the nucleon interpolating operator (see Eq. 2.24) that couples to QCD states with the same quantum numbers as the nucleon - i.e. the nucleon and its excited states. Therefore,

$$\langle\mathcal{O}\rangle = \int d^3z e^{-i\mathbf{p}'\cdot\mathbf{z}}\Gamma_{\beta\alpha}\langle\Omega|\chi(\mathbf{z},\tau)_\alpha\chi^\dagger_\beta(0)|\Omega\rangle = C_{\boldsymbol{\lambda}}(\tau,\mathbf{p}'), \tag{5.33}$$

the correlator (two-point function) of a nucleon. Finally, evaluating Eq. 5.31 at $\lambda_1 = \lambda_2 = 0$, we will get the mixed second derivative of the perturbed correlator. Hence we can equate the matrix element on the RHS of Eq. 5.31 to Eq. 5.25.

5.2.3 Vanishing First Order Shift

From the simple quantum mechanical arguments in 5.1, we saw that there were no linear terms in λ for our perturbed energies (Eq. 5.9). This was due to a choice of kinematics: at first order, the perturbing potential mixed a state $|p_1\rangle$ with a non-degenerate state $|p_1 \pm q^{(\prime)}\rangle$. As such, there was no linear shift in the energy.

Similarly, we want to show that, if we choose our $\mathbf{q}$ momenta such that $|\mathbf{p}'| \neq |\mathbf{p}' \pm \mathbf{q}^{(\prime)}|$, the first order shift $\partial E_{X,a}/\partial\lambda_i$ vanishes. Clearly, from Eq. 5.25, this would give our 'direct' derivative a much cleaner form.

We start by inserting Eqs. 5.29, 5.32 and 5.33 into Eq. 5.27:

$$\begin{aligned}&\frac{\partial C_{\boldsymbol{\lambda}}(\tau,\mathbf{p}')}{\partial\lambda_1}\Big|_{\lambda_1=\lambda_2=0} = C_{\boldsymbol{\lambda}}(\tau,\mathbf{p}')\Big\langle\frac{\partial S}{\partial\lambda_1}\Big\rangle\Big|_{\lambda_1=\lambda_2=0} \\ &- \Big\langle T\Big\{\int d^3z e^{-i\mathbf{p}'\cdot\mathbf{z}}\Gamma_{\beta\alpha}\chi_\alpha(\mathbf{z},\tau)\chi^\dagger_\beta(0)\int_{-\infty}^{\infty}d\tau'\int d^3y\big(e^{i\mathbf{q}\cdot\mathbf{y}} + e^{-i\mathbf{q}\cdot\mathbf{y}}\big)J(\mathbf{y},\tau')\Big\}\Big\rangle\Big|_{\lambda_1=\lambda_2=0}.\end{aligned} \tag{5.34}$$

A key detail to note about Eq. 5.34 (and all other matrix elements considered in this derivation) is that it's evaluated at $\lambda_1 = \lambda_2 = 0$, the unperturbed case. This means that the difficulties we mentioned in subsection 5.2.1 don't apply here: the Euclidean translation operator is simply $e^{-H\tau + i\hat{\mathbf{P}}\cdot\mathbf{z}}$, where the Hamiltonian and momentum operators are both unperturbed.

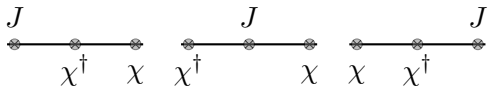

Figure 5.2: Graphical representation of the three cases of time-ordering in Eq. 5.35. In each subgraph, τ increases left to right.

From here on we suppress the projector, Dirac indices and evaluation at $\lambda_1 = \lambda_2 = 0$, but of course they're still being carried around, and all matrix elements will be in terms of unperturbed quantities. Looking closer at the second term of Eq. 5.34, we can expand the time-ordering (see figure 5.2):

$$\begin{aligned}
&\Big\langle T\Big\{\int d^3z e^{-i\mathbf{p}'\cdot\mathbf{z}}\chi(\mathbf{z},\tau)\chi^\dagger(0)\int_{-\infty}^{\infty}d\tau'\int d^3y\big(e^{i\mathbf{q}\cdot\mathbf{y}}+e^{-i\mathbf{q}\cdot\mathbf{y}}\big)J(\mathbf{y},\tau')\Big\}\Big\rangle \\
&=\int_{-\infty}^{\infty}d\tau'\int d^3zd^3y\big(e^{i\mathbf{q}\cdot\mathbf{y}}+e^{-i\mathbf{q}\cdot\mathbf{y}}\big)e^{-i\mathbf{p}'\cdot\mathbf{z}}\big\langle T\big\{\chi(\mathbf{z},\tau)\chi^\dagger(0)J(\mathbf{y},\tau')\big\}\big\rangle \\
&=\int_{-\infty}^{0}d\tau'\int d^3zd^3y\big(e^{i\mathbf{q}\cdot\mathbf{y}}+e^{-i\mathbf{q}\cdot\mathbf{y}}\big)e^{-i\mathbf{p}'\cdot\mathbf{z}}\big\langle\chi(\mathbf{z},\tau)\chi^\dagger(0)J(\mathbf{y},\tau')\big\rangle \\
&+\int_{0}^{\tau}d\tau'\int d^3zd^3y\big(e^{i\mathbf{q}\cdot\mathbf{y}}+e^{-i\mathbf{q}\cdot\mathbf{y}}\big)e^{-i\mathbf{p}'\cdot\mathbf{z}}\big\langle\chi(\mathbf{z},\tau)J(\mathbf{y},\tau')\chi^\dagger(0)\big\rangle \\
&+\int_{\tau}^{\infty}d\tau'\int d^3zd^3y\big(e^{i\mathbf{q}\cdot\mathbf{y}}+e^{-i\mathbf{q}\cdot\mathbf{y}}\big)e^{-i\mathbf{p}'\cdot\mathbf{z}}\big\langle J(\mathbf{y},\tau')\chi(\mathbf{z},\tau)\chi^\dagger(0)\big\rangle.
\end{aligned} \tag{5.35}$$

Now, each of the terms in Eq. 5.35 is simply a three-point function.

$$\begin{aligned}
&\Big\langle T\Big\{\int d^3z e^{-i\mathbf{p}'\cdot\mathbf{z}}\chi(\mathbf{z},\tau)\chi^\dagger(0)\int_{-\infty}^{\infty}d\tau'\int d^3y\big(e^{i\mathbf{q}\cdot\mathbf{y}}+e^{-i\mathbf{q}\cdot\mathbf{y}}\big)J(\mathbf{y},\tau')\Big\}\Big\rangle \\
&=\int_{-\infty}^{0}d\tau' C^{(3)}_{\chi\chi^\dagger J}(\mathbf{p}',\mathbf{q};\tau,0,\tau')+\int_{0}^{\tau}d\tau' C^{(3)}_{\chi J\chi^\dagger}(\mathbf{p}',\mathbf{p}'-\mathbf{q};\tau,\tau',0) \\
&+\int_{\tau}^{\infty}d\tau' C^{(3)}_{J\chi\chi^\dagger}(-\mathbf{q},\mathbf{p}'-\mathbf{q};\tau',\tau,0).
\end{aligned} \tag{5.36}$$

Explicit calculations of three point functions are given in appendix F. The calculations in appendix F only apply in the case where our momentum eigenstates are also eigenstates of our Hamiltonian. This is why it was important that our matrix elements are calculated in terms of unperturbed quantities. To quote the result of appendix F,

$$\begin{aligned}
C^{(3)}_{\mathcal{O}_1\mathcal{O}_2\mathcal{O}_3}(\mathbf{p}_1,\mathbf{p}_2;\tau_1,\tau_2,\tau_3) = \sum_{X,Y}&\frac{e^{-E_X(\mathbf{p}_1)(\tau_1-\tau_2)}}{2E_X(\mathbf{p}_1)}\frac{e^{-E_Y(\mathbf{p}_2)(\tau_2-\tau_3)}}{2E_Y(\mathbf{p}_2)} \\
&\times\langle\Omega|\mathcal{O}_1(0)|X(\mathbf{p}_1)\rangle\langle X(\mathbf{p}_1)|\mathcal{O}_2(0)|Y(\mathbf{p}_2)\rangle\langle Y(\mathbf{p}_2)|\mathcal{O}_3(0)|\Omega\rangle.
\end{aligned}$$

In the following we let our kinematics be such $|\mathbf{p}'| \neq |\mathbf{p}' \pm \mathbf{q}^{(\prime)}|$. Then, we will assume that this kinematic restriction implies $E_Y(\mathbf{p}') \neq E_X(\mathbf{p}' \pm \mathbf{q}^{(\prime)})$ for all hadronic states X, Y.

Therefore, the first integral in Eq. 5.36 is

$$\int_{-\infty}^{0} d\tau' C^{(3)}_{\chi\chi^\dagger J}(\mathbf{p}',\mathbf{q};\tau,0,\tau') = \sum_{X,Y} \frac{e^{-E_X(\mathbf{p}')\tau}}{4E_X(\mathbf{p}')E_Y^2(\mathbf{q})} \times \langle\Omega|\chi(0)|X(\mathbf{p}')\rangle\langle X(\mathbf{p}')|\chi^\dagger(0)|Y(\mathbf{q})\rangle\langle Y(\mathbf{q})|J(0)|\Omega\rangle. \tag{5.37}$$

The second integral is

$$\int_{0}^{\tau} d\tau' C^{(3)}_{\chi J\chi^\dagger}(\mathbf{p}',\mathbf{p}'-\mathbf{q};\tau,\tau',0) = \sum_{X,Y} \frac{e^{-E_Y(\mathbf{p}'-\mathbf{q})\tau} - e^{-E_X(\mathbf{p}')\tau}}{4E_X(\mathbf{p}')E_Y(\mathbf{p}'-\mathbf{q})\big(E_X(\mathbf{p}')-E_Y(\mathbf{p}'-\mathbf{q})\big)} \times \langle\Omega|\chi(0)|X(\mathbf{p}')\rangle\langle X(\mathbf{p}')|\chi^\dagger(0)|Y(\mathbf{p}'-\mathbf{q})\rangle\langle Y(\mathbf{p}'-\mathbf{q})|J(0)|\Omega\rangle. \tag{5.38}$$

The third integral is

$$\int_{\tau}^{\infty} d\tau' C^{(3)}_{J\chi\chi^\dagger}(-\mathbf{q},\mathbf{p}'-\mathbf{q};\tau',\tau,0) = \sum_{X,Y} \frac{e^{-E_Y(\mathbf{p}'-\mathbf{q})\tau}}{4E_Y(\mathbf{p}'-\mathbf{q})E_X^2(-\mathbf{q})} \times \langle\Omega|\mathcal{O}_1(0)|X(-\mathbf{q})\rangle\langle X(-\mathbf{q})|\mathcal{O}_2(0)|Y(\mathbf{p}'-\mathbf{q})\rangle\langle Y(\mathbf{p}'-\mathbf{q})|\mathcal{O}_3(0)|\Omega\rangle. \tag{5.39}$$

Now we compare the τ-dependence of Eqs. 5.34 and 5.24:

$$\sum_X e^{-E_{X,a}(\mathbf{p}')\tau}\left[\frac{\partial A_{X,a}(\mathbf{p}')}{\partial\lambda_1} - \tau\frac{\partial E_{X,a}(\mathbf{p}')}{\partial\lambda_1}A_{X,a}(\mathbf{p}')\right]\Big|_{\lambda_1=\lambda_2=0} = \sum_X C_1 e^{-E_X(\mathbf{p}')\tau} - \sum_{X,Y}\Big[C_2 e^{-E_X(\mathbf{p}')\tau} + C_3\big(e^{-E_Y(\mathbf{p}'-\mathbf{q})\tau} - e^{-E_X(\mathbf{p}')\tau}\big) + C_4 e^{-E_Y(\mathbf{p}'-\mathbf{q})\tau}\Big]. \tag{5.40}$$

The RHS uses Eq. 5.34, 5.37, 5.38, 5.39. Here the C_i are constant in Euclidean time, but otherwise depend on X, Y, momentum variables, etc. Hence, since $\frac{\partial E_{X,a}(\mathbf{p}')}{\partial\lambda_1}$ is the only τ-enhanced term in Eq. 5.40, matching like terms, $\frac{\partial E_{X,a}(\mathbf{p}')}{\partial\lambda_1} = 0$.

Since the perturbing Lagrangian density, Eq. 5.15, is symmetric under the simultaneous exchanges $\lambda_1 \leftrightarrow \lambda_2$ and $\mathbf{q} \leftrightarrow \mathbf{q}'$, we have an analogous result for the derivative with respect to λ_2:

$$\frac{\partial E_{X,a}(\mathbf{p}')}{\partial\lambda_1} = 0 = \frac{\partial E_{X,a}(\mathbf{p}')}{\partial\lambda_2}. \tag{5.41}$$

5.2.4 Second-Order Derivative

Using result Eq. 5.41, we can greatly simplify the direct derivative Eq. 5.25:

$$\frac{\partial^2 C_{\boldsymbol{\lambda}}(\tau,\mathbf{p}')}{\partial\lambda_1\partial\lambda_2}\Big|_{\lambda_1=\lambda_2=0} = \sum_{X,a} e^{-E_{X,a}(\mathbf{p}')\tau}\left[\frac{\partial^2 A_{X,a}(\mathbf{p}')}{\partial\lambda_1\partial\lambda_2} - \tau\frac{\partial^2 E_{X,a}(\mathbf{p}')}{\partial\lambda_1\partial\lambda_2}A_{X,a}(\mathbf{p}')\right]\Big|_{\lambda_1=\lambda_2=0}. \tag{5.42}$$

Now we compare this to the path integral derivative, by substituting Eq. 5.32 into Eq. 5.31:

$$\begin{aligned}\left.\frac{\partial^2 C_{\boldsymbol{\lambda}}(\tau,\mathbf{p})}{\partial\lambda_2\partial\lambda_1}\right|_{\lambda_1=\lambda_2=0} =& C_{\boldsymbol{\lambda}}(\tau,\mathbf{p}')\left\langle\frac{\partial S}{\partial\lambda_2}\right\rangle\left\langle\frac{\partial S}{\partial\lambda_1}\right\rangle\Bigg|_{\lambda_1=\lambda_2=0}\\ &-\left\langle T\left\{\int d^3z e^{-i\mathbf{p}'\cdot\mathbf{z}}\chi(\mathbf{z},\tau)\chi^\dagger(0)\frac{\partial S}{\partial\lambda_2}\right\}\right\rangle\left\langle\frac{\partial S}{\partial\lambda_1}\right\rangle\Bigg|_{\lambda_1=\lambda_2=0}\\ &-\left\langle T\left\{\int d^3z e^{-i\mathbf{p}'\cdot\mathbf{z}}\chi(\mathbf{z},\tau)\chi^\dagger(0)\frac{\partial S}{\partial\lambda_1}\right\}\right\rangle\left\langle\frac{\partial S}{\partial\lambda_2}\right\rangle\Bigg|_{\lambda_1=\lambda_2=0}\\ &+\left\langle T\left\{\int d^3z e^{-i\mathbf{p}'\cdot\mathbf{z}}\chi(\mathbf{z},\tau)\chi^\dagger(0)\frac{\partial S}{\partial\lambda_1}\frac{\partial S}{\partial\lambda_2}\right\}\right\rangle\Bigg|_{\lambda_1=\lambda_2=0}.\end{aligned} \tag{5.43}$$

Since the $\frac{\partial^2 E_{X,a}(\mathbf{p}')}{\partial\lambda_1\partial\lambda_2}$ term is the only term in Eq. 5.42 that is τ-enhanced, we will look for the τ-enhanced component of Eq. 5.43.

Note that the τ-dependence of the second and third terms on the RHS of Eq. 5.43 are three-point functions we considered in subsection 5.41. Hence these don't contain τ-enhanced contributions. Moreover, the first term's τ-dependence is entirely contained in the correlator, which is not τ-enhanced. Therefore, the only possible τ-enhanced contribution to Eq. 5.43 comes from the fourth term on the RHS.

Let's start by expanding this term using the explicit form of the action derivatives, Eqs. 5.29 and 5.30. Once again we drop the explicit evaluation at $\lambda_1 = \lambda_2 = 0$.

$$\begin{aligned}&\left\langle T\left\{\int d^3z e^{-i\mathbf{p}'\cdot\mathbf{z}}\chi(\mathbf{z},\tau)\chi^\dagger(0)\int_{-\infty}^{\infty}d\tau_1\int d^3y\big(e^{i\mathbf{q}\cdot\mathbf{y}}+e^{-i\mathbf{q}\cdot\mathbf{y}}\big)J(\mathbf{y},\tau_1)\right.\right.\\ &\left.\left.\times\int_{-\infty}^{\infty}d\tau_2\int d^3y'\big(e^{i\mathbf{q}'\cdot\mathbf{y}'}+e^{-i\mathbf{q}'\cdot\mathbf{y}'}\big)J(\mathbf{y}',\tau_2)\right\}\right\rangle\\ &=\int d^3z d^3y' d^3y e^{-i\mathbf{p}'\cdot\mathbf{z}}\big(e^{i\mathbf{q}\cdot\mathbf{y}}+e^{-i\mathbf{q}\cdot\mathbf{y}}\big)\big(e^{i\mathbf{q}'\cdot\mathbf{y}'}+e^{-i\mathbf{q}'\cdot\mathbf{y}'}\big)\\ &\times\left\{\int_{-\infty}^{0}d\tau_1\int_{-\infty}^{\tau_1}d\tau_2\Big\langle\chi(\mathbf{z},\tau)\chi^\dagger(0)J(\mathbf{y},\tau_1)J(\mathbf{y}',\tau_2)\Big\rangle\right.\\ &+\int_{0}^{\tau}d\tau_1\int_{-\infty}^{0}d\tau_2\Big\langle\chi(\mathbf{z},\tau)J(\mathbf{y},\tau_1)\chi^\dagger(0)J(\mathbf{y}',\tau_2)\Big\rangle\\ &+\int_{0}^{\tau}d\tau_1\int_{0}^{\tau_1}d\tau_2\Big\langle\chi(\mathbf{z},\tau)J(\mathbf{y},\tau_1)J(\mathbf{y}',\tau_2)\chi^\dagger(0)\Big\rangle\\ &+\int_{\tau}^{\infty}d\tau_1\int_{-\infty}^{0}d\tau_2\Big\langle J(\mathbf{y},\tau_1)\chi(\mathbf{z},\tau)\chi^\dagger(0)J(\mathbf{y}',\tau_2)\Big\rangle\\ &+\int_{\tau}^{\infty}d\tau_1\int_{0}^{\tau}d\tau_2\Big\langle J(\mathbf{y},\tau_1)\chi(\mathbf{z},\tau)J(\mathbf{y}',\tau_2)\chi^\dagger(0)\Big\rangle\\ &+\int_{\tau}^{\infty}d\tau_1\int_{\tau}^{\tau_1}d\tau_2\Big\langle J(\mathbf{y},\tau_1)J(\mathbf{y}',\tau_2)\chi(\mathbf{z},\tau)\chi^\dagger(0)\Big\rangle\\ &\left.+\Big[(\mathbf{y}',\tau_2)\leftrightarrow(\mathbf{y},\tau_1)\Big]\right\}.\end{aligned} \tag{5.44}$$

5.2.5 Four-Point Functions

Equation 5.44 gives us a total of twelve four-point functions multiplied by four separate Fourier projections. That gives a total of 48 integrals to evaluate. However, note that

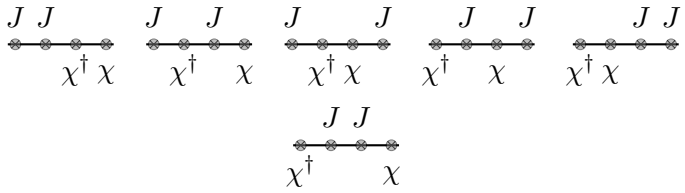

Figure 5.3: Graphical representation of the six cases of time-ordering. In each subgraph, τ increases left to right. The only region that produces τ-enhanced terms is the subgraph in the second line.

there are really only six different ways to order the J and χ operators in Euclidean time (see figure 5.3). Therefore, we consider the generalised integral

$$\int d^3z d^3y_1 d^3y_2 e^{-i\mathbf{p}'\cdot\mathbf{z}} e^{i\mathbf{q}\cdot\mathbf{y}_1} e^{i\mathbf{q}_2\cdot\mathbf{y}_2} \int_{-\infty}^{\infty} d\tau_1' \int_{-\infty}^{\infty} d\tau_2' \Big\langle T\Big\{\chi(\mathbf{z},\tau) J(\mathbf{y}_1,\tau_1') J(\mathbf{y}_2,\tau_2') \chi^\dagger(0)\Big\}\Big\rangle, \tag{5.45}$$

where $(\mathbf{y}_{1,2}, \tau_{1,2}')$ stand in for $(\mathbf{y}^{(\prime)}, \tau_{1,2})$, and $\mathbf{q}_{1,2}$ stand in for $\pm\mathbf{q}^{(\prime)}$. Without loss of generality, assume $\tau_1' > \tau_2'$. Then, Eq. 5.45 breaks up into the six cases shown in figure 5.3.

Here, our kinematic choices become very important. We already specified in subsection 5.2.3 that $|\mathbf{p}'| \neq |\mathbf{p}' \pm \mathbf{q}^{(\prime)}|$. From here on we will choose our $\mathbf{q}$s and $\mathbf{p}'$ such that $|\mathbf{p}'| = |\mathbf{p}' + \mathbf{q} - \mathbf{q}'|$. This is significant, since it implies $E_X(\mathbf{p}') = E_X(\mathbf{p}' + \mathbf{q} - \mathbf{q}')$ and hence we can have τ-enhanced terms.

Finally, in appendix F we give an explicit calculation of the four-point function, again assuming that we're using unperturbed quantities:

$$\begin{aligned} C^{(4)}_{\mathcal{O}_1\mathcal{O}_2\mathcal{O}_3\mathcal{O}_4}(\mathbf{p}_1,\mathbf{p}_2,\mathbf{p}_3;\tau_1,\tau_2,\tau_3,\tau_4) = \sum_{X,Y,Z} \frac{e^{-E_X(\mathbf{p}_1)(\tau_1-\tau_2)}}{2E_X(\mathbf{p}_1)} \frac{e^{-E_Y(\mathbf{p}_2)(\tau_2-\tau_3)}}{2E_Y(\mathbf{p}_2)} \frac{e^{-E_Z(\mathbf{p}_3)(\tau_3-\tau_4)}}{2E_Z(\mathbf{p}_3)} \\ \times \langle\Omega|\mathcal{O}_1(0)|X(\mathbf{p}_1)\rangle\langle X(\mathbf{p}_1)|\mathcal{O}_2(0)|Y(\mathbf{p}_2)\rangle\langle Y(\mathbf{p}_2)|\mathcal{O}_3(0)|Z(\mathbf{p}_3)\rangle\langle Z(\mathbf{p}_3)|\mathcal{O}_4(0)|\Omega\rangle. \end{aligned}$$

However, since we are just interested in the τ behaviour for the moment (to determine which term is τ-enhanced), we will only look at the exponentials given in the above equation and the integral of τ.

Case 1

The first case is $\tau > 0 > \tau_1' > \tau_2'$ (figure 5.3, top line far left). Looking at Eqs. 5.45 and the four-point function above, we have that

$$\mathbf{p}_1 = \mathbf{p}', \quad \mathbf{p}_2 = \mathbf{q}_1 + \mathbf{q}_2, \quad \mathbf{p}_3 = \mathbf{q}_2. \tag{5.46}$$

The integral in this case is therefore

$$\int_{-\infty}^{0} d\tau_1' \int_{-\infty}^{\tau_1'} d\tau_2' e^{-E_X(\mathbf{p}')\tau} e^{E_Y(\mathbf{q}_1+\mathbf{q}_2)\tau_1'} e^{-E_Z(\mathbf{q}_2)(\tau_1'-\tau_2')}. \tag{5.47}$$

which goes like a sum of exponentials $e^{-E\tau}$ in τ for any choice of kinematics.

Case 2

The second case is $\tau > \tau_1' > 0 > \tau_2'$ (figure 5.3, top line centre left).

$$\mathbf{p}_1 = \mathbf{p}', \quad \mathbf{p}_2 = \mathbf{p}' - \mathbf{q}_1, \quad \mathbf{p}_3 = \mathbf{q}_2. \tag{5.48}$$

The integral is

$$\int_0^\tau d\tau_1' \int_{-\infty}^0 d\tau_2' e^{-E_X(\mathbf{p}')(\tau-\tau_1')} e^{-E_Y(\mathbf{p}'-\mathbf{q}_1)(\tau_1'-\tau)} e^{-E_Z(\mathbf{q}_2)(\tau-\tau_2')}, \tag{5.49}$$

which is τ-enhanced for $E_X(\mathbf{p}') = E_Y(\mathbf{p}' - \mathbf{q}_1)$. Hence this integral is not τ-enhanced under our choice of kinematics.

Case 3

The third case is $\tau_1' > \tau > 0 > \tau_2'$ (figure 5.3, top line centre).

$$\mathbf{p}_1 = -\mathbf{q}_1, \quad \mathbf{p}_2 = \mathbf{p}' - \mathbf{q}_1, \quad \mathbf{p}_3 = \mathbf{q}_2. \tag{5.50}$$

$$\int_\tau^\infty d\tau_1' \int_{-\infty}^0 d\tau_2' e^{-E_X(-\mathbf{q}_1)(\tau_1'-\tau)} e^{-E_Y(\mathbf{p}'-\mathbf{q}_1)\tau} e^{E_Z(\mathbf{q}_2)\tau_2'}, \tag{5.51}$$

which has no possible τ-enhancement.

Case 4

The fourth case is $\tau_1' > \tau > \tau_2' > 0$ (figure 5.3, top line centre right).

$$\mathbf{p}_1 = -\mathbf{q}_1, \quad \mathbf{p}_2 = \mathbf{p}' - \mathbf{q}_1, \quad \mathbf{p}_3 = \mathbf{p}' - \mathbf{q}_1 - \mathbf{q}_2. \tag{5.52}$$

$$\int_\tau^\infty d\tau_1' \int_0^\tau d\tau_2' e^{-E_X(-\mathbf{q}_1)(\tau_1'-\tau)} e^{-E_Y(\mathbf{p}'-\mathbf{q}_1)(\tau-\tau_2')} e^{-E_Z(\mathbf{p}'-\mathbf{q}_1-\mathbf{q}_2)(\tau_2'-\tau)}, \tag{5.53}$$

which is τ-enhanced for $E_Y(\mathbf{p}' - \mathbf{q}_1) = E_Z(\mathbf{p}' - \mathbf{q}_1 - \mathbf{q}_2)$. Hence this integral is not τ-enhanced under our choice of kinematics.

Case 5

The fifth case is $\tau_1' > \tau_2' > \tau > 0$ (figure 5.3, top line far right).

$$\mathbf{p}_1 = -\mathbf{q}_1, \quad \mathbf{p}_2 = -\mathbf{q}_1 - \mathbf{q}_2, \quad \mathbf{p}_3 = \mathbf{p}' - \mathbf{q}_1 - \mathbf{q}_2. \tag{5.54}$$

$$\int_\tau^\infty d\tau_1' \int_\tau^{\tau_1'} d\tau_2' e^{-E_X(-\mathbf{q}_1)(\tau_1'-\tau_2')} e^{-E_Y(-\mathbf{q}_1-\mathbf{q}_2)(\tau_2'-\tau)} e^{-E_Z(\mathbf{p}'-\mathbf{q}_1-\mathbf{q}_2)\tau}, \tag{5.55}$$

which has no possible τ-enhancement.

Case 6

The sixth case is $\tau > \tau_1' > \tau_2' > 0$ (figure 5.3, bottom line).

$$\mathbf{p}_1 = \mathbf{p}', \quad \mathbf{p}_2 = \mathbf{p}' - \mathbf{q}_1, \quad \mathbf{p}_3 = \mathbf{p}' - \mathbf{q}_1 - \mathbf{q}_2. \tag{5.56}$$

The integral is

$$\int_0^\tau d\tau_1' \int_0^{\tau_1'} d\tau_2' e^{-E_X(\mathbf{p}')(t-\tau_1')} e^{-E_Y(\mathbf{p}'-\mathbf{q}_1)(\tau_1'-\tau_2')} e^{-E_Z(\mathbf{p}'-\mathbf{q}_1-\mathbf{q}_2)(\tau_2'-\tau)}. \tag{5.57}$$

This is the *only* integral for which any τ-enhancement is possible. Let $\mathbf{q}_1 = \mathbf{q}$ (and $\mathbf{y}_1 = \mathbf{y}$) and $\mathbf{q}_2 = -\mathbf{q}'$ (and $\mathbf{y}_2 = \mathbf{y}'$). Or $\mathbf{q}_1 = -\mathbf{q}'$ (and $\mathbf{y}_2 = \mathbf{y}$) and $\mathbf{q}_2 = \mathbf{q}$ (and $\mathbf{y}_2 = \mathbf{y}$). Hence the degeneracy is $E_X(\mathbf{p}') = E_Z(\mathbf{p}' - \mathbf{q} + \mathbf{q}')$ and $X = Z$, which is allowed by our kinematics.

So, if we make the substitution $E_Z(\mathbf{p}' - \mathbf{q} + \mathbf{q}') = E_X(\mathbf{p}') = E_X$, Eq. 5.57 becomes

$$e^{-E_X\tau} \int_0^\tau d\tau_1' \int_0^{\tau_1'} d\tau_2' e^{(E_X-E_Y)(\tau_1'-\tau_2')} = \frac{\tau e^{-E_X\tau}}{E_Y - E_X} + \frac{e^{-E_X\tau}}{(E_X-E_Y)^2}(e^{-(E_Y-E_X)\tau} - 1), \tag{5.58}$$

so we have a τ-enhanced component of the integral in Eq. 5.57 for the previously mentioned choices of momentum variables.

From Eq. 5.58, it seems possible that we could have $E_Y < E_X$, and therefore we would have a term that's not a decaying exponential. However, in the lattice calculation, we will be fitting to the exponential $\sum_X e^{-E_X\tau}$, and hence this picks out the term for which E_X is its lowest value, the energy of a nucleon with momentum $\mathbf{p}'$. Then, since we choose kinematics such that $|\mathbf{p}' \pm \mathbf{q}^{(\prime)}| > |\mathbf{p}'|$, we will always have $E_Y > E_X$, and hence the second term on the RHS of Eq. 5.58 is just a decaying exponential.

5.2.6 Enhanced Term

Now we know which terms give the τ-enhanced component to Eq. 5.44, and hence the only τ-enhanced contribution to the whole of Eq. 5.43: the terms for which $\tau > \tau_1 > \tau_2 > 0$ or $\tau > \tau_2 > \tau_1 > 0$. We denote this τ-enhanced component as

$$\Big[\partial_{\boldsymbol{\lambda}}^2 C\Big]_{\text{enh}}.$$

Let's first consider the term for which $\tau_1 > \tau_2$:

$$\begin{aligned}
\Big[\partial_{\boldsymbol{\lambda}}^2 C\Big]_{\text{enh}}\Big|_{\tau_1>\tau_2} &\equiv \int d^3z d^3y' d^3y e^{-i\mathbf{p}'\cdot\mathbf{z}} \big(e^{i\mathbf{q}\cdot\mathbf{y}} + e^{-i\mathbf{q}\cdot\mathbf{y}}\big)\big(e^{i\mathbf{q}'\cdot\mathbf{y}'} + e^{-i\mathbf{q}'\cdot\mathbf{y}'}\big) \\
&\quad \times \int_0^\tau d\tau_1 \int_0^{\tau_1} d\tau_2 \Big\langle \chi(\mathbf{z},\tau) J(\mathbf{y},\tau_1) J(\mathbf{y}',\tau_2) \chi^\dagger(0) \Big\rangle \\
&= \int d^3z d^3y' d^3y e^{-i\mathbf{p}'\cdot\mathbf{z}} \big(e^{i\mathbf{q}\cdot\mathbf{y}} + e^{-i\mathbf{q}\cdot\mathbf{y}}\big)\big(e^{i\mathbf{q}'\cdot\mathbf{y}'} + e^{-i\mathbf{q}'\cdot\mathbf{y}'}\big) \\
&\times \sum_{X_1,X_2,X_3} \int \frac{d^3p_1}{(2\pi)^3} \frac{d^3p_2}{(2\pi)^3} \frac{d^3p_3}{(2\pi)^3} \frac{1}{8E_{X_1}(\mathbf{p}_1)E_{X_2}(\mathbf{p}_2)E_{X_3}(\mathbf{p}_3)} \int_0^\tau d\tau_1 \int_0^{\tau_1} d\tau_2 \\
&\times e^{-E_{X_1}(\mathbf{p}_1)\tau + i\mathbf{p}_1\cdot\mathbf{z}} e^{E_{X_1}(\mathbf{p}_1)\tau_1 - i\mathbf{p}_1\cdot\mathbf{y}} e^{-E_{X_2}(\mathbf{p}_2)\tau_1 + i\mathbf{p}_2\cdot\mathbf{y}} e^{E_{X_2}(\mathbf{p}_2)\tau_2 - i\mathbf{p}_2\cdot\mathbf{y}'} e^{-E_{X_3}(\mathbf{p}_3)\tau_2 + i\mathbf{p}_3\cdot\mathbf{y}'} \\
&\times \langle\Omega|\chi(0)|X_1(\mathbf{p}_1)\rangle\langle X_1(\mathbf{p}_1)|J(0)|X_2(\mathbf{p}_2)\rangle\langle X_2(\mathbf{p}_2)|J(0)|X_3(\mathbf{p}_3)\rangle\langle X_3(\mathbf{p}_3)|\chi^\dagger(0)|\Omega\rangle.
\end{aligned} \tag{5.59}$$

Then, using the delta function definition,

$$\begin{aligned}
&\Big[\partial_{\boldsymbol{\lambda}}^2 C\Big]_{\text{enh}}\Big|_{\tau_1>\tau_2} = \\
&\sum_{X_1,X_2,X_3}\int d^3p_1 d^3p_2 d^3p_3 \frac{\delta_{\mathbf{p}_1,\mathbf{p}'}(\delta_{\mathbf{p}_2,\mathbf{p}_1-\mathbf{q}}+\delta_{\mathbf{p}_2,\mathbf{p}_1+\mathbf{q}})(\delta_{\mathbf{p}_3,\mathbf{p}_2-\mathbf{q}'}+\delta_{\mathbf{p}_3,\mathbf{p}_2+\mathbf{q}'})}{8E_{X_1}(\mathbf{p}_1)E_{X_2}(\mathbf{p}_2)E_{X_3}(\mathbf{p}_3)} \\
&\times e^{-E_{X_1}(\mathbf{p}_1)\tau}\int_0^\tau d\tau_1\int_0^{\tau_1} d\tau_2 e^{(E_{X_1}(\mathbf{p}_1)-E_{X_2}(\mathbf{p}_2))\tau_1}e^{(E_{X_2}(\mathbf{p}_2)-E_{X_3}(\mathbf{p}_3))\tau_2} \\
&\times \langle\Omega|\chi(0)|X_1(\mathbf{p}_1)\rangle\langle X_1(\mathbf{p}_1)|J(0)|X_2(\mathbf{p}_2)\rangle\langle X_2(\mathbf{p}_2)|J(0)|X_3(\mathbf{p}_3)\rangle\langle X_3(\mathbf{p}_3)|\chi^\dagger(0)|\Omega\rangle.
\end{aligned} \tag{5.60}$$

Note that we have simplified the notation: $\delta_{\mathbf{p}_1,\mathbf{p}_2} = \delta^{(3)}(\mathbf{p}_1-\mathbf{p}_2)$. Once we evaluate this integral, we have $\mathbf{p}_1 = \mathbf{p}'$, $\mathbf{p}_2 = \mathbf{p}' \pm \mathbf{q}$, and $\mathbf{p}_3 = \mathbf{p}'+\mathbf{q}+\mathbf{q}'$, or $\mathbf{p}_3 = \mathbf{p}'-\mathbf{q}+\mathbf{q}'$, or $\mathbf{p}_3 = \mathbf{p}'+\mathbf{q}-\mathbf{q}'$, or $\mathbf{p}_3 = \mathbf{p}'-\mathbf{q}-\mathbf{q}'$.

In our chosen kinematics, only one of these combinations ($\mathbf{p}_2 = \mathbf{p}'-\mathbf{q}$ and $\mathbf{p}_3 = \mathbf{p}'-\mathbf{q}+\mathbf{q}'$) produces equal energies and therefore a τ-enhancement. Here we introduce the momentum vector $\boldsymbol{\Delta} = \mathbf{q}-\mathbf{q}'$. So we focus on this combination of delta functions:

$$\begin{aligned}
&\Big[\partial_{\boldsymbol{\lambda}}^2 C\Big]_{\text{enh}}\Big|_{\tau_1>\tau_2} = \\
&\sum_{X_1,X_2,X_3}\int_0^\tau d\tau_1\int_0^{\tau_1} d\tau_2 \frac{e^{-E_{X_1}(\mathbf{p}')\tau}e^{(E_{X_1}(\mathbf{p}')-E_{X_2}(\mathbf{p}'-\mathbf{q}))\tau}e^{(E_{X_2}(\mathbf{p}'-\mathbf{q})-E_{X_3}(\mathbf{p}'-\boldsymbol{\Delta}))\tau_2}}{8E_{X_1}(\mathbf{p}')E_{X_2}(\mathbf{p}'-\mathbf{q})E_{X_3}(\mathbf{p}'-\boldsymbol{\Delta})} \\
&\times \langle\Omega|\chi(0)|X_1(\mathbf{p}')\rangle\langle X_1(\mathbf{p}')|J(0)|X_2(\mathbf{p}'-\mathbf{q})\rangle \\
&\times \langle X_2(\mathbf{p}'-\mathbf{q})|J(0)|X_3(\mathbf{p}'-\boldsymbol{\Delta})\rangle\langle X_3(\mathbf{p}'-\boldsymbol{\Delta})|\chi^\dagger(0)|\Omega\rangle
\end{aligned} \tag{5.61}$$

Now we take the limit of large Euclidean time τ so that the state X_1 goes to the nucleon, N. And similarly, since we must have $E_{X_3} = E_{X_1}$ to produce a τ-enhancement, we also have that X_3 goes to N. Then, for simplicity, we introduce the variables $\mathbf{p} = \mathbf{p}'-\boldsymbol{\Delta}$, $X_2 = X$, $E_X(\mathbf{p}'-\mathbf{q}) = E_X$, and $E_N(\mathbf{p}') = E_N(\mathbf{p}) = E_N$:

$$\begin{aligned}
&\Big[\partial_{\boldsymbol{\lambda}}^2 C\Big]_{\text{enh}}\Big|_{\tau_1>\tau_2} = \\
&\sum_X \frac{1}{8E_N^2E_X}e^{-E_N\tau}\int_0^\tau d\tau_1\int_0^{\tau_1} d\tau_2 e^{(E_N-E_X)\tau_1}e^{(E_X-E_N)\tau_2} \\
&\times \langle\Omega|\chi(0)|N(\mathbf{p}')\rangle\langle N(\mathbf{p}')|J(0)|X(\mathbf{p}'-\mathbf{q})\rangle\langle X(\mathbf{p}'-\mathbf{q})|J(0)|N(\mathbf{p})\rangle\langle N(\mathbf{p})|\chi^\dagger(0)|\Omega\rangle \\
&= \sum_X \frac{1}{8E_N^2E_X}\left[\frac{\tau e^{-E_N\tau}}{E_X-E_N}+\frac{e^{-E_N\tau}}{(E_N-E_X)^2}(e^{-(E_X-E_N)\tau}-1)\right] \\
&\times \langle\Omega|\chi(0)|N(\mathbf{p}')\rangle\langle N(\mathbf{p}')|J(0)|X(\mathbf{p}'-\mathbf{q})\rangle\langle X(\mathbf{p}'-\mathbf{q})|J(0)|N(\mathbf{p})\rangle\langle N(\mathbf{p})|\chi^\dagger(0)|\Omega\rangle.
\end{aligned} \tag{5.62}$$

Then, isolating the τ-enhanced term of Eq. 5.62, we get

$$\begin{aligned}
&\Big[\partial_{\boldsymbol{\lambda}}^2 C\Big]_{\text{enh}}\Big|_{\tau_1>\tau_2} = \tau e^{-E_N\tau} \\
&\times \sum_X \frac{\langle\Omega|\chi(0)|N(\mathbf{p}')\rangle\langle N(\mathbf{p}')|J(0)|X(\mathbf{p}'-\mathbf{q})\rangle\langle X(\mathbf{p}'-\mathbf{q})|J(0)|N(\mathbf{p})\rangle\langle N(\mathbf{p})|\chi^\dagger(0)|\Omega\rangle}{8E_N^2E_X(E_X-E_N)}.
\end{aligned} \tag{5.63}$$

Considering the $\tau_2 > \tau_1$ term, we similarly arrive at

$$\begin{aligned}\Big[\partial_{\boldsymbol{\lambda}}^2 C\Big]_{\text{enh}}\Big|_{\tau_2>\tau_1} &= \int d^3z d^3y' d^3y e^{-i\mathbf{p}'\cdot\mathbf{z}}\big(e^{i\mathbf{q}\cdot\mathbf{y}} + e^{-i\mathbf{q}\cdot\mathbf{y}}\big)\big(e^{i\mathbf{q}'\cdot\mathbf{y}'} + e^{-i\mathbf{q}'\cdot\mathbf{y}'}\big) \\ &\times \int_0^\tau d\tau_2 \int_0^{\tau_2} d\tau_1 \Big\langle \chi(\mathbf{z},\tau) J(\mathbf{y}',\tau_2) J(\mathbf{y},\tau_1)\chi^\dagger(0)\Big\rangle = \tau e^{-E_N\tau} \\ &\times \sum_X \frac{\langle\Omega|\chi(0)|N(\mathbf{p}')\rangle\langle N(\mathbf{p}')|J(0)|X(\mathbf{p}'+\mathbf{q}')\rangle\langle X(\mathbf{p}'+\mathbf{q}')|J(0)|N(\mathbf{p})\rangle\langle N(\mathbf{p})|\chi^\dagger(0)|\Omega\rangle}{8E_N^2 E_X(E_X - E_N)}.\end{aligned} \tag{5.64}$$

The notation here is a bit careless, since the terms E_X in Eq. 5.63 and 5.64 have different momenta. We make this explicit in the next equation.

If we combine Eqs. 5.63 and 5.64, dividing through by the $\tau e^{-E_N\tau}$ factor, we get

$$\begin{aligned}\frac{e^{E_N\tau}}{\tau}\Big[\partial_{\boldsymbol{\lambda}}^2 C\Big]_{\text{enh}} &= \frac{1}{4E_N^2}\sum_X \\ &\times \Bigg\{ \frac{\langle\Omega|\chi(0)|N(\mathbf{p}')\rangle\langle N(\mathbf{p}')|J(0)|X(\mathbf{p}'-\mathbf{q})\rangle\langle X(\mathbf{p}'-\mathbf{q})|J(0)|N(\mathbf{p})\rangle\langle N(\mathbf{p})|\chi^\dagger(0)|\Omega\rangle}{2E_X(\mathbf{p}'-\mathbf{q})(E_X(\mathbf{p}'-\mathbf{q}) - E_N)} \\ &+ \frac{\langle\Omega|\chi(0)|N(\mathbf{p}')\rangle\langle N(\mathbf{p}')|J(0)|X(\mathbf{p}'+\mathbf{q}')\rangle\langle X(\mathbf{p}'+\mathbf{q}')|J(0)|N(\mathbf{p})\rangle\langle N(\mathbf{p})|\chi^\dagger(0)|\Omega\rangle}{2E_X(\mathbf{p}'+\mathbf{q}')(E_X(\mathbf{p}'+\mathbf{q}') - E_N)} \Bigg\}\end{aligned} \tag{5.65}$$

This equation is proportional to the Compton tensor, even though this might not be immediately obvious. To show this we can first replace the momentum of the intermediate state X with a variable $\mathbf{p}_X$ and an integral over this variable with the appropriate delta functions:

$$\begin{aligned}\frac{e^{E_N\tau}}{\tau}\Big[\partial_{\boldsymbol{\lambda}}^2 C\Big]_{\text{enh}} &= \frac{1}{4E_N^2}\sum_X \int \frac{d^3p_X}{(2\pi)^3}\frac{(2\pi)^3(\delta_{\mathbf{p}_X,\mathbf{p}'-\mathbf{q}} + \delta_{\mathbf{p}_X,\mathbf{p}'+\mathbf{q}'})}{2E_X(\mathbf{p}_X)(E_X(\mathbf{p}_X) - E_N)} \\ &\times \langle\Omega|\chi(0)|N(\mathbf{p}')\rangle\langle N(\mathbf{p}')|J(0)|X(\mathbf{p}_X)\rangle\langle X(\mathbf{p}_X)|J(0)|N(\mathbf{p})\rangle\langle N(\mathbf{p})|\chi^\dagger(0)|\Omega\rangle.\end{aligned} \tag{5.66}$$

Using the Fourier transform definition of a delta function, we get

$$\begin{aligned}\frac{e^{E_N\tau}}{\tau}\Big[\partial_{\boldsymbol{\lambda}}^2 C\Big]_{\text{enh}} &= \frac{1}{4E_N^2}\sum_X \int \frac{d^3p_X}{(2\pi)^3}\int d^3z\Big(e^{i(\mathbf{p}_X-(\mathbf{p}'-\mathbf{q}))\cdot\mathbf{z}} + e^{i(\mathbf{p}_X-(\mathbf{p}'+\mathbf{q}'))\cdot\mathbf{z}}\Big) \\ &\times \frac{\langle\Omega|\chi(0)|N(\mathbf{p}')\rangle\langle N(\mathbf{p}')|J(0)|X(\mathbf{p}_X)\rangle\langle X(\mathbf{p}_X)|J(0)|N(\mathbf{p})\rangle\langle N(\mathbf{p})|\chi^\dagger(0)|\Omega\rangle}{2E_X(\mathbf{p}_X)(E_X(\mathbf{p}_X) - E_N)}.\end{aligned} \tag{5.67}$$

Then, we can use the fact that[‡]

$$\int_{-\infty}^{\infty} dt\Big[e^{-(E_1-E_2)t}\Theta(t) + e^{(E_1-E_2)t}\Theta(-t)\Big] = \frac{2}{E_1 - E_2}, \tag{5.68}$$

[‡]Here, $\Theta(t)$ is the Heaviside step function.

to reorganise Eq. 5.67:

$$\begin{aligned}\frac{e^{E_N\tau}}{\tau}\Big[\partial_{\boldsymbol{\lambda}}^2 C\Big]_{\text{enh}} &= \frac{1}{8E_N^2}\sum_X \int \frac{d^3p_X}{(2\pi)^3}\frac{1}{2E_X(\mathbf{p}_X)} \\ &\times \int d^3z\Big(e^{i(\mathbf{p}_X-(\mathbf{p}'-\mathbf{q}))\cdot\mathbf{z}} + e^{i(\mathbf{p}_X-(\mathbf{p}'+\mathbf{q}'))\cdot\mathbf{z}}\Big) \\ &\times \int_{-\infty}^{\infty} dz^0\big(e^{-(E_X(\mathbf{p}_X)-E_N)z^0}\Theta(z^0) + e^{(E_X(\mathbf{p}_X)-E_N)z^0}\Theta(-z^0)\big) \\ &\times \langle\Omega|\chi(0)|N(\mathbf{p}')\rangle\langle N(\mathbf{p}')|J(0)|X(\mathbf{p}_X)\rangle\langle X(\mathbf{p}_X)|J(0)|N(\mathbf{p})\rangle\langle N(\mathbf{p})|\chi^\dagger(0)|\Omega\rangle.\end{aligned} \tag{5.69}$$

Now, using translational invariance (again, this hinges on the fact that we are evaluating the matrix element at $\lambda_1 = \lambda_2 = 0$), this becomes

$$\begin{aligned}\frac{e^{E_N\tau}}{\tau}\Big[\partial_{\boldsymbol{\lambda}}^2 C\Big]_{\text{enh}} &= \frac{1}{8E_N^2}\sum_X \int \frac{d^3p_X}{(2\pi)^3}\frac{1}{2E_X(\mathbf{p}_X)}\int d^4z e^{-i\bar{\mathbf{q}}\cdot\mathbf{z}} \\ &\times \Big\{\Theta(z^0)\langle\Omega|\chi(0)|N(\mathbf{p}')\rangle\langle N(\mathbf{p}')|J(z/2)|X(\mathbf{p}_X)\rangle\langle X(\mathbf{p}_X)|J(-z/2)|N(\mathbf{p})\rangle\langle N(\mathbf{p})|\chi^\dagger(0)|\Omega\rangle \\ &+ \Theta(-z^0)\langle\Omega|\chi(0)|N(\mathbf{p}')\rangle\langle N(\mathbf{p}')|J(-z/2)|X(\mathbf{p}_X)\rangle\langle X(\mathbf{p}_X)|J(z/2)|N(\mathbf{p})\rangle\langle N(\mathbf{p})|\chi^\dagger(0)|\Omega\rangle\Big\}.\end{aligned} \tag{5.70}$$

Then, since

$$\mathbb{I} = \sum_X \int \frac{d^3p_X}{(2\pi)^3}\frac{1}{2E_X(\mathbf{p}_X)}|X(\mathbf{p}_X)\rangle\langle X(\mathbf{p}_X)|, \tag{5.71}$$

we have that Eq. 5.70 becomes

$$\begin{aligned}\frac{e^{E_N\tau}}{\tau}\Big[\partial_{\boldsymbol{\lambda}}^2 C\Big]_{\text{enh}} &= \frac{1}{8E_N^2} \\ &\times \langle\Omega|\chi(0)|N(\mathbf{p}')\rangle\int d^4z e^{-i\bar{\mathbf{q}}\cdot\mathbf{z}}\langle N(\mathbf{p}')|T\big[J(z/2)J(-z/2)\big]|N(\mathbf{p})\rangle\langle N(\mathbf{p})|\chi^\dagger(0)|\Omega\rangle.\end{aligned} \tag{5.72}$$

Compare this to the Euclidean off-forward Compton tensor (OFCT), the Wick rotation of Eq. 4.5:

$$T^{\mu\nu} = \int d^4z e^{i\bar{q}\cdot z}\langle P'|T\big[j^\mu(z/2)j^\nu(-z/2)\big]|P\rangle.$$

In our notation, $|P^{(\prime)}\rangle = |N(\mathbf{p}^{(\prime)})\rangle$. So we have that

$$\int d^4z e^{-i\bar{\mathbf{q}}\cdot\mathbf{z}}\langle N(\mathbf{p}')|T\big[J(z/2)J(-z/2)\big]|N(\mathbf{p})\rangle$$

is simply the Euclidean OFCT for the case that $\bar{q}^0 = 0$, $\mu = \nu = 3$, with only one flavour and unit charge. However, recall from Eq. 5.33, this is still carrying around a Dirac projector and sum over spins. Therefore, Eq. 5.72 is really

$$\frac{e^{E_N\tau}}{\tau}\Big[\partial_{\boldsymbol{\lambda}}^2 C\Big]_{\text{enh}} = \frac{1}{8E_N^2}\langle\Omega|\chi(0)|N(\mathbf{p}')\rangle T^{33}\langle N(\mathbf{p})|\chi^\dagger(0)|\Omega\rangle, \tag{5.73}$$

with kinematics $\bar{q}^0 = 0$.

Recall our expression for the direct derivative in Eq. 5.42:

$$\frac{\partial^2 C_{\boldsymbol{\lambda}}(\tau, \mathbf{p}')}{\partial\lambda_1\partial\lambda_2}\bigg|_{\lambda_1=\lambda_2=0} = \sum_{X,a} e^{-E_{X,a}(\mathbf{p}')\tau}\left[\frac{\partial^2 A_{X,a}(\mathbf{p}')}{\partial\lambda_1\partial\lambda_2} - \tau\frac{\partial^2 E_{X,a}(\mathbf{p}')}{\partial\lambda_1\partial\lambda_2}A_{X,a}(\mathbf{p}')\right]\bigg|_{\lambda_1=\lambda_2=0}.$$

The τ-enhanced term of the direct derivative is then

$$-\sum_{X,a} e^{-E_{X,a}(\mathbf{p}')\tau}\tau\frac{\partial^2 E_{X,a}(\mathbf{p}')}{\partial\lambda_1\partial\lambda_2}A_{X,a}(\mathbf{p}')\bigg|_{\lambda_1=\lambda_2=0}. \tag{5.74}$$

If we take the limit of large Euclidean time, then the tower of states X is dominated by the nucleon state N:

$$-\sum_{a} e^{-E_{N,a}(\mathbf{p}')\tau}\tau\frac{\partial^2 E_{N,a}(\mathbf{p}')}{\partial\lambda_1\partial\lambda_2}A_{N,a}(\mathbf{p}')\bigg|_{\lambda_1=\lambda_2=0}. \tag{5.75}$$

It is natural to ask what happens to the a quantum number at this stage, since we wish to equate Eq. 5.75 and Eq. 5.72. The former has a sum over this quantum number, while the latter doesn't. For the moment we will just state that all but one of the amplitudes $A_{N,a}$ vanish as we go to $\lambda_1 = \lambda_2 = 0$. In section 5.3 we will justify this statement. Hence Eq. 5.75 becomes

$$-e^{-E_N(\mathbf{p}')\tau}\tau\frac{\partial^2 E_N(\mathbf{p}')}{\partial\lambda_1\partial\lambda_2}A_N(\mathbf{p}')\bigg|_{\lambda_1=\lambda_2=0}. \tag{5.76}$$

Therefore, equating Eq. 5.76 (ignoring the τ-enhanced factor which will cancel) and Eq. 5.73 we arrive finally at our FH relation:

$$-A_N(\mathbf{p}')\frac{\partial^2 E}{\partial\lambda_1\partial\lambda_2}\bigg|_{\lambda_1=\lambda_2=0} = \frac{1}{8E_N^2}\langle\Omega|\chi(0)|N(\mathbf{p}')\rangle T_{33}\langle N(\mathbf{p})|\chi^\dagger(0)|\Omega\rangle\bigg|_{\lambda_1=\lambda_2=0}. \tag{5.77}$$

Recall from section 2.2 that

$$A_N(\mathbf{p}') = \frac{|\langle\Omega|\chi|N(\mathbf{p}')\rangle|^2}{2E_N(\mathbf{p}')}. \tag{5.78}$$

Therefore, Eq. 5.77 becomes

$$\frac{\partial^2 E}{\partial\lambda_1\partial\lambda_2}\bigg|_{\lambda_1=\lambda_2=0} = -\frac{\langle\Omega|\chi(0)|N(\mathbf{p}')\rangle T_{33}\langle N(\mathbf{p})|\chi^\dagger(0)|\Omega\rangle}{4E_N|\langle\Omega|\chi|N(\mathbf{p}')\rangle|^2}\bigg|_{\lambda_1=\lambda_2=0}. \tag{5.79}$$

Finally, since

$$\langle\Omega|\chi_\alpha(0)|X(\mathbf{p})\rangle = Z_{\chi,X}(\mathbf{p})u_\alpha(p,s), \tag{5.80}$$

$$\langle X(\mathbf{p})|\chi^\dagger_\alpha(0)|\Omega\rangle = Z^*_{\chi,X}(\mathbf{p})\bar{u}_\alpha(p,s), \tag{5.81}$$

it is convenient for chapter 6 to define

$$\tilde{T}^{\mu\nu} \equiv i\int d^4z e^{i\bar{q}\cdot z}\frac{1}{4}\sum_{\text{spins}}\Gamma_{\beta\alpha}u_\alpha(P')\langle P'|T[j^\mu(z/2)j^\nu(-z/2)]|P\rangle\bar{u}_\beta(P). \tag{5.82}$$

The above expression will become useful when we wish to compare terms from our operator product expansion to the lattice calculation.

Therefore, we have arrived at a Feynman-Hellmann relation of the form desired (Eq. 5.79). This is very powerful, since it allows us to extract a four-point function (proportional to the OFCT) from the energy shifts of two-point functions.

5.2.7 Comparison to Four-Point Function Methods

Lattice calculations of the *forward* Compton tensor through four-point function methods have been hampered by a persistent problem [115, 119, 142]. Any attempt to determine the OFCT through lattice four-point methods would face the same difficulty. Hence in this subsection we briefly explain what this problem is, and how the FH lattice calculation circumvents it.

A standard lattice four-point function, similar to the forward Compton tensor[§], has the form

$$W^{\mu\nu}(\tau) = \langle \chi \mathcal{J}^{\mu}(\tau)\mathcal{J}^{\nu}(0)\chi\rangle = e^{-(E_N+q^0-E_X)\tau}\langle N|J^{\mu}(0)|X\rangle\langle X|J^{\nu}(0)|N\rangle. \tag{5.83}$$

Martinelli [142] first pointed out that, due to the exponential term out the front, the dominant terms will be those for which the intermediate state's energy is minimised. Hence, for large Euclidean time, the intermediate state does not couple to a tower of states. Note that there are proposed methods of overcoming this difficulty [118].

By contrast, this problem does not apply to Feynman-Hellmann techniques. Primarily, this is because the Compton tensor as calculated via FH has completely different Euclidean time behaviour behaviour to Eq. 5.83: there is already an integral over Euclidean time in the energy shift we extract. From Eq. 5.58, the energy shift goes like

$$\sum_{Y} \tau e^{-E_Y\tau} \int d\tau' [\text{four-point function}],$$

where Y is the outgoing nucleon state, *not the intermediate state*. The integral over τ means that there is no weight factor for each intermediate hadronic state as in Eq. 5.83, and as such the current still couples to the full spectrum of intermediate states.

In this way, the Compton tensor we extract from the energy shift should be equivalent to the Euclidean OFCT in the large Euclidean momentum limit (see chapter 6).

5.3 The Perturbed States and Perturbed Correlator

Due to the fact that the quantity we wish to calculate is both second order and off-forward, our perturbing Lagrangian (Eq. 5.15) induces a non-trivial mixing of states. We have so far avoided the complications that arise from this mixing by: (1) taking quite an inexplicit form of the perturbed correlator (Eq. 5.23), and making assumptions about its behaviour in the $\boldsymbol{\lambda} \to 0$ limit; and (2) using the fact that the formal Feynman-Hellmann derivation evaluates all quantities at $\lambda_1 = \lambda_2 = 0$.

We will investigate this mixing behaviour by deriving approximate forms of the eigenstates of the perturbed Hamiltonian, and the perturbed correlator. The two main results

[§]In reality, this is the hadronic tensor from chapter 3.

of this section are: (1) justifying our assumption that only one of the amplitudes $A_{N,a}$ survives the $\boldsymbol{\lambda} \to 0$ limit, and (2) finding the values of λ that allow us to extract the perturbed energy eigenstates most cleanly in the lattice calculation.

5.3.1 Form of the Perturbed Correlator

The following is general for any FH calculation in which the perturbed Hamiltonian doesn't commute with the momentum operator. Consider a perturbed Lagrangian density: $\mathcal{L} = \mathcal{L}_{\text{QCD}} + \mathcal{L}_{\text{FH}}$. Similarly, our Hamiltonian will receive a modification: $H = H_{\text{QCD}} + H_{\text{FH}}$. And let the momentum operator be $\hat{\mathbf{P}}$.

Below, we make a simplifying assumption that will not change our overall arguments: we take the translation operator $\mathbb{T}$ to be unperturbed, so that $\mathbb{T} = \exp\{i\hat{\mathbf{P}} \cdot \mathbf{z}\}$. However, unlike the Hamiltonian, the eigenstates of the translation operator are the momentum eigenstates, *but not linear combinations of the momentum eigenstates.* This means that, unlike the perturbed Hamiltonian, there is a one-to-one correspondence between the spectrum of momentum eigenstates and the eigenstates of the perturbed translation operator. Hence we can write an eigenstate of the perturbed translation ($|X(\mathbf{p})\rangle_{\boldsymbol{\lambda}}$) operator as

$$|X(\mathbf{p})\rangle_{\boldsymbol{\lambda}} = |X(\mathbf{p})\rangle + \mathcal{O}(\lambda).$$

As such, since we use the *unperturbed* translation operator, we will have $\mathcal{O}(\lambda)$ corrections to the expressions for energy eigenstates we derive[**]. These corrections to the eigenstates don't affect any of our conclusions, as we will show.

Then, the perturbed correlator is

$$\begin{aligned} C_{\boldsymbol{\lambda}}(\tau, \mathbf{p}') &= \int d^3z e^{-i\mathbf{p}'\cdot\mathbf{z}} \langle\Omega|\chi(z)\chi^\dagger(0)|\Omega\rangle \\ &= \sum_Y \int \frac{d^3p}{(2\pi)^3} \frac{1}{2E_Y(\mathbf{p})} \int d^3z e^{-i\mathbf{p}'\cdot\mathbf{x}} \langle\Omega|\chi(z)|Y(\mathbf{p})\rangle\langle Y(\mathbf{p})|\chi^\dagger(0)|\Omega\rangle \\ &= \sum_Y \int \frac{d^3p}{(2\pi)^3} \frac{1}{2E_Y(\mathbf{p})} \int d^3z e^{i(\mathbf{p}-\mathbf{p}')\cdot\mathbf{z}} \langle\Omega|\chi(0)e^{-H(\boldsymbol{\lambda})t}|Y(\mathbf{p})\rangle\langle Y(\mathbf{p})|\chi^\dagger(0)|\Omega\rangle \\ &= \sum_Y \frac{1}{2E_Y(\mathbf{p}')} \langle\Omega|\chi(0)e^{-H(\boldsymbol{\lambda})t}|Y(\mathbf{p}')\rangle\langle Y(\mathbf{p}')|\chi^\dagger(0)|\Omega\rangle. \end{aligned} \tag{5.84}$$

Note that, by our previous assumption, this expression will have a $\mathcal{O}(\lambda)$ correction.

As in subsection 5.2.1, we introduce another basis of eigenstates $\{|X(a)\rangle\}$ that are eigenstates of the perturbed Hamiltonian and a new operator $\mathcal{A}$ and span the same space as the momentum eigenstates $\{|Y(\mathbf{p})\rangle\}$.

Recall Eq. 5.21, which implies Eq. 5.84 becomes

$$C_{\boldsymbol{\lambda}}(\tau, \mathbf{p}') = \sum_{X,a} e^{-E_{X,a}\tau} \langle\Omega|\chi(0)|X(a)\rangle \sum_Y c_{X,a}(\mathbf{p}', Y) \frac{\langle Y(\mathbf{p}')|\chi^\dagger(0)|\Omega\rangle}{2E_Y(\mathbf{p}')}. \tag{5.85}$$

[**]Note that this is quite similar to the case in QM perturbation theory from section 5.1, where the effective Hamiltonian's eigenstates were only approximations up to $\mathcal{O}(1)$ of the eigenstates of the perturbed Hamiltonian.

For large Euclidean time, the nucleon ground states dominate. Hence Eq. 5.85 becomes

$$C_{\boldsymbol{\lambda}}(\tau, \mathbf{p}') \approx \sum_a \frac{c_{N,a}(\mathbf{p}', N) e^{-E_{N,a}\tau}}{2E(\mathbf{p}')} \langle \Omega | \chi(0) | N(a) \rangle \langle N(\mathbf{p}') | \chi^\dagger(0) | \Omega \rangle. \tag{5.86}$$

Moreover, we have taken $Y = N$, since $c_{N,a}(\mathbf{p}', Y)$ will be small (proportional to higher powers of $\lambda_{1,2}$) for higher hadronic states. This is the second simplifying assumption we make. Again, it means that our expression for the perturbed correlator will have $\mathcal{O}(\lambda)$ corrections. However, as we will argue, these don't affect our results.

Suppose the momentum we project onto, $\mathbf{p}'$, has the following properties:

$$\begin{aligned} &\langle N(\mathbf{p}) | H(\boldsymbol{\lambda}) | N(\mathbf{p}') \rangle \neq 0, \\ &H_{\mathrm{QCD}} | N(\mathbf{p}) \rangle = H_{\mathrm{QCD}} | N(\mathbf{p}') \rangle = E_0 | N(\mathbf{p}') \rangle, \quad \mathbf{p} \neq \mathbf{p}'. \end{aligned}$$

In other words, the perturbed Hamiltonian mixes the nucleon state with momentum $\mathbf{p}'$, with another momentum eigenstate of degenerate energy. In principle, depending on how we choose the FH perturbation, these states could be subject to arbitrarily many degeneracies. However, in the case of our chosen perturbation, Eq. 5.15, the degeneracy is only twofold: states with momentum $\mathbf{p}'$ and hadronic state X are only mixed with states of momentum $\mathbf{p} = \mathbf{p}' - (\mathbf{q} - \mathbf{q}')$ and hadronic state X.

Hence for a two-fold degeneracy, Eq. 5.86 becomes

$$\begin{aligned} C_{\boldsymbol{\lambda}}(\tau, \mathbf{p}') \approx \frac{1}{2E(\mathbf{p}')} \Big[& c_{a_1}(\mathbf{p}') e^{-E_{N,a_1} t} \langle \Omega | \chi(0) | N(a_1) \rangle \langle N(\mathbf{p}') | \chi^\dagger(0) | \Omega \rangle \\ & + c_{a_2}(\mathbf{p}') e^{-E_{N,a_2} t} \langle \Omega | \chi(0) | N(a_2) \rangle \langle N(\mathbf{p}') | \chi^\dagger(0) | \Omega \rangle \Big]. \end{aligned} \tag{5.87}$$

The next step is to find an operator that commutes with our Hamiltonian to derive the basis of eigenstates of the Hamiltonian. To find such an operator, $\mathcal{A}$, we need that:

1. the operator commutes with the perturbed Hamiltonian: $[H(\boldsymbol{\lambda}), \mathcal{A}] = 0$;
2. the operator doesn't have the same eigenvalue for all the states in our basis (precluding e.g. the identity). This ensures that the quantum numbers associated with $\mathcal{A}$ allow us to distinguish states that are degenerate in energy.

5.3.2 Symmetries of the Hamiltonian

In this subsection, we will find the operator $\mathcal{A}$ that commutes with the perturbed Hamiltonian, and hence construct the eigenstates of the perturbed Hamiltonian. To start, we note that the QCD-only lattice Hamiltonian is independently invariant under charge conjugation (C), time-reversal (T), parity (P) and rotations by an angle of $\pi/2$. Hence a good starting point might be to construct $\mathcal{A}$ from these transformations. To commute with the whole (perturbed) Hamiltonian, we must also have that $\mathcal{A}$ commutes with the perturbing Hamiltonian H_{FH}. Therefore, we start by seeing how H_{FH} changes under the aforementioned transformations.

As we showed in subsection 5.2.1, the FH perturbation to the Lagrangian density is related to the Hamiltonian density by $\mathcal{H}_{\mathrm{FH}} = -\mathcal{L}_{\mathrm{FH}}$. Recall the form of the perturbing Lagrangian:

$$\mathcal{L}_{\mathrm{FH}} = \Big[\lambda_1 \big(e^{i\mathbf{q}\cdot\mathbf{x}} + e^{-i\mathbf{q}\cdot\mathbf{x}} \big) + \lambda_2 \big(e^{i\mathbf{q}'\cdot\mathbf{x}} + e^{-i\mathbf{q}'\cdot\mathbf{x}} \big) \Big] J(\mathbf{x}, \tau),$$

where we have that $J(\mathbf{x},\tau) = \bar{\psi}(\mathbf{x},\tau)\gamma^3\psi(\mathbf{x},\tau)$. Then, we will let $\mathbf{q} = (q^1, q^2, q^3)$ and $\mathbf{q}' = (-q^1, q^2, q^3)$; that is, they are related by a reflection of the x^1 axis. This choice is equivalent to the choice to have 'zero-skewness' kinematics. In chapter 6, we will show that this allows us to calculate the A and B generalised form factors. In a different kinematic region, we would need to consider different symmetries of the Hamiltonian.

Then, the perturbing Hamiltonian density is

$$\mathcal{H}_{\mathrm{FH}} = -\Big[\lambda_1\big(e^{i\mathbf{q}\cdot\mathbf{x}} + e^{-i\mathbf{q}\cdot\mathbf{x}}\big) + \lambda_2\big(e^{i\mathbf{q}'\cdot\mathbf{x}} + e^{-i\mathbf{q}'\cdot\mathbf{x}}\big)\Big]J(\mathbf{x},\tau),$$

and the perturbing Hamiltonian is

$$H_{\mathrm{FH}} = -\int d^3x\Big[\lambda_1\big(e^{i\mathbf{q}\cdot\mathbf{x}} + e^{-i\mathbf{q}\cdot\mathbf{x}}\big) + \lambda_2\big(e^{i\mathbf{q}'\cdot\mathbf{x}} + e^{-i\mathbf{q}'\cdot\mathbf{x}}\big)\Big]J(\mathbf{x},\tau).$$

A reflection off the x^1 axis is equivalent to a parity transform combined with a rotation about the x^1 axis by 180 degrees. Hence

$$\mathrm{P}_1 = R_1(\pi)\mathrm{P}. \tag{5.88}$$

Since $R_1(\pi)^2 = \mathbb{I} = \mathrm{P}^2$, we have that $\mathrm{P}_1^\dagger = \mathrm{P}R_1(\pi)$. And furthermore, P and $R_1(\pi)$ commute, so really $\mathrm{P}_1^\dagger = \mathrm{P}_1$ and $\mathrm{P}_1^2 = \mathbb{I}$.

Under this transformation, the perturbing Hamiltonian becomes:

$$\begin{aligned}
\mathrm{P}_1\mathcal{H}_{\mathrm{FH}}\mathrm{P}_1 &= -\,\mathrm{P}_1\Big[\lambda_1\big(e^{i\mathbf{q}\cdot\mathbf{x}} + e^{-i\mathbf{q}\cdot\mathbf{x}}\big) + \lambda_2\big(e^{i\mathbf{q}'\cdot\mathbf{x}} + e^{-i\mathbf{q}'\cdot\mathbf{x}}\big)\Big]J(\mathbf{x},\tau)\mathrm{P}_1 \\
&= -\,\Big[\lambda_1\big(e^{i\mathbf{q}\cdot\mathbf{x}} + e^{-i\mathbf{q}\cdot\mathbf{x}}\big) + \lambda_2\big(e^{i\mathbf{q}'\cdot\mathbf{x}} + e^{-i\mathbf{q}'\cdot\mathbf{x}}\big)\Big]\mathrm{P}_1 J(\mathbf{x},\tau)\mathrm{P}_1 \\
&= -\,\Big[\lambda_1\big(e^{i\mathbf{q}\cdot\mathbf{x}} + e^{-i\mathbf{q}\cdot\mathbf{x}}\big) + \lambda_2\big(e^{i\mathbf{q}'\cdot\mathbf{x}} + e^{-i\mathbf{q}'\cdot\mathbf{x}}\big)\Big]J(-x^1, x^2, x^3, \tau),
\end{aligned} \tag{5.89}$$

where the vector current doesn't flip sign since in our case it's oriented in the x^3 direction, whereas the reflection is along the x^1 axis. Therefore,

$$\begin{aligned}
\mathrm{P}_1 H_{\mathrm{FH}}\mathrm{P}_1 &= \mathrm{P}_1\int d^3x\mathrm{P}_1\mathrm{P}_1\mathcal{H}_{\mathrm{FH}}\mathrm{P}_1 \\
&= -\mathrm{P}_1\int d^3x\mathrm{P}_1\Big[\lambda_1\big(e^{i\mathbf{q}\cdot\mathbf{x}} + e^{-i\mathbf{q}\cdot\mathbf{x}}\big) + \lambda_2\big(e^{i\mathbf{q}'\cdot\mathbf{x}} + e^{-i\mathbf{q}'\cdot\mathbf{x}}\big)\Big]J(-x^1, x^2, x^3, \tau).
\end{aligned} \tag{5.90}$$

Note that

$$\mathrm{P}_1\int d^3x\mathrm{P}_1 = (-1)\int_{\infty}^{-\infty} dx^1\int_{-\infty}^{\infty} dx^2\int_{-\infty}^{\infty} dx^3 = \int d^3x.$$

And moreover if we do a substitution $\mathbf{x}\to\mathbf{y} = (-x^1, x^2, x^3)$, we have

$$\mathbf{q}\cdot\mathbf{x} = \mathbf{q}'\cdot\mathbf{y}, \quad \mathbf{q}'\cdot\mathbf{x} = \mathbf{q}\cdot\mathbf{y}.$$

Hence

$$\mathrm{P}_1 H_{\mathrm{FH}}\mathrm{P}_1 = -\int d^3y\Big[\lambda_1\big(e^{i\mathbf{q}'\cdot\mathbf{y}} + e^{-i\mathbf{q}'\cdot\mathbf{y}}\big) + \lambda_2\big(e^{i\mathbf{q}\cdot\mathbf{y}} + e^{-i\mathbf{q}\cdot\mathbf{y}}\big)\Big]J(\mathbf{y},\tau), \tag{5.91}$$

making the change of variables $\mathbf{x} \to \mathbf{y} = (-x^1, x^2, x^3)$.

If $\lambda_1 = \lambda_2$, Eq. 5.91 implies that the perturbing Hamiltonian commutes with the operator P_1, and therefore so does the full Hamiltonian:

$$[H(\lambda_1 = \lambda_2), \mathrm{P}_1] = 0.$$

Hence we take $\mathcal{A} = \mathrm{P}_1$, and the eigenstates of P_1 are the eigenstates of the Hamiltonian at $\lambda_1 = \lambda_2$.

On the other hand, if $\lambda_1 = -\lambda_2$, then we have that $H_{\mathrm{FH}}\mathrm{P}_1 = -\mathrm{P}_1 H_{\mathrm{FH}}$; it anti-commutes. Hence $\mathcal{A} \neq \mathrm{P}_1$. Instead, we want to combine P_1 with an operator that flips the sign of Eq. 5.91 without changing anything else. Note:

$$\mathrm{P}j^i(\mathbf{x},\tau)\mathrm{P} = -j^i(-\mathbf{x},\tau), \quad \mathrm{T}j^i(\mathbf{x},\tau)\mathrm{T} = -j^i(\mathbf{x},-\tau), \quad \mathrm{C}j^i(\mathbf{x},\tau)\mathrm{C} = -j^i(\mathbf{x},\tau).$$

Therefore, if we take the operator CP_1,

$$\begin{aligned}
\mathrm{CP}_1 H_{\mathrm{FH}} \mathrm{P}_1\mathrm{C} =& \mathrm{CP}_1 \int d^3x \mathrm{P}_1\mathrm{CCP}_1 \mathcal{H}_{\mathrm{FH}} \mathrm{P}_1\mathrm{C} \\
=& -\int d^3y \Big[\lambda_1\big(e^{i\mathbf{q}'\cdot\mathbf{y}} + e^{-i\mathbf{q}'\cdot\mathbf{y}}\big) + \lambda_2\big(e^{i\mathbf{q}\cdot\mathbf{y}} + e^{-i\mathbf{q}\cdot\mathbf{y}}\big)\Big] \mathrm{C}J(\mathbf{y},\tau)\mathrm{C} \\
=& +\int d^3y \Big[\lambda_1\big(e^{i\mathbf{q}'\cdot\mathbf{y}} + e^{-i\mathbf{q}'\cdot\mathbf{y}}\big) + \lambda_2\big(e^{i\mathbf{q}\cdot\mathbf{y}} + e^{-i\mathbf{q}\cdot\mathbf{y}}\big)\Big] J(\mathbf{y},\tau).
\end{aligned} \tag{5.92}$$

Hence CP_1 commutes with the perturbing Hamiltonian at $\lambda_1 = -\lambda_2$:

$$[H(\lambda_1 = -\lambda_2), \mathrm{CP}_1] = 0,$$

and therefore $\mathcal{A} = \mathrm{CP}_1$, and the eigenstates of CP_1 are the eigenstates of the Hamiltonian at $\lambda_1 = -\lambda_2$.

So if $\lambda_1 = \lambda_2$ and $\mathbf{p}_1 = (p^1, p^2, p^3)$ and $\mathbf{p}_2 = (-p^1, p^2, p^3)$, then the eigenstates of the full Hamiltonian are are eigenstates of P_1:

$$|\psi^{\pm}\rangle = \frac{1}{\sqrt{2}}\Big(|N(\mathbf{p}_1)\rangle \pm |N(\mathbf{p}_2)\rangle\Big). \tag{5.93}$$

And for $\lambda_1 = -\lambda_2$ the eigenstates of the full Hamiltonian are eigenstates of CP_1:

$$|\phi_1^{\pm}\rangle = \frac{1}{\sqrt{2}}\Big(|N(\mathbf{p}_1)\rangle \pm |\bar{N}(\mathbf{p}_2)\rangle\Big), \tag{5.94}$$

$$|\phi_2^{\pm}\rangle = \frac{1}{\sqrt{2}}\Big(|N(\mathbf{p}_2)\rangle \pm |\bar{N}(\mathbf{p}_1)\rangle\Big), \tag{5.95}$$

where $|\bar{N}\rangle$ is the anti-nucleon state.

If we insert these into Eq. 5.87, we get for the $\lambda_1 = \lambda_2$ case

$$\begin{aligned}
C_{\boldsymbol{\lambda}}(\tau,\mathbf{p}') \approx& \frac{1}{2E(\mathbf{p}')}\Big[e^{-E_{\psi^+}t}\Big(\langle\Omega|\chi(0)|N(\mathbf{p}')\rangle + \langle\Omega|\chi(0)|N(\mathbf{p})\rangle\Big)\langle N(\mathbf{p}')|\chi^\dagger(0)|\Omega\rangle \\
&+ e^{-E_{\psi^-}t}\Big(\langle\Omega|\chi(0)|N(\mathbf{p}')\rangle - \langle\Omega|\chi(0)|N(\mathbf{p})\rangle\Big)\langle N(\mathbf{p}')|\chi^\dagger(0)|\Omega\rangle\Big].
\end{aligned} \tag{5.96}$$

Similarly, for the $\lambda_1 = -\lambda_2$ case,

$$\begin{aligned} C_{\boldsymbol{\lambda}}(\tau, \mathbf{p}') \approx & \frac{1}{2E(\mathbf{p}')}\Big[e^{-E_{\phi_2^+}t}\Big(\langle\Omega|\chi(0)|N(\mathbf{p}')\rangle + \langle\Omega|\chi(0)|\bar{N}(\mathbf{p})\rangle\Big)\langle N(\mathbf{p}')|\chi^\dagger(0)|\Omega\rangle \\ & + e^{-E_{\phi_2^-}t}\Big(\langle\Omega|\chi(0)|N(\mathbf{p}')\rangle - \langle\Omega|\chi(0)|\bar{N}(\mathbf{p})\rangle\Big)\langle N(\mathbf{p}')|\chi^\dagger(0)|\Omega\rangle\Big]. \end{aligned} \tag{5.97}$$

Equations 5.96 and 5.97 are important results. In the free case, $\langle\Omega|\chi|N(\mathbf{p})\rangle = f(|\mathbf{p}|)$ (that is, they only depend on the magnitude of the momentum), and the same applies for the anti-nucleon. Therefore,

$$\langle\Omega|\chi(0)|N(\mathbf{p}')\rangle - \langle\Omega|\chi(0)|\bar{N}(\mathbf{p})\rangle = 0 = \langle\Omega|\chi(0)|N(\mathbf{p}')\rangle - \langle\Omega|\chi(0)|N(\mathbf{p})\rangle. \tag{5.98}$$

However, once we introduce the FH perturbation, the vacuum term has shifts proportional to λ and higher powers. Therefore,

$$\langle\Omega|\chi(0)|N(\mathbf{p}')\rangle - \langle\Omega|\chi(0)|N(\mathbf{p})\rangle \sim \mathcal{O}(\lambda), \tag{5.99}$$

and the same applies for the anti-nulceon overlap.

One immediate consequence of Eq. 5.96 and 5.97 is that we can show the assumption we made at the end of our FH derivation: all but one of the amplitudes vanish as the perturbation couplings go to zero.

From Eq. 5.87, we know that we can parameterise the perturbed correlator by

$$C_{\boldsymbol{\lambda}}(\tau) = \frac{1}{2E}\Big[A_1(\boldsymbol{\lambda})e^{-E_1(\boldsymbol{\lambda})\tau} + A_2(\boldsymbol{\lambda})e^{-E_2(\boldsymbol{\lambda})\tau}\Big] + \text{suppressed terms}, \tag{5.100}$$

From Eq. 5.96, along the line $\lambda_1 = \lambda_2$,

$$A_2(\boldsymbol{\lambda}) = \frac{1}{2}\Big[\langle\Omega|\chi(0)|N(\mathbf{p}')\rangle - \langle\Omega|\chi(0)|N(\mathbf{p})\rangle\Big]\langle N(\mathbf{p}')|\chi^\dagger(0)|\Omega\rangle, \tag{5.101}$$

and therefore

$$A_2(\boldsymbol{\lambda}) \xrightarrow{\boldsymbol{\lambda}\to 0} 0, \tag{5.102}$$

along this line. However, since we assumed that the perturbed correlator is at least twice differentiable in its λ variables, the above property must hold along all paths to the origin.

Hence, if we take τ sufficiently large for our nucleon terms to dominate, then the time-enhanced term from section 5.2 is

$$\begin{aligned} & -\sum_a e^{-E_{N,a}(\mathbf{p}')\tau}\tau\frac{\partial^2 E_{N,a}(\mathbf{p}')}{\partial\lambda_1\partial\lambda_2}A_{N,a}(\mathbf{p}')\Big|_{\lambda_1=\lambda_2=0} \\ & = \left(e^{-E_{N,1}(\mathbf{p}')\tau}\tau\frac{\partial^2 E_{N,1}(\mathbf{p}')}{\partial\lambda_1\partial\lambda_2}A_{N,1}(\mathbf{p}') + e^{-E_{N,2}(\mathbf{p}')\tau}\tau\frac{\partial^2 E_{N,2}(\mathbf{p}')}{\partial\lambda_1\partial\lambda_2}A_{N,2}(\mathbf{p}')\right)\Big|_{\lambda_1=\lambda_2=0} \\ & = e^{-E_{N,1}(\mathbf{p}')\tau}\tau\frac{\partial^2 E_{N,1}(\mathbf{p}')}{\partial\lambda_1\partial\lambda_2}A_{N,1}(\mathbf{p}')\Big|_{\lambda_1=\lambda_2=0}, \end{aligned} \tag{5.103}$$

since $A_{N,2} \xrightarrow{\boldsymbol{\lambda}\to 0} 0$.

Here, $A_{N,1} = A_N$, the unperturbed nucleon coefficient. Note that the simplifying assumptions at the start of the chapter, which amounted $\mathcal{O}(\lambda)$ corrections to the perturbed correlator, doesn't affect the above argument. Those higher order terms will of course vanish as the perturbation couplings go to zero, too.

5.3.3 Extracting the Energy Shift

In a more practical sense, Eqs. 5.96 and 5.97 tell us that the perturbed correlator is dominated by a single exponential term. This is because, along the lines $\lambda_1 = \pm\lambda_2$, one of the coefficients is $\mathcal{O}(1)$ and the other is $\mathcal{O}(\lambda)$. Therefore, we need not make a two-exponential fit to extract the eigen-energies of the perturbed Hamiltonian: these results ensure that only one of these eigen-energies dominates the correlator.

That is,

$$C_{\boldsymbol{\lambda}}(\tau)\Big|_{\lambda_1=\lambda_2=\lambda} \approx A(\lambda)e^{-E_{\psi^+}(\lambda)\tau}, \tag{5.104}$$

and

$$C_{\boldsymbol{\lambda}}(\tau)\Big|_{\lambda_1=-\lambda_2=\lambda} \approx \tilde{A}(\lambda)e^{-E_{\phi^+}(\lambda)\tau}, \tag{5.105}$$

for $\lambda \approx 0$.

From Eqs. 5.96 and 5.97,

$$A(\lambda)e^{-E_{\psi^+}(\lambda)\tau},\ \tilde{A}(\lambda)e^{-E_{\phi^+}(\lambda)\tau} \xrightarrow{\boldsymbol{\lambda}\to 0} A_N e^{-E_N\tau}, \tag{5.106}$$

the unperturbed propagator. Therefore, $E_{\psi^+}(\lambda)$ and $E_{\phi^+}(\lambda)$ are the same eigen-energy of the Hamiltonian, *but evaluated at different values of* λ_1, λ_2:

$$E(\lambda_1,\lambda_2)\Big|_{\lambda_1=\lambda_2=\lambda} = E_{\psi^+}(\lambda), \quad \text{and} \quad E(\lambda_1,\lambda_2)\Big|_{\lambda_1=-\lambda_2=\lambda} = E_{\phi^+}(\lambda). \tag{5.107}$$

Hence we can approximate the energy shift with a centered finite difference[††]:

$$\frac{\partial^2 E}{\partial\lambda_1\partial\lambda_2}\Big|_{\lambda_1=\lambda_2=0} = \lim_{\lambda\to 0}\frac{E(\lambda,\lambda)+E(-\lambda,-\lambda)-E(\lambda,-\lambda)-E(-\lambda,\lambda)}{4\lambda^2}, \tag{5.108}$$

and extract the centered difference by fitting to the correlator ratio

$$\frac{C(\lambda,\lambda)C(-\lambda,-\lambda)}{C(\lambda,-\lambda)C(\lambda,-\lambda)} \approx Ae^{-\Delta Et}, \tag{5.109}$$

where $\Delta E = E(\lambda,\lambda)+E(-\lambda,-\lambda)-E(\lambda,-\lambda)-E(-\lambda,\lambda)$. Once again, the assumptions that ignored some $\mathcal{O}(\lambda)$ corrections to the perturbed correlator doesn't affect this conclusion either. Since the $\mathcal{O}(\lambda)$ corrections will be suppressed, the correlator is dominated by one exponential along the lines $\lambda_1 = \pm\lambda_2$. Therefore, even in a more complete treatment that considers $\mathcal{O}(\lambda)$ corrections to the state, the above results will still hold.

[††]It is easy to derive this equation by taking $E(\lambda_1,\lambda_2)$ as a Taylor expansion in its λ variables.

Chapter 6

Off-Forward Scattering

In this chapter, we will examine the theoretical behaviour of the off-forward Compton tensor (OFCT), and show how generalised form factors (GFFs) can be extracted from a lattice calculation. Widespread interest in off-forward scattering began with a series of papers on generalised parton distributions (GPDs) [8, 9, 48, 49]. In particular, Ji showed that GPDs could be used to probe the spin structure of hadrons [9] (the Ji sum rule Eq. 4.32). Since then, almost all aspects of the OFCT have been intensively studied: its scaling [8, 48, 49, 143], factorisation [50, 144], electromagnetic gauge invariance and higher twist terms [145–149], among other properties have all been the subject of many papers.

However, almost all analyses of the nucleon OFCT are limited to a frame in which kinematics are dominated by two collinear lightlike vectors, and usually to deeply virtual Compton scattering (DVCS) kinematics. While this frame is a good approximation for high-energy scattering, it is the opposite of what we would like for our lattice kinematics.

As we have already discussed in previous chapters, the Euclidean spacetime of the lattice implies that we may only have spacelike momentum vectors. As such, the existing perturbative expansions in terms of lightlike Minkowski vectors can not be directly compared to our lattice calculation. Moreover, this means we can not compare to DVCS kinematics where the outgoing photon is on-shell (lightlike). Finally, since we extract the Feynman-Hellmann energy shift using lattice spectroscopy, we need small nucleon momenta for a clean signal. Therefore, we must do much of the theoretical work ourselves to derive results that match onto our lattice calculation.

First, in section 6.1 we will decompose the OFCT into its tensor structures and Lorentz scalar coefficients. Similar decompositions were performed by Bardeen and Tung [150] and Tarrach [151], and more recently by Lu [152]. In particular, we specialise our decomposition to suit the kinematics used in the lattice calculation.

In section 6.2 we will perform an OPE on the OFCT, using almost exactly the same method as in section 3.2. There have already been numerous perturbative calculations of the OFCT, in multiple different formalisms. Most prominently, the collinear factorisation method of Ellis, Furmanski and Petronzio [67, 68] has been used to calculate the OFCT up to twist-two [9] (recall Eq. 4.11) and twist three [146, 147] accuracy. Less prominent but still quite common is the light-ray operator method* [153, 154], which was used to calculate a perturbative expansion of the OFCT to twist three accuracy [148, 155]. These methods suffer from the aforementioned difficulty: they use a frame in which the nucleon's

*This is sometimes also referred to as the 'non-local operator product expansion', since it is an OPE in a basis of non-local operators. However, to avoid confusion in this thesis, we always refer to the local OPE as just 'the OPE' and the non-local OPE as 'the light-ray method'.

momenta are dominated by collinear lightlike vectors, and hence they can not be compared to our lattice calculation.

As has already been discussed in section 3.2, the OPE has a natural correspondence with lattice calculations: it uses Euclidean kinematics, and allows for arbitrarily slow-moving hadrons. There already exist multiple OPEs of the OFCT in the literature, starting with very early studies by Watanabe [156, 157] that pre-date interest in GPDs, and are therefore unsuited to compare to the lattice calculation. Later OPEs were also carried out by Chen [143] and White [145]. Neither of these analyses can be compared directly to results from the lattice calculation in the present thesis, since they assume the target hadron is a boson, and therefore the twist-two local operators (as in Eq. 3.50) have a much simpler off-forward matrix element:

$$\langle P'|\mathcal{O}_f^{(n)\mu_1\ldots\mu_n}|P\rangle = \sum_{i=0,2,4}^{n} \Delta^{\{\mu_1}\ldots\Delta^{\mu_i}\bar{P}^{\mu_{i+1}}\ldots\bar{P}^{\mu_n\}}G^f_{n+1,i}(t). \tag{6.1}$$

Of course, for those more theoretical studies, this assumption avoids a cluttered and a messy final result, while not impinging on results regarding, for instance, factorisation and scaling. However, dealing with the far messier form of the nucleon off-forward matrix elements (see Eq. 4.15) is necessary if we want to extract nucleon GFFs from our lattice calculation. For this reason, we must also do our own OPE on the OFCT.

Finally, in section 6.3, we will look at the analytic structure of the OFCT, first by delineating where the OFCT has cuts in the complex plane when the relevant momentum variables are taken complex. Secondly, we will derive a non-perturbative dispersion relation, and lastly, we will discuss the analytic continuation of the OFCT from Euclidean space, where the lattice calculation takes place, to Minkowski space.

6.1 Tensor Decomposition

To decompose the OFCT into its tensor structure and scalar coefficients, we use a general recipe with Bardeen and Tung [150] and Tarrach [151] as our guides:

1. take all the relevant tensor structures given in Tarrach [151];
2. reorganise these with the Gordon identity;
3. construct a gauge projector from the conditions given by Bardeen and Tung [150], and use this to find the gauge invariant form of the Compton tensor.

6.1.1 Kinematics and Definitions

Before we begin, let's reiterate all the relevant definitions. Note that for the whole of this chapter, we are working in Minkowski space.

First, we use the following basis of linearly independent momentum vectors:

$$\bar{P} = \frac{1}{2}(P + P'), \quad \bar{q} = \frac{1}{2}(q + q'), \quad \Delta = P' - P = q - q'.$$

Then, due to the fact that $P^2 = M^2$ is fixed in Minkowski space, we can form at most four linearly independent Lorentz scalars. We choose the following (as in Eq. 4.3),

$$\bar{Q}^2 = -\bar{q}^2, \quad \bar{\omega} = \frac{2\bar{P}\cdot\bar{q}}{\bar{Q}^2}, \quad t = \Delta^2, \quad \xi = -\frac{\bar{q}\cdot\Delta}{2\bar{P}\cdot\bar{q}}.$$

In this thesis, the main kinematic region we consider is the zero-skewness region[†]:

$$\xi = 0 \iff \Delta\cdot\bar{q} = 0 \iff q^2 = 0 = q'^2. \tag{6.2}$$

Using these kinematics we can isolate the twist-two A and B GFFs introduced in chapter 4, and hence these are what we calculate from our lattice calculation in chapter 7. Therefore, this is the kinematic region we will restrict ourselves to in the tensor decomposition.

Finally, as in section 3.2, we only consider the component of the OFCT that is symmetrised in its Lorentz indices:

$$T^{\mu\nu}_{\text{symm}} = \frac{1}{2}\Big[T^{\mu\nu} + T^{\nu\mu}\Big]. \tag{6.3}$$

Since we will calculate the diagonal component T^{33} (by Eq. 5.79), only the symmetric part of the OFCT is relevant to our lattice calculation.

6.1.2 Relevant Tensor Structures

The OFCT is invariant under the discrete symmetries (parity, time-reversal and charge conjugation), and it must further satisfy the crossing symmetry,

$$T^{\mu\nu}(q, P; q', P') = T^{\nu\mu}(-q', P; -q, P'). \tag{6.4}$$

Using these restrictions and the basis $\{\gamma^\mu, P^\mu, P'^\mu, q^\mu, q'^\mu\}$, Tarrach [151] determined all possible tensor structures that can contribute to the off-forward scattering of a nucleon. Of these[‡], we only select structures that are gauge-independent (that is, no q or q' terms with uncontracted indices)[§] and that are symmetric under $\mu \leftrightarrow \nu$:

$$g^{\mu\nu}, \quad g^{\mu\nu}\bar{\not{q}}, \quad \bar{P}^\mu\bar{P}^\nu, \quad \bar{P}^\mu\bar{P}^\nu\bar{\not{q}}, \quad \bar{P}^\mu\gamma^\nu + \bar{P}^\nu\gamma^\mu, \quad (\bar{P}^\mu\gamma^\nu + \bar{P}^\nu\gamma^\mu)\bar{\not{q}} - \bar{\not{q}}(\bar{P}^\mu\gamma^\nu + \bar{P}^\nu\gamma^\mu). \tag{6.5}$$

The unprojected OFCT $\tilde{T}^{\mu\nu}$ is then built up from the linear combination of these tensor structures:

$$\tilde{T}^{\mu\nu} = \bar{u}(P')\Big[\sum_i K_i \ell_i^{\mu\nu}\Big]u(P), \tag{6.6}$$

where $\ell_i^{\mu\nu}$ is one of the terms in the statement 6.5, and K_i is a Lorentz scalar coefficient that depends on the variables $\bar{Q}^2, t$ and $\bar{\omega}$ (we have chosen $\xi = 0$ and hence we lose one of our Lorentz scalars).

[†]Recall that we referenced this fact in section 5.19 in deriving the symmetries of the perturbed Hamiltonian.
[‡]See Tarrach [151] for the full list.
[§]One can always construct a general gauge invariant tensor structure in this way, since the Ward identities ensure that gauge-dependent (e.g. $q^\mu q^\nu$) parts, and gauge-independent (e.g. $g^{\mu\nu}$) must cancel one another, and hence the Lorentz scalar coefficients of the gauge-independent contributions determines that of the gauge-independent — they're linearly dependent.

Once again referring to Tarrach [151], the coefficient of the $(\bar{P}^\mu\gamma^\nu+\bar{P}^\nu\gamma^\mu)\not{\bar{q}}-\not{\bar{q}}(\bar{P}^\mu\gamma^\nu+\bar{P}^\nu\gamma^\mu)$ component vanishes in the region $q^2=q'^2$, and hence we do not consider it.

Since they will come up a lot, we define the Dirac bilinears

$$\tau_1^\mu=\bar{u}(P')\gamma^\mu u(P),\quad \tau_2^\mu=\bar{u}(P')\frac{\sigma^{\mu\alpha}i\Delta_\alpha}{2M}u(P).$$

Therefore, the unprojected component of the OFCT is

$$\tilde{T}^{\mu\nu}=K_1g^{\mu\nu}\bar{u}(P')u(P)+K_2g^{\mu\nu}\bar{q}\cdot\tau_1+K_3\bar{P}^\mu\bar{P}^\nu\bar{u}(P')u(P)+K_4\bar{P}^\mu\bar{P}^\nu\bar{q}\cdot\tau_1+K_5\bar{P}^{\{\mu}\tau_1^{\nu\}}. \tag{6.7}$$

In the above expression, we have two Dirac bilinears: $\bar{u}(P')u(P)$ and $\bar{u}(P')\gamma^\mu u(P)$. It will be convenient, when we need to compare this to the OPE, to use the Gordon identity (Eq. 4.13),

$$\bar{u}(P')\gamma^\mu u(P)=\bar{u}(P')\left(\frac{\bar{P}^\mu}{M}+\frac{i\sigma^{\mu\nu}\Delta_\nu}{2M}\right)u(P),$$

to reorganise Eq. 6.7.

First, using the Gordon identity, we have that

$$\bar{P}^\mu\bar{u}(P')u(P)=M\big(\tau_1^\mu-\tau_2^\mu\big)\quad\Rightarrow\quad\bar{u}(P')u(P)=\frac{M}{\bar{P}\cdot\bar{q}}\big(\tau_1\cdot\bar{q}-\tau_2\cdot\bar{q}\big). \tag{6.8}$$

Hence Eq. 6.7 becomes

$$\begin{aligned}\tilde{T}^{\mu\nu}=&-\frac{M}{\bar{P}\cdot\bar{q}}K_1g^{\mu\nu}\bar{q}\cdot\tau_2+\Big(K_2+\frac{M}{\bar{P}\cdot\bar{q}}K_1\Big)g^{\mu\nu}\bar{q}\cdot\tau_1\\&-MK_3\bar{P}^{\{\mu}\tau_2^{\nu\}}+K_4\bar{P}^\mu\bar{P}^\nu\bar{q}\cdot\tau_1+\Big(K_5+MK_3\Big)\bar{P}^{\{\mu}\tau_1^{\nu\}}.\end{aligned} \tag{6.9}$$

Once again, we note the linear independence of the scalar coefficients to re-write the Compton tensor as

$$\tilde{T}^{\mu\nu}=K_1'g^{\mu\nu}\bar{q}\cdot\tau_1+K_2'g^{\mu\nu}\bar{q}\cdot\tau_2+K_3'\bar{P}^{\{\mu}\tau_2^{\nu\}}+K_4'\bar{P}^\mu\bar{P}^\nu\bar{q}\cdot\tau_1+K_5'\bar{P}^{\{\mu}\tau_1^{\nu\}}. \tag{6.10}$$

To compare this to the OPE it is helpful if our expression also has a $\bar{P}^\mu\bar{P}^\nu\bar{q}\cdot\tau_2$ term. We can easily re-express this, again using the Gordon identity:

$$\bar{P}^\mu\bar{P}^\nu\bar{q}\cdot\tau_1+\bar{P}\cdot\bar{q}\bar{P}^{\{\mu}\tau_2^{\nu\}}=\bar{P}^\mu\bar{P}^\nu\bar{q}\cdot\tau_2+\bar{P}\cdot\bar{q}\bar{P}^{\{\mu}\tau_1^{\nu\}}. \tag{6.11}$$

Using this relation, Eq. 6.10 becomes

$$\begin{aligned}\tilde{T}^{\mu\nu}=&K_1'g^{\mu\nu}\bar{q}\cdot\tau_1+K_2'g^{\mu\nu}\bar{q}\cdot\tau_2+(K_3'-\bar{P}\cdot\bar{q}K_6')\bar{P}^{\{\mu}\tau_2^{\nu\}}+(K_4'-K_6')\bar{P}^\mu\bar{P}^\nu\bar{q}\cdot\tau_1\\&+(K_5'+\bar{P}\cdot\bar{q}K_6')\bar{P}^{\{\mu}\tau_1^{\nu\}}+K_6'\bar{P}^\mu\bar{P}^\nu\bar{q}\cdot\tau_2.\end{aligned} \tag{6.12}$$

Clearly, we have just added zero to Eq. 6.10. Again, we redefine the coefficients in Eq. 6.12 to get

$$\begin{aligned}\tilde{T}^{\mu\nu}=&[K_1''\bar{q}\cdot\tau_1+K_2''\bar{q}\cdot\tau_2]g^{\mu\nu}+[K_3''\bar{q}\cdot\tau_1+K_4''\bar{q}\cdot\tau_2]\bar{P}^\mu\bar{P}^\nu\\&+K_5''\bar{P}^{\{\mu}\tau_1^{\nu\}}+K_6''\bar{P}^{\{\mu}\tau_2^{\nu\}}.\end{aligned} \tag{6.13}$$

For convenience, in the future we will simply replace $K_i'' \to K_i$.

6.1.3 Gauge Projection

We will define a gauge projector $I^{\mu\nu}$ as a tensor that satisfies two conditions from [150]:

1. if M^μ is a fully gauge invariant quantity, then

$$I^{\mu\nu} M_\nu = M^\mu; \tag{6.14}$$

2. it satisfies the Ward identities; for us, these are $q_\mu I^{\mu\nu} = 0 = q'_\nu I^{\mu\nu}$.

However, even in the most general case, the gauge projector is not unique. Compare the projector from Bardeen and Tung, $I^{\mu\nu} = g^{\mu\nu} - q'^\mu q^\nu / q \cdot q'$, to the two different projectors used in Eichmann and Fischer [158], $I_1^{\mu\mu'} = g^{\mu\mu'} - q^\mu q^{\mu'}/q^2$ and $I_2^{\nu\nu'} = g^{\nu\nu'} - q'^\nu q'^{\nu'}/q'^2$, for the μ and ν respectively.

Hence we will construct a gauge projector that is simplest for our situation but satisfies our stipulations for a gauge projector. Since we are only interested in the symmetric component of the Compton tensor, our Ward identities $q_\mu T^{\mu\nu} = 0$ and $q'_\nu T^{\mu\nu} = 0$ can be added and subtracted to one another to get $\Delta_\mu T^{\mu\nu} = 0 = \bar{q}_\mu T^{\mu\nu}$.

Moreover, since we are focussed on the symmetric Compton tensor,

$$T^{\mu\nu} = I_{\mu\mu'} I_{\nu'\nu} T_{\mu'\nu'} = I_{\nu\mu'} I_{\nu'\mu} T_{\mu'\nu'} = I_{\nu\nu'} I_{\mu'\mu} T_{\mu'\nu'} = I_{\mu'\mu} I_{\nu\nu'} T_{\mu'\nu'}.$$

Hence a symmetrised gauge projector is sufficient.

A general ansatz for the symmetrised gauge projector is

$$I^{\mu\nu} = A_1 g^{\mu\nu} + A_2 \Delta^\mu \Delta^\nu + A_3 \bar{q}^\mu \bar{q}^\nu + A_4 \big(\bar{q}^\mu \Delta^\nu + \Delta^\mu \bar{q}^\nu\big), \tag{6.15}$$

where the A_i are Lorentz scalars. Since $\bar{q} \cdot \Delta = 0$ in our kinematics (recall the Eq. 6.2), by applying the gauge conditions we find that $A_4 = 0$. Hence the restricted gauge projector is

$$I^{\mu\nu} = g^{\mu\nu} - \frac{\Delta^\mu \Delta^\nu}{\Delta^2} - \frac{\bar{q}^\mu \bar{q}^\nu}{\bar{q}^2}. \tag{6.16}$$

Acting with this gauge projector on the unprojected decomposition Eq. 6.13, we get our final decomposition:

$$\begin{aligned} T^{\mu\nu} =& [K_1 \bar{q} \cdot \tau_1 + K_2 \bar{q} \cdot \tau_2] \left(g^{\mu\nu} - \frac{\Delta^\mu \Delta^\nu}{\Delta^2} - \frac{\bar{q}^\mu \bar{q}^\nu}{\bar{q}^2} \right) \\ &+ [K_3 \bar{q} \cdot \tau_1 + K_4 \bar{q} \cdot \tau_2] \left(\bar{P}^\mu - \frac{\bar{P} \cdot \bar{q}}{\bar{q}^2} \bar{q}^\mu \right) \left(\bar{P}^\nu - \frac{\bar{P} \cdot \bar{q}}{\bar{q}^2} \bar{q}^\nu \right) \\ &+ K_5 \left(\bar{P}^{\{\mu} - \frac{\bar{P} \cdot \bar{q}}{\bar{q}^2} \bar{q}^{\{\mu} \right) \left(\tau_1^{\nu\}} - \frac{\tau_1 \cdot \bar{q}}{\bar{q}^2} \bar{q}^{\nu\}} \right) \\ &+ K_6 \left(\bar{P}^{\{\mu} - \frac{\bar{P} \cdot \bar{q}}{\bar{q}^2} \bar{q}^{\{\mu} \right) \left(\tau_2^{\nu\}} - \frac{\tau_2 \cdot \bar{q}}{\bar{q}^2} \bar{q}^{\nu\}} \right). \end{aligned} \tag{6.17}$$

6.2 Operator Product Expansion

The tensor decomposition in Eq. 6.17 is entirely non-perturbative. As in chapter 3, we want to perform a leading-order OPE to divide the coefficient functions K_i into their perturbative and non-perturbative parts. The process we follow is exactly the same as the forward OPE:

1. perform a coordinate space OPE; we will argue that the coordinate space OPE from chapter 3 is sufficient for our purposes;
2. take the off-forward matrix element of this operator;
3. Fourier transform this using the same process as in chapter 3, only with more Fourier conjugate variables.

6.2.1 OPE Kinematics

In this section we relax our restriction that $\xi = 0$. The physical Minkowski space generalised Bjorken limit is

$$\bar{P}\cdot\bar{q}\to\infty,\ \bar{Q}^2\to\infty,\quad |\bar{\omega}|\geq 1,\ \text{fixed and finite.}$$

However, as in section 3.2, this is not the limit we take in the OPE.

If we have Euclidean momenta, then

$$\bar{\omega} = \frac{2\bar{P}\cdot\bar{q}}{\bar{Q}^2} \sim \frac{|\bar{P}|}{\bar{Q}^2}. \tag{6.18}$$

In Minkoswki space, $\bar{P}^2 = M^2 - t/4$ and hence $\bar{P}^2/\bar{Q}^2$ terms are target mass corrections that should vanish on the physical light-cone. So, as in chapter 3, we define a large Euclidean momentum limit:

$$\bar{Q}^2\to\infty,\quad \bar{\omega}\to 0.$$

Therefore, in our off-forward OPE we will use the same trick we used in the forward OPE: keep terms of order $\bar{\omega}$ and throw out terms of order $M^2/\bar{Q}^2$ and $t/\bar{Q}^2$, even they are of the same order as $\bar{\omega}$[**].

Again, as in the forward OPE, even though the limit $\bar{Q}^2\to\infty$ and $\bar{\omega}\to 0$ is most naturally taken in Euclidean space, we do not explicitly evaluate this in Euclidean space. Nonetheless, our final expression can be compared to Euclidean lattice results.

6.2.2 Coordinate Space OPE

Recall the OPE of the leading-twist current product, symmetrised in its Lorentz indices (Eq. 3.55), from section 3.2:

$$T[j_\mu(z/2)j_\nu(-z/2)]_{\text{symm}} = -2\sum_f e_f^2 S^\rho(z)\Big\{\mathcal{S}_{\mu\rho\nu\kappa}\sum_{n=1,3,5}^{\infty}\frac{(-i)^n}{n!}z_{\mu_1}...z_{\mu_n}\mathcal{O}_f^{(n+1)\kappa\mu_1...\mu_n}\Big\}.$$

[**] Of course, these corrections don't actually vanish completely. In chapter 7 we will discuss some difficulties related to this assumption when it comes to interpreting our lattice results.

This expression is independent of what states it is sandwiched between. However, recall that this expression was equivalent to taking the handbag contributions of the short-distance OPE. Therefore, we need to be sure that handbag contributions dominate. Following the arguments of Diehl et al. [159], we note that for $t \ll \bar{Q}^2$ (that is, the soft momentum transfer is much smaller than the hard) handbag terms should dominate the off-forward process. Hence this OPE is a good approximation for our purposes so long as we stay in a kinematic regime where $t \ll \bar{Q}^2$.

6.2.3 'Total' Derivative Operators

Before we actually perform the OPE calculation, we will take a quick detour to discuss 'total' derivative operators. These operators have a vanishing *forward* matrix element and are hence not considered in the standard deep inelastic scattering OPE. However, for off-forward kinematics they contribute to the OFCT, and need to be discussed.

Recall the basis of local twist-two operators we have so far focussed on (Eq. 3.50):

$$\mathcal{O}_f^{(n)\mu_1\ldots\mu_n}(X) = \bar{\psi}_f(X)\gamma^{\{\mu_1} i\overset{\leftrightarrow}{D}^{\mu_2}\ldots i\overset{\leftrightarrow}{D}^{\mu_n\}}\psi_f(X) - \text{traces}.$$

We define the 'total' or 'overall' derivative operators as

$$\widehat{\mathcal{O}}_f^{(m,n)\mu_1\ldots\mu_m\mu_{m+1}\ldots\mu_n}(X) = (-i)^m\partial_X^{\mu_1}\ldots\partial_X^{\mu_m}\mathcal{O}_f^{(n)\mu_{m+1}\ldots\mu_n}(X), \quad n > m. \tag{6.19}$$

Note that the derivatives need not be covariant, since they act on one of the operators in Eq. 3.50, which are gauge invariant.

The off-forward matrix element of the operators in Eq. 6.19 is

$$\langle P'|\widehat{\mathcal{O}}_f^{(m,n)\mu_1\ldots\mu_m\mu_{m+1}\ldots\mu_n}(X)|P\rangle\Big|_{X=0} = \Delta^{\mu_1}\ldots\Delta^{\mu_m}\langle P'|\mathcal{O}_f^{(n-m)\mu_{m+1}\ldots\mu_n}|P\rangle. \tag{6.20}$$

Therefore, they vanish in the forward case ($\Delta = 0$), and hence why they are generally not considered in the classic derivations of the forward OPE.

Although the operators in Eq. 6.19 don't have definite twist, we can get their leading-twist component by symmetrising their indices and subtracting traces:

$$\begin{aligned}&[\widehat{\mathcal{O}}_f^{(m,n)\mu_1\ldots\mu_n}(X)]_{\text{twist-two}}\\ &\quad= (-i)^m\partial_X^{\{\mu_1}\ldots\partial_X^{\mu_m}\bar{\psi}_f(X)\gamma^{\mu_{m+1}}i\overset{\leftrightarrow}{D}^{\mu_{m+2}}\ldots i\overset{\leftrightarrow}{D}^{\mu_n\}}\psi_f(X) - \text{traces}, \quad n > m.\end{aligned} \tag{6.21}$$

Therefore, it is natural to ask why these operators don't contribute to the leading-order handbag terms (Eq. 3.55).

Scalar OPE

The OPE result from Eq. 3.55 is completely general, and is equivalent to a full OPE at twist-two with leading-order Wilson coefficients. This is almost axiomatic, since the leading-order term of the OPE should be the current product for zero coupling. However, Eq. 3.55 doesn't contain any of the operators from Eq. 6.21. Here, we show through a simplified OPE how their contribution to the leading-order OPE vanishes.

First, we will assume that our target particle is a spin zero particle (such as a pion), and hence the matrix element of one of the usual twist-two operators is

$$\langle P'|\mathcal{O}_f^{(n)\mu_1\ldots\mu_n}|P\rangle = \sum_{i=0,2,4}^{n} \Delta^{\{\mu_1}\ldots\Delta^{\mu_i}\bar{P}^{\mu_{i+1}}\ldots\bar{P}^{\mu_n\}} A^f_{n+1,i}(t). \tag{6.22}$$

Where these $A^f_{n,i}$ are generalised form factors (GFFs) are related to the Mellin moments of (isosinglet pion) GPDs by

$$\int_{-1}^{1} dx x^n H^f(x,\xi,t) = \sum_{i=0,2,4}^{n} (-2\xi)^i A^f_{n+1,i}(t). \tag{6.23}$$

Then, we consider a twist-two OPE, where we assume scalar currents for simplicity:

$$\begin{aligned} T(P,q;P',q') &= \int d^4z e^{i\bar{q}\cdot z}\langle P'|T[j(z/2)j(-z/2)]|P\rangle \\ &= \sum_{i,n,m} c^{(i)}_{n,m}(\bar{Q}^2)\frac{2^n}{(\bar{Q}^2)^n}\bar{q}_{\mu_1}\ldots\bar{q}_{\mu_n}\langle P'|\widehat{\mathcal{O}}^{(m,n)\mu_1\ldots\mu_n}|P\rangle, \end{aligned} \tag{6.24}$$

where $\widehat{\mathcal{O}}^{(m,n)\mu_1\ldots\mu_n}$ are the operators from Eq. 6.19, so they include the leading-twist part of the total derivative operators (Eq. 6.21) as well as the non-leading-twist. Note that i here denotes the order to which the Wilson coefficients are expanded, and hence $i = 0$ corresponds to the tree-level expansion.

From Eq. 6.20, the OPE becomes

$$T = \sum_{i,n,m} c^{(i)}_{n,m}(\bar{Q}^2)(-2\xi\bar{\omega})^m \frac{2^{n-m}}{(\bar{Q}^2)^{n-m}}\bar{q}_{\mu_{m+1}}\ldots\bar{q}_{\mu_n}\langle P'|\widehat{\mathcal{O}}^{(n-m)\mu_{m+1}\ldots\mu_n}|P\rangle, \tag{6.25}$$

where we have dropped the momentum arguments of the scalar Compton tensor, T. Further, we can insert Eq. 6.22 into this expansion:

$$\begin{aligned} T &= \sum_{i,n,m} c^{(i)}_{n,m}(\bar{Q}^2)(-2\xi\bar{\omega})^m \sum_{j=0,2,4}^{n-m} (-2\xi\bar{\omega})^j \bar{\omega}^{n-m-j} A_{n-m,j}(t) \\ &= \sum_{i,n,m} c^{(i)}_{n,m}(\bar{Q}^2)(-2\xi)^m \bar{\omega}^n \sum_{j=0,2,4}^{n-m} (-2\xi)^j A_{n-m,j}(t). \end{aligned} \tag{6.26}$$

Finally, using Eq. 6.23, this becomes

$$T = \sum_{i,n,m} c^{(i)}_{n,m}(\bar{Q}^2)(-2\xi)^m \bar{\omega}^n \int_{-1}^{1} dx x^{n-m-1} H(x,\xi,t). \tag{6.27}$$

Therefore, the term

$$\sum_{i,n,m} c^{(i)}_{n,m}(\bar{Q}^2)(-2\xi)^m \bar{\omega}^n$$

can be compared to the tree-level parton amplitude to calculate the value of the Wilson coefficients.

A calculation of the leading-order Wilson coefficients diagrams to get $c^{(0)}_{n,m}$ is fairly straightforward; Chen found [143] that the tree-level amplitude is

$$\mathcal{M}^{(0)} \propto \sum_{n=2,4,6}^{\infty} \bar{\omega}^n. \tag{6.28}$$

Therefore, the leading-order Wilson coefficients are

$$c^{(0)}_{n,m} \propto \delta_{m,0}, \tag{6.29}$$

and hence at leading-order all total derivative terms vanish, including their twist-two components.

Leading Twist Gauge Invariance

The fact that these total derivative contributions vanish at leading-order has implications for the EM gauge invariance of the OFCT. It is well-known that the symmetric component of the leading-twist OFCT violates EM gauge invariance (see Refs. [146, 155, 160]). Since we only consider a Compton tensor that is symmetric in its Lorentz indices, the final result of our OPE will therefore not satisfy EM gauge invariance.

The EM gauge invariance of the symmetric OFCT may be thought of as satisfying its Ward identities,

$$q_\mu T^{\mu\nu}_{\text{symm}} = 0 = q'_\nu T^{\mu\nu}_{\text{symm}} \quad \Rightarrow \quad \bar{q}_\mu T^{\mu\nu}_{\text{symm}} = 0 = \Delta_\mu T^{\mu\nu}_{\text{symm}}, \tag{6.30}$$

or as current conservation,

$$\begin{gathered} \frac{\partial}{\partial (X \pm z/2)_\rho} T[j^{\{\mu}(X+z/2)j^{\nu\}}(X-z/2)] = 0, \\ \frac{\partial}{\partial X_\rho} T[j^{\{\mu}(X+z/2)j^{\nu\}}(X-z/2)] = 0 = \frac{\partial}{\partial z_\rho} T[j^{\{\mu}(X+z/2)j^{\nu\}}(X-z/2)]. \end{gathered} \tag{6.31}$$

Note that X is the center position of the current product, which we have so far set to zero without loss of generality.

At leading-twist, it can be shown [155] that

$$\frac{\partial}{\partial X_\rho} T[j^{\{\mu}(X+z/2)j^{\nu\}}(X-z/2)] \neq 0, \quad \frac{\partial}{\partial z_\rho} T[j^{\{\mu}(X+z/2)j^{\nu\}}(X-z/2)] = 0, \tag{6.32}$$

and hence the leading-twist component of the current product doesn't satisfy EM gauge invariance.

Note that, due to translational invariance of the currents,

$$\begin{aligned} \frac{\partial}{\partial X_\rho} \langle P'|T[j^{\{\mu}(X+z/2)j^{\nu\}}(X-z/2)]|P\rangle =& \frac{\partial}{\partial X_\rho} e^{i\Delta\cdot X} \langle P'|T[j^{\{\mu}(z/2)j^{\nu\}}(-z/2)]|P\rangle \\ =& i\Delta^\rho e^{i\Delta\cdot X} \langle P'|T[j^{\{\mu}(z/2)j^{\nu\}}(-z/2)]|P\rangle. \end{aligned} \tag{6.33}$$

Therefore, in the forward case where $\Delta = 0$, the matrix element of the current product is EM gauge invariant, and hence our final result in section 3.2 satisfied its Ward identities. It is only for off-forward kinematics, where $\Delta \neq 0$, that the leading-twist amplitude violates EM gauge invariance. Moreover, as is suggested by Eq. 6.33, EM gauge invariance will be satisfied up to terms linear in Δ.

In the light-ray operator method it has been found that, by including total derivatives of leading-twist operators, EM gauge invariance can be restored [148, 149, 155]. Identical results were found in the OPE formalism [145]. To give an example, take the matrix element

$$\langle P'|\widehat{\mathcal{O}}_f^{(2,n)\mu\nu\mu_1\ldots\mu_n}(X)|P\rangle\Big|_{X=0} = \Delta^\mu\Delta^\nu\langle P'|\mathcal{O}_f^{(n)\mu_1\ldots\mu_n}|P\rangle. \tag{6.34}$$

Even though the operator $\widehat{\mathcal{O}}_f^{(2,n)\mu\nu\mu_1\ldots\mu_n}(X)$ is a non-leading-twist operator, Eq. 6.34 is a leading-twist term. And the term in Eq. 6.34 is what is needed to restore EM gauge invariance.

In our OPE, we will find the same result: EM gauge invariance of the leading-twist OPE is broken by terms linear in Δ. To restore it we could include total derivatives of leading-twist operators as in the aforementioned studies. However, it has been found [155] that including total derivative operators is equivalent to the *ad hoc* inclusion of minimal terms linear in Δ that restore gauge invariance (such as in Ref. [161]), plus twist-three terms. As such, we will opt to simply include the minimal terms that restore EM gauge invariance.

6.2.4 Matrix Element

Recall the decomposition of the off-forward matrix elements of the local twist-two operators in Eq. 4.15:

$$\begin{aligned}\langle P'|\mathcal{O}_f^{(n+1)\kappa\mu_1\ldots\mu_n}|P\rangle = \bar{u}(P')\gamma^{\{\kappa}u(P)\sum_{j=0,2,4}^{n}A_{n+1,j}^f(t)\Delta^{\mu_1}\ldots\Delta^{\mu_j}\bar{P}^{\mu_{j+1}}\ldots\bar{P}^{\mu_n\}}\\ + \bar{u}(P')\frac{\sigma^{\{\kappa\alpha}i\Delta_\alpha}{2M}u(P)\sum_{j=0,2,4}^{n}B_{n+1,j}^f(t)\Delta^{\mu_1}\ldots\Delta^{\mu_j}\bar{P}^{\mu_{j+1}}\ldots\bar{P}^{\mu_n\}}\\ + C_{n+1}^f(t)\mathrm{mod}(n,2)\frac{1}{M}\bar{u}(P')u(P)\Delta^{\{\kappa}\Delta^{\mu_1}\ldots\Delta^{\mu_n\}}.\end{aligned} \tag{6.35}$$

Therefore,

$$\begin{aligned} z_{\mu_1}...z_{\mu_n}\langle P'|\mathcal{O}_f^{(n+1)\kappa\mu_1...\mu_n}|P\rangle \\ &= \sum_{j=0,2,4}^{n} c_{n,j}^{(1)}(\Delta\cdot z)^j(\bar{P}\cdot z)^{n-j}\left[\tau_1^\kappa A_{n+1,j}^f(t)+\tau_2^\kappa B_{n+1,j}^f(t)\right] \\ &+ \sum_{j=0,2,4}^{n} c_{n,j}^{(2)}(\Delta\cdot z)^j(\bar{P}\cdot z)^{n-j-1}\bar{P}^\kappa\left[A_{n+1,j}^f(t)\tau_1\cdot z+B_{n+1,j}^f(t)\tau_2\cdot z\right] \\ &+ \sum_{j=0,2,4}^{n} c_{n,j}^{(3)}(\Delta\cdot z)^{j-1}(\bar{P}\cdot z)^{n-j}\Delta^\kappa\left[A_{n+1,j}^f(t)\tau_1\cdot z+B_{n+1,j}^f(t)\tau_2\cdot z\right] \\ &+ \Delta^\kappa(\Delta\cdot z)^n C_{n+1}^f(t)\mathrm{mod}(n,2)\frac{1}{M}\overline{u}(P')u(P), \end{aligned} \tag{6.36}$$

where we determine the c from combinatorics.

The general expression for a symmetrised rank-$(n+1)$ tensor is

$$T^{\{\kappa\mu_1...\mu_n\}} = \frac{1}{(n+1)!}\sum_{\sigma\in S_{n+1}} T^{\nu_{\sigma(1)}...\nu_{\sigma(n+1)}}, \tag{6.37}$$

where S_{n+1} is the group of permutations of the numbers $1,2,...,n+1$, and σ is an element of S_{n+1}. For instance, we can take an element of S_{n+1} $\sigma_0=(1,2,3,4,...,n+1)$, and denote the i^{th} term in σ_0 by $\sigma_0(i)$. We let $\nu_1=\kappa$ and $\nu_j=\mu_{j-1}$. To calculate the c coefficients in Eq. 6.36, we first note that there are $(n+1)!$ elements of S_{n+1}, and hence $(n+1)!$ ways to permute the indices. If we fix the first index $\sigma(1)=1$, and calculate the number of permutations, we can then find $c_{n,j}^{(1)}$. Fixing one element of S_{n+1} leaves n free terms; therefore, there are $n!$ such permutations with $\sigma(1)=1$.

Similarly, if we hold $\sigma(l)=1$ for some $2\le l\le j+1$, this is equivalent to calculating $c_{n,j}^{(3)}$. So there are $n!$ permutations for each value of l, since for each we're just holding one index fixed. And furthermore, there are j values of l. Therefore, $jn!$ permutations in total.

Finally, if we hold $\sigma(k)=1$ for some $k\ge j+2$, this is equivalent to calculating $c_{n,j}^{(2)}$. There are $n!$ permutations for each value of k, and $n-j$ values of k. Therefore, there are $(n-j)n!$ permutations in total.

$$T^{\{\kappa\mu_1...\mu_n\}} = \frac{1}{(n+1)!}\left(\sum_{\sigma(1)=1} + \sum_{\substack{\sigma(l)=1\\ 2\le l\le j+1}} + \sum_{\substack{\sigma(k)=1\\ k\ge j+2}}\right) T^{\nu_{\sigma(1)}...\nu_{\sigma(n+1)}}. \tag{6.38}$$

The three c values are

$$c_{n,j}^{(1)} = \frac{n!}{(n+1)!} = \frac{1}{n+1}, \quad c_{n,j}^{(2)} = \frac{(n-j)n!}{(n+1)!} = \frac{n-j}{n+1} \quad c_{n,j}^{(3)} = \frac{jn!}{(n+1)!} = \frac{j}{n+1}. \tag{6.39}$$

Substituting these counting factors, Eq. 6.36 becomes

$$\begin{aligned} z_{\mu_1}...z_{\mu_n}\langle P'|\mathcal{O}_f^{(n+1)\kappa\mu_1...\mu_n}|P\rangle = \\ &\sum_{j=0,2,4}^{n}\frac{1}{n+1}(\Delta\cdot z)^j(\bar{P}\cdot z)^{n-j}\big[\tau_1^\kappa A_{n+1,j}^f(t)+\tau_2^\kappa B_{n+1,j}^f(t)\big] \\ &+\sum_{j=0,2,4}^{n}\frac{n-j}{n+1}(\Delta\cdot z)^j(\bar{P}\cdot z)^{n-j-1}\bar{P}^\kappa\big[A_{n+1,j}^f(t)\tau_1\cdot z+B_{n+1,j}^f(t)\tau_2\cdot z\big] \\ &+\sum_{j=0,2,4}^{n}\frac{j}{n+1}(\Delta\cdot z)^{j-1}(\bar{P}\cdot z)^{n-j}\Delta^\kappa\big[A_{n+1,j}^f(t)\tau_1\cdot z+B_{n+1,j}^f(t)\tau_2\cdot z\big] \\ &+\Delta^\kappa(\Delta\cdot z)^n C_{n+1}^f(t)\mathrm{mod}(n,2)\frac{1}{M}\overline{u}(P')u(P). \end{aligned} \tag{6.40}$$

Finally, the leading-twist term of the matrix element is

$$\begin{aligned} &\langle P'|T[j_\mu(z/2)j_\nu(-z/2)]|P\rangle = -2\sum_f e_f^2 S^\rho(z)\mathcal{S}_{\mu\rho\nu\kappa}\sum_{n=1,3,5}^{\infty}\frac{(-i)^n}{n!} \\ &\times\sum_{j=0,2,4}^{n}\Big\{\frac{1}{n+1}(\Delta\cdot z)^j(\bar{P}\cdot z)^{n-j}\big[\tau_1^\kappa A_{n+1,j}^f(t)+\tau_2^\kappa B_{n+1,j}^f(t)\big] \\ &+\frac{n-j}{n+1}(\Delta\cdot z)^j(\bar{P}\cdot z)^{n-j-1}\bar{P}^\kappa\big[A_{n+1,j}^f(t)\tau_1\cdot z+B_{n+1,j}^f(t)\tau_2\cdot z\big] \\ &+\frac{j}{n+1}(\Delta\cdot z)^{j-1}(\bar{P}\cdot z)^{n-j}\Delta^\kappa\delta_{j,0}\big[A_{n+1,j}^f(t)\tau_1\cdot z+B_{n+1,j}^f(t)\tau_2\cdot z\big] \\ &+\Delta^\kappa(\Delta\cdot z)^n C_{n+1}^f(t)\frac{1}{M}\overline{u}(P')u(P)\Big\}, \end{aligned} \tag{6.41}$$

where we have dropped the $\mathrm{mod}(n,2)$ due to the sum over n.

6.2.5 Fourier Transform

The off-forward Compton tensor (Eq. 4.5) is then simply the suitable Fourier transform of Eq. 6.41:

$$T^{\mu\nu} = i\int d^4z e^{i\bar{q}\cdot z}\langle P'|T\big[j^\mu(z/2)j^\nu(-z/2)\big]|P\rangle.$$

Here, we will only give a basic outline of the process of the Fourier transform. Even though it is simply an extension of the Fourier transform performed in section 3.2, the details (given in appendix G) are quite involved and not very physically enlightening.

The general procedure is given below.

1. Substitute Eq. 6.41 into the OFCT.

2. Introduce Fourier conjugates,

$$(\bar{P}\cdot z)^n = i^n \int_{-\infty}^{\infty} d\chi e^{i\chi\bar{P}\cdot z}\frac{\partial^n}{\partial\chi^n}\delta(\chi), \tag{6.42a}$$

$$(\Delta\cdot z)^n = i^n \int_{-\infty}^{\infty} d\eta e^{i\eta\Delta\cdot z}\frac{\partial^n}{\partial\eta^n}\delta(\eta), \tag{6.42b}$$

$$\tau_m\cdot z = i\int_{-\infty}^{\infty} d\tilde{\chi}_m e^{i\tilde{\chi}_m\tau_m\cdot z}\frac{\partial}{\partial\tilde{\chi}_m}\delta(\tilde{\chi}_m), \qquad m=1,2, \text{ with indices not summed.} \tag{6.42c}$$

3. Pull the exponentials introduced above through to the reduced propagator

$$\int d^4z e^{i(\bar{q}+\eta\Delta)\cdot z}S^\rho(z) = \frac{i(\bar{q}^\rho+\eta\Delta^\rho)}{(\bar{q}+\eta\Delta)^2}, \tag{6.43a}$$

$$\int d^4z e^{i(\bar{q}+\chi\bar{P}+\eta\Delta)\cdot z}S^\rho(z) = \frac{i(\bar{q}^\rho+\chi\bar{P}^\rho+\eta\Delta^\rho)}{(\bar{q}+\chi\bar{P}+\eta\Delta)^2}, \tag{6.43b}$$

$$\int d^4z e^{i(\bar{q}+\chi\bar{P}+\eta\Delta+\tilde{\chi}_m\tau_m)\cdot z}S^\rho(z) = \frac{i(\bar{q}^\rho+\chi\bar{P}^\rho+\eta\Delta^\rho+\tilde{\chi}_m\tau_m^\rho)}{(\bar{q}+\chi\bar{P}+\eta\Delta+\tilde{\chi}_m\tau_m)^2}. \tag{6.43c}$$

Here, $\tilde{\omega}_i = 2\bar{q}\cdot\tau_i/\bar{Q}^2$ and the m indices aren't summed.

4. Use the identity, Eq. 3.60

$$\int_a^b dx\mathcal{F}(x)\frac{\partial^n}{\partial x^n}\delta(x-y) = (-1)^n\frac{\partial^n}{\partial x^n}\mathcal{F}(x)\bigg|_{x=y},$$

to evaluate the propagators.

The final result is

$$\begin{aligned}
T^{\mu\nu} = &\sum_f e_f^2\sum_{n=2,4,6}^{\infty}\sum_{j=0,2,4}^{n-1}\Bigg\{\frac{4}{\bar{Q}^2}\frac{1}{n}\bar{\omega}^{n-2}(-2\xi)^{j-1}[\tau_1^{\{\mu}A^f_{n,j}(t)+\tau_2^{\{\mu}B^f_{n,j}(t)]\\
&\times\Big[\bar{\omega}(-2\xi)\bar{q}^{\nu\}}+\frac{2(n-j-1)}{n-1}(-2\xi)\bar{P}^{\nu\}}+\frac{2j}{n-1}\Delta^{\nu\}}\Big]\\
&+\frac{4}{\bar{Q}^2}\frac{1}{n}\bar{\omega}^{n-3}(-2\xi)^{j-2}[A^f_{n,j}(t)\tilde{\omega}_1+B^f_{n,j}(t)\tilde{\omega}_2]\\
&\times\Big((n-j-1)\bar{\omega}(-2\xi)^2\bar{P}^{\{\mu}\bar{q}^{\nu\}}+\frac{2(n-j-1)j}{n-1}(-2\xi)\bar{P}^{\{\mu}\Delta^{\nu\}}+j\bar{\omega}(-2\xi)\Delta^{\{\mu}\bar{q}^{\nu\}}\\
&+\frac{j(j-1)}{n-1}\Delta^\mu\Delta^\nu+\frac{(n-j-1)(n-j-2)}{n-1}\bar{\omega}(-2\xi)^2\bar{P}^\mu\bar{P}^\nu\Big)\\
&+2\delta_{j,0}\bar{\omega}^{n-3}(-2\xi)^{n-2}C^f_n(t)(\tilde{\omega}_1-\tilde{\omega}_2)\Big((-2\xi)\bar{\omega}\Delta^{\{\mu}\bar{q}^{\nu\}}+\Delta^\mu\Delta^\nu\Big)\\
&-g^{\mu\nu}\bar{\omega}^n\Big((-2\xi)^j[A^f_{n,j}(t)\frac{\tilde{\omega}_1}{\bar{\omega}}+B^f_{n,j}(t)\frac{\tilde{\omega}_2}{\bar{\omega}}]\\
&+\delta_{j,0}(-2\xi)^nC^f_n(t)(\frac{\tilde{\omega}_1}{\bar{\omega}}-\frac{\tilde{\omega}_2}{\bar{\omega}})\Big)\Bigg\}.
\end{aligned} \tag{6.44}$$

6.2.6 Restricted Kinematic Regions

Clearly, Eq. 6.44 is deeply unpleasant and contains far too many moving parts to be compared to a lattice calculation. However, if we consider two restricted kinematic regions, we can not only greatly simplify Eq. 6.44, we can arrive at equations that allow us to extract the A and B form factors, and the C form factors separately.

First Region: Isolate C Form Factors

First, we consider the region $\bar{P}\cdot\bar{q}=0\Rightarrow\bar{\omega}=0$. This region is less important to us because we do not use these kinematics in our lattice calculation in chapter 7. However, below we will show that in principle one can use this kinematic region to extract the C form factors.

First, we look at just the metric term[††] of Eq. 6.44, without yet applying the condition $\bar{\omega}=0$:

$$\sum_f e_f^2 \sum_{n=2,4,6}^{\infty} \bar{\omega}^n \sum_{j=0,2,4}^{n-1} \Big((-2\xi)^j [A^f_{n,j}(t)\frac{\tilde{\omega}_1}{\bar{\omega}} + B^f_{n,j}(t)\frac{\tilde{\omega}_2}{\bar{\omega}}] + (-2\xi)^n \delta_{j,0} C^f_n(t)(\frac{\tilde{\omega}_1}{\bar{\omega}} - \frac{\tilde{\omega}_2}{\bar{\omega}}) \Big). \tag{6.45}$$

Using the Gordon identity (Eq. 4.13), we can write $(\tilde{\omega}_1-\tilde{\omega}_2)/\bar{\omega}=\bar{u}(P')u(P)/M$. Therefore, Eq. 6.45 becomes

$$\sum_f e_f^2 \sum_{n=2,4,6}^{\infty} \sum_{j=0,2,4}^{n-1} \Big((-2\xi)^j \bar{\omega}^{n-1} [\tilde{\omega}_1 A^f_{n,j}(t) + \tilde{\omega}_2 B^f_{n,j}(t)] + \frac{\bar{u}(P')u(P)}{M} \bar{\omega}^n (-2\xi)^n \delta_{j,0} C^f_n(t) \Big). \tag{6.46}$$

Note that $-2\xi\bar{\omega}=2\Delta\cdot\bar{q}/\bar{Q}^2$. It is convenient to define

$$\zeta = \frac{\Delta\cdot\bar{q}}{\bar{Q}^2}. \tag{6.47}$$

Now when we apply the $\bar{P}\cdot\bar{q}=0$ condition, all terms in Eq. 6.46 will vanish when the power of $\bar{\omega}$ is strictly greater than the power of ξ. Hence, at $\bar{P}\cdot\bar{q}=0$ Eq. 6.46 becomes

$$\sum_f e_f^2 \sum_{n=2,4,6}^{\infty} \Big(\zeta^{n-1} [\tilde{\omega}_1 A^f_{n,n-1}(t) + \tilde{\omega}_2 B^f_{n,n-1}(t)] + \frac{\bar{u}(P')u(P)}{M} \zeta^n C^f_n(t) \Big). \tag{6.48}$$

Note that the term that emerged from our Feynman-Hellmann relation Eq. 5.82 contained a sum over spins and additional Dirac structure. Therefore, if we choose the Dirac projector Γ_{unpol} as in appendix H, we have that $\tilde{\omega}_m \propto \bar{\omega}$, which of course vanishes in this kinematic regime. Hence we can safely ignore the $\tilde{\omega}$ terms, and Eq. 6.48 becomes

$$\frac{\bar{u}(P')u(P)}{M} \sum_f e_f^2 \sum_{n=2,4,6}^{\infty} 2^n \zeta^n C^f_n(t). \tag{6.49}$$

[††] We assume here that the lattice kinematics have been chosen so as to isolate the metric term; in practice this is not too difficult to do.

If we choose the kinematics that isolate the metric term ($\bar{q}^3 = \bar{P}^3 = \Delta^3 = 0$) and set $\bar{\omega} = 0$, we then have the result

$$\frac{1}{4}\sum_{\text{spins}} \Gamma^{\text{unpol}}_{\beta\alpha} u_\alpha(P') T^{33}(\zeta, t, \bar{Q}^2) \bar{u}_\beta(P) \propto \sum_f e_f^2 \sum_{n=2,4,6}^{\infty} 2^n \zeta^n C_n^f(t). \tag{6.50}$$

Since ζ and ξ are linearly dependent, we need not write our amplitude as a function of both.

Note that for DVCS kinematics $\zeta = 1 + \mathcal{O}(t/Q^2)$. Therefore, in the case of DVCS, Eq. 6.50 is similar to results that have been obtained with dispersion relation methods [82–85]. Physically, this region is interesting because it allows us to access the C_2 term (the D-term), and higher C_n GFFs.

Second Region: Isolate A and B Form Factors

The second kinematic region we consider is the zero skewness region (recall Eq. 6.2):

$$\Delta \cdot \bar{q} = 0 \iff \xi = 0 = \zeta \iff q^2 = q'^2.$$

This is the more important kinematic region to this thesis, since it's the kinematics for the lattice calculation, and hence why we took time to do a tensor decomposition in this region. Moreover, recall from section 4.2 that the zero-skewness region is where the H^f can be interpreted as the Fourier transform of the spatial distribution of partons, and the $A_{2,0}$ and $B_{2,0}$ GFFs are the form factors of the EMT that is relevant to the Ji sum rule. Therefore, this is physically a very important region.

Here, we simply apply the condition $\xi = 0$ to Eq. 6.44, noting that while this term may appear to have poles in ξ from the $(-2\xi)^{j-1}$ and $(-2\xi)^{j-2}$ terms, it doesn't since these terms have counting factors like j and $j(j-1)$, respectively. Therefore, in the zero skewness case Eq. 6.44 becomes

$$\begin{aligned} T^{\mu\nu} = &\sum_f e_f^2 \sum_{n=2,4,6}^{\infty} \Bigg\{ \frac{4}{\bar{Q}^2}\frac{2}{n}\bar{\omega}^{n-2}[\tau_1^{\{\mu} A_n^f(t) + \tau_2^{\{\mu} B_n^f(t)]\bar{P}^{\nu\}} \\ &+ \frac{4}{\bar{Q}^2}\frac{n-2}{n}\bar{\omega}^{n-3}\bar{P}^\mu\bar{P}^\nu(\tilde{\omega}_1 A_n^f(t) + \tilde{\omega}_2 B_n^f(t)) + \frac{4}{\bar{Q}^2}\frac{1}{n}\bar{\omega}^{n-1}[\tau_1^{\{\mu} A_n^f(t) + \tau_2^{\{\mu} B_n^f(t)]\bar{q}^{\nu\}} \\ &+ \frac{4}{\bar{Q}^2}\frac{n-1}{n}\bar{\omega}^{n-2}\bar{P}^{\{\mu}\bar{q}^{\nu\}}(\tilde{\omega}_1 A_n^f(t) + \tilde{\omega}_2 B_n^f(t)) - g^{\mu\nu}\bar{\omega}^{n-1}(\tilde{\omega}_1 A_n^f(t) + \tilde{\omega}_2 B_n^f(t)) \Bigg\}, \end{aligned} \tag{6.51}$$

where we have introduced the notation $A_n(t) = A_{n,0}(t)$ and $B_n(t) = B_{n,0}(t)$. Notice that Eq. 6.51 doesn't satisfy EM gauge invariance (the Ward identities $q_\mu T^{\mu\nu} = 0$ and $q'_\nu T^{\mu\nu} = 0$). While $\bar{q}_\mu T^{\mu\nu} = 0$,

$$\Delta_\mu T^{\mu\nu} = -\Delta^\nu \sum_f e_f^2 \sum_{n=2,4,6}^{\infty} \bar{\omega}^{n-1}(\tilde{\omega}_1 A_n^f(t) + \tilde{\omega}_2 B_n^f(t)), \tag{6.52}$$

which is not zero. As we explained in subsection 6.2.3, this is what we what we should expect.

Therefore, as we discussed in subsection 6.2.3, we simply add in the necessary terms to make it gauge invariant:

$$
\begin{aligned}
&T^{\mu\nu}(\bar{\omega}, t, \bar{Q}^2) = \\
&\sum_f e_f^2 \sum_{n=2,4,6}^{\infty} \Bigg\{ \bar{\omega}^{n-1} \big[A_n^f(t) \frac{2\bar{q}\cdot\tau_1}{\bar{Q}^2} + B_n^f(t) \frac{2\bar{q}\cdot\tau_2}{\bar{Q}^2} \big] \Big(-g^{\mu\nu} + \frac{\Delta^\mu \Delta^\nu}{\Delta^2} + \frac{\bar{q}^\mu \bar{q}^\nu}{\bar{q}^2} \Big) \\
&+ \frac{4}{\bar{Q}^2} \frac{n-2}{n} \bar{\omega}^{n-3} \big[A_n^f(t) \frac{2\bar{q}\cdot\tau_1}{\bar{Q}^2} + B_n^f(t) \frac{2\bar{q}\cdot\tau_2}{\bar{Q}^2} \big] \Big(\bar{P}^\mu - \frac{\bar{P}\cdot\bar{q}}{\bar{q}^2}\bar{q}^\mu \Big) \Big(\bar{P}^\nu - \frac{\bar{P}\cdot\bar{q}}{\bar{q}^2}\bar{q}^\nu \Big) \\
&+ \frac{4}{\bar{Q}^2} \frac{2}{n} \bar{\omega}^{n-2} \Bigg[A_n^f(t) \Big(\bar{P}^{\{\mu} - \frac{\bar{P}\cdot\bar{q}}{\bar{q}^2}\bar{q}^{\{\mu} \Big) \Big(\tau_1^{\nu\}} - \frac{\tau_1\cdot\bar{q}}{\bar{q}^2}\bar{q}^{\nu\}} \Big) \\
&+ B_n^f(t) \Big(\bar{P}^{\{\mu} - \frac{\bar{P}\cdot\bar{q}}{\bar{q}^2}\bar{q}^{\{\mu} \Big) \Big(\tau_2^{\nu\}} - \frac{\tau_2\cdot\bar{q}}{\bar{q}^2}\bar{q}^{\nu\}} \Big) \Bigg] \Bigg\}.
\end{aligned}
\tag{6.53}
$$

In the above equation, all we have done is add a term proportional to $\Delta^\mu\Delta^\nu$; that is, the minimal tensor structure to make the leading twist term gauge invariant, as in Ref. [161]. Moreover, note that this result has the same tensor structure as our decomposition in the previous section (Eq. 6.17).

Relation to Lattice Quantity

Finally, we insert the result of the leading-twist Compton tensor in Eq. 6.53 into Eq. 5.82, which is related to the Feynman-Hellmann energy shifts. Recall, Eq. 5.82

$$
\tilde{T}^{\mu\nu} \equiv i \int d^4 z e^{i\bar{q}\cdot z} \frac{1}{4} \sum_{\text{spins}} \Gamma_{\beta\alpha} u_\alpha(P') \langle P' | T[j^\mu(z/2) j^\nu(-z/2)] | P \rangle \bar{u}_\beta(P).
$$

The leading-twist zero-skewness term is, restricting the Lorentz indices to $i, j = 1, 2, 3$,

$$
\begin{aligned}
\tilde{T}_{ij}(\bar{\omega}, t, \bar{Q}^2) = \sum_f e_f^2 \sum_{n=2,4,6}^{\infty} &\bar{\omega}^n \big[N_1 A_n^f(t) + N_2 B_n^f(t) \big] \\
&\times \Big(\frac{\bar{P}_i \bar{q}_j + \bar{P}_j \bar{q}_i}{\bar{P}\cdot\bar{q}} + \frac{\bar{Q}^2}{(\bar{P}\cdot\bar{q})^2} \bar{P}_i \bar{P}_j + \frac{\Delta_i \Delta_j}{\Delta^2} - g_{ij} \Big).
\end{aligned}
\tag{6.54}
$$

In Eq. 6.54, N_1 and N_2 are given by

$$
\begin{aligned}
N_1 \bar{\mathbf{p}}_i &= \frac{1}{8} \text{tr} \Big\{ (\mathbb{I} + \gamma^0)(\not{P}' + M) \gamma^i (\not{P} + M) \Big\}, \\
N_2 \bar{\mathbf{p}}_i &= \frac{1}{8} \text{tr} \Big\{ (\mathbb{I} + \gamma^0)(\not{P}' + M) \frac{\sigma^{i\alpha} i \Delta_\alpha}{2M} (\not{P} + M) \Big\},
\end{aligned}
\tag{6.55}
$$

where $\bar{\mathbf{p}}_i$ is the spatial component of $\bar{P}^\mu$. The $\mathbb{I} + \gamma^0$ term simply corresponds to our choice of Dirac projector that we use in the lattice calculation. Refer to appendix H for explicit

calculations. Choosing the unpolarised projector and $i = j = 3$, Eq. 6.54 becomes

$$\begin{aligned}\tilde{T}_{ij}(\bar{\omega}, t, \bar{Q}^2) = &\sum_f e_f^2 \sum_{n=2,4,6}^{\infty} \bar{\omega}^n \big[(E+M)A_n^f(t) - \frac{t}{4M} B_n^f(t)\big] \\ &\times \left(\frac{\bar{P}_i \bar{q}_j + \bar{P}_j \bar{q}_i}{\bar{P}\cdot\bar{q}} + \frac{\bar{Q}^2}{(\bar{P}\cdot\bar{q})^2} \bar{P}_i \bar{P}_j + \frac{\Delta_i \Delta_j}{\Delta^2} - g_{ij} \right).\end{aligned} \tag{6.56}$$

6.3 Analytic Properties

We now wish to investigate the analytic properties of the OFCT. First, we will perform a dispersion relation on the OFCT, which is useful since it is completely non-perturbative (in contrast to the dispersion relation in section 3.2) and comes simply from the analytic properties of the amplitude, rather than needing to use the OPE relation. Second, by examining the analytic properties of the OFCT we will show exactly how the Euclidean lattice calculation contains information relating to physical Minkowski GPDs.

6.3.1 Analytic Properties of the Off-Forward Compton Tensor

Before we start doing anything we need to know where the discontinuities in the complex plane are when we take the relevant momentum variables complex. As is standard, we assume that our scattering amplitudes are analytic functions of their momentum variables at every point off the real axis.

One can show (see appendix C) that the OFCT has the form

$$\begin{aligned}T^{\mu\nu} = \sum_X \Big[&\frac{\langle P'|j^\mu(0)|X(\mathbf{P}+\mathbf{q})\rangle\langle X(\mathbf{P}+\mathbf{q})|j^\nu(0)|P\rangle}{P_X^0 - (P^0+q^0) - i\epsilon} \\ &+ \frac{\langle P'|j^\nu(0)|X(\mathbf{P}-\mathbf{q}')\rangle\langle X(\mathbf{P}-\mathbf{q}')|j^\mu(0)|P\rangle}{P_X^0 - (P^0-q'^0) - i\epsilon}\Big].\end{aligned} \tag{6.57}$$

Therefore, we have discontinuities in our amplitude where the intermediate state goes on-shell: at $P_X^0 = P^0 + q^0$ or $P_X^0 = P^0 - q'^0$.

In the incoming nucleon's rest frame, this becomes

$$(P_X^0)^2 = (P^0+q^0)^2 \quad \Rightarrow \quad M_X^2 + \mathbf{q}^2 = M^2 + 2q^0 M + (q^0)^2 \quad \Rightarrow \quad M_X^2 = (P+q)^2.$$

Similarly,

$$(P_X^0)^2 = (P^0-q'^0)^2 \quad \Rightarrow \quad M_X^2 + \mathbf{q}'^2 = M^2 - 2q'^0 M + (q'^0)^2 \quad \Rightarrow \quad M_X^2 = (P-q')^2.$$

Hence the discontinuities are where the invariant mass of the intermediate state is $M_X^2 = (P+q)^2$ or $M_X^2 = (P-q')^2$. We can use this to determine where the cuts of each of the coefficient functions K_i in Eq. 6.17 are in terms of $\bar{\omega}$ and $\zeta = \bar{q}\cdot\Delta/\bar{Q}^2$. To do this we note that, as in the forward case, our inelastic condition means that $M_X^2 \geq M^2$:

$$M_X^2 = (P+q)^2 = (\bar{P}+\bar{q})^2 = \bar{P}^2 + 2\bar{P}\cdot\bar{q} - \bar{Q}^2 = -\bar{Q}^2(1-\bar{\omega}) + \bar{P}^2 \geq M^2, \tag{6.58}$$

and

$$M_X^2 = (P - q')^2 = (\bar{P} - \bar{q})^2 = \bar{P}^2 - 2\bar{P}\cdot\bar{q} - \bar{Q}^2 = -\bar{Q}^2(1+\bar{\omega}) + \bar{P}^2 \geq M^2, \qquad (6.59)$$

for the crossed graph. Recall that $\bar{P}^2 = M^2 - t/4$. Therefore, in the complex $\bar{\omega}$, Eq. 6.58 implies the discontinuities are for $\bar{\omega} \geq 1 + t/(4\bar{Q}^2)$, and from Eq. 6.59, $\bar{\omega} \leq -1 - t/(4\bar{Q}^2)$.

Now if we set $\bar{P}\cdot\bar{q} = 0$, we have in both Eqs. 6.58 and 6.59, $M_X^2 = \bar{P}^2 - \bar{Q}^2 \geq M^2$, for intermediate state on-shell, and hence $-\bar{Q}^2 \geq -t/4$. Since $|\bar{Q}| \gg M, |t|$, we must either have $q^2 > 0$ and/or $q'^2 > 0$. This implies two possible regions for a cut:

$$0 < q^2 = (\bar{q} + \Delta/2)^2 = t/4 + \Delta\cdot\bar{q} - \bar{Q}^2 \quad \Rightarrow \quad \zeta > 1 - \frac{t}{4\bar{Q}^2}. \qquad (6.60)$$

$$0 < q'^2 = (\bar{q} - \Delta/2)^2 = t/4 - \Delta\cdot\bar{q} - \bar{Q}^2 \quad \Rightarrow \quad \zeta < -1 + \frac{t}{4\bar{Q}^2}. \qquad (6.61)$$

So, we consider two cases:

1. $\Delta\cdot\bar{q} = 0$ and therefore there are no singularities in the amplitude due to ζ. The amplitude is expanded in $\bar{\omega}$, and is analytic everywhere except the cuts at $|\bar{\omega}| \geq 1 + t/4\bar{Q}^2$;

2. $\bar{P}\cdot\bar{q} = 0$ and therefore there are no singularities in the amplitude due to $\bar{\omega}$. The amplitude is expanded in ζ, and is analytic everywhere except for the cuts $|\zeta| \geq 1 - t/4\bar{Q}^2$.

6.3.2 A General Dispersion Relation

Now it is possible to derive a dispersion relation using these analytic features.

Instead of deriving two separate dispersion relations for these two cases, we note that they are essentially the same case with different momentum variables. Let the scattering amplitude be $\mathcal{M}(\alpha, t, \bar{Q}^2)$, with α being either ζ or ω and its thresholds either at $\pm(1 - t/4\bar{Q}^2)$ or $\pm(1 + t/4\bar{Q}^2)$, respectively. For simplicity, we take $1 \pm t/4\bar{Q}^2 \approx 1$, by the fact that we have chosen $t \ll \bar{Q}^2$.

First, note that the Lorentz scalar coefficients of the scattering amplitude (the K_i in Eq. 6.17) have the same analyticity as the whole scattering amplitude. Therefore, we apply Cauchy's theorem to one of the scalar coefficients of the OFCT $K_i(\alpha, t, \bar{Q}^2)$ at some fixed values of the momentum transfer variables $t, \bar{Q}^2$:

$$K_i(\alpha, t, \bar{Q}^2) = \frac{1}{2\pi i}\oint d\alpha' \frac{K_i(\alpha', t, \bar{Q}^2)}{\alpha' - \alpha}. \qquad (6.62)$$

To evaluate this integral we take the contour given in figure 6.1. Letting the contour along the cuts be a distance $\epsilon > 0$ above or below the real axis, we can write Eq. 6.62 as

$$\begin{aligned} K_i(\alpha, t, \bar{Q}^2) = \frac{1}{2\pi i}\Big[&\int_1^\infty d\alpha' \frac{K_i(\alpha' + i\epsilon, t, \bar{Q}^2) - K_i(\alpha' - i\epsilon, t, \bar{Q}^2)}{\alpha' - \alpha} \\ &+ \int_{-\infty}^{-1} d\alpha' \frac{K_i(\alpha' + i\epsilon, t, \bar{Q}^2) - K_i(\alpha' - i\epsilon, t, \bar{Q}^2)}{\alpha' - \alpha}\Big] + \text{arc contributions}. \end{aligned} \qquad (6.63)$$

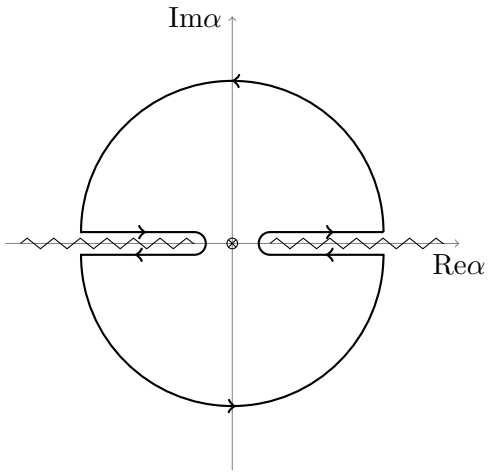

Figure 6.1: Contour for two dispersion relations with $\alpha = \omega$ or ζ. The cuts on the real axis start at $\alpha \approx 1$. The radius of the contour is taken to ininfity.

Now we let $\alpha' \to -\alpha'$ in the second integral. For simplicity we suppress the $t, \bar{Q}^2$ arguments:

$$\begin{aligned} K_i(\alpha) =& \frac{1}{2\pi i}\Big[\int_1^\infty d\alpha' \frac{K_i(\alpha'+i\epsilon) - K_i(\alpha'-i\epsilon)}{\alpha'-\alpha} \\ &- \int_\infty^1 d\alpha' \frac{-K_i(-\alpha'+i\epsilon) + K_i(-\alpha'-i\epsilon)}{-\alpha'-\alpha}\Big] + \text{arcs}. \end{aligned} \tag{6.64}$$

From the crossing symmetry, $q \to -q'$ and $q' \to -q$, we note that under crossing $\bar{\omega} \to -\bar{\omega}$ and $\zeta \to -\zeta$, but the whole amplitude remains invariant. Hence $K_i(\alpha, t, \bar{Q}^2) = K_i(-\alpha, t, \bar{Q}^2)$. Moreover, the Schwarz reflection principle states that a function with real number boundary value on the real axis has the property $f^*(z) = f(z^*)$ [47]. Therefore, Eq. 6.64 becomes

$$K_i(\alpha) = \frac{1}{\pi i}\int_1^\infty d\alpha' [K_i(\alpha'+i\epsilon) - K_i(\alpha'-i\epsilon)]\Big(\frac{1}{\alpha'-\alpha} + \frac{1}{\alpha+\alpha'}\Big) + \text{arcs}. \tag{6.65}$$

By the Schwarz reflection principle $K_i(z) - K_i(z^*) = 2i\text{Im}\big[K_i(z)\big]$, and hence we will define a spectral function: $\rho_i(z) = \frac{2}{\pi}\text{Im}\big[K_i(z)\big]$. Note that, unlike the forward (inclusive) case, there is no way to associate this spectral function with the cross section of another process; that is, the optical theorem can not be applied here.

Therefore,

$$K_i(\alpha) = 2\int_1^\infty d\alpha' \rho(\alpha')\Big(\frac{1}{\alpha'-\alpha} + \frac{1}{\alpha+\alpha'}\Big) + \text{arcs}. \tag{6.66}$$

Further, we to subtract off the component of $K_i(\alpha)$ that is constant in α: $K_i(\alpha = 0)$. This will allow for better comparison to the OPE, and remove the arc contributions. Using Eq. 6.66,

$$K_i(0) = 2\int_1^\infty d\alpha' \frac{2\rho(\alpha')}{\alpha'} + \text{arcs}. \tag{6.67}$$

Therefore,

$$\begin{aligned} K_i(\alpha) - K_i(0) =& 2\int_1^\infty d\alpha' \rho(\alpha') \Big(\frac{1}{\alpha' - \alpha} + \frac{1}{\alpha + \alpha'} - \frac{2}{\alpha'} \Big) \\ =& 4\alpha^2 \int_1^\infty d\alpha' \frac{\rho(\alpha')}{\alpha'(\alpha'^2 - \alpha^2)}. \end{aligned} \tag{6.68}$$

Substituting the variable $x = 1/\alpha'$, and assuming α is sufficiently small,

$$K_i(\alpha) - K_i(0) = 4\alpha^2 \int_0^1 dx x \frac{\tilde{\rho}(x)}{1 - (\alpha x)^2} = 4 \sum_{n=2,4,6}^{\infty} \alpha^n \int_0^1 dx x^{n-1} \tilde{\rho}(x). \tag{6.69}$$

For instance, if $\alpha = \bar{\omega}$, then looking at K_1 in Eq. 6.17, we have from the OPE

$$K_1(\bar{\omega}, t) = \sum_{n=2,4,6} \bar{\omega}^n A_n^f(t). \tag{6.70}$$

Then, in zero-skewness kinematics

$$\int_0^1 dx x^{n-1} H_f^{(+)}(x,t) = A_n^f(t), \tag{6.71}$$

where $H_f^{(+)}(x,t) = H(x,t) - H(-x,t)$ is the singlet GPD. An identical expression holds if we replace $H \to E$ and $A \to B$. Therefore, the OPE prediction is

$$\lim_{\bar{Q}^2 \to \infty} \tilde{\rho}(x,t,\bar{Q}^2) = H_f^{(+)}(x,t), \quad \text{and} \quad \lim_{\bar{Q}^2 \to \infty} K_1(\bar{\omega} = 0, t, \bar{Q}^2) = 0. \tag{6.72}$$

However, previous Feynman-Hellmann calculations of the forward Compton tensors [123, 162] found that in the forward case the $\omega = 0$ term asymptotes to a non-zero value for large Q^2. We will discuss this 'subtraction term' for the OFCT in chapter 7.

6.3.3 Comparison to Euclidean Space and Lattice

In the preceding chapters, we have commented on the difficulties of extracting information about physical Minkowski space from Euclidean lattice calculations. Here, as a conclusion to our theoretical results, we will show exactly what information can be determined from Euclidean space calculations, and how our continuum OPE performed in this chapter can be interpreted in light of operator mixing on the lattice.

The OPE we have just performed (Eq. 6.53) essentially has the form

$$\lim_{q \to \infty} \int d^4 z e^{i\bar{q}\cdot z} T[j(z/2) j(-z/2)] \simeq \sum_n c_n(\bar{q}^2) \bar{q}_{\mu_1} ... \bar{q}_{\mu_n} \mathcal{O}_n^{\mu_1 .. \mu_n}(0), \tag{6.73}$$

here ignoring the Lorentz structure. Therefore, its matrix element is simply the sum of the matrix elements of the local operators. As we discussed in section 4.4, local operators are 'signature agnostic': they have the same value whether calculated in Minkowski or Euclidean space. So as long as we stay in the region of Euclidean kinematics, we can compare our results derived in Minkowski space (for instance, Eq. 6.56) to the Euclidean lattice results.

Moreover, unlike chapter 3, we do not need to perform a perturbative dispersion relation to relate the matrix elements of the local operators to GPDs; we already did that work in section 3.3, and arrived at the polynomiality relationship Eq. 4.19. Therefore, by applying a polynomial fit to our lattice results, choosing the correct kinematics, we should be able to extract GPD moments.

However, as we mentioned in section 4.4, the lattice breaks the Lorentz symmetry of the continuum. Hence leading twist operators mix with non-leading twist operators. Therefore, unless we perform a continuum extrapolation (varying the size of the lattice spacing and fitting to this behaviour), we can only use the continuum OPE (and continuum dispersion relation) performed in this chapter as guides of how we expect the lattice OFCT to behave, and how to interpret it physically.

Moreover, the Euclidean kinematics do somewhat hamper our ability to access higher GPD moments. This is most obvious when we look at a simplified OPE of a Compton tensor:

$$\lim_{\bar{q}\to\infty} T \simeq \sum_n \bar{\omega}^n A_n(t). \tag{6.74}$$

Note that in the unphysical region, $|\bar{\omega}| \leq 1$, only the first few operators, $A_n(t)$ appreciably contribute to the amplitude. By contrast, all the moments are required to full reconstruct the GPDs.

In principle, analytic continuity ensures that we can recover the contribution of all operators. However, this would require a lattice calculation with 'infinite' precision. In reality, many of the terms in the polynomial $\bar{\omega}^N A_N(t)$ will be smaller than the error bars. This means that with traditional fitting procedures we can only accurately access a finite number of moments, which are nonetheless enough to reconstruct the original parton distributions [163].

In the next chapter, we present the results of our lattice calculation.

Chapter 7

Numerical Calculation

In this chapter we present the results of a lattice calculation of the off-forward Compton tensor (OFCT), performed using the Feynman-Hellmann (FH) method as outlined in chapter 5. It is an extension of previous work calculating the forward Compton tensor using FH techniques [122, 123, 139, 140, 162]. We will further compare the results of this proof-of-principle calculation to the leading-twist OFCT from chapter 6.

In contrast to other hadronic observables, relatively little work has been done to extract GPD-related quantities on the lattice. In the vast majority of such studies, generalised form factors (GFFs) are determined through standard three-point function methods [56–64]. As we mentioned in section 4.4, due to the broken Lorentz symmetry on the lattice, only the first few GFFs can be determined from this method. The highest GFF calculated so far is $A_{3,0}$ [61]. Most such studies, however, limit themselves to the $A_{2,0}$, $B_{2,0}$ and C_2 form factors, which parameterise the QCD energy-momentum tensor. In addition to many quasi-PDF papers (see Ref. [111] for a review), there has also been one investigation of pion quasi-GPDs [65].

Consequently, the FH calculation of the OFCT presented in this chapter is quite different from previous lattice studies of GPD-related quantities. As such, it may allow us to determine previously inaccessible GPD-related information. First and most importantly, we can calculate many higher GFFs than the local operator methods. This would require more work than is presented in this thesis, although the initial results are promising. From a tower of GFFs, using the fact that they parameterise GPD Mellin moments (Eq. 4.19), one can in principle reconstruct GPDs [163]. To fully extract many GFFs, however, we would need a wide spread of t and $\bar{\omega}$ values. Moreover, we can investigate the scaling behaviour of GPDs with $\bar{Q}^2$.

The structure of this chapter follows: In section 7.1, we explain how the lattice calculation was performed, giving details of the FH perturbation, kinematics, and lattice specifications. Then, we discuss, using results from chapters 5 and 6, how to extract GFFs from this calculation.

In section 7, we present the main results of this lattice calculation:

1. An exponential fit to the relevant ratios of correlators. This shows the quality of our signal.

2. The behaviour of the energy shifts as functions of λ_1 and λ_2, the FH parameters, which confirms the quadratic λ behaviour of the energy shift.

3. The $\bar{\omega}$ dependence of this signal, which allows us to access the interesting physical information.

4. A comparison of the OFCT, as calculated in this work, to the forward Compton tensor as calculated in previous Feynman-Hellmann lattice studies [123, 162], and a comparison to a simple model GPD.

In the final section, we discuss the results, finding them to largely be in agreement with the behaviour predicted in previous chapters as well as with previous lattice studies and the simple phenomenological model. However, our method of comparison at this stage only provides a glimpse of what may be possible in the future. Finally, we discuss some obstacles to overcome and avenues of further investigation.

7.1 Introduction and Setup

7.1.1 Lattice Details

The key quantities of the lattice ensembles used in our calculations are given in the table below. In particular, we highlight the fact that this calculation uses a larger-than-physical pion mass (more than three times the physical mass), and is on the SU(3) flavour symmetric line: $m_u = m_d = m_s$.

	Ensemble values for this calculation
$(N_L)^3 \times N_T$	$32^3 \times 64$
N_f	2+1
(κ_s, κ_l)	$(0.120900, 0.120900)$
β	5.50
m_π	466(13) MeV
a	0.074(2) fm

7.1.2 Perturbed Correlators

In a Feynman-Hellmann calculation, we calculate the nucleon two-point correlators with a perturbation to the standard QCD Lagrangian. As we mentioned in chapter 5, we choose the following perturbation to the standard QCD Lagrangian:

$$\mathcal{L}_{\text{FH}} = \Big[\lambda_1\big(e^{i\mathbf{q}\cdot\mathbf{y}} + e^{-i\mathbf{q}\cdot\mathbf{y}}\big) + \lambda_2\big(e^{i\mathbf{q}'\cdot\mathbf{y}} + e^{-i\mathbf{q}'\cdot\mathbf{y}}\big)\Big]\bar{\psi}(y)\gamma^3\psi(y).$$

Then, as discussed in chapter 6, we limit ourselves to zero-skewness kinematics (Eq. 6.2), $q^2 = q'^2$. Therefore, since there is no temporal component of the q vectors in our FH shift, we must have $|\mathbf{q}| = |\mathbf{q}'|$.

We calculated two sets of perturbed correlators for different kinematics. For the first set of correlators, we chose $\frac{L}{2\pi}\mathbf{q} = (3, 2, 0)$ and $\frac{L}{2\pi}\mathbf{q}' = (2, 3, 0)$, which satisfy the zero-skewness condition. Note that L is the lattice length, and we ignore the factor of $L/2\pi$ from here on when giving momentum vectors. For the second set of correlators, we chose $\mathbf{q} = (1, 5, 0)$ and $\mathbf{q}' = (-1, 5, 0)$, which also satisfy zero skewness. The choice of the $\mathbf{q}^{(\prime)}$ vectors limits what our values of $\mathbf{p}^{(\prime)}$ may be, since we must always have the intermediate term of greater energy to extract a meaningful signal.

For both sets of correlators, we calculated eight different pairs of λ values that are necessary to isolate the off-forward term*:

*Note that these λ values are chosen to give correlators that lie on the $\lambda_1 = \lambda_2$ and $\lambda_1 = -\lambda_2$ lines, as discussed in chapter 5.3.

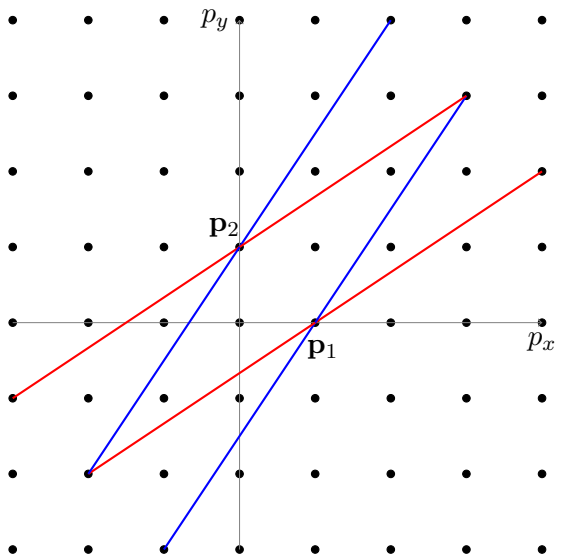

Figure 7.1: Diagram in momentum space showing how the momentum values mix under the perturbing Lagrangian for the first set of correlators. For each momentum value there is a tower of hadronic states with the same quantum numbers as the nucleon. The red lines are $\mathbf{q}$ vectors, and the blue lines are $\mathbf{q}'$ vectors.

λ_1	λ_2
0.025	0.025
0.025	-0.025
-0.025	0.025
-0.025	-0.025
0.05	0.05
0.05	-0.05
-0.05	0.05
-0.05	-0.05

With these sets of correlators, we then choose a value of the three momentum to Fourier project onto; this is the outgoing nucleon momentum $\mathbf{p}'$. We also define $\mathbf{p} \equiv \mathbf{p}' - \mathbf{q} + \mathbf{q}'$. In general, the source momenta may be $\mathbf{p}' + n_1\mathbf{q} + n_2\mathbf{q}'$ for n_1 and n_2 integers (see figure 7.1). However, as we showed in chapter 5, the sink momentum will be $\mathbf{p}$ for the dominant contributions to the energy shift.

Recall that we defined $\bar{\omega} = 2\bar{P} \cdot \bar{q}/\bar{Q}^2$. For our lattice kinematics this becomes

$$\bar{\omega} = \frac{2(\mathbf{p} + \mathbf{p}') \cdot (\mathbf{q} + \mathbf{q}')}{(\mathbf{q} + \mathbf{q}')^2}.$$

First Set

The first set of correlators have $\mathbf{q} = (3, 2, 0)$ and $\mathbf{q}' = (2, 3, 0)$. The OFCT extracted from this has $t = -2$ and $\bar{Q}^2 = 12.5$. We will neglect factors of $(2\pi/L)^2$ in momentum squared variables. In physical units, this is $t = -0.55$ GeV^2 and $\bar{Q}^2 = 3.44$ GeV^2. Therefore, the only reasonable $\bar{\omega}$ value we can extract is given in the table below.

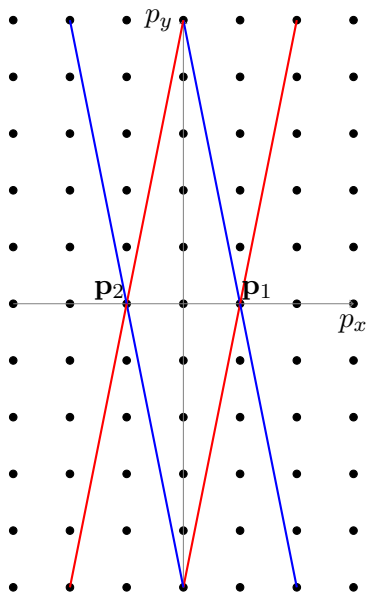

Figure 7.2: Diagram in momentum space for the second set of correlators. The red lines are $\mathbf{q}$ vectors and the blue lines are $\mathbf{q}'$ vectors.

$\mathbf{p}$	$\mathbf{p}'$	$\bar{\omega}$	momentum sq.
$(1,0,0)$	$(0,1,0)$	2/5	1

We can only use these values of $\mathbf{p}$ and $\mathbf{p}'$, since any higher momentum values (for instance, $(2,1,0)$ and $(1,2,0)$) will have intermediate states of *lower energy* than the incoming outgoing states, thus preventing us from extracting a meaningful signal.

Second Set

The second set of correlators had $\mathbf{q} = (1,5,0)$ and $\mathbf{q}' = (-1,5,0)$. So the OFCT extracted from this calculation has $t = -4$ and $\bar{Q}^2 = 25$. In physical units, this is $t = -1.10$ GeV^2 and $\bar{Q}^2 = 6.85$ GeV^2. The momentum mixing induced by the perturbing Lagrangian for these kinematics is given in figure 7.2.

Using this set of correlators, we can calculate a wider range of $\bar{\omega}$ values:

$\mathbf{p}$	$\mathbf{p}'$	$\bar{\omega}$	momentum sq.
$(1,-2,0)$	$(1,-2,0)$	-4/5	5
$(1,-1,0)$	$(1,-1,0)$	-2/5	2
$(1,0,0)$	$(-1,0,0)$	0	1
$(1,1,0)$	$(-1,1,0)$	2/5	2
$(1,2,0)$	$(-1,2,0)$	4/5	5

This wider spread in the possible $\bar{\omega}$ values means that most of the analysis was performed on this second set of correlators.

7.1.3 Ratios

Recall the expression for a finite difference equation that approximates a mixed derivative:

$$\left.\frac{\partial^2 E_N}{\partial\lambda_1\partial\lambda_2}\right|_{\lambda_1=\lambda_2=0} = \frac{E_N(\lambda,\lambda)+E_N(-\lambda,-\lambda)-E_N(\lambda,-\lambda)-E_N(-\lambda,\lambda)}{4\lambda^2}, \tag{7.1}$$

for some $\lambda \approx 0$. We denote the energy shift

$$\Delta E(\lambda) \equiv E_N(\lambda,\lambda)+E_N(-\lambda,-\lambda)-E_N(\lambda,-\lambda)-E_N(-\lambda,\lambda). \tag{7.2}$$

Then, we define the correlator ratio,

$$R(\mathbf{p}',\lambda) \equiv \frac{C(\mathbf{p}',\lambda,\lambda)C(\mathbf{p}',-\lambda,-\lambda)}{C(\mathbf{p}',\lambda,-\lambda)C(\mathbf{p}',-\lambda,\lambda)}, \tag{7.3}$$

where $C(\mathbf{p}',\lambda_1,\lambda_2)$ is the perturbed correlator calculated with the FH shift Eq. 5.15 and projected onto three momentum $\mathbf{p}'$ at the sink.

Therefore, as we argued in section 5.3, for large Euclidean time and the right choice of λ values,

$$R(\mathbf{p}',\lambda) \to Ae^{-\Delta E\tau}. \tag{7.4}$$

So if we fit an exponential to a ratio such as Eq. 7.3, we can extract the energy shift Eq. 7.2.

Recall the FH relation Eq. 5.79 from chapter 5:

$$\frac{\Delta E(\mathbf{p}')}{4\lambda^2} \approx -\frac{\langle\Omega|\chi(0)|N(\mathbf{p}')\rangle T_{33}\langle N(\mathbf{p})|\chi^\dagger(0)|\Omega\rangle}{4E_N|\langle\Omega|\chi|N(\mathbf{p}')\rangle|^2}, \tag{7.5}$$

where T_{33} is the $\mu=\nu=3$ component of the OFCT, as defined in Eq. 4.5.

Then the overlaps are

$$\langle\Omega|\chi_\alpha(0)|X(\mathbf{p})\rangle = Z_{\chi,X}(\mathbf{p})u_\alpha(p,s),$$

$$\langle X(\mathbf{p})|\chi^\dagger_\alpha(0)|\Omega\rangle = Z^*_{\chi,X}(\mathbf{p})\bar{u}_\alpha(p,s).$$

Therefore, inserting this into the FH relation, we get

$$\frac{\Delta E(\mathbf{p}')}{4\lambda^2} \approx -\frac{Z^*_N(\mathbf{p}')Z_N(\mathbf{p})\tilde{T}_{33}}{4E_N|\langle\Omega|\chi|N(\mathbf{p}')\rangle|^2}, \tag{7.6}$$

where $\tilde{T}^{33}$ is the OFCT-like object we defined in Eq. 5.82, which was the OFCT sandwiched on either side by spinors and a sum over spins and Dirac projector out the front.

Therefore, isolating the OFCT part of this equation we get

$$-\frac{\Delta E(\mathbf{p}')}{\lambda^2}\frac{E_N|\langle\Omega|\chi|N(\mathbf{p}')\rangle|^2}{Z^*_N(\mathbf{p}')Z_N(\mathbf{p})} \approx \tilde{T}^{33}, \tag{7.7}$$

To evaluate the term on the LHS of Eq. 7.7, first note that by rotational invariance (of integer values of $\pi/2$), we have that

$$Z_N(\mathbf{p}_1)u(\mathbf{p}_1) = \langle\Omega|\chi|N(\mathbf{p}_1)\rangle = \langle\Omega|\chi|N(\mathbf{p}_2)\rangle = Z_N(\mathbf{p}_2)u(\mathbf{p}').$$

And moreover, since we have been carrying around the same sum over spins and trace, we have

$$|\langle\Omega|\chi|N(\mathbf{p})\rangle|^2 = \frac{1}{4}|Z_N(\mathbf{p})|^2 \sum_{s,s'} \left[\Gamma_{\text{unpol}}\right]_{\beta\alpha} u_\alpha(P,s')u\bar{u}_\beta(P,s) = \frac{1}{2}|Z_N(\mathbf{p})|^2(E_N+M).$$

Inserting this into Eq. 7.7, we get

$$-\frac{\Delta E(\mathbf{p}')}{2\lambda^2}E_N(E_N+M) \approx \tilde{T}^{33}, \tag{7.8}$$

Now, we need to use our results from chapter 6 to match the Feynman-Hellmann shift at large $\bar{Q}^2$ to the OPE.

Recall Eq. 6.56 from the OPE:

$$\begin{aligned}\tilde{T}_{ij}(\bar{\omega},t) = &\sum_f e_f^2 \sum_{n=2,4,6}^{\infty} \bar{\omega}^n \left[(E_N+M)A_n^f(t) - \frac{t}{4M}B_n^f(t)\right] \\ &\times \left(\frac{\bar{P}_i\bar{q}_j + \bar{P}_j\bar{q}_i}{\bar{P}\cdot\bar{q}} + \frac{\bar{Q}^2}{(\bar{P}\cdot\bar{q})^2}\bar{P}_i\bar{P}_j + \frac{\Delta_i\Delta_j}{\Delta^2} - g_{ij}\right).\end{aligned}$$

In our kinematics with $\bar{P}^3 = \bar{q}^3 = \Delta^3 = 0$, this becomes

$$\tilde{T}_{33}(\bar{\omega},t) = \sum_f e_f^2 \sum_{n=2,4,6}^{\infty} \bar{\omega}^n \left[(E_N+M)A_n^f(t) - \frac{t}{4M}B_n^f(t)\right]. \tag{7.9}$$

However, since we only choose one flavour of current at a time with unit charge, this is really

$$\tilde{T}_{33}^f(\bar{\omega},t) = \sum_{n=2,4,6}^{\infty} \bar{\omega}^n \left[(E_N+M)A_n^f(t) - \frac{t}{4M}B_n^f(t)\right]. \tag{7.10}$$

Inserting this result in Eq. 7.8, we get

$$-\frac{\Delta E(\mathbf{p}')}{2\lambda^2}E_N(E_N+M) \approx \sum_{n=2,4,6}^{\infty} \bar{\omega}^n \left[(E_N+M)A_n^f(t) - \frac{t}{4M}B_n^f(t)\right], \tag{7.11}$$

where the choice of $f = u, d$ depends on what quark current we use in the FH perturbation.

It is then convenient to define the following

$$\mathcal{A}^f(\bar{\omega},t) \equiv \sum_{n=2,4,6}^{\infty} \bar{\omega}^n A_n^f(t), \quad \mathcal{B}^f(\bar{\omega},t) \equiv \sum_{n=2,4,6}^{\infty} \bar{\omega}^n B_n^f(t). \tag{7.12}$$

Of course, these have $\Lambda_{\text{QCD}}/\bar{Q}$ corrections when we compare to the lattice calculation, but for ease of notation we will not consider such corrections for the moment.

In particular, we will calculate the quantity

$$-\frac{\Delta E(\mathbf{p}')}{\lambda^2}E_N \approx \frac{2}{(E_N+M)}\left[(E_N+M)\mathcal{A}^f(\bar{\omega},t) - \frac{t}{4M}\mathcal{B}^f(\bar{\omega},t)\right], \tag{7.13}$$

as this reduces to the forward Compton tensor, as calculated using Feynman-Hellmann techniques in Ref. [123, 162], as $t \to 0$.

Moreover, for a conjugate pair of momenta, $\mathbf{p}_1$ and $\mathbf{p}_2$, such that $\mathbf{p}_2 = \mathbf{p}_1 - \mathbf{\Delta}$, we will calculate the product of two ratios,

$$R(\mathbf{p}_1) \times R(\mathbf{p}_2),$$

which should give us four times Eq. 7.10.

And the ratio of the two ratios

$$R(\mathbf{p}_1)/R(\mathbf{p}_2),$$

which we expect to be consistent with zero.

7.2 Results

In this section we present all the main results of our lattice calculation: (1) the effective mass as a function of Euclidean time, which tells us the quality of the signal; (2) the λ dependence of the energy shift, which confirms that it is dominated by second order terms; (3) the energy shift as a function of $\bar{\omega}$, which allows us to compare our results to the OFCT; and finally, (4) the towers of GFFs (Eq. 7.10), normalised using the results from the previous section. We will compare these final results to the forward Compton tensor, as calculated using lattice FH techniques, and a simple phenomenological model.

For the sake of brevity, we have only included a small selection of plots that best convey our results. Additional plots, including many down quark results, can be found in appendix I.

7.2.1 Effective Mass

First, recall that we are interested in two different types of ratios:

1. The ratio that isolates the off-forward component, $R(\mathbf{p}')$ as in Eq. 7.3,

$$R(\mathbf{p}', \lambda) \equiv \frac{C(\mathbf{p}', \lambda, \lambda)C(\mathbf{p}', -\lambda, -\lambda)}{C(\mathbf{p}', \lambda, -\lambda)C(\mathbf{p}', -\lambda, \lambda)}.$$

2. And the product and ratio of this ratio: $R(\mathbf{p}_1) \times R(\mathbf{p}_2)$ and $R(\mathbf{p}_1)/R(\mathbf{p}_2)$.

The effective mass may be taken of each both types of ratio. This is defined by

$$\Delta E_{\text{eff}}(\tau) = \frac{1}{\delta\tau} \log\left(\frac{R(\tau)}{R(\tau + \delta\tau)}\right). \tag{7.14}$$

For the first set of correlators, the effective mass plot for the ratio, $R(\mathbf{p}')$, as defined in Eq. 7.3, is given in figure 7.3. Similarly, for the second set of correlators, the same ratio $R(\mathbf{p}')$ is given in figure 7.4.

The exponential fits to the ratios (figures 7.3 and figure 7.4) are largely 'good': they have small error bars, low noise/signal ratio, and conform to the effective mass plot. However, the fitting window starts quite early in Euclidean time: $\tau = 4a - 11a$ for figure 7.3, and $\tau = 3a - 8a$ for figure 7.4.

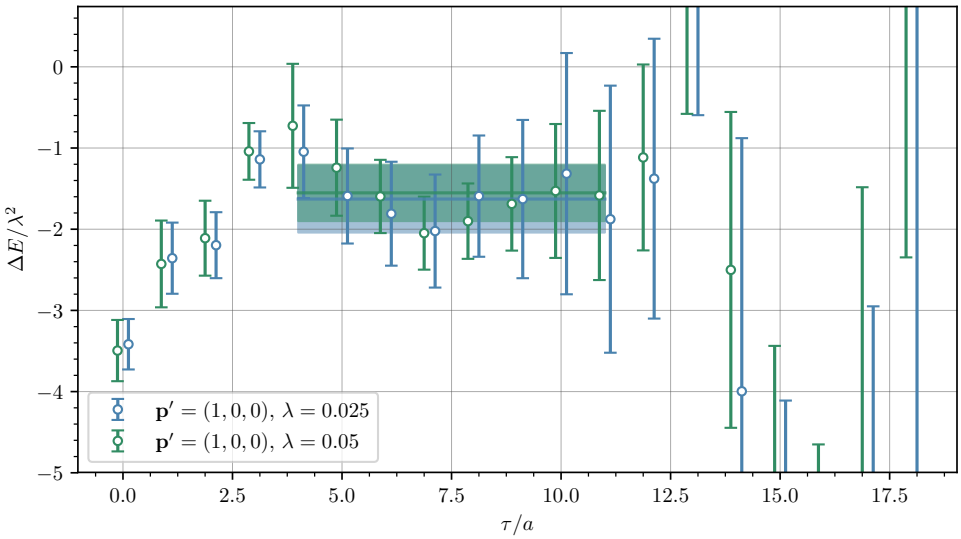

Figure 7.3: Effective mass plot for the ratio $R(\mathbf{p})$, with the first set of correlators. Shaded bands are exponential fits to the energy shift.

The effective masses for other kinematics, for all down quark results, and for the $R(\mathbf{p}_1) \times R(\mathbf{p}_2)$ and $R(\mathbf{p}_1)/R(\mathbf{p}_2)$ ratios results can be found in appendix I.

7.2.2 λ Dependence

In our Feynman-Hellman derivation from chapter 5, we assumed that there were no linear terms in λ in our energy shift. We can test this explicitly by taking the quantity defined in Eq. 7.2, $\Delta E(\lambda)$, and subtracting off the energy shift at $\bar{\omega} = 0$. Then, we fit the function $f(\lambda) = a\lambda + b\lambda^2$ to this subtracted $\Delta E(\lambda)$.

For the case of $\bar{\mathbf{p}} = (0, 1, 0)$, we find that the parameters of the model function are $a = 0.0012 \pm 0.0168$, and $b = -5.29 \pm 0.54$. Hence the linear term is consistent with zero, in line with our assumption for the FH derivation. We plot $b\lambda^2$ against the subtracted energy shift in figure 7.5.

7.2.3 $\bar{\omega}$ Dependence

Next, we are interested in how these energy shifts behave as functions of $\bar{\omega}$. For this analysis, we limit our focus to the second set of correlators, since we only calculated one $\bar{\omega}$ value from the first set. The $\bar{\omega}$ dependence of the up quark energy shifts from $R(\mathbf{p}_1)$ and $R(\mathbf{p}_2)$ are given in figures 7.6 and 7.7. The $\bar{\omega}$ dependence of the up quark energy shifts of $R(\mathbf{p}_1) \times R(\mathbf{p}_2)$ and $R(\mathbf{p}_1)/R(\mathbf{p}_2)$ are given in figure 7.8. Additional results are in appendix I.

We expect the energy shift of the ratios $R(\mathbf{p}_1)$ and $R(\mathbf{p}_2)$ to have quadratic dominated $\bar{\omega}$ dependence from Eq. 7.11. Moreover, we should see that the energy shift extracted from $R(\mathbf{p}_1)$ is consistent with that extracted from $R(\mathbf{p}_2)$.

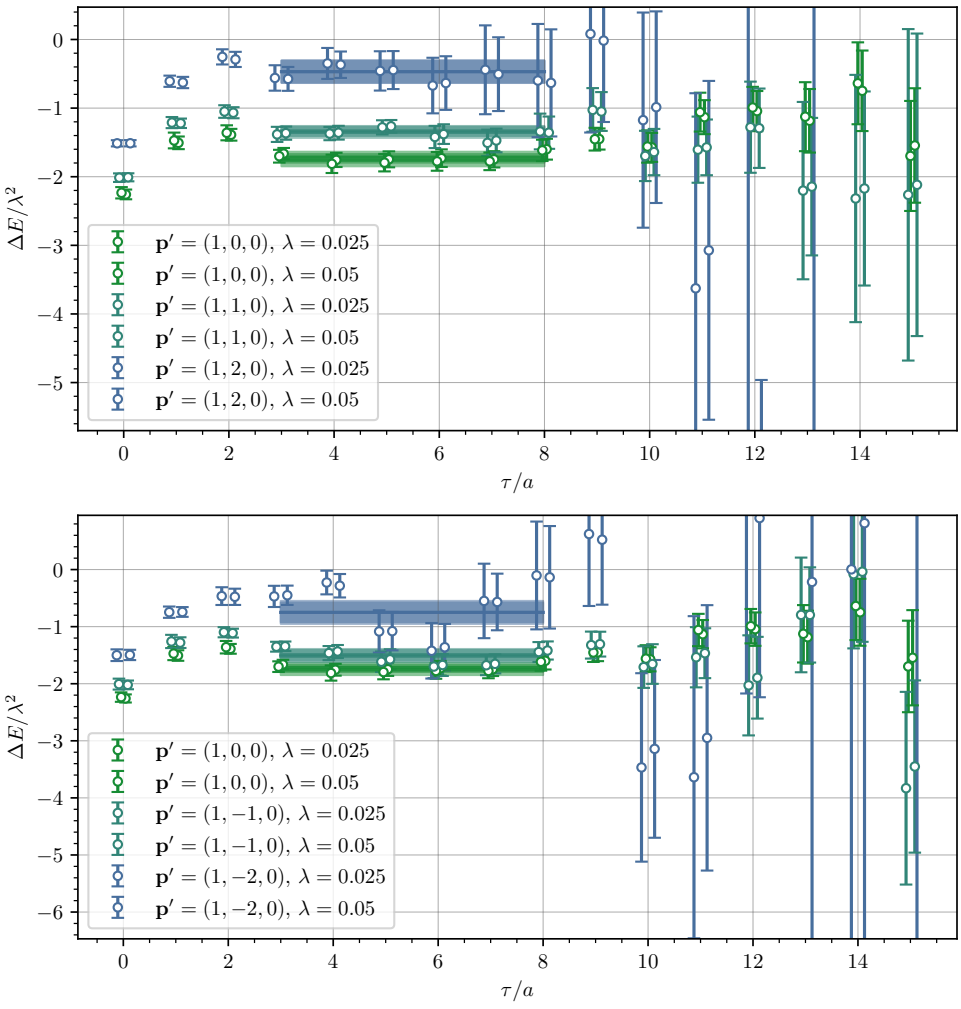

Figure 7.4: Effective mass plot for the ratios $R(\mathbf{p}_1)$, with the second set of correlators. Note that the values of the sink momentum all have $p_x = 1$.

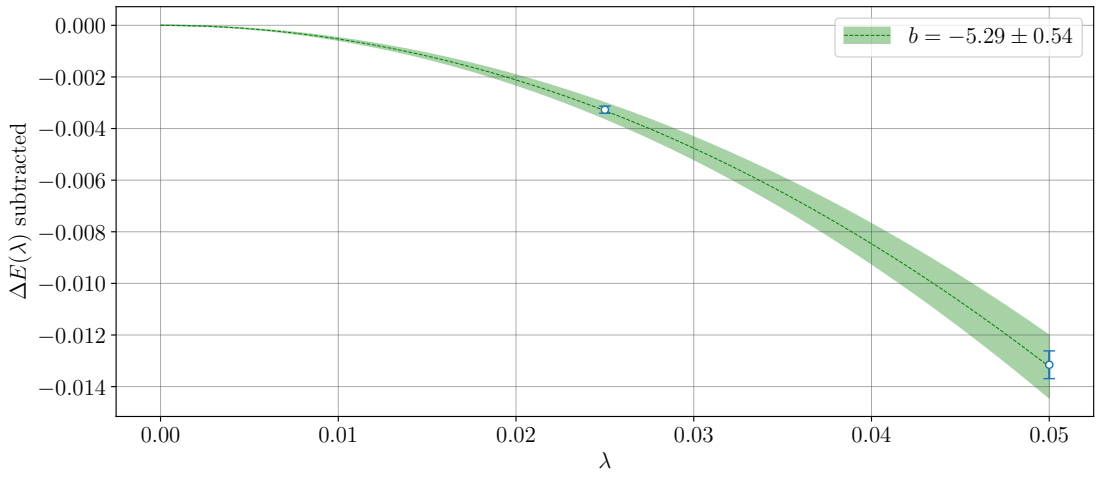

Figure 7.5: The energy shift $\Delta E(\lambda)$ with the $\bar{\omega} = 0$ term subtracted for up quarks.

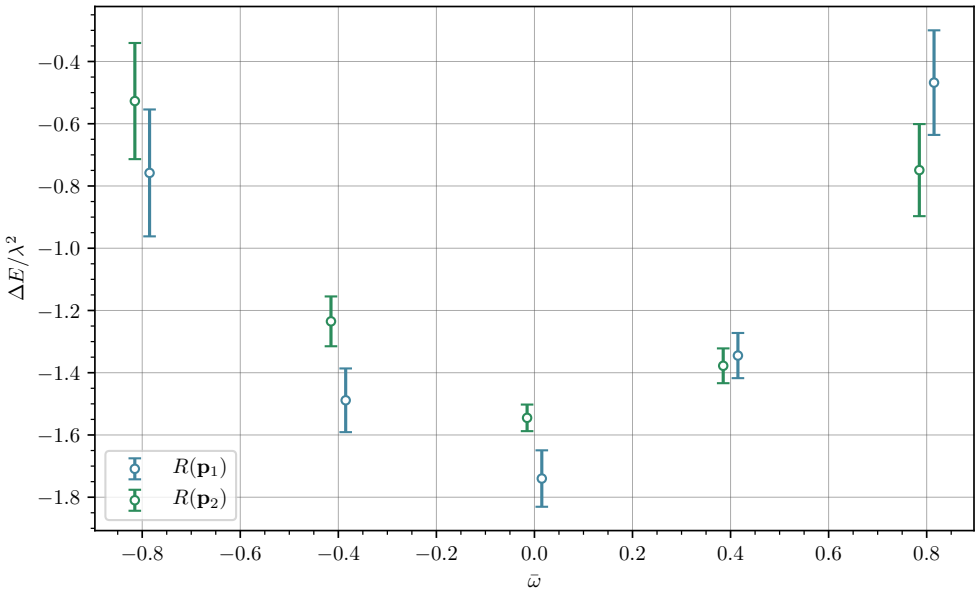

Figure 7.6: The energy shift normalised by $1/\lambda^2$ as a function of $\bar{\omega}$. The two λ values have been averaged.

However, there is also a very large $\bar{\omega} = 0$ term (see figure 7.6), which we call the 'subtraction term' — we will consider this in greater detail in the discussion. So we also present the energy shifts with the $\bar{\omega} = 0$ term subtracted in figure 7.7.

We also expect that the product of the two ratios $R(\mathbf{p}_1) \times R(\mathbf{p}_2)$ isolates Eq. 7.10, and therefore has quadratic-dominated $\bar{\omega}$ dependence. The $R(\mathbf{p}_1)/R(\mathbf{p}_2)$ should be consistent with zero. The subtracted energy shifts of these ratios is presented in figure 7.8.

This is largely what we see; however, note that the $\bar{\omega} > 0$ values of $R(\mathbf{p}_1)/R(\mathbf{p}_2)$ are not consistent with zero as we would expect.

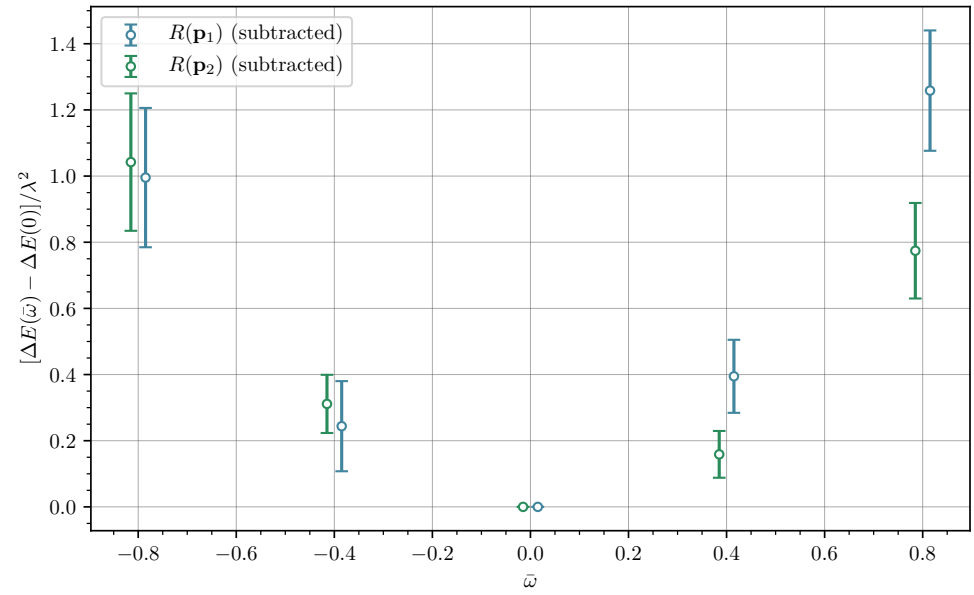

Figure 7.7: The same energy shift as figure 7.6, except with the $\bar{\omega} = 0$ terms subtracted off.

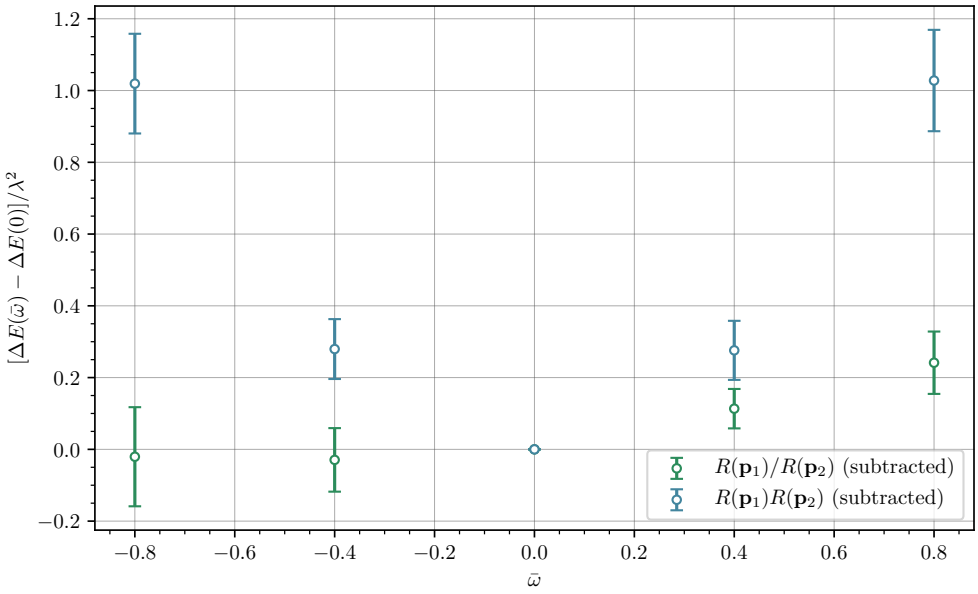

Figure 7.8: The energy shifts of $R(\mathbf{p}_1) \times R(\mathbf{p}_2)$ and $R(\mathbf{p}_1)/R(\mathbf{p}_2)$ with the $\bar{\omega} = 0$ value subtracted.

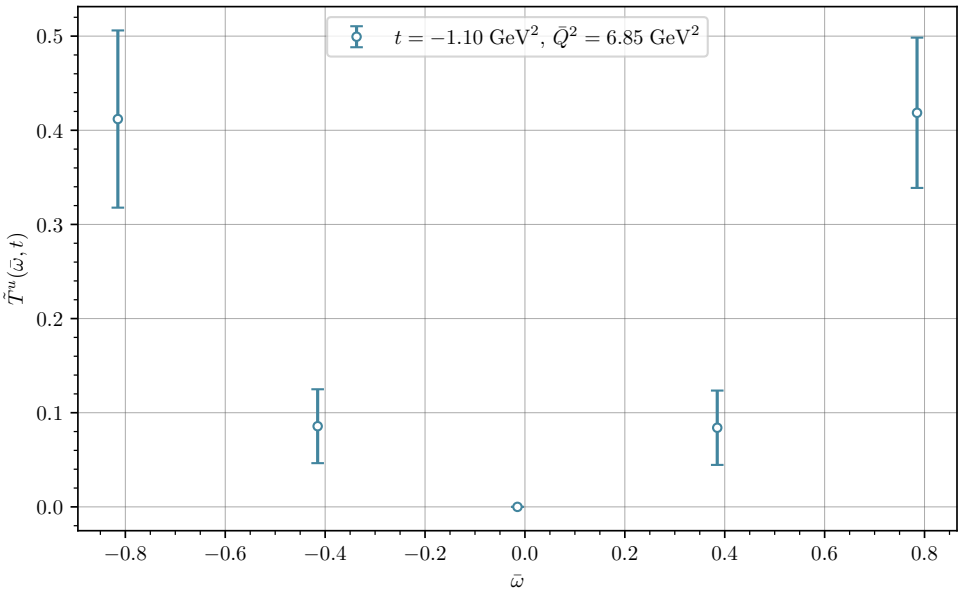

Figure 7.9: The energy shifts from figure 7.8 normalised to give the towers of up quark GFFs.

7.2.4 Towers of GFFs

Finally, we apply all the correct normalisations to get the two towers of GFFs, which we will combine into the quantity

$$\tilde{T}^f(\bar{\omega}, t) = \frac{2}{(E_N + M)}\left[(E_N + M)\mathcal{A}^f(\bar{\omega}, t) - \frac{t}{4M}\mathcal{B}^f(\bar{\omega}, t)\right].$$

The results for this quantity are given in figure 7.9 for up quarks and figure 7.10 for down quarks.

Note that

$$\tilde{T}^u(\omega, t = 0) = 2 \sum_{n=2,4,6}^{\infty} \omega^n a_n^u,$$

where a_n^u are up quark PDF moments (recall the relationship between PDFs and GPDs from Eq. 4.21). This allows us to compare directly the off-forward and forward towers of moments, which we do by comparing our calculation to the calculation of the forward Compton tensor with lattice Feynman-Hellmann techniques in Re. [162]. This comparison is presented in figures 7.11 and 7.12.

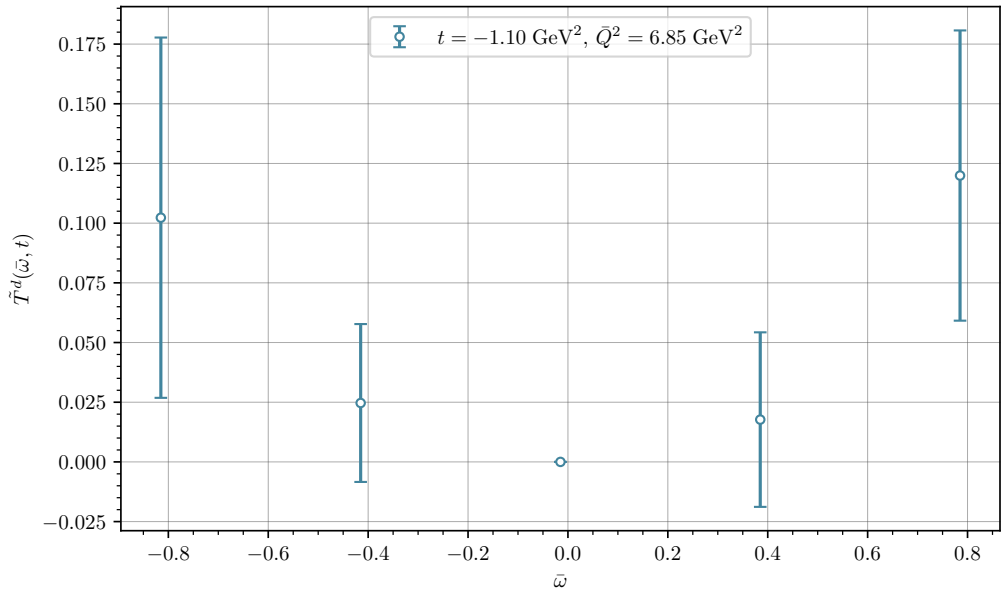

Figure 7.10: The down quark energy shifts, normalised to give the towers of down quark GFFs.

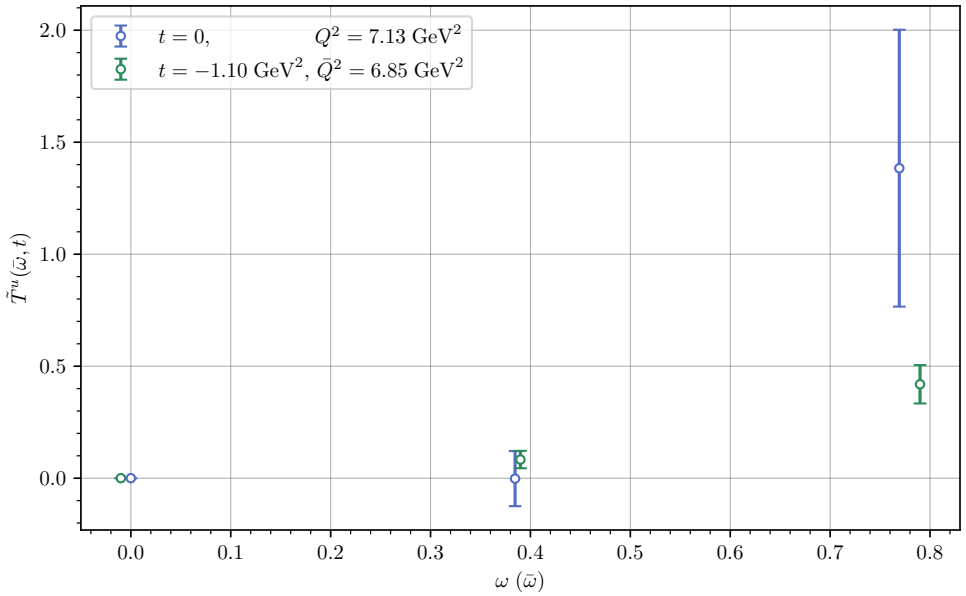

Figure 7.11: The forward Compton tensor ($\mathcal{A}^u(\omega, t = 0)$), as calculated in Ref. [162], compared to the towers of GFFs.

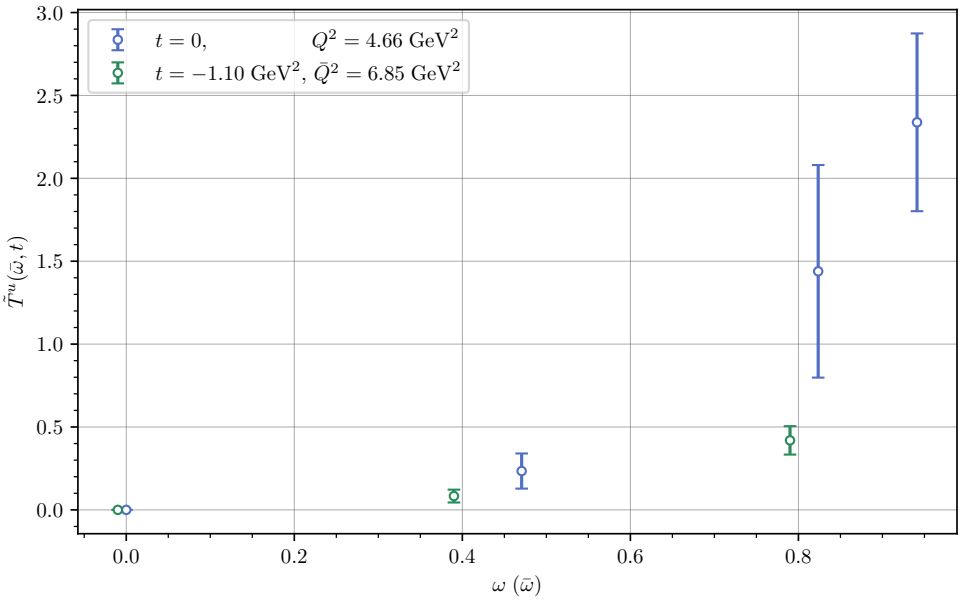

Figure 7.12: The same comparison as figure 7.11, with a different value of Q^2 for the forward Compton tensor.

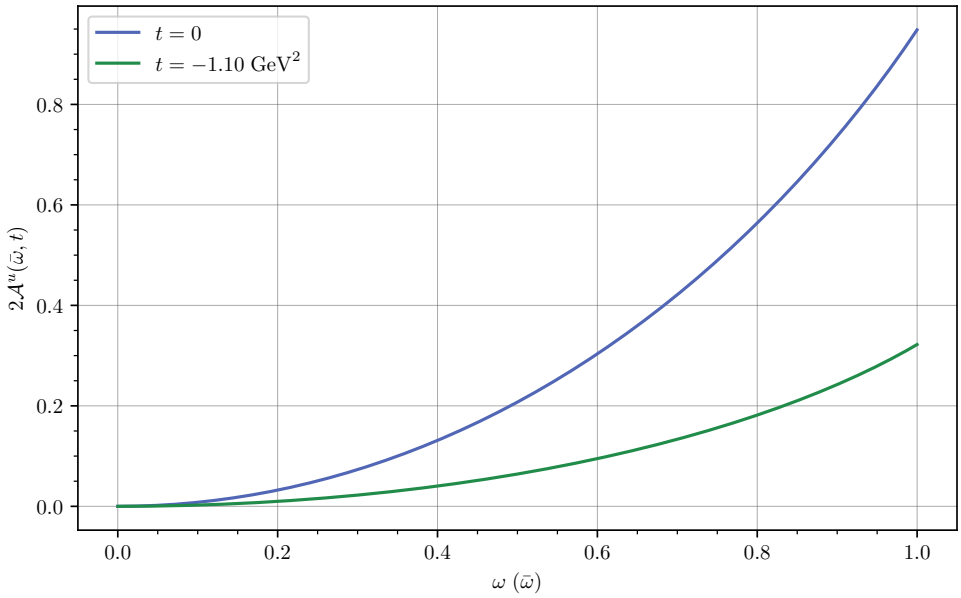

Figure 7.13: PDFs extracted from experiment used to find the zero-skewness forward and off-forward Compton tensors.

We can use a rough phenomenological model of GPDs to test whether our results are of the right magnitude. We use PDFs from the MMHT 2014 set at $Q_0^2 = 1$ GeV^2, next-to-next-to leading-order [164]. Then, we can construct a comparable tower of PDF moments from

$$\mathcal{A}^u(\omega, t=0) = \sum_{n=2,4,6}^{\infty} \omega^n \int_0^1 dx x^{n-1} \big[q_u(x) + \bar{q}_u(x)\big].$$

For the GPDs we use a very simple Regge-based ansatz [55, 165–167], which at zero skewness is

$$H^f(x,t) - H^f(-x,t) = x^{-\alpha' t}(q_f(x) + \bar{q}_f(x)),$$

for $\alpha' = 0.9$ GeV^{-2}. Hence the off-forward Compton tensor is

$$\mathcal{A}^u(\bar{\omega}, t) = \sum_{n=2,4,6}^{\infty} \bar{\omega}^n \int_0^1 dx x^{n-1-\alpha' t} \big[q_u(x) + \bar{q}_u(x)\big].$$

These towers of moments from the phenomenological fits are given in figure 7.13. Note that our use of these results is very rough: we have not got the same values of the scaling variable Q^2 (or $\bar{Q}^2$) and we have not done any error analysis.

Summary of Results

To summarise the first three main results: (1) from the effective mass plots, the fits are largely good, but start quite early in Euclidean time; (2) the λ behaviour is consistent with a quadratic, as we expect from chapter 5; (3) the $\bar{\omega}$ behaviour is consistent with the OPE, except the perhaps the $\bar{\omega} > 0$ behaviour of the $R(\mathbf{p}_1)/R(\mathbf{p}_2)$ energy shift (figure 7.8).

7.3 Discussion

In this section, we interpret the results from the proof-of-principle calculation. Of course, since this calculation is exploratory, much of the discussion in this section is premature and not as rigorous as we would like. Nonetheless, we can conclude that our results present a great deal of potential for future studies.

First, we look at the t behaviour of our results, and compare this with previous studies. Then, we note some of the unique features of the method we have used in this calculation, such as the subtraction term and spacelike target mass corrections, and propose how these can be interpreted and controlled. Finally, we outline some avenues of further research.

7.3.1 t Behaviour

The t dependence of our results is particularly important because this reflects the non-perturbative behaviour of the GFFs.

$t = -2$ versus $t = -4$

We can investigate the t behaviour by comparing the two sets of correlators: the first set at $t = -2$ and the second at $t = -4$. In physical units, $t = -0.55$ GeV^2 and $t = -1.10$ GeV^2, respectively. Therefore, by this comparison, we can *tentatively* compare the t dependence

of the OFCT. This is tentative because there is a very large difference in $\bar{Q}^2$ between the two sets. Moreover, we have no subtraction term for the $t = -2$ set that would allow us to compare the GFF towers of each.

However, we can get the $\bar{\omega} = 2/5$ term from each set of correlators, which gives some credence to our comparison. The results are given in the table below.

	$\mathbf{p}'$	$a\lambda$	$\bar{Q}^2$	$\bar{\omega}$	$\Delta E/\lambda^2$
First Set	$(1,0,0)$	0.025	12.5	2/5	-1.572 ± 0.403
$(t = -2)$	$(1,0,0)$	0.05	12.5	2/5	-1.531 ± 0.357
$(t = -0.55\ \text{GeV}^2)$	$(0,1,0)$	0.025	12.5	2/5	-1.421 ± 0.328
	$(0,1,0)$	0.05	12.5	2/5	-1.428 ± 0.228
Second Set	$(1,1,0)$	0.025	25	2/5	-1.336 ± 0.075
$(t = -4)$	$(1,1,0)$	0.05	25	2/5	-1.364 ± 0.083
$(t = -1.10\ \text{GeV}^2)$	$(-1,1,0)$	0.025	25	2/5	-1.371 ± 0.058
	$(-1,1,0)$	0.05	25	2/5	-1.379 ± 0.059

Taken at face-value, therefore, there is a decrease in the signal with increased t, as we would expect.

$t = 0$ **versus** $t = 4$

We can make a more robust comparison of the forward Compton tensor, as calculated in [123, 162], and the OFCT calculated in the present thesis. There is a relatively small difference in the scaling variable: $Q^2 = 17$ and $Q^2 = 26$, compared to $\bar{Q}^2 = 25$ for the OFCT. In physical units, $Q^2 = 4.66\ \text{GeV}^2$ and $Q^2 = 7.13\ \text{GeV}^2$, respectively, and $\bar{Q}^2 = 6.85\ \text{GeV}^2$.

Similarly, the λ values for the forward Compton tensor are $a\lambda = 0.0125$, and 0.025 for $Q^2 = 17$, and $a\lambda = 5 \times 10^{-5}$, and 5×10^{-6} for $Q^2 = 26$. This is compared to $a\lambda = 0.025$ and 0.05 for the OFCT. Moreover, we have the subtraction term ($\omega = 0$ or $\bar{\omega} = 0$) for both calculations.

Finally, we note the difference between the coefficients of the two towers of GFFs:

$$\sum_{n=2,4,6}^{\infty} \bar{\omega}^n \big[(E_N + M)A_n^f(t) + \frac{t}{4M} B_n^f(t)\big].$$

Since $-t/[4M(E_N + M)] \approx 0.08$, our results are dominated by the $\mathcal{A}^f(\bar{\omega}, t)$ towers.

Therefore, we can interpret the comparison of these two calculations as the tower of GFFs $\mathcal{A}^u(\bar{\omega}, t)$ at different values of t: the forward Compton tensor is the tower of GFFs at $t = 0$ (i.e. a tower of PDF moments), and the OFCT is the same object at $t = -4$ (or $t = -1.10\ \text{GeV}^2$ in physical units). From figures 7.11 and 7.12, we can see a significant decrease in the size of the OFCT from $t = 0$ to $t = -4$.

Comparison to Simple Phenomenological Model

The t behaviour of figures 7.11 and 7.12 is consistent with the t behaviour of the phenomenological PDF and GPD towers in figure 7.13. However, the FH-calculated quantities are approximately twice the magnitude of the model ones. This is similar to the case of PDF moments, where lattice calculations from three point functions are significantly

larger than those extracted from experiment [111]. However, we must caution that the simple Regge-based ansatz used here is no substitute for a complete analysis, using more advanced and accurate phenomenological fits.

Comparison to Three-Point Functions

Previous lattice studies that calculate GFFs from three point functions [56–62] have consistently found the t behaviour of the $n = 2$ GFFs has a dipole form:

$$A^f_{2,0}(t) = \frac{A^f_{2,0}(0)}{(1 - t/M^2)^2},$$

with a similar behaviour for the other $n = 2$ GFFs. As such, we expect the towers of quadratic term in the towers of moments to decrease with $-t$. This is what we see in figures 7.11 and 7.12.

7.3.2 Unique Features of the Present Calculation

Subtraction Term

In previous studies of the forward Compton tensor from lattice FH techniques, it was found that there was a significant contribution from the energy shift at $\omega = 0$; this term is known as the subtraction term [122, 123, 162]. Moreover, it was found that this term *doesn't scale to zero* with $Q^2 \to \infty$, as we'd expect from the OPE[†], but rather scaled to a non-zero value with large Q^2. Similarly, in our results for the OFCT, we find a large contribution at $\bar{\omega} = 0$ (see figures I.5 and 7.6). While we don't have the $\bar{Q}^2$ behaviour to see whether this term vanishes, it is likely that it won't.

There are two possible sources of the subtraction term. First, it is possible that it's a discretisation error. As we argued in chapter 3, the large Q^2 (or $\bar{Q}^2$) limit probes the short distance limit $|z^\mu| \to 0$. However, on the lattice have a non-zero minimum spacing, the lattice spacing. As such, this subtraction term could simply be a lattice artefact from discretisation. In Refs. [123, 162], it was found that at least part of the subtraction term was a lattice artefact.

On the other hand, the subtraction term could contain interesting physical information (of course, once the part that's a lattice artefact is removed). However, for this to be the case would require us to rethink the validity of the OPE for deep inelastic processes, which has so far been very successful.

Following previous studies of the forward Compton tensor, we will assume that once we subtract off the term at $\bar{\omega} = 0$, the subtracted quantity behaves like the OPE prediction for the OFCT (Eq. 6.56). As such, we interpret our subtracted quantities as towers of GFFs.

Spacelike Target Mass Corrections

Here, we will briefly outline one subtlety in using the twist-two OPE. In the following section for simplicity we will limit our discussion to forward scattering, but the results

[†]However, non-perturbative results such as the dispersion relation (section 6.3) don't make any strict predictions about its value.

apply equally to off-forward. From chapters 3 and 6, the leading-twist local operators in the operator product expansion (OPE) are (Eq. 3.50)

$$\mathcal{O}_f^{(n)\mu_1\ldots\mu_n} = \bar{\psi}_f \gamma^{\{\mu_1} i\overset{\leftrightarrow}{D}^{\mu_2} \ldots i\overset{\leftrightarrow}{D}^{\mu_n\}} \psi_f - \text{traces},$$

where traces were any terms proportional to $g^{\mu_i\mu_j}$. These traces are suppressed by powers of P^2/Q^2, which may be large with Euclidean kinematics. Therefore, the trace terms may actually contribute significantly to the Euclidean Compton tensor due to these spacelike target mass corrections, and hence we must consider their contributions.

Consider the forward matrix element of the spin two operator (flavour index suppressed) *without the traces subtracted*:

$$\frac{4q_{\mu_1}q_{\mu_2}}{Q^4}\langle P|\mathcal{O}_2^{(\text{unsub})\mu_1\mu_2}|P\rangle = \omega^2 a_2 + \frac{P^2}{Q^2}\tilde{a}_2, \tag{7.15}$$

where a_2 is the usual parton distribution function (PDF) moment, and $\tilde{a}_2$ is the reduced matrix element of the operator that is usually subtracted.

Then, we can subtract off the $\omega = 0$ term, which corresponds to the $\mathbf{p} = 0$ in the usual kinematics, where this is the spatial component of P^μ. Therefore, we get

$$\frac{4q_{\mu_1}q_{\mu_2}}{Q^4}\langle P|\mathcal{O}_2^{(\text{unsub})\mu_1\mu_2}|P\rangle - \langle P|\mathcal{O}_2^{(\text{unsub})\mu_1\mu_2}|P\rangle\Big|_{\omega=0} = \omega^2 a_2 + \frac{P^2 - M^2}{Q^2}\tilde{a}_2. \tag{7.16}$$

Hence so long as $(P^2 - M^2)/Q^2 = 2\mathbf{p}^2/Q^2 \ll \omega$, this first moment is fine. This problem stems from the Euclidean signature, where it is possible for $P^2 \neq M^2$.

Now consider the $n = 4$ operator:

$$\frac{16q_{\mu_1}\ldots q_{\mu_4}}{Q^8}\langle P|\mathcal{O}_4^{(\text{unsub})\mu_1\ldots\mu_4}|P\rangle = \omega^4 a_4 + \frac{P^2}{Q^2}\omega^2\tilde{a}_4^{(1)} + \left(\frac{P^2}{Q^2}\right)^2\tilde{a}_4^{(2)}. \tag{7.17}$$

Note that the $\omega = 0$ subtraction term will not remove the $\frac{P^2}{Q^2}\omega^2$ term. However, it will be suppressed compared to the leading ω^2 term, especially if $\mathbf{p}$ is kept small.

Analogous conditions hold in off-forward kinematics, where we now would like to keep $\bar{\omega} \gg \bar{\mathbf{p}}^2/\bar{Q}^2$ and $\boldsymbol{\Delta}^2/\bar{Q}^2$. This only means we need to be judicious in how we choose our kinematics; it isn't a fundamental problem.

Similarly, in quasi-distributions studies trace terms need to be suppressed by taking P_z large [109]. Therefore, borrowing ideas from quasi-distributions, it may be useful to fit at each power of $\bar{\omega}$ to the ansatz $a + b/\bar{Q}^2$ [168, 169].

Here we have shown how to avoid only one type of higher twist correction — there are of course other sources of higher twist terms.

7.3.3 Future Prospects

The exploratory calculation carried out in this chapter is just a first step in extracting GPDs from lattice Feynman-Hellmann techniques. In this section we suggest possible avenues of investigation for future studies.

Separation of $\mathcal{A}$ and $\mathcal{B}$ Towers

Since our ultimate aim is the calculation of GFFs, we need to first separate out the towers of A and B GFFs. This may involve changing the spin-parity projection, or calculating different elements of the OFCT such as T^{44}.

Higher Moments

The most exciting feature of this calculation is that it allows us to extract higher GFFs, from which it is possible in principle to reconstruct GPDs.

Already, sophisticated fitting techniques have been applied to similar studies of the forward Compton tensor [170]. The moment fitting would largely be the same as in the forward study, since for zero-skewness kinematics the GFFs are straightforward Mellin moments of GPDs:

$$\int_{-1}^{1} dx x^{n-1} H^f(x, \xi = 0, t) = A^f_{2,0}(t), \quad \int_{-1}^{1} dx x^{n-1} E^f(x, \xi = 0, t) = B^f_{2,0}(t). \tag{7.18}$$

For an extraction of the t dependence of higher GPD moments, we would need to calculate many more sets of correlators, vary both momentum transfer variables t and $\bar{Q}^2$, and $\bar{\omega}$. Moreover, it is likely that the kinematics would need to extend beyond a two-dimensional plane, and as such we would have to use the 'conserved' current operator (see Ref. [162]). Similarly, larger lattice volumes will likely be needed for more densely distributed values of $\bar{\omega}$ and t.

Non-zero Skewness and D-term

Recall from chapter 6 that the kinematic regime $\bar{P} \cdot \bar{q} = 0$ allows us to extract C_n GFFs (Eq. 6.50):

$$\frac{1}{4} \sum_{\text{spins}} \Gamma^{\text{unpol}}_{\beta\alpha} u_\alpha(P') T^{33} \bar{u}_\beta(P) \propto \sum_f e_f^2 \sum_{n=2,4,6}^{\infty} 2^n \zeta^n C^f_n(t),$$

where $\zeta = \Delta \cdot \bar{q} / \bar{Q}^2$. For lattice studies this becomes

$$\zeta = \frac{2(\mathbf{q} - \mathbf{q}') \cdot (\mathbf{q} + \mathbf{q}')}{(\mathbf{q} + \mathbf{q}')^2}.$$

This calculation is completely achievable; the only drawback being that it is more computationally expensive than the calculation carried out in this chapter. This is because if we want a range of ζ values, we must vary $\bar{q}$, and hence each new ζ value requires a new set of correlators.

$\mathbf{q}$	$\mathbf{q}'$	ζ
$(1,5,0)$	$(-1,5,0)$	0
$(4,4,0)$	$(2,4,0)$	$12/25$
$(5,3,0)$	$(3,3,0)$	$16/25$
$(6,0,0)$	$(4,0,0)$	$20/25$

Note that $\mathbf{p} = (-1,0,0)$, $\mathbf{p}' = (1,0,0)$, $\bar{\omega} = 0$ and $\bar{Q}^2 = 25$ are fixed in the table above. See figure 7.14. This would give us access to the quark D-term, which we discussed extensively in section 4.2.

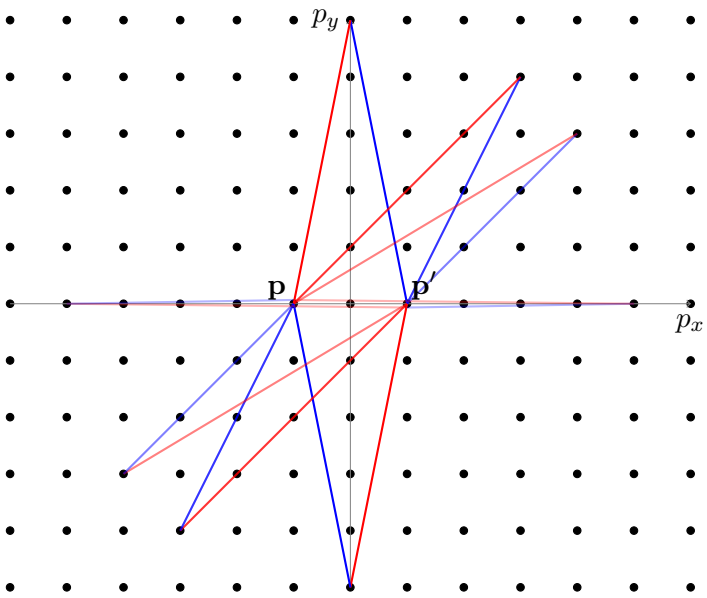

Figure 7.14: Diagram representing the kinematics to isolate the C_n GFFs. Note that the lines along the p_x axis have been made slightly off-axis for clarity.

Therefore, the present lattice calculation is simply the start of many possible applications of FH techniques to help unravel the structure of hadrons through GPDs.

Chapter 8

Conclusions and Outlook

Generalised parton distributions (GPDs) offer us the opportunity to significantly deepen our understanding of hadron structure. However, on the lattice and in experiment, they are hard to determine. On the lattice, the fundamental problem to overcome is the mismatch between the high-energy partonic description and the Euclidean spacetime of numerical calculations.

In this thesis, we presented a novel method to calculate GPDs through lattice Feynman-Hellmann techniques. This required first developing the Feynman-Hellmann formalisms necessary to calculate the off-forward Compton tensor (OFCT) in chapter 5. These results are analogous to previous Feynman-Hellmann derivations (for instance, Refs. [133, 139, 162]). Due to the non-trivial mixing induced by our perturbing Lagrangian, we considered the effects of this mixing on the perturbed correlator in detail. This analysis guided our choice of the perturbation couplings, $\lambda_{1,2}$. However, we didn't perform any numerical calculations at other combinations of λ values, and further investigation (numerical and analytic) of this mixing behaviour would be interesting.

In chapter 6, we performed an operator product expansion (OPE) on the OFCT, and thereby related it to the Mellin moments of GPDs. The behaviour of the nucleon OFCT found in this chapter is consistent with previous studies in different formalisms. Moreover, with the correct choice of kinematics, the OPE allows for the extraction of generalised form factors (GFFs). Since lattice calculations must use large but finite $\bar{Q}^2$, further study of the higher twist contributions to the OFCT will make GFF fits more accurate.

Finally, in chapter 7, we presented a proof-of-principle numerical computation using these methods. Although this calculation and its analysis was exploratory, the initial results look very promising. Most notably, the comparison of the forward Compton tensor to the OFCT showed t behaviour consistent with a simple phenomenological model. Hence this exploratory calculation sets the stage for far more work calculating the Euclidean OFCT.

However promising these initial results are, it will still require a great deal more work to realise the full potential of this method. First, we need to be able to separate the $\mathcal{A}$ and $\mathcal{B}$ towers of GFFs. Then, to calculate higher GFFs, we need a greater spread of $\bar{\omega}$ and t values than the ones presented in this thesis. Moreover, since the subtraction term is so poorly understood, greater work must be done (both for off-forward and forward calculations) to determine to what extent it is a lattice artefact.

Second, it will be highly revealing to look at the $\bar{Q}^2$ behaviour of the amplitude. This may be compared to theoretical predictions of the scaling behaviour, and will moreover help isolate the leading-twist part of the OFCT.

Additionally, there are certain systematic improvements to the lattice calculation that would likely improve the results, including excited state control, physical point extrapolation, and application of the parity expanded variational analysis (PEVA) [171].

In summary, we have shown the first steps in determining GFFs from lattice Feynman-Hellmann techniques, and presented the results of an exploratory calculation. Although there is still much work to do, these results lay the groundwork for future studies.

Appendix A

Notation and Standard Results

Metrics

We use the convention for the Minkowski metric,

$$g^{\mu\nu} = g_{\mu\nu} = \text{diag}(1, -1, -1, -1).$$

Units

We use physical units $\hbar = c = 1$, and so we measure all quantities in terms of their energy dimension:

$$[\text{energy}] = [\text{mass}] = \frac{1}{[\text{length}]} = \frac{1}{[\text{time}]}.$$

Minkowski Triangle Inequality

For two *future-pointing timelike* Lorentz vectors a and b, we have the Minkowski triangle inequality:

$$\sqrt{(a+b)^2} \geq \sqrt{a^2} + \sqrt{b^2}.$$

Note that this is the reverse of the Euclidean triangle inequality. Then, as with the Euclidean triangle inequality, we can get the *reverse* triangle inequality:

$$\sqrt{(a-b)^2} \leq \left|\sqrt{a^2} - \sqrt{b^2}\right|.$$

This last result is an easy way to check if a virtual photon must be spacelike or timelike.

Symmetrisation of Indices

Symmetrisation and anti-symmetrisation of two indices, respectively, is denoted

$$a^{\{\mu\nu\}} = \frac{1}{2}(a^{\mu\nu} + a^{\nu\mu}), \quad a^{[\mu\nu]} = \frac{1}{2}(a^{\mu\nu} - a^{\nu\mu}). \tag{A.1}$$

Therefore, $a^{\mu\nu} = a^{\{\mu\nu\}} + a^{[\mu\nu]}$.

The general expression for a symmetrised rank-n tensor is

$$T^{\{\mu_1 \ldots \mu_n\}} = \frac{1}{n!} \sum_{\sigma \in S_n} T^{\nu_{\sigma(1)} \cdots \nu_{\sigma(n)}}, \tag{A.2}$$

where S_n is the group of permutations of the numbers $1, 2, ..., n$, and σ is an element of S_n. Here, we denote a component of some group element $\sigma \in S_n$ as $\sigma(1) \in [1, 2, ..., n]$.

Appendix B

Operator Product Expansion: Traditional Approach

In this appendix, we show how to perform the operator product expansion (OPE) using the traditional approach (we use Refs. [14,28,31] as our guides). The basic argument goes:

1. Assume that the OPE relation (Eq. 3.34) applies to the time-ordered product of currents. As we mentioned before, for non-perturbative operators, the OPE is merely a conjecture.

2. Use dimensional power-counting arguments to deduce a basis of leading-order operators.

3. Given this basis of operators and constraints such as Lorentz covariance, current conservation etc., one can construct the leading-order (as $z \to 0$) OPE of the current product.

4. Using perturbation theory, one can calculate the Wilson coefficients to a given order.

Therefore, for the time-ordered product of currents, we start with the assumption that a relation of the form

$$A(z)B(0) \xrightarrow{z\to 0} \sum_i c_i(z)\mathcal{O}_i(0)$$

applies to the product of currents.

As is convention, we parameterise the OPE for the current product in an equivalent but slightly different way:

$$T[j(z)j(0)] \xrightarrow{z\to 0} \sum_{n,i} C_n^{(i)}(z^2) z_{\mu_1}...z_{\mu_n}\mathcal{O}_i^{\mu_1\cdots\mu_n}(0). \tag{B.1}$$

Note that $C_n^{(i)}(z^2)$ are the *reduced Wilson coefficients*, and the full Wilson coefficient is

$$C_n^{(i)}(z^2) z_{\mu_1}...z_{\mu_n}. \tag{B.2}$$

Here, we must play a subtle game similar to section 3: even though we are doing a short-distance expansion, we actually want the part of the OPE that is relevant to the light-cone. For the term

$$C_n^{(i)}(z^2) z_{\mu_1}...z_{\mu_n},$$

in the light-cone limit $z^2 \to 0$, the terms $z_{\mu_1}...z_{\mu_n}$ *do not affect the singularity of the overall Wilson coefficient*, but for the short-distance limit they do. Therefore, we will only consider the singularity of the reduced Wilson coefficients $C_n^{(i)}(z^2)$, so that we keep all the terms we need to analytically continue back to the light-cone.

Power Counting: Canonical Dimension

Now we are ready to consider the degree of the singularity in $C_n^{(i)}(z^2)$. Let's start by considering the canonical dimension of each operator (for an interacting theory, this will be altered by the anomalous dimension). We count dimension in terms of mass, so $[M] = 1$ and for a spacetime coordinate $[z] = -1$. Then, since the RHS of Eq. B.1 must have the same dimension as the LHS, the dimension of $C_n^{(i)}(z^2)$ is

$$d_{C_{i,n}} = -d_{\mathcal{O}_{i,n}} + n + 2d_j, \tag{B.3}$$

where $d_{\mathcal{O}_{i,n}}$ is the dimension of the operator $\mathcal{O}_i^{\mu_1...\mu_n}$, we get a dimension of $-n$ from $z_{\mu_1}...z_{\mu_n}$, and d_j is the dimension of a current. Then, since the only dimensionful parameter that $C_n^{(i)}(z^2)$ can depend on is z^2, we have that in the limit $z^2 \to 0$,

$$\lim_{z^2\to 0} C_n^{(i)}(z^2) \sim \lim_{z^2\to 0} (z^2)^{(d_{\mathcal{O}_{i,n}} - n - 2d_j)/2}. \tag{B.4}$$

Therefore, we introduce the 'twist' of an operator as $\tau = d_{\mathcal{O}_{i,n}} - n$. And hence from Eq. B.4, the operator with the lowest twist will have the most singular coefficient, and hence will contribute the most in the limit $z^2 \to 0$. Note that if we only considered the operators that were relevant in the short-distance limit, it wouldn't be the lowest twist operators that contribute most, but those with lowest dimension $d_{\mathcal{O}_{i,n}}$.

Leading Twist Operators

More generally, the twist of an operator is defined as $\tau \equiv$ dimension $-$ spin [172]. For instance, the spin of a quark field is $1/2$, while its dimension is $[\psi] = 3/2$ (recall the QCD Lagrangian, Eq. 2.10), and hence the twist of a quark field is 1. Similarly, the twist of the gluon field strength tensor is also 1. Therefore, the lowest twist terms one can have are twist-two, since our operators must be bilinears in our particle fields. On the other hand, the covariant derivative has canonical dimension $[D_\mu] = 1$ and spin 1, so overall twist 0. Hence we can add as many of these as we like, and so the light-cone OPE has an infinite number of leading-order terms in contrast to the short distance OPE.

Moreover, to have definite spin, an operator must belong to an irreducible representation of the Lorentz group. This means it must be symmetrised in its Lorentz indices and have any terms proportional to $g^{\mu_i\mu_j}$ (traces) subtracted (the justifications for this are quite involved; see Ref. [173]).

Therefore, the basis of twist-two operators is

$$\mathcal{O}_f^{(n)\mu_1...\mu_n}(X) = \bar{\psi}_f(X)\gamma^{\{\mu_1} i\overset{\leftrightarrow}{D}^{\mu_2}...i\overset{\leftrightarrow}{D}^{\mu_n\}}\psi_f(X) - \text{traces}, \tag{B.5}$$

$$\tilde{\mathcal{O}}_f^{(n)\mu_1...\mu_n}(X) = \bar{\psi}_f(X)\gamma^{\{\mu_1}\gamma^5 i\overset{\leftrightarrow}{D}^{\mu_2}...i\overset{\leftrightarrow}{D}^{\mu_n\}}\psi_f(X) - \text{traces}. \tag{B.6}$$

These are the same operators used in chapter 3. As per the discussion in section 6.2, technically we also need to include operators with total derivatives. However, we will follow the standard presentation of the OPE and leave these out.

For gluons, the twist two operators are

$$\mathcal{O}_g^{(n)\mu_1\ldots\mu_n}(X) = F_\alpha^{\{\mu_1}(X) i\overset{\leftrightarrow}{D}^{\mu_2}\ldots i\overset{\leftrightarrow}{D}^{\mu_n\}} F^{\alpha\mu_n\}}(X) - \text{traces}. \tag{B.7}$$

The leading-order Wilson coefficients for any operators with gluon fields will be zero, since adding gluon lines to the leading order handbag diagrams introduces terms of order α_S^2. Therefore, once again going by the traditional presentation of the OPE, we do not give these operators in our final result.

Form of Current Product

Getting this basis of operators is really the difficult part of the expansion. Once we know them, we can find the OPE by applying general properties of the current product: Lorentz covariance; crossing symmetry, which eliminates q-odd terms in the symmetric Compton tensor; and current conservation ($\partial_z j(z) = 0$).

Then, the OPE of the time-ordered current product is

$$\begin{aligned} T[j^\mu(z)j^\nu(0)] \xrightarrow{z\to 0} & (\partial_\mu\partial_\nu - g_{\mu\nu}\partial^2) \sum_{n=0,2,4}^{\infty} C_n^{(1)}(z^2) z_{\mu_1}\ldots z_{\mu_n} \mathcal{O}_n^{\mu_1\ldots\mu_n}(0) \\ & + (g_{\mu\kappa}\partial_\rho\partial_\nu + g_{\rho\nu}\partial_\mu\partial_\kappa - g_{\mu\kappa}g_{\nu\rho}\partial^2 - g_{\mu\nu}\partial_\rho\partial_\kappa) \sum_{n=0,2,4}^{\infty} C_n^{(2)}(z^2) z_{\mu_1}\ldots z_{\mu_n} \mathcal{O}_{n+2}^{\mu\nu\mu_1\ldots\mu_n}(0). \end{aligned} \tag{B.8}$$

After evaluating the Wilson coefficients to first order (born-level diagrams), this OPE gives the same result as the free field approximation from chapter 3.

Appendix C

Analyticity of the Compton Tensor

In this appendix, we show how to derive a form of the Compton tensor in which the coordinate space integral has been performed and hence the cuts along the real axis are manifest.

We start by expanding the time-ordering of the OFCT:

$$T^{\mu\nu} = i\int d^4z e^{i\bar{q}\cdot z}\Big[\langle P'|j^\mu(z/2)j^\nu(-z/2)|P\rangle\Theta(z^0) + \langle P'|j^\nu(-z/2)j^\mu(z/2)|P\rangle\Theta(-z^0)\Big], \tag{C.1}$$

where Θ is the Heaviside step function*. Inserting a complete set of states, and using the translation operator,

$$\begin{aligned} T^{\mu\nu} =& \sum_X i\int\frac{d^3P_X}{(2\pi)^3}\frac{1}{2P_X^0}\int d^4z\Big[e^{i(\bar{q}+\bar{P}-P_X)\cdot z}\langle P'|j^\mu(0)|X\rangle\langle X|j^\nu(0)|P\rangle\Theta(z^0) \\ &+ e^{i(\bar{q}+P_X-\bar{P})\cdot z}\langle P'|j^\nu(0)|X\rangle\langle X|j^\mu(0)|P\rangle\Theta(-z^0)\Big], \end{aligned} \tag{C.2}$$

where P_X is the four momentum of state $|X\rangle$. Now apply the definition of the Dirac delta:

$$\begin{aligned} T^{\mu\nu} =& \sum_X (2\pi)^3 i\int\frac{d^3P_X}{(2\pi)^3}\frac{1}{2P_X^0}\int dz^0 \\ &\times\Big[\delta^{(3)}(\bar{\mathbf{q}}+\bar{\mathbf{P}}-\mathbf{P_X})e^{iz^0(\bar{q}^0+\bar{P}^0-P_X^0)}\langle P'|j^\mu(0)|X\rangle\langle X|j^\nu(0)|P\rangle\Theta(z^0) \\ &+\delta^{(3)}(\bar{\mathbf{q}}+\mathbf{P_X}-\bar{\mathbf{P}})e^{iz^0(\bar{q}^0+P_X^0-\bar{P}^0)}\langle P'|j^\nu(0)|X\rangle\langle X|j^\mu(0)|P\rangle\Theta(-z^0)\Big]. \end{aligned} \tag{C.3}$$

The integral representation of the step function is

$$\Theta(z^0) = \frac{1}{2\pi i}\lim_{\epsilon\to 0^+}\int_{-\infty}^{\infty} ds\frac{e^{isz^0}}{s-i\epsilon}, \tag{C.4}$$

where we evaluate Eq. C.4 with a semi-circle contour in the upper half of the complex plane, whose radius goes to infinity. Then,

$$\Theta(z^0) = \lim_{\epsilon\to 0^+}\begin{cases} e^{-\epsilon z^0} & \text{if } z^0 > 0 \\ 0 & \text{if } z^0 < 0, \end{cases} \tag{C.5}$$

*Even though quark fields anti-commute, quark currents commute, since they contain two quark fields that pick up two negative signs.

$$\Theta(-z^0) = \lim_{\epsilon\to 0^+} \begin{cases} 0 & \text{if } z^0 > 0 \\ e^{\epsilon z^0} & \text{if } z^0 < 0. \end{cases} \tag{C.6}$$

Now we can evaluate Eq. C.3:

$$\int_{-\infty}^{\infty} dz^0 e^{iz^0(\bar{q}^0+\bar{P}^0-P_X^0)}\Theta(z^0) = \frac{-i}{P_X^0 - \bar{q}^0 - \bar{P}^0 - i\epsilon}, \tag{C.7}$$

$$\int_{-\infty}^{\infty} dz^0 e^{iz^0(\bar{q}^0-\bar{P}^0+P_X^0)}\Theta(-z^0) = \frac{-i}{P_X^0 + \bar{q}^0 - \bar{P}^0 - i\epsilon}, \tag{C.8}$$

where from now on we suppress the limit $\epsilon \to 0^+$. Putting Eqs. C.7 and C.8 into Eq. C.3, we get

$$\begin{aligned} T^{\mu\nu}(P,q;P',q') = \sum_X \Big[& \frac{\langle P'|j^\mu(0)|X(\mathbf{P}+\mathbf{q})\rangle\langle X(\mathbf{P}+\mathbf{q})|j^\nu(0)|P\rangle}{P_X^0 - (P^0+q^0) - i\epsilon} \\ & + \frac{\langle P'|j^\nu(0)|X(\mathbf{P}-\mathbf{q}')\rangle\langle X(\mathbf{P}-\mathbf{q}')|j^\mu(0)|P\rangle}{P_X^0 - (P^0-q'^0) - i\epsilon} \Big]. \end{aligned} \tag{C.9}$$

Therefore, we have discontinuities in our amplitude where the intermediate state goes on-shell: at $P_X^0 = P^0 + q^0$ or $P_X^0 = P^0 - q'^0$.

For the forward Compton tensor $\Delta = 0$, Eq. C.9 becomes

$$\begin{aligned} T^{\mu\nu}(P,q) = \sum_X \Big[& \frac{\langle P'|j^\mu(0)|X(\mathbf{P}+\mathbf{q})\rangle\langle X(\mathbf{P}+\mathbf{q})|j^\nu(0)|P\rangle}{P_X^0 - (P^0+q^0) - i\epsilon} \\ & + \frac{\langle P'|j^\nu(0)|X(\mathbf{P}-\mathbf{q})\rangle\langle X(\mathbf{P}-\mathbf{q})|j^\mu(0)|P\rangle}{P_X^0 - (P^0-q^0) - i\epsilon} \Big]. \end{aligned} \tag{C.10}$$

This gives that the discontinuities are at $|\omega| \geq 1$.

Appendix D

Light-Cone Coordinates

In this section, we show how to expand a set of momentum vectors, in a hadron's infinite momentum frame, in terms of the collinear light-cone vectors that appear throughout this thesis.

Given two lightlike vectors a^μ and $\bar{a}^\mu$ such that $a \cdot \bar{a} = 1$, we write any Lorentz vector as

$$k^\mu = (\bar{a} \cdot k)a^\mu + (a \cdot k)\bar{a}^\mu + k_\perp^\mu, \tag{D.1}$$

where $k_\perp \cdot a = 0 = k_\perp \cdot \bar{a}$. This is sometimes called the 'Sudakov decomposition'.

We will apply this to the case of off-forward scattering, where we choose a frame (the centre of mass frame) such that $a \cdot \bar{P} = 1$ and $\xi = -a \cdot \Delta/2$. Then, Eq. D.1 implies that

$$\bar{P}^\mu = \frac{M^2 - t/4}{2} a^\mu + \bar{a}^\mu, \tag{D.2a}$$

$$\Delta^\mu = (M^2 - t/4)\xi a^\mu - 2\xi\bar{a}^\mu + \Delta_\perp^\mu, \tag{D.2b}$$

$$\bar{q}^\mu = -\frac{1}{\bar{\omega}}\bar{a}^\mu + \frac{\bar{Q}^2\bar{\omega}}{2} a^\mu, \tag{D.2c}$$

where we have assumed that the transverse components of $\bar{P}$ and $\bar{q}$ are very small. Moreover, we only recover the usual Lorentz scalars from the above light-cone decomposition up to terms of order $M^2/\bar{Q}^2$ and $t/\bar{Q}^2$, which of course we take to be vanishingly small.

In the forward case, we have the same a and $\bar{a}$ but chosen so that $a \cdot P = 1$. Then,

$$P^\mu = \frac{M^2}{2} a^\mu + \bar{a}^\mu, \tag{D.3a}$$

$$q^\mu = -x\bar{a}^\mu + \frac{\bar{Q}^2}{2x} a^\mu, \tag{D.3b}$$

where x is the Bjorken variable.

Finally, for some vector k it is common to see the notation $k^+ = k \cdot a$ and $k^- = k \cdot \bar{a}$.

Appendix E

Electromagnetic Form Factors

Throughout this thesis, we discuss electromagnetic (EM) form factors. Like parton distribution functions, these are some of the most important hadronic observables, and are related to GPDs by Eq. 4.24.

EM form factors parameterise *elastic* electron-nucleon scattering: $e^-(k) + N(P) \to e^-(k') + N(P')$. See figure E. The scattering matrix of this process is given by

$$i\mathcal{M}(e^-N \to e^-N) = \bar{u}(k')\gamma_\mu u(k)\langle P'|j^\mu(0)|P\rangle, \tag{E.1}$$

where, as in all previous chapters, j^μ is the hadronic current:

$$j^\mu(z) = \sum_f e_f^2 \bar{\psi}_f(z)\gamma^\mu\psi_f(z).$$

We denote $Q^2 = (P' - P)^2$. Note that, by the Minkowski triangle inequality, we can show that q is a spacelike vector.

Therefore, the matrix element can be expanded

$$\langle P'|j^\mu(0)|P\rangle = \bar{u}(P')\left[\gamma^\mu F_1(Q^2) + \frac{i\sigma^{\mu\nu}\Delta_\nu}{2M}F_2(Q^2)\right]u(P). \tag{E.2}$$

The Lorentz scalar functions F_1 and F_2 are the EM form factors of the nucleon, known as the Pauli and Dirac form factors, respectively. They are non-perturbative quantities, and therefore can only be measured from experiment or calculated from first principles on the lattice.

In the GPD-form factor comparison (Eq. 4.24), the momentum transfer denoted Q^2 here is actually the soft momentum transfer in GPDs: $Q^2 = t$.

Non-relativistically, form factors have been interpreted as the three-dimensional Fourier transforms of charge and magnetisation distributions. However, a more correct interpretation [174] is that the Pauli and Dirac form factors are *two-dimensional* Fourier transforms of the charge and magnetisation densities, respectively, in the infinite momentum frame:

$$\rho_E(\mathbf{b}) = \int_0^\infty \frac{d|Q|}{2\pi}|Q|J_0(|Q||\mathbf{b}|)F_1(Q^2) \tag{E.3a}$$

$$\rho_M(\mathbf{b}) = |\mathbf{b}|\sin^2(\phi)\int_0^\infty \frac{d|Q|}{2\pi}Q^2J_1(|Q||\mathbf{b}|)F_2(Q^2), \tag{E.3b}$$

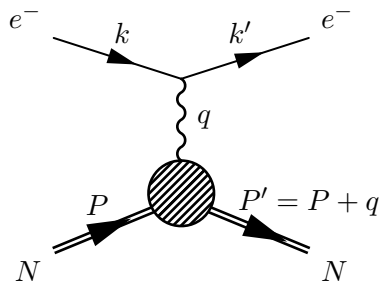

Figure E.1: The Feynman diagram for elastic electron-nucleon scattering.

where $J_{0,1}$ are the cylindrical Bessel functions of the first and second kind, **b** is the impact parameter and ϕ is the angle between the polarisation and the impact parameter. The formalism used to derive this relation is the same as the one used in section 4.2 when discussing the interpretation of GPDs as the Fourier transform of spatial distributions of quarks.

Three- and Four-Point Functions (Ch. 5)

In this appendix, we derive the form of three- and four-point functions necessary for the Feynman-Hellmann calculation in chapter 5.

Three-Point Function

Note that for a complete set of states $\{|X(\mathbf{p})\rangle\}$, we have that

$$\mathbb{I} = \sum_X \int \frac{d^3p}{(2\pi)^3} \frac{1}{2E_X(\mathbf{p})} |X(\mathbf{p})\rangle\langle X(\mathbf{p})|. \tag{F.1}$$

Therefore, for three translationally invariant operators, we define the three-point correlator

$$\begin{aligned} C^{(3)}_{\mathcal{O}_1\mathcal{O}_2\mathcal{O}_3}(x_1, x_2, x_3) \equiv & \langle\Omega|\mathcal{O}_1(x_1)\mathcal{O}_2(x_2)\mathcal{O}_3(x_3)|\Omega\rangle \\ = & \sum_{X,Y} \int \frac{d^3p_1}{(2\pi)^3} \frac{d^3p_2}{(2\pi)^3} \frac{1}{4E_X(\mathbf{p}_1)E_Y(\mathbf{p}_2)} \\ & \langle\Omega|\mathcal{O}_1(x_1)|X(\mathbf{p}_1)\rangle\langle X(\mathbf{p}_1)|\mathcal{O}_2(x_2)|Y(\mathbf{p}_2)\rangle\langle Y(\mathbf{p}_2|\mathcal{O}_3(x_3)|\Omega\rangle, \end{aligned} \tag{F.2}$$

where we have made the vacuum states explicit. Then, using translational invariance Eq. F.2 becomes

$$\begin{aligned} & C^{(3)}_{\mathcal{O}_1\mathcal{O}_2\mathcal{O}_3}(x_1, x_2, x_3) \\ & = \sum_{X,Y} \int \frac{d^3p_1}{(2\pi)^3} \frac{d^3p_2}{(2\pi)^3} \frac{1}{4E_X(\mathbf{p}_1)E_Y(\mathbf{p}_2)} \\ & \times e^{-E_X(\mathbf{p}_1)\tau_1 + i\mathbf{p}_1\cdot\mathbf{x_1}} e^{(E_X(\mathbf{p}_1) - E_Y(\mathbf{p}_2))\tau_2 - i(\mathbf{p}_1 - \mathbf{p}_2)\cdot\mathbf{x_2}} e^{E_Y(\mathbf{p}_2)\tau_3 - i\mathbf{p}_2\cdot\mathbf{x_3}} \\ & \times \langle\Omega|\mathcal{O}_1(0)|X(\mathbf{p}_1)\rangle\langle X(\mathbf{p}_1)|\mathcal{O}_2(0)|Y(\mathbf{p}_2)\rangle\langle Y(\mathbf{p}_2)|\mathcal{O}_3(0)|\Omega\rangle \\ & = \sum_{X,Y} \sum_{\mathbf{p}_1,\mathbf{p}_2} \frac{\Delta^3p_1}{(2\pi)^3} \frac{\Delta^3p_2}{(2\pi)^3} \frac{e^{-E_X(\mathbf{p}_1)(\tau_1 - \tau_2)}}{2E_X(\mathbf{p}_1)} \frac{e^{-E_Y(\mathbf{p}_2)(\tau_2 - \tau_3)}}{2E_Y(\mathbf{p}_2)} e^{i\mathbf{p}_1\cdot(\mathbf{x}_1 - \mathbf{x}_2)} e^{i\mathbf{p}_2\cdot(\mathbf{x}_2 - \mathbf{x}_3)} \\ & \times \langle\Omega|\mathcal{O}_1(0)|X(\mathbf{p}_1)\rangle\langle X(\mathbf{p}_1)|\mathcal{O}_2(0)|Y(\mathbf{p}_2)\rangle\langle Y(\mathbf{p}_2)|\mathcal{O}_3(0)|\Omega\rangle. \end{aligned} \tag{F.3}$$

The Fourier-projected three-point function is defined as

$$C^{(3)}_{\mathcal{O}_1\mathcal{O}_2\mathcal{O}_3}(\mathbf{p}_1,\mathbf{p}_2;\tau_1,\tau_2,\tau_3) \equiv \int d^3x_1 d^3x_2 e^{-i\mathbf{p}_1\cdot(\mathbf{x}_1-\mathbf{x}_2)} e^{-i\mathbf{p}_2\cdot(\mathbf{x}_2-\mathbf{x}_3)} C^{(3)}_{\mathcal{O}_1\mathcal{O}_2\mathcal{O}_3}(x_1,x_2,x_3). \tag{F.4}$$

Using the delta definition and Eq. F.3, this becomes

$$\begin{aligned} C^{(3)}_{\mathcal{O}_1\mathcal{O}_2\mathcal{O}_3}(\mathbf{p}_1,\mathbf{p}_2;\tau_1,\tau_2,\tau_3) = \sum_{X,Y} &\frac{e^{-E_X(\mathbf{p}_1)(\tau_1-\tau_2)}}{2E_X(\mathbf{p}_1)} \frac{e^{-E_Y(\mathbf{p}_2)(\tau_2-\tau_3)}}{2E_Y(\mathbf{p}_2)} \\ &\times \langle\Omega|\mathcal{O}_1(0)|X(\mathbf{p}_1)\rangle\langle X(\mathbf{p}_1)|\mathcal{O}_2(0)|Y(\mathbf{p}_2)\rangle\langle Y(\mathbf{p}_2)|\mathcal{O}_3(0)|\Omega\rangle. \end{aligned} \tag{F.5}$$

Four-Point Function

As before, we can simplify our working by introducing the general four-point function of four translationally invariant operators:

$$\begin{aligned} &C^{(4)}_{\mathcal{O}_1\mathcal{O}_2\mathcal{O}_3\mathcal{O}_4}(x_1,x_2,x_3,x_4) \equiv \langle\Omega|\mathcal{O}_1(x_1)\mathcal{O}_2(x_2)\mathcal{O}_3(x_3)\mathcal{O}_4(x_4)|\Omega\rangle \\ &= \sum_{X,Y,Z} \int \frac{d^3p_1}{(2\pi)^3}\frac{d^3p_2}{(2\pi)^3}\frac{d^3p_3}{(2\pi)^3} \frac{1}{8E_X(\mathbf{p}_1)E_Y(\mathbf{p}_2)E_Z(\mathbf{p}_3)} \\ &\times \langle\Omega|\mathcal{O}_1(x_1)|X(\mathbf{p}_1)\rangle\langle X(\mathbf{p}_1)|\mathcal{O}_2(x_2)|Y(\mathbf{p}_2)\rangle\langle Y(\mathbf{p}_2)|\mathcal{O}_3(x_3)|Z(\mathbf{p}_3)\rangle\langle Z(\mathbf{p}_3)|\mathcal{O}_4(x_4)|\Omega\rangle, \end{aligned} \tag{F.6}$$

Then, using translational invariance Eq. F.6 becomes

$$\begin{aligned} &C^{(4)}_{\mathcal{O}_1\mathcal{O}_2\mathcal{O}_3\mathcal{O}_4}(x_1,x_2,x_3,x_4) \\ &= \sum_{X,Y,Z} \int \frac{d^3p_1}{(2\pi)^3}\frac{d^3p_2}{(2\pi)^3}\frac{d^3p_3}{(2\pi)^3} \frac{1}{8E_X(\mathbf{p}_1)E_Y(\mathbf{p}_2)E_Z(\mathbf{p}_3)} \\ &\times e^{-E_X(\mathbf{p}_1)\tau_1 + i\mathbf{p}_1\cdot\mathbf{x_1}} e^{(E_X(\mathbf{p}_1)-E_Y(\mathbf{p}_2))\tau_2 - i(\mathbf{p}_1-\mathbf{p}_2)\cdot\mathbf{x_2}} e^{(E_Y(\mathbf{p}_2)-E_Z(\mathbf{p}_3))\tau_3 - i(\mathbf{p}_2-\mathbf{p}_3)\cdot\mathbf{x_3}} e^{E_Z(\mathbf{p}_3)\tau_4 - i\mathbf{p}_3\cdot\mathbf{x_4}} \\ &\times \langle\Omega|\mathcal{O}_1(0)|X(\mathbf{p}_1)\rangle\langle X(\mathbf{p}_1)|\mathcal{O}_2(0)|Y(\mathbf{p}_2)\rangle\langle Y(\mathbf{p}_2)|\mathcal{O}_3(0)|Z(\mathbf{p}_3)\rangle\langle Z(\mathbf{p}_3)|\mathcal{O}_4(0)|\Omega\rangle \\ &= \sum_{X,Y,Z} \int \frac{d^3p_1}{(2\pi)^3}\frac{d^3p_2}{(2\pi)^3}\frac{d^3p_3}{(2\pi)^3} \frac{e^{-E_X(\mathbf{p}_1)(\tau_1-\tau_2)}}{2E_X(\mathbf{p}_1)} \frac{e^{-E_Y(\mathbf{p}_2)(\tau_2-\tau_3)}}{2E_Y(\mathbf{p}_2)} \frac{e^{-E_Z(\mathbf{p}_3)(\tau_3-\tau_4)}}{2E_Z(\mathbf{p}_3)} \\ &\times e^{i\mathbf{p}_1\cdot(\mathbf{x}_1-\mathbf{x}_2)} e^{i\mathbf{p}_2\cdot(\mathbf{x}_2-\mathbf{x}_3)} e^{i\mathbf{p}_3\cdot(\mathbf{x}_3-\mathbf{x}_4)} \\ &\times \langle\Omega|\mathcal{O}_1(0)|X(\mathbf{p}_1)\rangle\langle X(\mathbf{p}_1)|\mathcal{O}_2(0)|Y(\mathbf{p}_2)\rangle\langle Y(\mathbf{p}_2)|\mathcal{O}_3(0)|Z(\mathbf{p}_3)\rangle\langle Z(\mathbf{p}_3)|\mathcal{O}_4(0)|\Omega\rangle. \end{aligned} \tag{F.7}$$

The Fourier-projected four-point function is defined as

$$\begin{aligned} &G^{(4)}_{\mathcal{O}_1\mathcal{O}_2\mathcal{O}_3\mathcal{O}_4}(\mathbf{p}_1,\mathbf{p}_2,\mathbf{p}_3;\tau_1,\tau_2,\tau_3,\tau_4) \equiv \\ &\int d^3x_1 d^3x_2 d^3x_3 e^{-i\mathbf{p}_1\cdot(\mathbf{x}_1-\mathbf{x}_2)} e^{-i\mathbf{p}_2\cdot(\mathbf{x}_2-\mathbf{x}_3)} e^{-i\mathbf{p}_3\cdot(\mathbf{x}_3-\mathbf{x}_4)} C^{(4)}_{\mathcal{O}_1\mathcal{O}_2\mathcal{O}_3\mathcal{O}_4}(x_1,x_2,x_3,x_4). \end{aligned} \tag{F.8}$$

Using the delta function and Eq. F.7, Eq. F.8 becomes

$$
\begin{aligned}
&G^{(4)}_{\mathcal{O}_1\mathcal{O}_2\mathcal{O}_3\mathcal{O}_4}(\mathbf{p}_1,\mathbf{p}_2,\mathbf{p}_3;\tau_1,\tau_2,\tau_3,\tau_4) \\
&= \sum_{X,Y,Z} \frac{e^{-E_X(\mathbf{p}_1)(\tau_1-\tau_2)}}{2E_X(\mathbf{p}_1)} \frac{e^{-E_Y(\mathbf{p}_2)(\tau_2-\tau_3)}}{2E_Y(\mathbf{p}_2)} \frac{e^{-E_Z(\mathbf{p}_3)(\tau_3-\tau_4)}}{2E_Z(\mathbf{p}_3)} \\
&\times \langle\Omega|\mathcal{O}_1(0)|X(\mathbf{p}_1)\rangle\langle X(\mathbf{p}_1)|\mathcal{O}_2(0)|Y(\mathbf{p}_2)\rangle\langle Y(\mathbf{p}_2)|\mathcal{O}_3(0)|Z(\mathbf{p}_3)\rangle\langle Z(\mathbf{p}_3)|\mathcal{O}_4(0)|\Omega\rangle.
\end{aligned}
\tag{F.9}
$$

Details of Off-Forward OPE (Ch. 6)

Here, we give the details of the Fourier transform of the coordinate space OPE from chapter 6.

To begin, we insert our coordinate space matrix element (Eq. 6.41) into the off-forward Compton tensor (OFCT),

$$T^{\mu\nu} = i \int d^4z e^{i\bar{q}\cdot z} \langle P'|T\big[j^\mu(z/2)j^\nu(-z/2)\big]|P\rangle.$$

This gives us

$$\begin{aligned} T_{\mu\nu} = &-2i \int d^4z e^{i\bar{q}\cdot z} \sum_f e_f^2 S^\rho(z) \mathcal{S}_{\mu\rho\nu\kappa} \sum_{n=1,3,5}^{\infty} \frac{(-i)^n}{n!} \\ &\times \sum_{j=0,2,4}^{n} \Big\{ \frac{1}{n+1}(\Delta\cdot z)^j(\bar{P}\cdot z)^{n-j}\big[\tau_1^\kappa A^f_{n+1,j}(t) + \tau_2^\kappa B^f_{n+1,j}(t)\big] \\ &+ \frac{n-j}{n+1}(\Delta\cdot z)^j(\bar{P}\cdot z)^{n-j-1}\bar{P}^\kappa\big[A^f_{n+1,j}(t)\tau_1\cdot z + B^f_{n+1,j}(t)\tau_2\cdot z\big] \\ &+ \frac{j}{n+1}(\Delta\cdot z)^{j-1}(\bar{P}\cdot z)^{n-j}\Delta^\kappa\big[A^f_{n+1,j}(t)\tau_1\cdot z + B^f_{n+1,j}(t)\tau_2\cdot z\big] \\ &+ \Delta^\kappa\delta_{j,0}(\Delta\cdot z)^n C^f_{n+1}(t)\frac{1}{M}\overline{u}(P')u(P)\Big\}. \end{aligned} \tag{G.1}$$

Now, as in the forward case, we introduce Fourier conjugate variables, this time using four Fourier conjugates:

$$(\bar{P}\cdot z)^n = i^n \int_{-\infty}^{\infty} d\chi e^{i\chi\bar{P}\cdot z}\frac{\partial^n}{\partial\chi^n}\delta(\chi), \tag{G.2a}$$

$$(\Delta\cdot z)^n = i^n \int_{-\infty}^{\infty} d\eta e^{i\eta\Delta\cdot z}\frac{\partial^n}{\partial\eta^n}\delta(\eta), \tag{G.2b}$$

$$\tau_m\cdot z = i\int_{-\infty}^{\infty} d\tilde{\chi}_m e^{i\tilde{\chi}_m\tau_m\cdot z}\frac{\partial}{\partial\tilde{\chi}_m}\delta(\tilde{\chi}_m), \quad m=1,2, \text{ with indices not summed.} \tag{G.2c}$$

So Eq. G.1 becomes

$$\begin{aligned}
T_{\mu\nu} = &-2i\sum_f e_f^2 \mathcal{S}_{\mu\rho\nu\kappa} \sum_{n=1,3,5}^{\infty} \frac{(-i)^n i^n}{n!} \Bigg\{ \sum_{j=0,2,4}^{n} \Bigg[\frac{1}{n+1} [\tau_1^\kappa A^f_{n+1,j}(t) + \tau_2^\kappa B^f_{n+1,j}(t)] \\
&\times \int d\eta e^{i\eta\Delta\cdot z} \frac{\partial^j}{\partial\eta^j}\delta(\eta) \int d\chi e^{i\chi\bar{P}\cdot z} \frac{\partial^{n-j}}{\partial\chi^{n-j}}\delta(\chi) \\
&+ \frac{n-j}{n+1}\bar{P}^\kappa \big[A^f_{n+1,j}(t) \int d\tilde{\chi}_1 e^{i\tilde{\chi}_1\tau_1\cdot z} \frac{\partial}{\partial\tilde{\chi}_1}\delta(\tilde{\chi}_1) + B^f_{n+1,j}(t) \int d\tilde{\chi}_2 e^{i\tilde{\chi}_2\tau_2\cdot z} \frac{\partial}{\partial\tilde{\chi}_2}\delta(\tilde{\chi}_2) \big] \\
&\times \int d\eta e^{i\eta\Delta\cdot z} \frac{\partial^j}{\partial\eta^j}\delta(\eta) \int d\chi e^{i\chi\bar{P}\cdot z} \frac{\partial^{n-j-1}}{\partial\chi^{n-j-1}}\delta(\chi) \\
&+ \frac{j}{n+1}\Delta^\kappa \big[A^f_{n+1,j}(t) \int d\tilde{\chi}_1 e^{i\tilde{\chi}_1\tau_1\cdot z} \frac{\partial}{\partial\tilde{\chi}_1}\delta(\tilde{\chi}_1) + B^f_{n+1,j}(t) \int d\tilde{\chi}_2 e^{i\tilde{\chi}_2\tau_2\cdot z} \frac{\partial}{\partial\tilde{\chi}_2}\delta(\tilde{\chi}_2) \big] \\
&\times \int d\eta e^{i\eta\Delta\cdot z} \frac{\partial^{j-1}}{\partial\eta^{j-1}}\delta(\eta) \int d\chi e^{i\chi\bar{P}\cdot z} \frac{\partial^{n-j}}{\partial\chi^{n-j}}\delta(\chi) \Bigg] \\
&+ \Delta^\kappa C^f_{n+1}(t) \frac{1}{M}\overline{u}(P')u(P) \int d\eta e^{i\eta\Delta\cdot z} \frac{\partial^n}{\partial\eta^n}\delta(\eta) \Bigg\} \int d^4z e^{i\bar{q}\cdot z} S^\rho(z).
\end{aligned} \tag{G.3}$$

Pulling all the exponentials through to the propagator terms we have

$$\int d^4z e^{i(\bar{q}+\eta\Delta)\cdot z} S^\rho(z) = \frac{i(\bar{q}^\rho + \eta\Delta^\rho)}{(\bar{q}+\eta\Delta)^2}, \tag{G.4}$$

$$\int d^4z e^{i(\bar{q}+\chi\bar{P}+\eta\Delta)\cdot z} S^\rho(z) = \frac{i(\bar{q}^\rho + \chi\bar{P}^\rho + \eta\Delta^\rho)}{(\bar{q}+\chi\bar{P}+\eta\Delta)^2}, \tag{G.5}$$

$$\int d^4z e^{i(\bar{q}+\chi\bar{P}+\eta\Delta+\tilde{\chi}_m\tau_m)\cdot z} S^\rho(z) = \frac{i(\bar{q}^\rho + \chi\bar{P}^\rho + \eta\Delta^\rho + \tilde{\chi}_m\tau_m^\rho)}{(\bar{q}+\chi\bar{P}+\eta\Delta+\tilde{\chi}_m\tau_m)^2}, \tag{G.6}$$

where $\tilde{\omega}_m = 2\tau_m\cdot\bar{q}/\bar{Q}^2$, and again the m indices are not summed. Physically, it is useful to think of χ, $\tilde{\chi}_i$ as the longitudinal momentum fractions, and η as the transverse momentum fraction.

Now, using the identity Eq. 3.60

$$\int_a^b dx \mathcal{F}(x) \frac{\partial^n}{\partial x^n}\delta(x-y) = (-1)^n \frac{\partial^n}{\partial x^n}\mathcal{F}(x)\Big|_{x=y},$$

we can evaluate all the terms in Eq. G.3. First, using Eq. G.4,

$$\begin{aligned}
&\int d\eta \frac{\partial^n}{\partial\eta^n}\delta(\eta) \int d^4z e^{i(\bar{q}+\eta\Delta)\cdot z} S^\rho(z) = (-1)^n \frac{\partial^n}{\partial\eta^n} \frac{i(\bar{q}^\rho+\eta\Delta^\rho)}{(\bar{q}+\eta\Delta)^2}\Big|_{\eta=0} \\
&= -\frac{i}{\bar{Q}^2}(-1)^n \sum_{k=0}^{\infty} (\bar{q}^\rho \delta_{k,n} k! + \Delta^\rho \delta_{k+1,n}(k+1)!)(-2\xi\bar{\omega})^k \\
&= \frac{i}{\bar{Q}^2} n!((-2\xi)\bar{\omega}\bar{q}^\rho + \Delta^\rho)(-2\xi\bar{\omega})^{n-1},
\end{aligned} \tag{G.7}$$

where we can Taylor expand around $\eta = 0$, since this is where the derivative is taken.

It pays to do the integral with Eq. G.5 more carefully. First, since we will end up evaluating $\chi = \eta = 0$, we can take these variables arbitrarily small and expand the propagator as a Taylor series in them around zero:

$$\begin{aligned}
&\int d\chi \frac{\partial^{n-j}}{\partial\chi^{n-j}}\delta(\chi)\int d\eta\frac{\partial^j}{\partial\eta^j}\delta(\eta)\int d^4z e^{i(\bar{q}+\chi\bar{P}+\eta\Delta)\cdot z}S^\rho(z)\\
&=\int d\chi \frac{\partial^{n-j}}{\partial\chi^{n-j}}\delta(\chi)\int d\eta\frac{\partial^j}{\partial\eta^j}\delta(\eta)\frac{i(\bar{q}^\rho+\chi\bar{P}^\rho+\eta\Delta^\rho)}{(\bar{q}+\chi\bar{P}+\eta\Delta)^2}\\
&=-\frac{i}{\bar{Q}^2}(-1)^n\frac{\partial^{n-j}}{\partial\chi^{n-j}}\frac{\partial^j}{\partial\eta^j}\sum_{k=0}^{\infty}\sum_{l=0}^{k}\frac{k!}{(k-l)!l!}(\chi\bar{\omega})^{k-l}(\eta(-2\xi\bar{\omega}))^l[\bar{q}^\rho+\chi\bar{P}^\rho+\eta\Delta^\rho]\Big|_{\chi=\eta=0}\\
&=\frac{i}{\bar{Q}^2}\sum_{k=0}^{\infty}\sum_{l=0}^{k}\frac{k!}{(k-l)!l!}\bar{\omega}^{k-l}(-2\xi\bar{\omega})^l\Big[\delta_{l,j}\delta_{k-l,n-j}l!(k-l)!\bar{q}^\rho\\
&+\delta_{l,j}\delta_{k-l+1,n-j}l!(k-l+1)!\bar{P}^\rho+\delta_{l+1,j}\delta_{k-l,n-l}(l+1)!(k-l)!\Delta^\rho\Big]\\
&=\frac{i}{\bar{Q}^2}\bar{\omega}^{n-1}(-2\xi)^{j-1}n!\Big[\bar{\omega}(-2\xi)\bar{q}^\rho+\frac{n-j}{n}(-2\xi)\bar{P}^\rho+\frac{j}{n}\Delta^\rho\Big].
\end{aligned}\tag{G.8}$$

For the largest propagator Eq. G.6,

$$\begin{aligned}
&\int d\tilde{\chi}_m\frac{\partial}{\partial\tilde{\chi}_m}\delta(\tilde{\chi}_m)\int d\chi\frac{\partial^J}{\partial\chi^J}\delta(\chi)\int d\eta\frac{\partial^K}{\partial\eta^K}\delta(\eta)\int d^4z e^{i(\bar{q}+\chi\bar{P}+\eta\Delta+\tilde{\chi}_m\tau_m)\cdot z}S^\rho(z)\\
&=\int d\tilde{\chi}_m\frac{\partial}{\partial\tilde{\chi}_m}\delta(\tilde{\chi}_m)\int d\chi\frac{\partial^J}{\partial\chi^J}\delta(\chi)\int d\eta\frac{\partial^K}{\partial\eta^K}\delta(\eta)\frac{i(\bar{q}^\rho+\chi\bar{P}^\rho+\eta\Delta^\rho+\tilde{\chi}_m\tau_m^\rho)}{(\bar{q}+\chi\bar{P}+\eta\Delta+\tilde{\chi}_m\tau_m)^2}\\
&=-\frac{i}{\bar{Q}^2}\int d\tilde{\chi}_m\frac{\partial}{\partial\tilde{\chi}_m}\delta(\tilde{\chi}_m)\int d\chi\frac{\partial^J}{\partial\chi^J}\delta(\chi)\int d\eta\frac{\partial^K}{\partial\eta^K}\delta(\eta)\\
&\times(\bar{q}^\rho+\chi\bar{P}^\rho+\eta\Delta^\rho+\tilde{\chi}_m\tau_m^\rho)\sum_{k=0}^{\infty}(\chi\bar{\omega}-2\eta\xi\bar{\omega}+\tilde{\chi}_m\tilde{\omega}_m)^k.
\end{aligned}\tag{G.9}$$

Then, using the trinomial theorem*, we get

$$\begin{aligned}
&\int d\tilde{\chi}_m \frac{\partial}{\partial\tilde{\chi}_m}\delta(\tilde{\chi}_m)\int d\chi\frac{\partial^J}{\partial\chi^J}\delta(\chi)\int d\eta\frac{\partial^K}{\partial\eta^K}\delta(\eta)\int d^4z e^{i(\bar{q}+\chi\bar{P}+\eta\Delta+\tilde{\chi}_m\tau_m)\cdot z}S^\rho(z)\\
&=-\frac{i}{\bar{Q}^2}(-1)^n\frac{\partial}{\partial\tilde{\chi}_m}\frac{\partial^J}{\partial\chi^J}\frac{\partial^K}{\partial\eta^K}\\
&\times\sum_{k=0}^{\infty}\sum_{\substack{j,l,m\\ j+l+m=k}}^{k}\frac{k!}{j!l!m!}(\chi\bar{\omega})^j(-2\eta\xi\bar{\omega})^l(\tilde{\chi}_m\tilde{\omega}_m)^m[\bar{q}^\rho+\chi\bar{P}^\rho+\eta\Delta^\rho+\tilde{\chi}_m\tau_m^\rho]\Big|_{\chi=\eta=\tilde{\chi}_m=0}\\
&=\frac{i}{\bar{Q}^2}\sum_{k=0}^{\infty}\sum_{\substack{j,l,m\\ j+l+m=k}}^{k}\frac{k!}{j!l!m!}\bar{\omega}^j(-2\xi\bar{\omega})^l\tilde{\omega}_m^m[\delta_{m,1}\delta_{J,j}\delta_{K,l}j!l!\bar{q}^\rho+\delta_{m,1}\delta_{J,j+1}\delta_{K,l}(j+1)!l!\bar{P}^\rho\\
&+\delta_{m,1}\delta_{J,j}\delta_{K,l+1}j!(l+1)!\Delta^\rho+\delta_{m,0}\delta_{J,j}\delta_{K,l}j!l!\tau_m^\rho]\\
&=\frac{i}{\bar{Q}^2}(J+K+1)!\bar{\omega}^{J-1}(-2\xi\bar{\omega})^{K-1}\Big[\bar{\omega}(-2\xi\bar{\omega})\tilde{\omega}_m\bar{q}^\rho+\frac{J}{J+K+1}(-2\xi\bar{\omega})\tilde{\omega}_m\bar{P}^\rho\\
&+\frac{K}{J+K+1}\bar{\omega}\tilde{\omega}_m\Delta^\rho+\frac{1}{J+K+1}\bar{\omega}(-2\xi\bar{\omega})\tau_m^\rho\Big].
\end{aligned}\tag{G.10}$$

Noting that $J+K+1=n$ for both cases, Eq. G.10 becomes

$$=\frac{i}{\bar{Q}^2}n!\bar{\omega}^{J-1}(-2\xi\bar{\omega})^{K-1}\Big[\bar{\omega}(-2\xi\bar{\omega})\tilde{\omega}_m\bar{q}^\rho+\frac{J}{n}(-2\xi\bar{\omega})\tilde{\omega}_m\bar{P}^\rho+\frac{K}{n}\bar{\omega}\tilde{\omega}_m\Delta^\rho+\frac{1}{n}\bar{\omega}(-2\xi\bar{\omega})\tau_m^\rho\Big].\tag{G.11}$$

*The trinomial theorem is a straightforward extension of the binomial theorem: $(a+b+c)^n=\sum_{\substack{i,j,k\\ i+j+k=n}}\frac{(i+j+k)!}{i!j!k!}a^ib^jc^k$.

Putting Eq. G.7-G.11 into Eq. G.3, we get

$$
\begin{aligned}
T_{\mu\nu} =& \frac{2}{\bar{Q}^2}\sum_f e_f^2 \mathcal{S}_{\mu\rho\nu\kappa}\Bigg\{\sum_{n=1,3,5}^{\infty}\sum_{j=0,2,4}^{n}\Bigg[\frac{1}{n+1}[\tau_1^\kappa A^f_{n+1,j}(t)+\tau_2^\kappa B^f_{n+1,j}(t)]\bar{\omega}^{n-1}(-2\xi)^{j-1}\\
&\times\Big[\bar{\omega}(-2\xi)\bar{q}^\rho+\frac{n-j}{n}(-2\xi)\bar{P}^\rho+\frac{j}{n}\Delta^\rho\Big]+\frac{n-j}{n+1}\bar{\omega}^{n-2}(-2\xi)^{j-1}\bar{P}^\kappa\Bigg[A^f_{n+1,j}(t)\\
&\times\Big(\bar{\omega}(-2\xi)\tilde{\omega}_1\bar{q}^\rho+\frac{n-j-1}{n}(-2\xi)\tilde{\omega}_1\bar{P}^\rho+\frac{j}{n}\tilde{\omega}_1\Delta^\rho+\frac{1}{n}\bar{\omega}(-2\xi)\tau_1^\rho\Big)\\
&+B^f_{n+1,j}(t)\Big(\bar{\omega}(-2\xi)\tilde{\omega}_2\bar{q}^\rho+\frac{n-j-1}{n}(-2\xi)\tilde{\omega}_2\bar{P}^\rho+\frac{j}{n}\tilde{\omega}_2\Delta^\rho+\frac{1}{n}\bar{\omega}(-2\xi)\tau_2^\rho\Big)\Bigg]\\
&+\frac{j}{n+1}\bar{\omega}^{n-2}(-2\xi)^{j-2}\Delta^\kappa\\
&\times\Bigg[A^f_{n+1,j}(t)\Big(\bar{\omega}(-2\xi)\tilde{\omega}_1\bar{q}^\rho+\frac{n-j}{n}(-2\xi)\tilde{\omega}_1\bar{P}^\rho+\frac{j-1}{n}\tilde{\omega}_1\Delta^\rho+\frac{1}{n}\bar{\omega}(-2\xi)\tau_1^\rho\Big)\\
&+B^f_{n+1,j}(t)\Big(\bar{\omega}(-2\xi)\tilde{\omega}_2\bar{q}^\rho+\frac{n-j}{n}(-2\xi)\tilde{\omega}_2\bar{P}^\rho+\frac{j-1}{n}\tilde{\omega}_2\Delta^\rho+\frac{1}{n}\bar{\omega}(-2\xi)\tau_2^\rho\Big)\Bigg]\Bigg]\\
&+(-2\xi\bar{\omega})^{n-1}\Delta^\kappa C^f_{n+1}(t)\frac{1}{M}\overline{u}(P')u(P)\Big((-2\xi)\bar{\omega}\bar{q}^\rho+\Delta^\rho\Big)\Bigg\}.
\end{aligned}
\tag{G.12}
$$

After expanding $\mathcal{S}_{\mu\rho\nu\kappa}=g_{\mu\rho}g_{\nu\kappa}+g_{\mu\kappa}g_{\nu\rho}-g_{\mu\nu}g_{\rho\kappa}$ (ignoring terms of the order $M^2/\bar{Q}^2$ and $t/\bar{Q}^2$ as usual) and collecting like terms, we have

$$
\begin{aligned}
T^{\mu\nu} =& \sum_f e_f^2\sum_{n=1,3,5}^{\infty}\sum_{j=0,2,4}^{n}\Bigg\{\frac{4}{\bar{Q}^2}\frac{1}{n+1}\bar{\omega}^{n-1}(-2\xi)^{j-1}[\tau_1^{\{\mu}A^f_{n+1,j}(t)+\tau_2^{\{\mu}B^f_{n+1,j}(t)]\\
&\times\Big[\bar{\omega}(-2\xi)\bar{q}^{\nu\}}+\frac{2(n-j)}{n}(-2\xi)\bar{P}^{\nu\}}+\frac{2j}{n}\Delta^{\nu\}}\Big]\\
&+\frac{4}{\bar{Q}^2}\frac{1}{n+1}\bar{\omega}^{n-2}(-2\xi)^{j-2}[A^f_{n+1,j}(t)\tilde{\omega}_1+B^f_{n+1,j}(t)\tilde{\omega}_2]\\
&\times\Big((n-j)\bar{\omega}(-2\xi)^2\bar{P}^{\{\mu}\bar{q}^{\nu\}}+\frac{2(n-j)j}{n}(-2\xi)\bar{P}^{\{\mu}\Delta^{\nu\}}+j\bar{\omega}(-2\xi)\Delta^{\{\mu}\bar{q}^{\nu\}}\\
&+\frac{j(j-1)}{n}\Delta^\mu\Delta^\nu+\frac{(n-j)(n-j-1)}{n}\bar{\omega}(-2\xi)^2\bar{P}^\mu\bar{P}^\nu\Big)\\
&+2\delta_{j,0}\bar{\omega}^{n-2}(-2\xi)^{n-1}C^f_{n+1}(t)(\tilde{\omega}_1-\tilde{\omega}_2)\Big((-2\xi)\bar{\omega}\Delta^{\{\mu}\bar{q}^{\nu\}}+\Delta^\mu\Delta^\nu\Big)\\
&-g^{\mu\nu}\bar{\omega}^{n+1}\Big((-2\xi)^j[A^f_{n+1,j}(t)\frac{\tilde{\omega}_1}{\bar{\omega}}+B^f_{n+1,j}(t)\frac{\tilde{\omega}_2}{\bar{\omega}}]\\
&+\delta_{j,0}(-2\xi)^{n+1}C^f_{n+1}(t)(\frac{\tilde{\omega}_1}{\bar{\omega}}-\frac{\tilde{\omega}_2}{\bar{\omega}})\Big)\Bigg\}.
\end{aligned}
\tag{G.13}
$$

Finally, shifting the indices of Eq. G.13, we get

$$
\begin{aligned}
T^{\mu\nu} = \sum_f e_f^2 \sum_{n=2,4,6}^{\infty} \sum_{j=0,2,4}^{n-1} \Bigg\{ & \frac{4}{\bar{Q}^2} \frac{1}{n} \bar{\omega}^{n-2} (-2\xi)^{j-1} [\tau_1^{\{\mu} A_{n,j}^f(t) + \tau_2^{\{\mu} B_{n,j}^f(t)] \\
& \times \Big[\bar{\omega}(-2\xi) \bar{q}^{\nu\}} + \frac{2(n-j-1)}{n-1} (-2\xi) \bar{P}^{\nu\}} + \frac{2j}{n-1} \Delta^{\nu\} } \Big] \\
& + \frac{4}{\bar{Q}^2} \frac{1}{n} \bar{\omega}^{n-3} (-2\xi)^{j-2} [A_{n,j}^f(t) \tilde{\omega}_1 + B_{n,j}^f(t) \tilde{\omega}_2] \\
& \times \Big((n-j-1) \bar{\omega} (-2\xi)^2 \bar{P}^{\{\mu} \bar{q}^{\nu\}} + \frac{2(n-j-1)j}{n-1} (-2\xi) \bar{P}^{\{\mu} \Delta^{\nu\}} + j \bar{\omega} (-2\xi) \Delta^{\{\mu} \bar{q}^{\nu\}} \\
& + \frac{j(j-1)}{n-1} \Delta^\mu \Delta^\nu + \frac{(n-j-1)(n-j-2)}{n-1} \bar{\omega} (-2\xi)^2 \bar{P}^\mu \bar{P}^\nu \Big) \\
& + 2\delta_{j,0} \bar{\omega}^{n-3} (-2\xi)^{n-2} C_n^f(t) (\tilde{\omega}_1 - \tilde{\omega}_2) \Big((-2\xi) \bar{\omega} \Delta^{\{\mu} \bar{q}^{\nu\}} + \Delta^\mu \Delta^\nu \Big) \\
& - g^{\mu\nu} \bar{\omega}^n \Big((-2\xi)^j [A_{n,j}^f(t) \frac{\tilde{\omega}_1}{\bar{\omega}} + B_{n,j}^f(t) \frac{\tilde{\omega}_2}{\bar{\omega}}] \\
& + \delta_{j,0} (-2\xi)^n C_n^f(t) (\frac{\tilde{\omega}_1}{\bar{\omega}} - \frac{\tilde{\omega}_2}{\bar{\omega}}) \Big) \Bigg\}.
\end{aligned}
\tag{G.14}
$$

Dirac Bilinears and Traces (Ch. 6)

In our lattice calculations, we project our the spin structure of the nucleon correlator with a projection matrix Γ:

$$c_{\chi\chi}(z,0) = \frac{1}{4}\sum_{\text{spins}} \Gamma_{\beta\alpha}\langle\Omega|\chi_\alpha(\mathbf{z},\tau)\chi^\dagger_\beta(0)|\Omega\rangle.$$

This projection is carried through the Feynman-Hellmann calculation, and hence our off-forward Compton tensor also has its spin structure projected out as above*.

Therefore, we define

$$\begin{aligned}\mathcal{F}(\Gamma_{\text{proj}},\Gamma_{\text{op}}) &\equiv \frac{1}{4}\sum_{s,s'}\big[\Gamma_{\text{proj}}\big]_{\beta\alpha}u_\alpha(P',s')\bar{u}_\gamma(P',s')\big[\Gamma_{\text{op}}\big]_{\gamma\delta}u_\delta(P,s)\bar{u}_\beta(P,s)\\ &= \frac{1}{4}\text{tr}\Big\{\Gamma_{\text{proj}}(\not{P}'+M)\Gamma_{\text{op}}(\not{P}+M)\Big\}.\end{aligned} \tag{H.1}$$

For our lattice calculation, we only use the unpolarised projector, which in Minkowski space is

$$\Gamma_{\text{unpol}} = \frac{1}{2}(\mathbb{I}+\gamma^0). \tag{H.2}$$

Note that this is using the Minkowski Clifford algebra.

$$\mathcal{F}(\Gamma_{\text{unpol}},\gamma^i) = \frac{1}{2}\Big(\big(E(\mathbf{p}')+M\big)\mathbf{p}_i + \big(E(\mathbf{p})+M\big)\mathbf{p}'_i\Big).$$

$$\mathcal{F}(\Gamma_{\text{unpol}},\frac{i\sigma^{ij}\boldsymbol{\Delta}_j}{2M}) = \frac{1}{4M}\epsilon_{ijk}\boldsymbol{\Delta}_j[\mathbf{p}\times\mathbf{p}']_k = \frac{1}{4M}\Big[\boldsymbol{\Delta}\times(\bar{\mathbf{p}}\times\boldsymbol{\Delta})\Big]_i.$$

In the frame of our lattice calculation, we have $E(\mathbf{p}') = E(\mathbf{p}) = E$, and $\bar{\mathbf{p}}\perp\boldsymbol{\Delta}$. Therefore, the above results become

$$\mathcal{F}(\Gamma_{\text{unpol}},\gamma^i) = (E+M)\bar{\mathbf{p}}_i.$$

$$\mathcal{F}(\Gamma_{\text{unpol}},\frac{i\sigma^{ij}\boldsymbol{\Delta}_j}{2M}) = \frac{1}{4M}\Big[\boldsymbol{\Delta}\times(\bar{\mathbf{p}}\times\boldsymbol{\Delta})\Big]_i = -\frac{t}{4M}\bar{\mathbf{p}}_i.$$

We have used the vector triple product identity, $\mathbf{a}\times(\mathbf{b}\times\mathbf{c}) = (\mathbf{a}\cdot\mathbf{c})\mathbf{b} - (\mathbf{a}\cdot\mathbf{b})\mathbf{c}$, in the last line above.

*Since the form of off-forward nucleon Dirac bilinears is so non-trivial [175], this projection tidies up a great deal of the unpleasant form of our nucleon OPE.

Hence, for their spatial components, the bilinears become

$$\tau_1^i \to (E+M)\bar{\mathbf{p}}_i, \quad \tau_2^i \to -\frac{t}{4M}\bar{\mathbf{p}}_i.$$

And in the frame of our lattice calculation, the $\tilde{\omega}_i$ terms become

$$\frac{2\bar{q}\cdot\tau_1}{\bar{Q}^2} \to (E+M)\bar{\omega}, \quad \frac{2\bar{q}\cdot\tau_2}{\bar{Q}^2} \to -\frac{t}{4M}\bar{\omega}.$$

Appendix I

Additional Lattice Results (Ch. 7)

In this appendix, we present the additional results of our lattice calculation. For the up quarks, these largely consist of different effective mass results. For the down quarks, this appendix includes all results except the down quark GFF towers, which were presented in chapter 7.

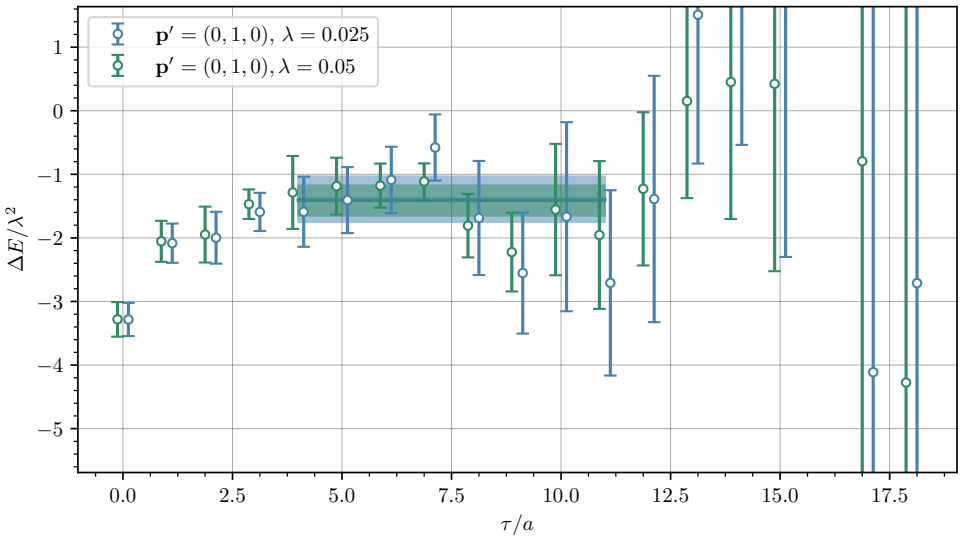

Figure I.1: Effective mass plot for the ratios $R(\mathbf{p})$, with the first set of correlators. Shaded bands are exponential fits to the energy shift.

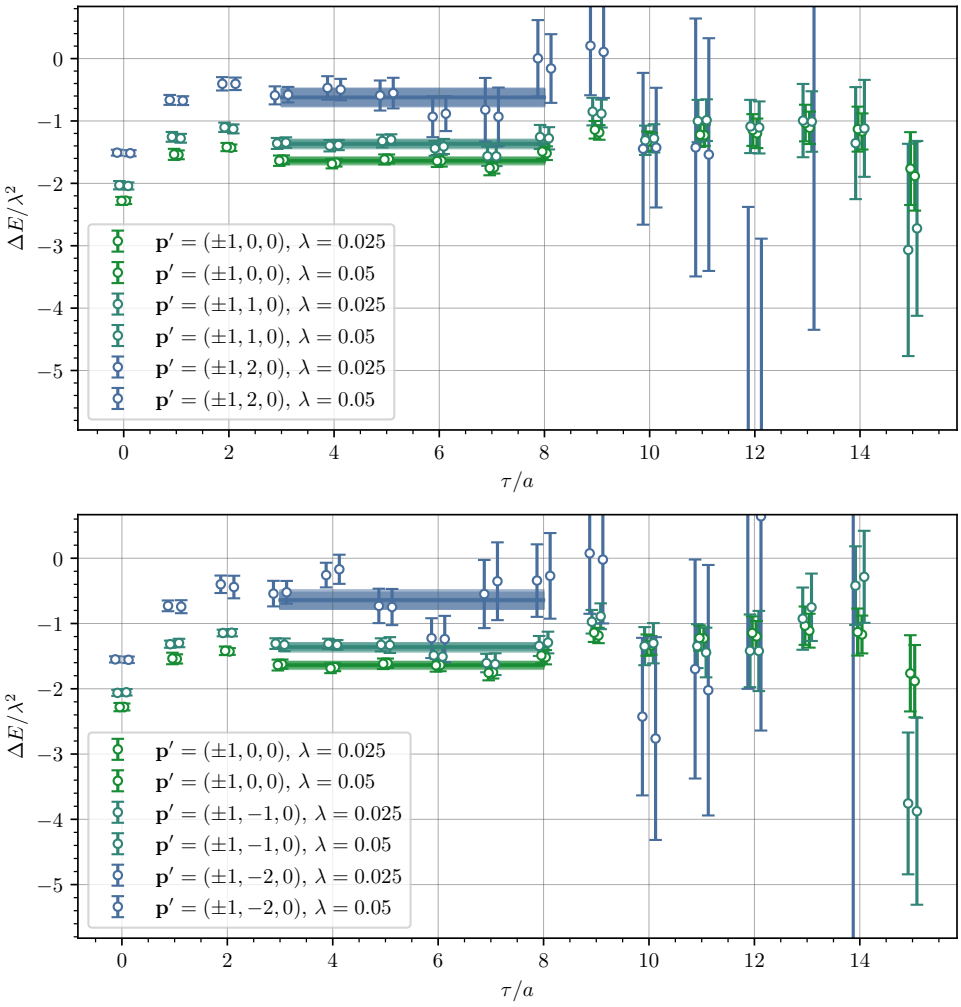

Figure I.2: Effective mass plot for $R(\mathbf{p}_1) \times R(\mathbf{p}_2)$ for up quarks.

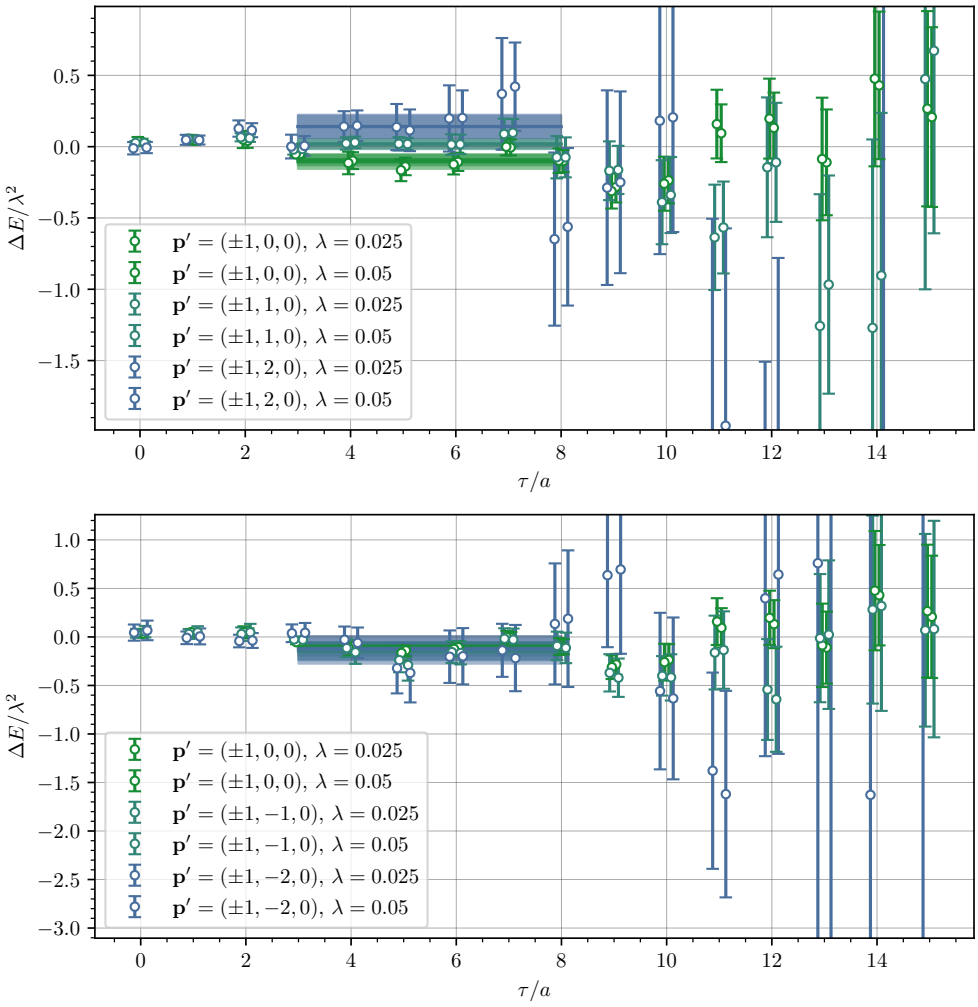

Figure I.3: Effective mass plot for $R(\mathbf{p}_1)/R(\mathbf{p}_2)$ for up quarks.

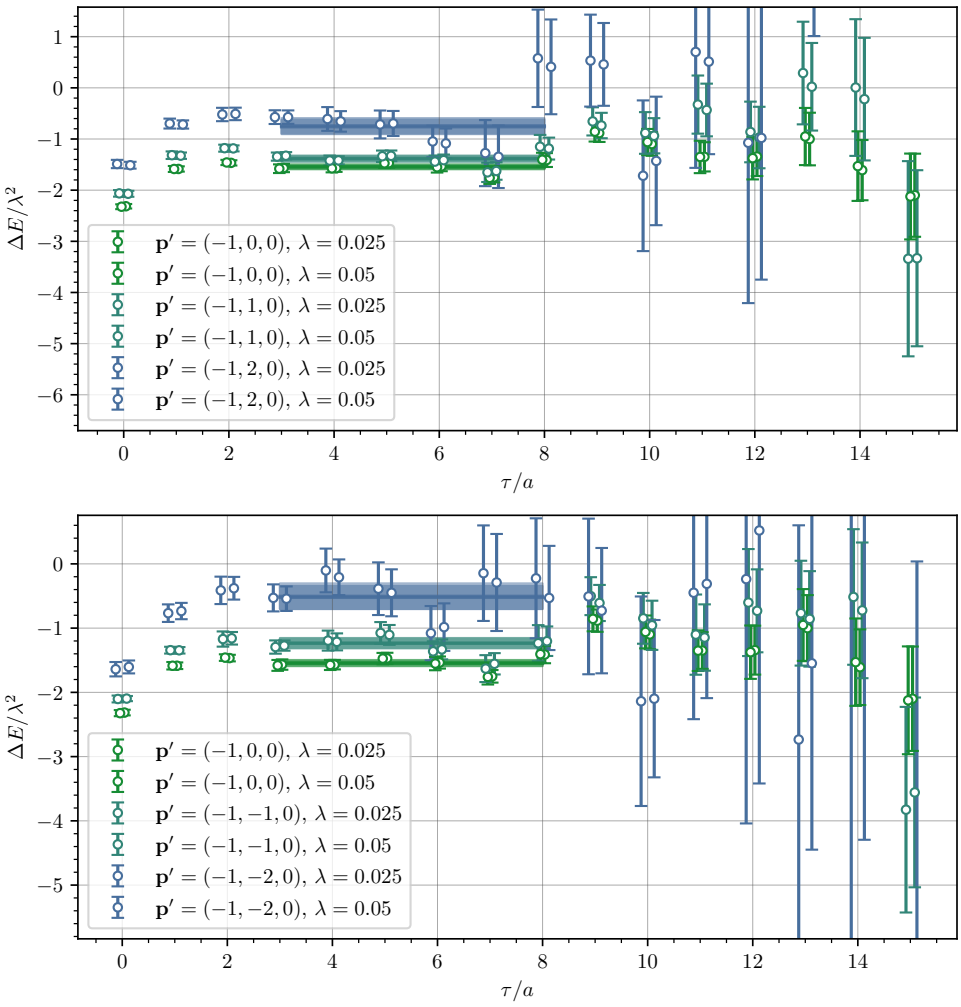

Figure I.4: Effective mass plot for the ratios $R(\mathbf{p}_2)$ for up quarks. Note that the values of the sink momentum all have $p_x = -1$.

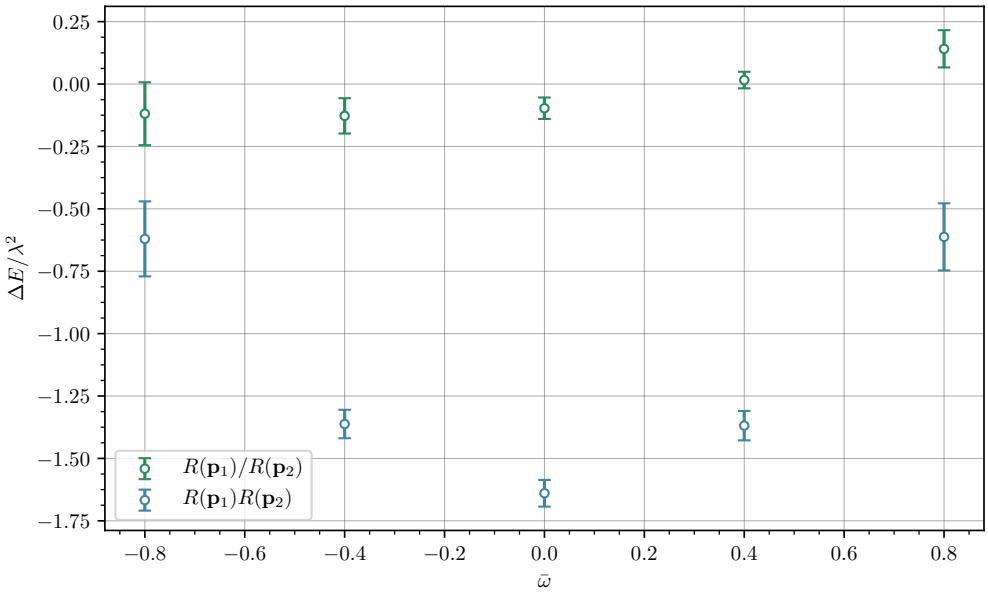

Figure I.5: The up quark energy shifts of the ratio and product as functions of $\bar{\omega}$.

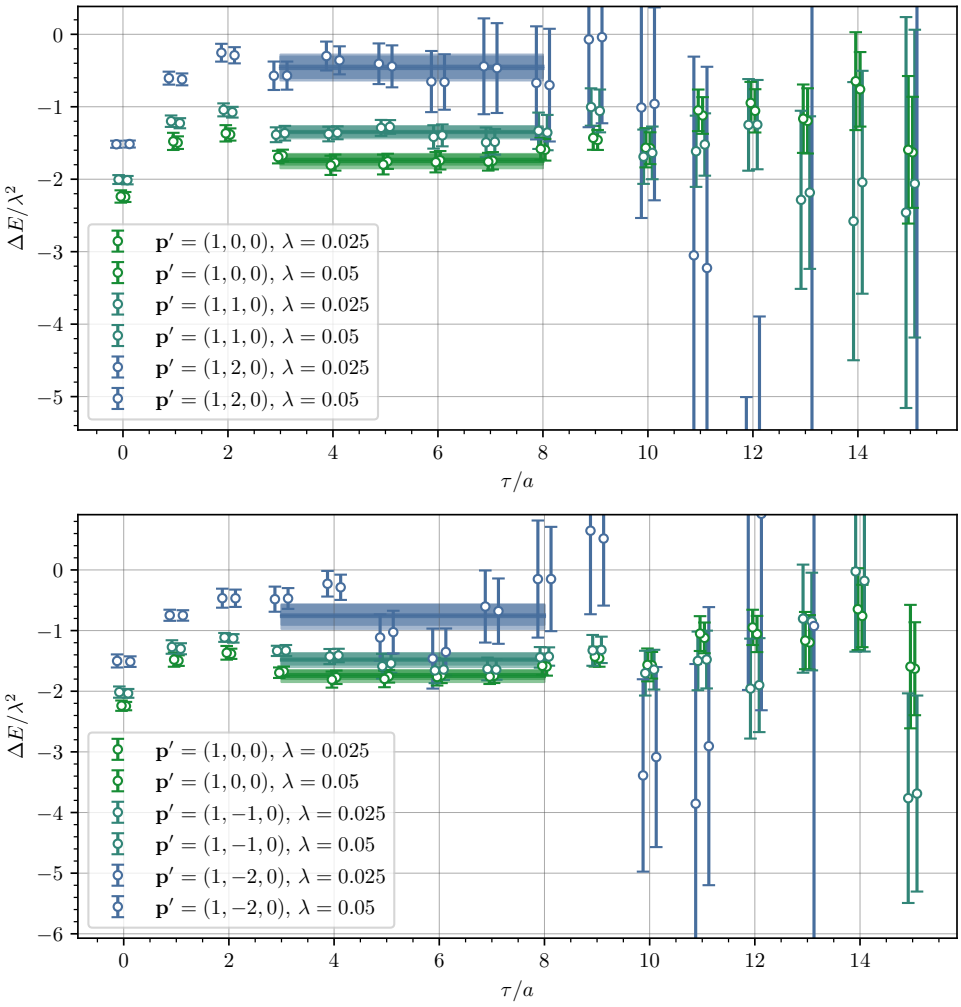

Figure I.6: The effective mass of $R(\mathbf{p}_1)$ for down quarks.

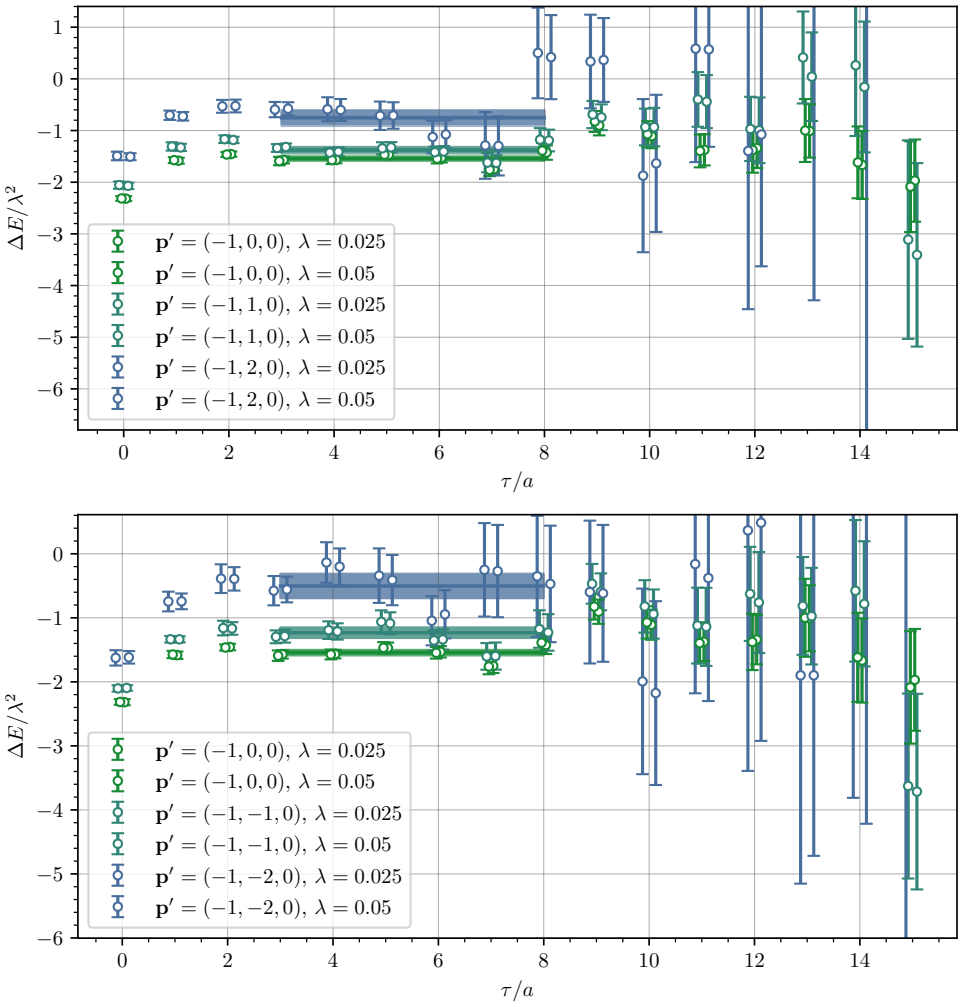

Figure I.7: The effective mass of $R(\mathbf{p}_2)$ for down quarks.

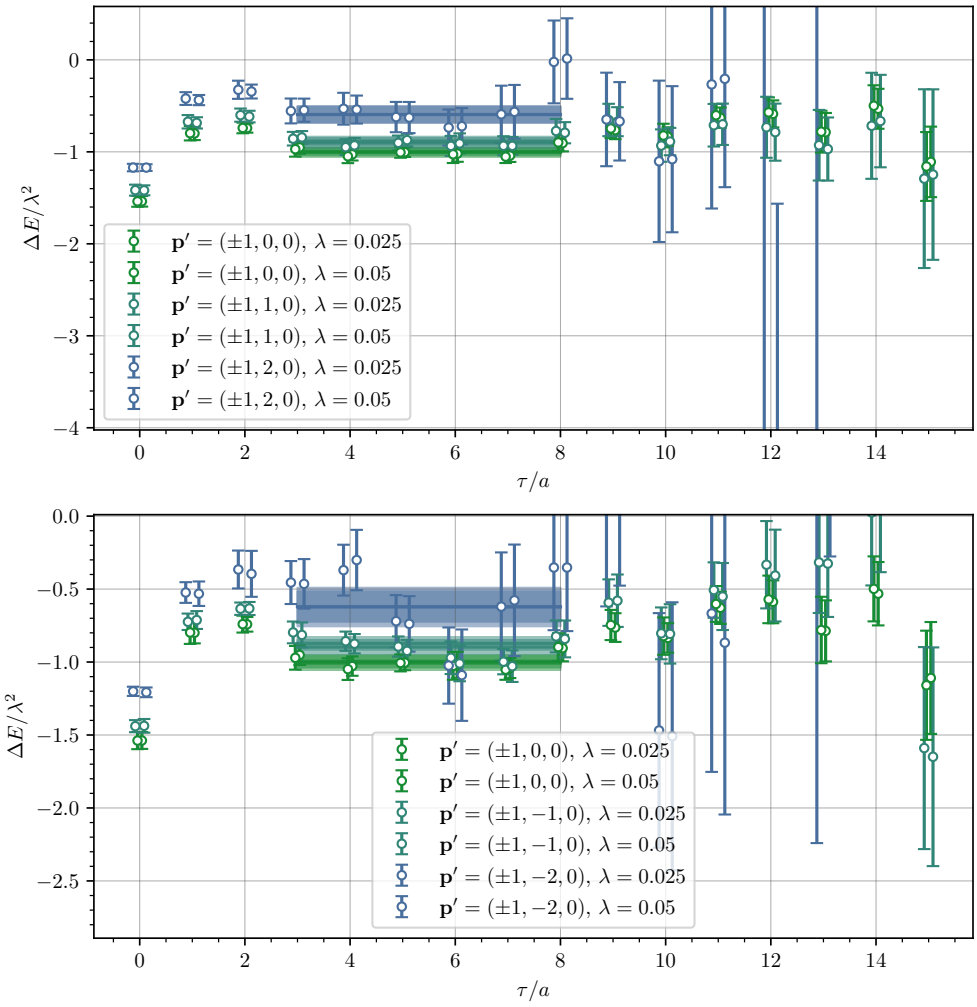

Figure I.8: The effective mass of $R(\mathbf{p}_1) \times R(\mathbf{p}_2)$ for down quarks.

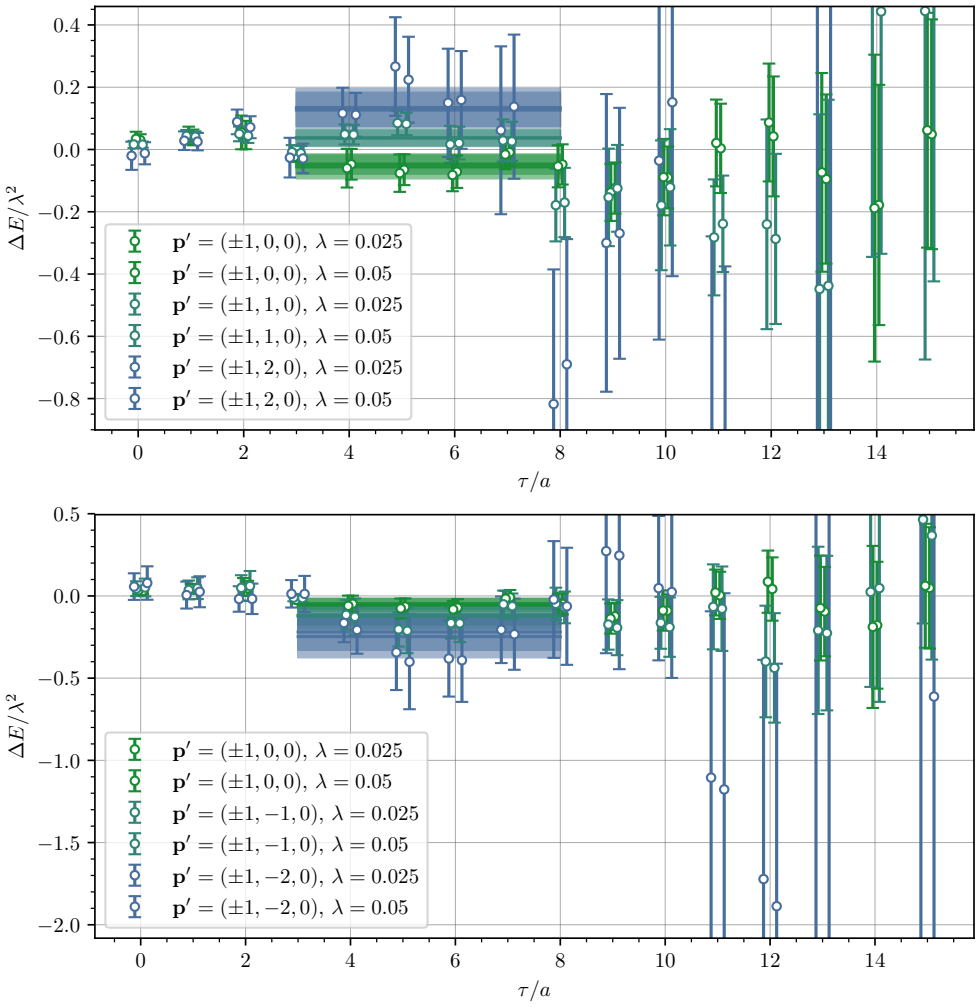

Figure I.9: The effective mass of $R(\mathbf{p}_1)/R(\mathbf{p}_2)$ for down quarks.

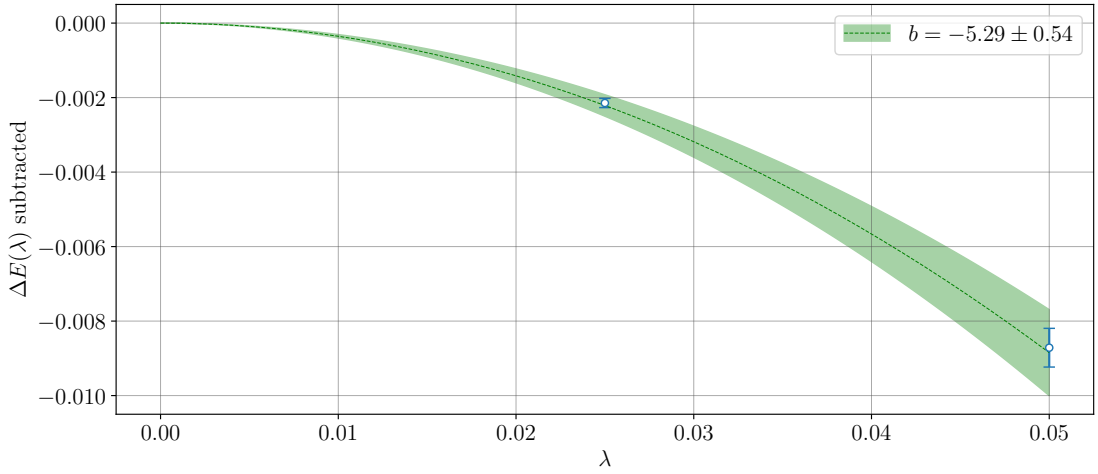

Figure I.10: The energy shift $\Delta E(\lambda)$ with the $\bar{\omega} = 0$ term subtracted for down quarks.

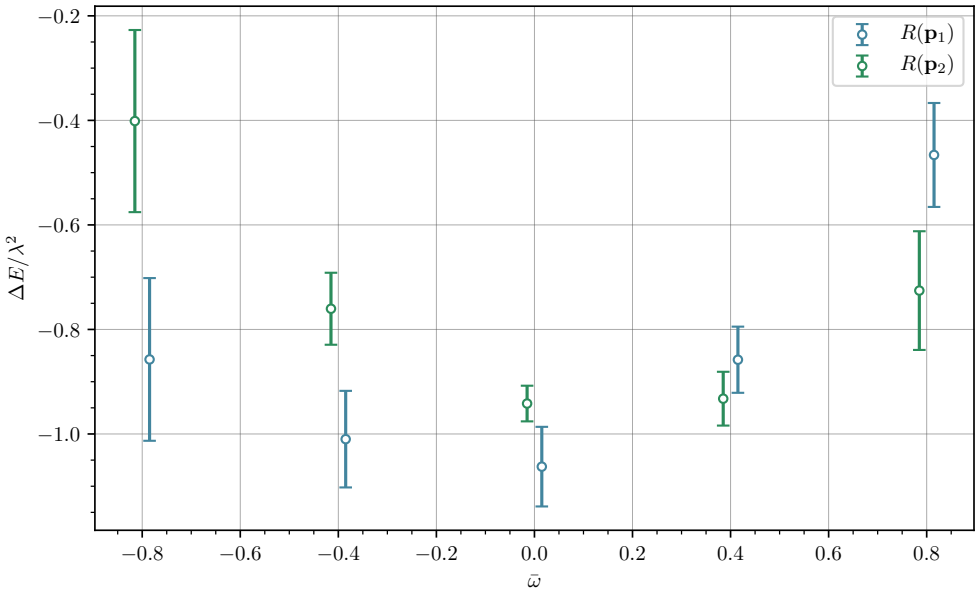

Figure I.11: The energy shift for down quarks normalised by $1/\lambda^2$ as a function of $\bar{\omega}$. The two λ values have been averaged.

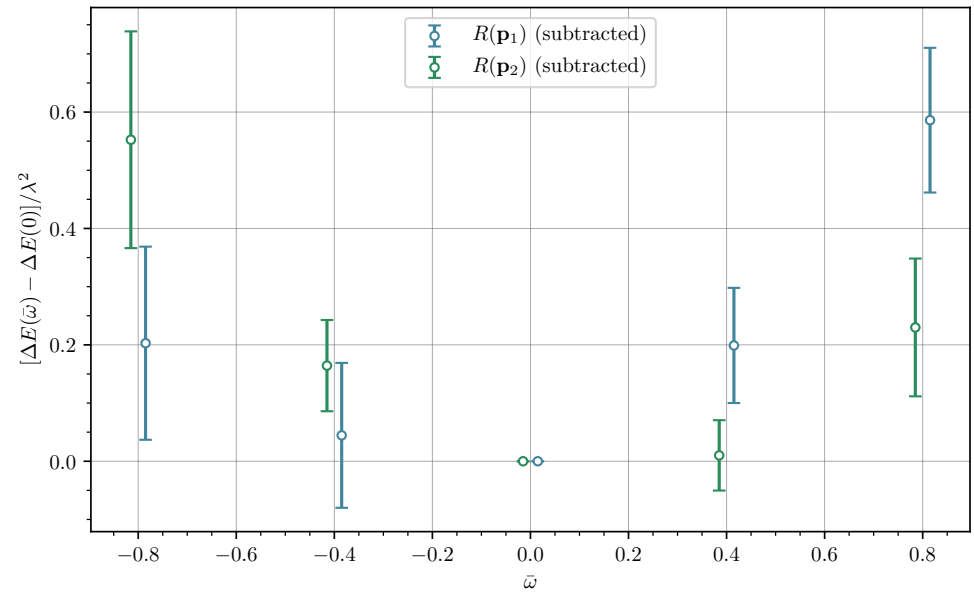

Figure I.12: The same energy shift as figure I.11, except with the $\bar{\omega} = 0$ terms subtracted off.

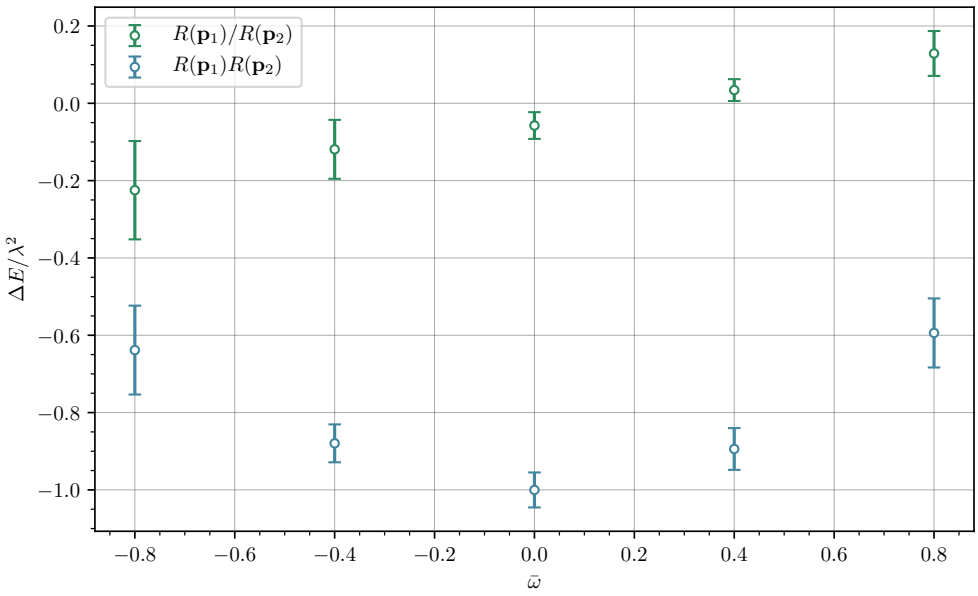

Figure I.13: The down quark energy shifts for the ratio and product as functions of $\bar{\omega}$.

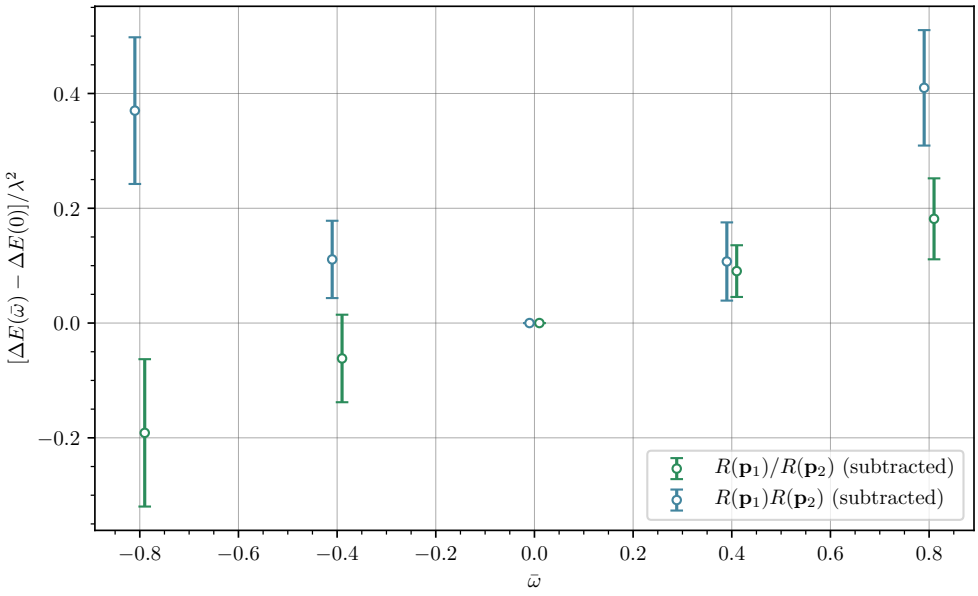

Figure I.14: The same energy shifts as in figure I.14, except with the $\bar{\omega} = 0$ value subtracted from each point.

Bibliography

[1] S. J. Brodsky and G. P. Lepage, "Exclusive Processes in Quantum Chromodynamics," *Adv. Ser. Direct. High Energy Phys.*, vol. 5, pp. 93–240, 1989.

[2] H. Geiger and E. Marsden, "On a diffuse reflection of the alpha-particles," *Proceedings of the Royal Society of London. Series A, Containing Papers of a Mathematical and Physical Character*, vol. 82, no. 557, pp. 495–500, 1909.

[3] E. Rutherford, "The scattering of alpha and beta particles by matter and the structure of the atom," *Phil. Mag. Ser.6*, vol. 21, pp. 669–688, 1911.

[4] H. Yukawa, "On the Interaction of Elementary Particles I," *Proc. Phys. Math. Soc. Jap.*, vol. 17, pp. 48–57, 1935.

[5] M. Gell-Mann, "A Schematic Model of Baryons and Mesons," *Phys. Lett.*, vol. 8, pp. 214–215, 1964.

[6] E. D. Bloom, D. H. Coward, H. DeStaebler, J. Drees, G. Miller, L. W. Mo, R. E. Taylor, M. Breidenbach, J. I. Friedman, G. C. Hartmann, and H. W. Kendall, "High-energy inelastic e-p scattering at 6 degrees and 10 degrees," *Phys. Rev. Lett.*, vol. 23, pp. 930–934, Oct 1969.

[7] K. G. Wilson, "Confinement of Quarks," *Phys. Rev.*, vol. D10, pp. 2445–2459, 1974.

[8] D. Müller, D. Robaschik, B. Geyer, F.-M. Dittes, and J. Hořejši, "Wave functions, evolution equations and evolution kernels from light-ray operators of qcd," *Fortschritte der Physik/Progress of Physics*, vol. 42, no. 2, p. 101–141, 1994.

[9] X. Ji, "Gauge-Invariant Decomposition of Nucleon Spin," *Phys. Rev. Lett.*, vol. 78, pp. 610–613, 1997.

[10] M. Burkardt, "Impact parameter dependent parton distributions and off-forward parton distributions for $\zeta \to 0$," *Phys. Rev. D*, vol. 62, p. 071503, Sep 2000.

[11] M. V. Polyakov and P. Schweitzer, "Forces inside hadrons: Pressure, surface tension, mechanical radius, and all that," *International Journal of Modern Physics A*, vol. 33, p. 1830025, Sep 2018.

[12] T. Kinoshita, "Quantum Electrodynamics - From a Personal Perspective," *NATO Sci. Ser. B*, vol. 352, pp. 9–26, 1996.

[13] F. Myhrer and A. W. Thomas, "Understanding the proton's spin structure," *Journal of Physics G: Nuclear and Particle Physics*, vol. 37, p. 023101, Jan 2010.

[14] T. Muta, *Foundations of Quantum Chromodynamics: An Introduction to Perturbative Methods in Gauge Theories, (3rd ed.)*, vol. 78 of *World scientific Lecture Notes in Physics*. Hackensack, N.J.: World Scientific, 2010.

[15] N. K. Nielsen, "Asymptotic Freedom as a Spin Effect," *Am. J. Phys.*, vol. 49, p. 1171, 1981.

[16] F. Wilczek, "Asymptotic freedom," 1996.

[17] A. M. Jaffe and E. Witten, "Quantum Yang-Mills theory," 2000.

[18] B. Sheikholeslami and R. Wohlert, "Improved Continuum Limit Lattice Action for QCD with Wilson Fermions," *Nucl. Phys.*, vol. B259, p. 572, 1985.

[19] C. Gattringer and C. B. Lang, "Quantum chromodynamics on the lattice," *Lect. Notes Phys.*, vol. 788, pp. 1–343, 2010.

[20] R. Gupta, "Introduction to lattice qcd," 1998.

[21] M. Gell-Mann, "The Symmetry group of vector and axial vector currents," *Physics Physique Fizika*, vol. 1, pp. 63–75, 1964.

[22] R. P. Feynman, "Very high-energy collisions of hadrons," *Phys. Rev. Lett.*, vol. 23, pp. 1415–1417, 1969.

[23] J. D. Bjorken and E. A. Paschos, "Inelastic Electron Proton and gamma Proton Scattering, and the Structure of the Nucleon," *Phys. Rev.*, vol. 185, pp. 1975–1982, 1969.

[24] S. Weinberg, "Nonabelian Gauge Theories of the Strong Interactions," *Phys. Rev. Lett.*, vol. 31, pp. 494–497, 1973.

[25] S. Coleman and D. J. Gross, "Price of asymptotic freedom," *Phys. Rev. Lett.*, vol. 31, pp. 851–854, Sep 1973.

[26] D. J. Gross and F. Wilczek, "Ultraviolet behavior of non-abelian gauge theories," *Phys. Rev. Lett.*, vol. 30, pp. 1343–1346, Jun 1973.

[27] J. Collins, "Foundations of perturbative QCD," *Camb. Monogr. Part. Phys. Nucl. Phys. Cosmol.*, vol. 32, pp. 1–624, 2011.

[28] J. C. Collins, *Renormalization*, vol. 26 of *Cambridge Monographs on Mathematical Physics*. Cambridge University Press, 1986.

[29] M. D. Schwartz, *Quantum Field Theory and the Standard Model*. Cambridge University Press, 2014.

[30] M. E. Peskin and D. V. Schroeder, *An Introduction to quantum field theory*. Reading, USA: Addison-Wesley, 1995.

[31] C. Itzykson and J. B. Zuber, *Quantum Field Theory*. International Series In Pure and Applied Physics, New York: McGraw-Hill, 1980.

[32] A. V. Manohar, "An introduction to spin dependent deep inelastic scattering," 1992.

[33] J. D. Bjorken, "Asymptotic sum rules at infinite momentum," *Phys. Rev.*, vol. 179, pp. 1547–1553, Mar 1969.

[34] Y. Frishman, "Scale invariance and current commutators near the light cone," *Phys. Rev. Lett.*, vol. 25, pp. 966–969, Oct 1970.

[35] R. L. Jaffe, "Light-cone dominance in the presence of singularities elsewhere in coordinate space," *Phys. Rev. D*, vol. 6, pp. 716–719, Jul 1972.

[36] J. M. Cornwall, "Spectral representations and their application to inclusive processes," *Phys. Rev. D*, vol. 5, pp. 2868–2877, Jun 1972.

[37] R. A. Brandt and G. Preparata, "Operator product expansions near the light cone," *Nucl. Phys.*, vol. B27, pp. 541–567, 1971.

[38] Y. Frishman, "Light Cone and Short Distances," *Phys. Rept.*, vol. 13, p. 1, 1974.

[39] K. G. Wilson, "Nonlagrangian models of current algebra," *Phys. Rev.*, vol. 179, pp. 1499–1512, 1969.

[40] W. Zimmermann, "Composite operators in the perturbation theory of renormalizable interactions," *Annals of Physics*, vol. 77, pp. 536–569, May 1973.

[41] K. G. Wilson and W. Zimmermann, "Operator product expansions and composite field operators in the general framework of quantum field theory," *Commun. Math. Phys.*, vol. 24, pp. 87–106, 1972.

[42] P. Otterson and W. Zimmermann, "On the directional dependence of composite field operators," *Comm. Math. Phys.*, vol. 24, no. 2, pp. 107–132, 1972.

[43] V. A. Novikov, M. A. Shifman, A. I. Vainshtein, and V. I. Zakharov, "Wilson's Operator Expansion: Can It Fail?," *Nucl. Phys.*, vol. B249, pp. 445–471, 1985.

[44] M. Shifman, "QCD sum rules: Bridging the gap between short and large distances," *Nucl. Phys. Proc. Suppl.*, vol. 207-208, pp. 298–305, 2010.

[45] J. Fischer and I. Vrkoč, "Operator-product expansion and analyticity," *International Journal of Modern Physics A*, vol. 14, p. 4819–4840, Dec 1999.

[46] R. P. a. Kanwal, *Generalized Functions Theory and Applications*. Springer eBooks, third edition. ed., 2004.

[47] R. Zwicky, "A brief introduction to dispersion relations and analyticity," 2016.

[48] A. V. Radyushkin, "Nonforward parton distributions," *Physical Review D*, vol. 56, p. 5524–5557, Nov 1997.

[49] X. Ji, "Deeply virtual compton scattering," *Physical Review D*, vol. 55, p. 7114–7125, Jun 1997.

[50] J. C. Collins, L. Frankfurt, and M. Strikman, "Factorization for hard exclusive electroproduction of mesons in qcd," *Physical Review D*, vol. 56, p. 2982–3006, Sep 1997.

[51] M. Polyakov, "Generalized parton distributions and strong forces inside nucleons and nuclei," *Physics Letters B*, vol. 555, p. 57–62, Feb 2003.

[52] M. V. Polyakov and P. Schweitzer, "Mechanical properties of particles," 2018.

[53] C. Lorcé, H. Moutarde, and A. P. Trawiński, "Revisiting the mechanical properties of the nucleon," *The European Physical Journal C*, vol. 79, p. 89, Jan 2019.

[54] K. Kumerički, S. Liuti, and H. Moutarde, "Gpd phenomenology and dvcs fitting," *The European Physical Journal A*, vol. 52, Jun 2016.

[55] M. Guidal, H. Moutarde, and M. Vanderhaeghen, "Generalized parton distributions in the valence region from deeply virtual compton scattering," *Reports on Progress in Physics*, vol. 76, p. 066202, May 2013.

[56] P. Hägler, J. W. Negele, D. B. Renner, W. Schroers, T. Lippert, and K. Schilling, "Moments of nucleon generalized parton distributions in lattice qcd," *Physical Review D*, vol. 68, Aug 2003.

[57] M. Göckeler, R. Horsley, D. Pleiter, P. E. L. Rakow, A. Schäfer, G. Schierholz, and W. Schroers, "Generalized parton distributions from lattice qcd," *Physical Review Letters*, vol. 92, Jan 2004.

[58] M. Ohtani, D. Brommel, M. Göckeler, P. Hägler, R. Horsley, Y. Nakamura, D. Pleiter, P. E. L. Rakow, A. Schäfer, G. Schierholz, W. Schroers, H. Stuben, and J. M. Zanotti, "Moments of generalized parton distributions and quark angular momentum of the nucleon," in *Proceedings, 25th International Symposium on Lattice field theory (Lattice 2007): Regensburg, Germany, July 30-August 4, 2007*, vol. LATTICE2007, p. 158, 2007.

[59] P. Hägler, W. Schroers, J. Bratt, J. W. Negele, A. V. Pochinsky, R. G. Edwards, D. G. Richards, M. Engelhardt, G. T. Fleming, B. Musch, and et al., "Nucleon generalized parton distributions from full lattice qcd," *Physical Review D*, vol. 77, May 2008.

[60] J. D. Bratt, R. G. Edwards, M. Engelhardt, P. Hägler, H. W. Lin, M. F. Lin, H. B. Meyer, B. Musch, J. W. Negele, K. Orginos, and et al., "Nucleon structure from mixed action calculations using $2 + 1$ flavors of asqtad sea and domain wall valence fermions," *Physical Review D*, vol. 82, Nov 2010.

[61] C. Alexandrou, J. Carbonell, M. Constantinou, P. A. Harraud, P. Guichon, K. Jansen, C. Kallidonis, T. Korzec, and M. Papinutto, "Moments of nucleon generalized parton distributions from lattice qcd," *Physical Review D*, vol. 83, Jun 2011.

[62] A. Sternbeck and M. Göckeler and Ph. Hägler and R. Horsley and Y. Nakamura and A. Nobile and D. Pleiter and P. E. L. Rakow and A. Schäfer and G. Schierholz and J. Zanotti, "First moments of the nucleon generalized parton distributions from lattice QCD," *PoS*, vol. LATTICE2011, p. 177, 2011.

[63] P. Shanahan and W. Detmold, "Gluon gravitational form factors of the nucleon and the pion from lattice qcd," *Physical Review D*, vol. 99, Jan 2019.

[64] P. Shanahan and W. Detmold, "Pressure distribution and shear forces inside the proton," *Physical Review Letters*, vol. 122, Feb 2019.

[65] J.-W. Chen, H.-W. Lin, and J.-H. Zhang, "Pion generalized parton distribution from lattice qcd," 2019.

[66] X. Ji, "Off-forward parton distributions," *Journal of Physics G: Nuclear and Particle Physics*, vol. 24, p. 1181–1205, Jul 1998.

[67] R. K. Ellis, W. Furmanski, and R. Petronzio, "Unraveling Higher Twists," *Nucl. Phys.*, vol. B212, p. 29, 1983.

[68] X. Ji, "The Nucleon structure functions from deep inelastic scattering with electroweak currents," *Nucl. Phys.*, vol. B402, pp. 217–250, 1993.

[69] X. Ji and R. F. Lebed, "Counting form factors of twist-two operators," *Physical Review D*, vol. 63, Mar 2001.

[70] E. Leader and M. Anselmino, "A crisis in the parton model: Where, oh where is the proton's spin?," *Z. Phys.*, vol. C41, p. 239, 1988.

[71] J. Ashman *et al.*, "A measurement of the spin asymmetry and determination of the structure function g1 in deep inelastic muon-proton scattering," *Physics Letters B*, vol. 206, no. 2, pp. 364 – 370, 1988.

[72] F. Belinfanté, "On the current and the density of the electric charge, the energy, the linear momentum and the angular momentum of arbitrary fields," *Physica*, vol. 7, no. 5, pp. 449 – 474, 1940.

[73] Wikipedia, the free encyclopedia, "Components of the stress-energy tensor," 2008. [Online; accessed January 15, 2020].

[74] M. Burkardt, "Impact parameter space interpretation for generalized parton distributions," *International Journal of Modern Physics A*, vol. 18, p. 173–207, Jan 2003.

[75] D. E. Soper, "Infinite-momentum helicity states," *Phys. Rev. D*, vol. 5, pp. 1956–1962, Apr 1972.

[76] M. Diehl, "Generalized parton distributions in impact parameter space," *The European Physical Journal C*, vol. 25, p. 223–232, Sep 2002.

[77] J. P. Ralston and B. Pire, "Femtophotography of protons to nuclei with deeply virtual compton scattering," *Physical Review D*, vol. 66, Dec 2002.

[78] N. G. Stefanis, C. Alexandrou, T. Horn, H. Moutarde, and I. Scimemi, "Round table: Nucleon tomography. what can we do better today than rutherford 100 years ago?," *EPJ Web of Conferences*, vol. 137, p. 01003, 2017.

[79] M. V. Polyakov and C. Weiss, "Skewed and double distributions in the pion and the nucleon," *Physical Review D*, vol. 60, Nov 1999.

[80] M. V. Polyakov and A. G. Shuvaev, "On "dual" parametrizations of generalized parton distributions," 2002.

[81] N. Kivel, M. V. Polyakov, and M. Vanderhaeghen, "Deeply virtual compton scattering on the nucleon: Study of the twist-3 effects," *Physical Review D*, vol. 63, May 2001.

[82] I. V. Anikin and O. V. Teryaev, "Dispersion relations and subtractions in hard exclusive processes," *Physical Review D*, vol. 76, Sep 2007.

[83] O. V. Teryaev, "Analytic properties of hard exclusive amplitudes," 2005.

[84] M. Diehl and D. Ivanov, "Dispersion representations for hard exclusive processes: beyond the born approximation," *The European Physical Journal C*, vol. 52, p. 919–932, Oct 2007.

[85] B. Pasquini, M. Polyakov, and M. Vanderhaeghen, "Dispersive evaluation of the d-term form factor in deeply virtual compton scattering," *Physics Letters B*, vol. 739, p. 133–138, Dec 2014.

[86] V. D. Burkert, L. Elouadrhiri, and F. X. Girod, "The pressure distribution inside the proton," *Nature*, vol. 557, pp. 396–399, 2018.

[87] C. Adloff, V. Andreev, B. Andrieu, T. Anthonis, V. Arkadov, A. Astvatsatourov, A. Babaev, J. Bähr, P. Baranov, E. Barrelet, and et al., "Measurement of deeply virtual compton scattering at hera," *Physics Letters B*, vol. 517, p. 47–58, Sep 2001.

[88] S. Chekanov, M. Derrick, D. Krakauer, J. Loizides, S. Magill, B. Musgrave, J. Repond, R. Yoshida, M. Mattingly, P. Antonioli, and et al., "Measurement of deeply virtual compton scattering at hera," *Physics Letters B*, vol. 573, p. 46–62, Oct 2003.

[89] "Measurement of deeply virtual compton scattering at hera," *The European Physical Journal C*, vol. 44, p. 1–11, Sep 2005.

[90] A. Airapetian, N. Akopov, Z. Akopov, E. Aschenauer, W. Augustyniak, R. Avakian, A. Avetissian, E. Avetisyan, S. Belostotski, N. Bianchi, and et al., "Measurement of double-spin asymmetries associated with deeply virtual compton scattering on a transversely polarized hydrogen target," *Physics Letters B*, vol. 704, p. 15–23, Oct 2011.

[91] A. Airapetian, N. Akopov, Z. Akopov, E. C. Aschenauer, W. Augustyniak, R. Avakian, A. Avetissian, E. Avetisyan, H. P. Blok, and et al., "Beam-helicity and beam-charge asymmetries associated with deeply virtual compton scattering on the unpolarised proton," *Journal of High Energy Physics*, vol. 2012, Jul 2012.

[92] F. Gautheron *et al.*, "COMPASS-II Proposal," 2010.

[93] M. Defurne, M. Amaryan, K. A. Aniol, M. Beaumel, H. Benaoum, P. Bertin, M. Brossard, A. Camsonne, J.-P. Chen, E. Chudakov, and et al., "E00-110 experiment at jefferson lab hall a: Deeply virtual compton scattering off the proton at 6 gev," *Physical Review C*, vol. 92, Nov 2015.

[94] H. Jo, F. Girod, H. Avakian, V. Burkert, M. Garçon, M. Guidal, V. Kubarovsky, S. Niccolai, P. Stoler, K. Adhikari, and et al., "Cross sections for the exclusive photon electroproduction on the proton and generalized parton distributions," *Physical Review Letters*, vol. 115, Nov 2015.

[95] E. Seder, A. Biselli, S. Pisano, S. Niccolai, G. Smith, K. Joo, K. Adhikari, M. Amaryan, M. Anderson, S. Anefalos Pereira, and et al., "Longitudinal target-spin asymmetries for deeply virtual compton scattering," *Physical Review Letters*, vol. 114, Jan 2015.

[96] J. Dudek, R. Ent, R. Essig, K. S. Kumar, C. Meyer, R. D. McKeown, Z. E. Meziani, G. A. Miller, M. Pennington, D. Richards, and et al., "Physics opportunities with the 12 gev upgrade at jefferson lab," *The European Physical Journal A*, vol. 48, Dec 2012.

[97] A. Accardi *et al.*, "Electron ion collider: The next qcd frontier - understanding the glue that binds us all," 2012.

[98] M. Guidal, "A fitter code for deep virtual compton scattering and generalized parton distributions," *The European Physical Journal A*, vol. 37, p. 319–332, Sep 2008.

[99] K. Kumerički, D. Müller, and A. Schäfer, "Neural network generated parametrizations of deeply virtual compton form factors," *Journal of High Energy Physics*, vol. 2011, Jul 2011.

[100] H. Moutarde, "Extraction of the compton form factor h from deeply virtual compton scattering measurements at jefferson lab," *Physical Review D*, vol. 79, May 2009.

[101] K. Kumerički and D. Müller, "Deeply virtual compton scattering at small x_b and the access to the gpd h," *Nuclear Physics B*, vol. 841, p. 1–58, Dec 2010.

[102] T. Lautenschlager, D. Müller, and A. Schäfer, "Global analysis of generalized parton distributions – collider kinematics –," 2013.

[103] J. O. Gonzalez-Hernandez, S. Liuti, G. R. Goldstein, and K. Kathuria, "Interpretation of the flavor dependence of nucleon form factors in a generalized parton distribution model," *Physical Review C*, vol. 88, Dec 2013.

[104] D. Müller, T. Lautenschlager, K. Passek-Kumerički, and A. Schäfer, "Towards a fitting procedure to deeply virtual meson production — the next-to-leading order case," *Nuclear Physics B*, vol. 884, p. 438u(P)2013546, Jul 2014.

[105] B. Berthou, D. Binosi, N. Chouika, L. Colaneri, M. Guidal, C. Mezrag, H. Moutarde, J. Rodríguez-Quintero, F. Sabatié, P. Sznajder, and J. Wagner, "Partons: Partonic tomography of nucleon software. a computing framework for the phenomenology of generalized parton distributions," 2015.

[106] R. A. Briceño, M. T. Hansen, and C. J. Monahan, "Role of the euclidean signature in lattice calculations of quasidistributions and other nonlocal matrix elements," *Physical Review D*, vol. 96, Jul 2017.

[107] S. Capitani and G. RosSi, "Deep inelastic scattering in improved lattice qcd (i). the first moment of structure functions," *Nuclear Physics B*, vol. 433, p. 351–389, Jan 1995.

[108] G. Beccarini, M. Bianchi, S. Capitani, and G. Rossi, "Deep inelastic scattering in improved lattice qcd (ii). the second moment of structure functions," *Nuclear Physics B*, vol. 456, p. 271–295, Dec 1995.

[109] X. Ji, "Parton physics on a euclidean lattice," *Physical Review Letters*, vol. 110, Jun 2013.

[110] X. Ji, "Parton physics from large-momentum effective field theory," 2014.

[111] H.-W. Lin, E. R. Nocera, F. Olness, K. Orginos, J. Rojo, A. Accardi, C. Alexandrou, A. Bacchetta, G. Bozzi, J.-W. Chen, and et al., "Parton distributions and lattice qcd calculations: A community white paper," *Progress in Particle and Nuclear Physics*, vol. 100, p. 107–160, May 2018.

[112] G. Rossi and M. Testa, "Note on lattice regularization and equal-time correlators for parton distribution functions," *Physical Review D*, vol. 96, Jul 2017.

[113] G. Rossi and M. Testa, "Euclidean versus minkowski short distance," *Physical Review D*, vol. 98, Sep 2018.

[114] K.-F. Liu and S.-J. Dong, "Origin of difference between u-bar and d-bar partons in the nucleon," *Physical Review Letters*, vol. 72, p. 1790–1793, Mar 1994.

[115] U. Aglietti, M. Ciuchini, G. Corbò, E. Franco, G. Martinelli, and L. Silvestrini, "Model independent determination of the shape function for inclusive b decays and of the structure functions in dis," *Physics Letters B*, vol. 432, p. 411–420, Jul 1998.

[116] K.-F. Liu, "Parton distribution function from the hadronic tensor on the lattice," 2016.

[117] J. Liang, K.-F. Liu, and Y.-B. Yang, "Lattice calculation of hadronic tensor of the nucleon," *EPJ Web of Conferences*, vol. 175, p. 14014, 2018.

[118] J. Liang, T. Draper, K.-F. Liu, A. Rothkopf, and Y.-B. Yang, "Towards the nucleon hadronic tensor from lattice qcd," 2019.

[119] W. Detmold and C.-J. D. Lin, "Deep inelastic scattering and the operator product expansion in lattice qcd," *Annalen der Physik*, vol. 322, no. 10, pp. 891–921, 1905.

[120] W. Detmold, I. Kanamori, C. J. D. Lin, S. Mondal, and Y. Zhao, "Moments of pion distribution amplitude using operator product expansion on the lattice," 2018.

[121] Y.-Q. Ma and J.-W. Qiu, "Exploring partonic structure of hadrons using ab initio lattice qcd calculations," *Phys. Rev. Lett.*, vol. 120, p. 022003, Jan 2018.

[122] A. Chambers, R. Horsley, Y. Nakamura, H. Perlt, P. Rakow, G. Schierholz, A. Schiller, K. Somfleth, R. Young, J. Zanotti, and et al., "Nucleon structure functions from operator product expansion on the lattice," *Physical Review Letters*, vol. 118, Jun 2017.

[123] K. Somfleth *et al.* 2020.

[124] R. P. Feynman, "Forces in molecules," *Phys. Rev.*, vol. 56, pp. 340–343, Aug 1939.

[125] H. Hellmann, *Einführung in die Quantenchemie*. Leipzig: Franz Deuticke, 1937.

[126] P. Güttinger, "Das Verhalten von Atomen im magnetischen Drehfeld," *Zeitschrift fur Physik*, vol. 73, pp. 169–184, Mar 1932.

[127] S. Dinter, V. Drach, R. Frezzotti, G. Herdoiza, K. Jansen, and G. Rossi, "Sigma terms and strangeness content of the nucleon with $n_f = 2 + 1 + 1$ twisted mass fermions," *Journal of High Energy Physics*, vol. 2012, Aug 2012.

[128] R. Horsley, Y. Nakamura, H. Perlt, D. Pleiter, P. E. L. Rakow, G. Schierholz, A. Schiller, H. Stüben, F. Winter, and J. M. Zanotti, "Hyperon sigma terms for $2 + 1$ quark flavors," *Physical Review D*, vol. 85, Feb 2012.

[129] S. Dürr, Z. Fodor, T. Hemmert, C. Hoelbling, J. Frison, S. D. Katz, S. Krieg, T. Kurth, L. Lellouch, T. Lippert, and et al., "Sigma term and strangeness content of octet baryons," *Physical Review D*, vol. 85, Jan 2012.

[130] P. E. Shanahan, A. W. Thomas, and R. D. Young, "Sigma terms from an su(3) chiral extrapolation," *Physical Review D*, vol. 87, Apr 2013.

[131] A. Chambers, R. Horsley, Y. Nakamura, H. Perlt, D. Pleiter, P. Rakow, G. Schierholz, A. Schiller, H. Stüben, R. Young, and et al., "Feynman-hellmann approach to the spin structure of hadrons," *Physical Review D*, vol. 90, Jul 2014.

[132] W. Detmold, "Flavor singlet physics in lattice qcd with background fields," *Physical Review D*, vol. 71, Mar 2005.

[133] C. Bouchard, C. C. Chang, T. Kurth, K. Orginos, and A. Walker-Loud, "On the feynman-hellmann theorem in quantum field theory and the calculation of matrix elements," *Physical Review D*, vol. 96, Jul 2017.

[134] M. J. Savage, P. E. Shanahan, B. C. Tiburzi, M. L. Wagman, F. Winter, S. R. Beane, E. Chang, Z. Davoudi, W. Detmold, K. Orginos, and et al., "Proton-proton fusion and tritium β decay from lattice quantum chromodynamics," *Physical Review Letters*, vol. 119, Aug 2017.

[135] R. Horsley, R. Millo, Y. Nakamura, H. Perlt, D. Pleiter, P. Rakow, G. Schierholz, A. Schiller, F. Winter, and J. Zanotti, "A lattice study of the glue in the nucleon," *Physics Letters B*, vol. 714, p. 312–316, Aug 2012.

[136] A. Chambers, J. Dragos, R. Horsley, Y. Nakamura, H. Perlt, D. Pleiter, P. Rakow, G. Schierholz, A. Schiller, K. Somfleth, and et al., "Electromagnetic form factors at large momenta from lattice qcd," *Physical Review D*, vol. 96, Dec 2017.

[137] A. Chambers, R. Horsley, Y. Nakamura, H. Perlt, D. Pleiter, P. Rakow, G. Schierholz, A. Schiller, H. Stüben, R. Young, and et al., "Disconnected contributions to the spin of the nucleon," *Physical Review D*, vol. 92, Dec 2015.

[138] R. Horsley, Y. Nakamura, H. Perlt, D. Pleiter, P. E. L. Rakow, G. Schierholz, A. Schiller, H. Stüben, R. D. Young, and J. M. Zanotti, "The strange quark contribution to the spin of the nucleon," 2019.

[139] A. J. Chambers, *Hadron structure and the Feynman-Hellmann theorem in lattice quantum chromodynamics*. PhD thesis, The University of Adelaide, 2017.

[140] A. Hannaford-Gunn, R. Horsley, Y. Nakamura, H. Perlt, P. E. L. Rakow, G. Schierholz, K. Somfleth, H. Stüben, R. D. Young, and J. M. Zanotti, "Scaling and higher twist in the nucleon compton amplitude," 2020.

[141] K. Gottfried and T.-M. Yan, *Quantum Mechanics: Fundamentals*. Springer, 01 2003.

[142] G. Martinelli, "Lattice results in hadron phenomenology," in *Particles and nuclei. Proceedings, 14th International Conference, PANIC'96, Williamsburg, USA, May 22-28, 1996*, pp. 88–104, 1996.

[143] Z. Chen, "Non-forward and unequal mass virtual compton scattering," *Nuclear Physics B*, vol. 525, p. 369–383, Aug 1998.

[144] X. Ji and J. Osborne, "One-loop corrections and all order factorization in deeply virtual compton scattering," *Physical Review D*, vol. 58, Sep 1998.

[145] B. E. White, "Factorization in deeply virtual compton scattering: local ope formalism and structure functions," *Journal of Physics G: Nuclear and Particle Physics*, vol. 28, p. 203–221, Jan 2002.

[146] I. V. Anikin, B. Pire, and O. V. Teryaev, "On the gauge invariance of the DVCS amplitude," *Phys. Rev.*, vol. D62, p. 071501, 2000.

[147] M. Penttinen, M. V. Polyakov, A. G. Shuvaev, and M. Strikman, "DVCS amplitude in the parton model," *Phys. Lett.*, vol. B491, pp. 96–100, 2000.

[148] A. Belitsky and D. Müller, "Twist-three effects in two-photon processes," *Nuclear Physics B*, vol. 589, p. 611–630, Nov 2000.

[149] A. Radyushkin and C. Weiss, "Dvcs amplitude with kinematical twist-3 terms," *Physics Letters B*, vol. 493, p. 332–340, Nov 2000.

[150] W. A. Bardeen and W.-K. Tung, "Invariant amplitudes for photon processes," *Phys. Rev.*, vol. 173, pp. 1423–1433, Sep 1968.

[151] R. Tarrach, "Invariant Amplitudes for Virtual Compton Scattering Off Polarized Nucleons Free from Kinematical Singularities, Zeros and Constraints," *Nuovo Cim.*, vol. A28, p. 409, 1975.

[152] W. Lu, "Form factor description of the non-collinear compton scattering tensor," 1997.

[153] S. A. Anikin and O. I. Zavialov, "Short-distance and light-cone expansions for products of currents," *Annals of Physics*, vol. 116, pp. 135–166, Nov 1978.

[154] I. I. Balitsky and V. M. Braun, "Evolution Equations for QCD String Operators," *Nucl. Phys.*, vol. B311, pp. 541–584, 1989.

[155] A. V. Radyushkin and C. Weiss, "Deeply virtual compton scattering amplitude at the tree level: Transversality, twist-3, and factorization," *Physical Review D*, vol. 63, Apr 2001.

[156] K. Watanabe, "Elastic Scattering and Hadron Dynamics at Short Distances," *Progress of Theoretical Physics*, vol. 66, pp. 1003–1024, 09 1981.

[157] K. Watanabe, "Operator Product Expansion and Integral Representation for Two Photon Processes," *Prog. Theor. Phys.*, vol. 67, p. 1834, 1982.

[158] G. Eichmann and C. S. Fischer, "Nucleon compton scattering in the dyson-schwinger approach," *Physical Review D*, vol. 87, Feb 2013.

[159] M. Diehl, T. Gousset, B. Pire, and J. P. Ralston, "Testing the handbag contribution to exclusive virtual Compton scattering," *Phys. Lett.*, vol. B411, pp. 193–202, 1997.

[160] A. Belitsky and A. Radyushkin, "Unraveling hadron structure with generalized parton distributions," *Physics Reports*, vol. 418, p. 1–387, Oct 2005.

[161] P. Guichon and M. Vanderhaeghen, "Virtual compton scattering off the nucleon," *Progress in Particle and Nuclear Physics*, vol. 41, p. 125–190, 1998.

[162] K. Somfleth, *Hadron Structure Using Feynman–Hellmann Theorem.* PhD thesis, The University of Adelaide, 2020.

[163] F. Ynduráin, "Reconstruction of the deep inelastic structure functions from their moments," *Physics Letters B*, vol. 74, no. 1, pp. 68 – 72, 1978.

[164] L. A. Harland-Lang, A. D. Martin, P. Motylinski, and R. S. Thorne, "Parton distributions in the lhc era: Mmht 2014 pdfs," *The European Physical Journal C*, vol. 75, May 2015.

[165] K. Goeke, M. Polyakov, and M. Vanderhaeghen, "Hard exclusive reactions and the structure of hadrons," *Progress in Particle and Nuclear Physics*, vol. 47, p. 401–515, Jan 2001.

[166] V. Guzey and M. Polyakov, "Dual parameterization of generalized parton distributions and a description of dvcs data," *The European Physical Journal C*, vol. 46, p. 151–156, Mar 2006.

[167] M. Diehl and W. Kugler, "Some numerical studies of the evolution of generalized parton distributions," *Physics Letters B*, vol. 660, p. 202–211, Feb 2008.

[168] H.-W. Lin, J.-W. Chen, S. D. Cohen, and X. Ji, "Flavor structure of the nucleon sea from lattice qcd," *Physical Review D*, vol. 91, Mar 2015.

[169] J.-W. Chen, S. D. Cohen, X. Ji, H.-W. Lin, and J.-H. Zhang, "Nucleon helicity and transversity parton distributions from lattice qcd," *Nuclear Physics B*, vol. 911, p. 246–273, Oct 2016.

[170] R. Horsley, Y. Nakamura, H. Perlt, P. E. L. Rakow, G. Schierholz, K. Somfleth, R. D. Young, and J. M. Zanotti, "Structure functions from the compton amplitude," 2020.

[171] F. M. Stokes, W. Kamleh, and D. B. Leinweber, "Opposite-parity contaminations in lattice nucleon form factors," *Physical Review D*, vol. 99, Apr 2019.

[172] D. J. Gross and S. B. Treiman, "Light-cone structure of current commutators in the gluon-quark model," *Phys. Rev. D*, vol. 4, pp. 1059–1072, Aug 1971.

[173] B. Geyer, M. Lazar, and D. Robaschik, "Decomposition of non-local light-cone operators into harmonic operators of definite twist," *Nuclear Physics B*, vol. 559, p. 339–377, Oct 1999.

[174] G. A. Miller, "Transverse charge densities," *Annual Review of Nuclear and Particle Science*, vol. 60, p. 1–25, Nov 2010.

[175] C. Lorcé, "New explicit expressions for dirac bilinears," *Physical Review D*, vol. 97, Jan 2018.